ORNL-2994
UC-41 - Health and Safety

HEALTH PHYSICS DIVISION

ANNUAL PROGRESS REPORT

FOR PERIOD ENDING JULY 31, 1960

OAK RIDGE NATIONAL LABORATORY
operated by
UNION CARBIDE CORPORATION
for the
U.S. ATOMIC ENERGY COMMISSION

Printed in USA. Price $4.00. Available from the
Office of Technical Services
Department of Commerce
Washington 25, D.C.

ORNL-2994
UC-41 — Health and Safety
TID-4500 (15th ed.)

Contract No. W-7405-eng-26

HEALTH PHYSICS DIVISION ANNUAL PROGRESS REPORT

For Period Ending July 31, 1960

K. Z. Morgan, Director

DATE ISSUED

OCT 24 1960

OAK RIDGE NATIONAL LABORATORY
Oak Ridge, Tennessee
operated by
UNION CARBIDE CORPORATION
for the
U.S. ATOMIC ENERGY COMMISSION

SUMMARY

1. RADIOACTIVE WASTE DISPOSAL

Low-Level Waste Water Treatment

Investigations of the distribution of radioactivity in the effluent from the process waste treatment plant showed that approximately 50% of the outgoing activity is associated with the suspended solids. Studies have been made of the effects of several coagulant aids on the removal of these suspended solids.

Disposal of ORNL Wastes

The study of open waste pits at ORNL was discontinued in 1959. Emphasis is now placed on studies of the disposal of intermediate-level waste in a newly designed covered pit (waste pit 5) and the development of soil-column disposal and disposal by fracturing.

Burial ground 4 was closed, and 5 was opened in 1959. Although radioactivity was found in wells, seeps, and streams in and around burial ground 4, the amount of activity contributed to White Oak Creek is so small that it is difficult to measure.

Evaluation of Consequences of Disposal to ORNL Environs

The more hazardous fission products are adsorbed by the dominantly clay soils of the ORNL area; this provides a safety factor in the case of accidental releases of radioactive cations. There are three shortcomings in the natural environment at ORNL: (1) the high rainfall results in leaching of adsorbed activity; (2) due to low soil permeability, surface runoff leads to erosion and sediment transport; and (3) the heterogeneity of ground-water movement patterns makes monitoring difficult.

Clinch River Studies

A comprehensive study of the Clinch River, downstream from White Oak Creek, has been started in cooperation with several state and Federal agencies. The purpose of the study is to obtain fundamental information

on the physical, chemical, and biological dynamics of a flowing, freshwater ecosystem which is receiving large volumes of low-level radioactive wastes.

Sorption and Retention by Minerals and Compounds

Cesium-sorptive capacity of several minerals was measured in simulated waste solutions and was found to vary with mineral structure, ion exchange capacity, and saturating cation.

For strontium removal from waste solution, apatite (rock phosphate) and variscite minerals were found to be potentially useful materials.

Soil-Column Studies

Several materials were investigated for sorption of cesium and strontium from solutions similar to the ORNL intermediate-level liquid wastes. Vermiculites with added PO_4^{---} were satisfactory for removal of cesium and strontium. Clinoptilolite and Florida pebble phosphate also appear promising for column application.

Disposal in Salt Formations

Theoretical studies and both field and laboratory experiments are under way to define and solve the problems involved in the storage of liquid and solid wastes in natural salt deposits. Temperatures obtained in the field experiments are in agreement with theoretical calculations. Radiolytic gas production is a more serious problem than chemical gas production with Purex-type wastes.

Disposal of Radioactive Waste by Hydraulic Fracturing

Tests are under way to determine the feasibility of injecting large volumes of radioactive waste into rock formations by hydraulic fracturing. A preliminary experiment, in which 26,000 gal of Cs^{137}-tagged cement was injected at a depth of 290 ft, resulted in the production of a nearly horizontal thin sheet of grout.

Related Cooperative Projects

A number of investigations have been made by and in cooperation with other groups, both governmental and private. Eight engineers and scientists from other countries have worked for varying lengths of time as members of the Radioactive Waste Disposal Section.

2. ECOLOGICAL RESEARCH

White Oak Lake Bed Studies

The biological community developing on the contaminated White Oak Lake bed illustrates the movement of Sr^{90} and Cs^{137} from soil to plants to animals. Little change in soil Sr^{90} from 1958 to 1959 suggests a decrease in former losses due to physical processes. In the upper soil, Cs^{137} and Co^{60} have remained almost the same (except for decay) since the lake was drained. Morphological features in two plant species (sedges) are affected more by the different site factors on the lake bed than by the differing dose rates. Rates of uptake of radionuclides by plants (smartweed) decrease relative to rates of plant growth throughout the growing season.

Only a minute fraction of the Sr^{90} and Cs^{137} taken up by plants is found in the insects at any one time, but laboratory studies of elimination rates led to estimates that about 3 to 5% of the radionuclides taken up by plants pass through the insects in the ecosystem.

Analyses of IBM data for over 4300 small-mammal captures from the lake bed and other study areas include estimations of population parameters for small mammals which are significant for new work on radiation effects. Radioassay studies of the small mammals show that concentrations of Cs^{137} in insect and mammal herbivores per unit area are similar, but the concentration of Sr^{90} is three times as high in mammals as in insects.

Forest Studies

Theoretical studies included the use of analog computers to simulate the cycle of movement of chemical elements and isotopes through ecological systems. In 1959–60, studies emphasizing methodology were illustrated by the flow of C and C^{14} in very simple model systems. Direct extensions

should help predict how rapidly other isotopes might become distributed in more complex systems.

Tracer experiments on translocation in dogwood trees showed how Sr^{85} lags behind Ca^{45}, while both lag far behind K^{42}. Like K^{42}, Cs^{134} in white oaks moved rapidly from trunks into foliage, then quickly began leaching out of intact or plucked leaves, and started reappearing in other plants within a few weeks — a rapid ecological cycle. Slower movements of Ru^{106}, Co^{60}, and Sr^{85}, which were introduced in tagged tree litter on top of soil, were approximately proportional to the rate of litter weight loss. New work on soil arthropods, bacteria, and fungi is helping to explain large differences in the rate of litter breakdown which were measured in conifer and deciduous forests of Oak Ridge and the Great Smoky Mountains. These studies, and others on biomass and productivity of pine forests, included extensive chemical and gamma-spectrometric analyses. The latter provided new information on several local sources of radioactive contamination. A vegetation and soil survey is helping to plan future experiments and land use in the Oak Ridge AEC-Controlled Area.

Clinch River Studies

The first year of Clinch River investigations determined which species of bottom organisms were present and their relative abundance. Tubificid worms are being used as an experimental organism for uptake and excretion studies with radioisotopes, and their role in the turnover and transport of river bottom sediments is being evaluated. Chronic, low-level radiation effects on bottom organism populations are being studied by means of chromosome analyses of the salivary glands of Chironomus tentans larvae. Crayfish, Cambarus longulus longerostris Ort., have been used in the study of the uptake and excretion of Sr^{85}, and similar investigations are now under way with Co^{60}.

3. RADIATION PHYSICS AND DOSIMETRY

Theoretical Physics of Dosimetry

Further estimates of the stopping power of heavy ions in tissue have been made. An investigation has been made of instabilities resulting from the passage of an electric beam through a dielectric medium.

A code for the computation of the space-independent slowing-down spectrum of low-energy electrons in an ideal Fermi-Dirac electron gas is nearly complete. A method is proposed for evaluating the energy dependence of the cross section for electron attachment from data on the dependence of this process on applied electric field in swarm experiments with noble gases. Calculations of neutron and gamma leakage from some bare critical assemblies which are of interest in the dosimetry of critical accidents have been made. A Monte Carlo study of the penetration of gamma rays in spherical inhomogeneous media has been carried out. Codes have been written for the evaluation of the energy response of neutron dosimeters.

Experimental Physics of Dosimetry

Studies of electron attachment in a mixture of water vapor and argon will lead to the cross section for the dissociation of the water molecule into H^- and OH. Similar experiments in water vapor and carbon dioxide indicate that no dissociation occurs, and that the cross section for direct attachment is small. Measurements of the diffusion of electrons in H_2, N_2, CH_4, and C_2H_4 enabled calculations of the ratios of mean drift velocities to the diffusion coefficients and the ratios of mean agitation energies of the electrons to thermal agitation energies of the gas molecules. The electronic mean free paths, average energy losses per collision, and collision cross sections were calculated from these data and the assumption of a Druyvesteyn electron-velocity distribution. Measurements of the pulse-height distribution in a proportional counter from single electrons reveal agreement with theory. Calorimetric measurements of electron stopping power in gold at low energies by a null method yield results 20% or more above that predicted by the Bethe theory. A redesign of the calorimeter to reduce scattering effects and improve accuracy has been carried out and should enable determination of whether or not the

above disagreement is real. A preliminary search for light of 837-A wavelength from electron-irradiated aluminum has been made by using an accelerator as a source of electrons and a Seya-Namioka vacuum ultraviolet spectrograph. No sharp line has been found as yet, although the theories of Ferrell and Ritchie predict that the conduction-electron plasma should radiate at this wavelength as it decays to the ground state. To enable further studies of the electron slowing-down spectra in irradiated media, the calculation of the transmission and resolution of the spherical condenser spectrometer for large sources were programmed for the IBM 704, and the favorable results have led to plans for early construction of such an instrument. The strong dependence of the light output of anthracene on the rate of energy loss from an energetic particle traversing this material has suggested that anthracene can be employed in an LET meter. Layers as thin as 0.19 mg/cm^2 have been vacuum-evaporated on a photomultiplier and have produced usable pulse-height distribution when irradiated with alpha particles.

Dosimetry Methods

A G-M tube dosimeter has been developed which measures gamma-ray dose rate from 0.1 mr/hr to 150 r/hr. It is energy independent above 150 kev and is very insensitive to both fast and thermal neutrons. Neutron-flux spectra in the threshold-detector units may be determined by counting the fission fragments from thin layers of U^{235}, Np^{237}, and U^{238} with silicon-gold surface barrier diodes. The shielding and scattering effects of a concrete wall, the human body, and the threshold-detector units have been determined, using threshold-detection methods. A dosimeter belt containing glass-rod dosimeters and several sulfur, gold, and cadmium-shielded gold samples has been developed which serves to indicate the orientation of an individual during exposure. A source field is being prepared at the Nevada Test Site for use in calibration and intercomparison of instrumentation in aircraft for radiation surveys used by several government agencies and contractors.

Dosimetry Applications

Studies to determine the shielding afforded by residences against radiation fallout have been continued. The activation of blood sodium by neutrons has been evaluated for dosimetric purposes, and monitoring systems for nuclear accidents have been improved. A comprehensive experiment was conducted at the Boris Kidrič Institute in Vinča, Yugoslavia, to determine the radiation exposures of the six persons exposed during an accident in 1958.

Physics of Tissue Damage

Radiation-induced thermoluminescence has been studied for 4 proteins and 23 L-amino acid preparations. The powdered crystalline samples were irradiated at liquid-nitrogen temperature and subsequently warmed to room temperature. Glow curves — plots of intensity of light emission vs temperature — are presented for these preparations. From considerations of the intensities of peaks in the glow curves and the temperatures at which they occur, four conclusions are drawn, as shown below.

1. The glow curves from proteins are not the sum of the glow curves of the constituent amino acids (properly weighted for per cent content) in their isolated crystalline form.

2. Chemical composition exerts the greatest influence on the thermoluminescence from amino acids.

3. The crystalline system to which an amino acid belongs seems to play only a minor or negligible role in determining the nature of the glow curves.

4. Small changes in the level of purity may exert a relatively strong influence on the thermoluminescence from some amino acids.

4. INTERNAL DOSIMETRY

Estimation of Internal Dose

The dose from a short-term exposure, or from a single intake of radioactive material, has been estimated and compared with the dose from continuous exposure to the same material. It is found that if a continuous exposure level is set so that after 50 years of ingestion at

this level the critical organ is exposed at a dose rate of R rems per quarter, then a single intake equal in amount to that ingested during a quarter of continuous exposure will deliver a total dose of R rems to the same organ during the 50 years immediately following the single ingestion.

As an aid in the analysis of distribution and elimination data, an iterative curve-fitting procedure, the fractionator method, has been derived. The procedure yields tenable estimates of the function parameters and converges in all cases tried, for those forms which have been studied — a sum of exponentials and a polynominal.

Data on the variability of the normal distribution of 48 isotopes in humans is being studied. This data was obtained by analysis of normal human tissue by emission spectrometry, neutron activation, and dry flame photometry.

Applied Radiobiology

Animal inhalation study programs, mentioned in previous progress reports, have been completed. In a study of chronic inhalation of U_3O_8 in beagles, it was seen that the concentration of uranium in the lung tends to equilibrate within about six to nine months. The urinary uranium excretion rate may be correlated with the lung burden — the ratio of the equilibrated value of lung burden to the excretion rate is approximately 520.

An expolding-wire aerosol generator for the production of U_3O_8 aerosols has been constructed and is undergoing tests. Preliminary results show that typical fume particles 0.02 μ in diameter are produced and that the yield is about (85 ± 4)% for 10-mg uranium wires.

Measurements of the absorption of uranium from the gastrointestinal tract into the bloodstream are being made in mongrel dogs. Seven dogs given single oral doses of UO_2F_2 absorbed 1.55% of the administered dose (standard deviation 0.21%), and their patterns of urinary uranium excretion rate do not appear to be significantly different from that seen in a study of intravenous injection of $UO_2(NO_3)_2 \cdot 6H_2O$ in dogs.

The study of the deposition of uranium in the rat kidney following intravenous injection of soluble uranium compounds, previously reported, has been extended to a new dose level (0.001 μg of uranium per gram of

body weight) and also extended in time to six months. There appears to be a different retention pattern for the various dose levels, the high doses being characterized by longer retention times in the kidney.

A method, previously developed, of determining the nonuniform distribution factor, N, of uranium in the rat kidney by track counting in autoradiograms has been carried forward and compared with the alpha activity in corresponding ashed material. Ten kidneys were counted. The greatest amount of activity was observed in the cortex of eight of these for which the average N is 1.33 and the range is 1.1 to 1.4. The ninth and tenth kidneys showed more activity in the medulla and gave an N_m of 1.5. From the results of six ashed kidneys, the average N was found to be 1.3 with a range of 1.06 to 1.48.

5. EDUCATION, TRAINING, AND CONSULTATION

The need for trained health physicists, both here and abroad, continues. In addition to the AEC Fellows, several foreign students and Air Force officers completed the Fellowship Program at Vanderbilt University and Oak Ridge. A combined lecture and laboratory course covering the principal aspects of health physics has become an integral part of the international ORSORT program. To provide training in health physics for AEC personnel and personnel from state departments of health, an eight-week course in health physics has been established.

It is anticipated that in the future more training in health physics will be provided for ORNL personnel and for foreigh students on an individual basis.

CONTENTS

1. RADIOACTIVE WASTE DISPOSAL

LOW LEVEL WASTE WATER TREATMENT

K. E. Cowser T. Tamura
H. J. Wyrick K. F. Eschle[2]
D. A. Gardiner[1] T. Subbaratnam[3]

There is an increasing demand for information on the treatment and disposal of large volumes of waste containing low levels of radioactivity. The process waste treatment plant at ORNL,[4,5] in addition to serving the needs of the Laboratory for effluent control, is an excellent facility with which to demonstrate the efficiency and economics of various treatment methods in a single-stage system.

This plant employs a $CaCO_3$ precipitation for removal of Sr^{90} and the addition of clay for removal of Cs^{137} from ORNL process waste. After a standard procedure for determining lime-soda ash dosages was established (March 1958), strontium removals averaged 84% and were as high as 94% for periods of a week. The removal of total rare earths averaged 86%, and, with identifiable quantities of Pm^{147} recently released to the system, the removal of this fission product was found to average 94%. Small amounts of plutonium and curium were also detected in the waste; the average removal of gross alpha activity was about 90%. With the continuous addition of clay, beginning in October 1958, cobalt removal averaged 78% and ruthenium removal, 76%. The removal of cesium averaged 80, 84, and 86%, with clay doses of 100, 150, and 200 ppm, respectively. The removal of gross beta activity averaged 88%.

The combination of treatment variables, that is, lime, soda ash, returned sludge, calcium chloride, and clay, and the use of coagulant aids to obtain the optimum removal of Sr^{90} and Cs^{137} were investigated. Also,

---

[1]Mathematics Panel, ORNL.

[2]Alien guest from Reactor A. G., Würenlingen (AG), Switzerland.

[3]Alien guest from Atomic Energy Establishment, Trombay, Bombay, India.

[4]K. E. Cowser and R. J. Morton, Proc. Am. Soc. Civil Engrs. 85, SA 3, 55–76 (1959).

[5]M. C. Culbreath, Proc. Am. Soc. Civil Engrs. 85, SA 3, 41–53 (1959).

additional work was directed toward an understanding of the reactions of specific scavenging processes.

An Experimental Procedure for Optimizing Treatment Efficiency

In a previous report,[6] three phases of a four-phase experimental procedure for optimizing the treatment of low-level waste water were described. Since then, the fourth phase has been designed and the experimental program completed.[7] Removal of 96% of the Sr^{90} and 95% of the Cs^{137} contained in ORNL process wastes has been demonstrated in laboratory experiments.

Figures 1.1 and 1.2 summarize the completed program. Figure 1.1 illustrates the results in terms of the percentage of Sr^{90} removed, and

[6]E. G. Struxness et al., H-P Ann. Prog. Rep. July 31, 1959, ORNL-2806, p 3–6.

[7]D. A. Gardiner and K. E. Cowser, "Optimization of Radionuclide Removal from Low-Level Process Wastes by the Use of Response Surface Methods," submitted for publication in Health Phys.

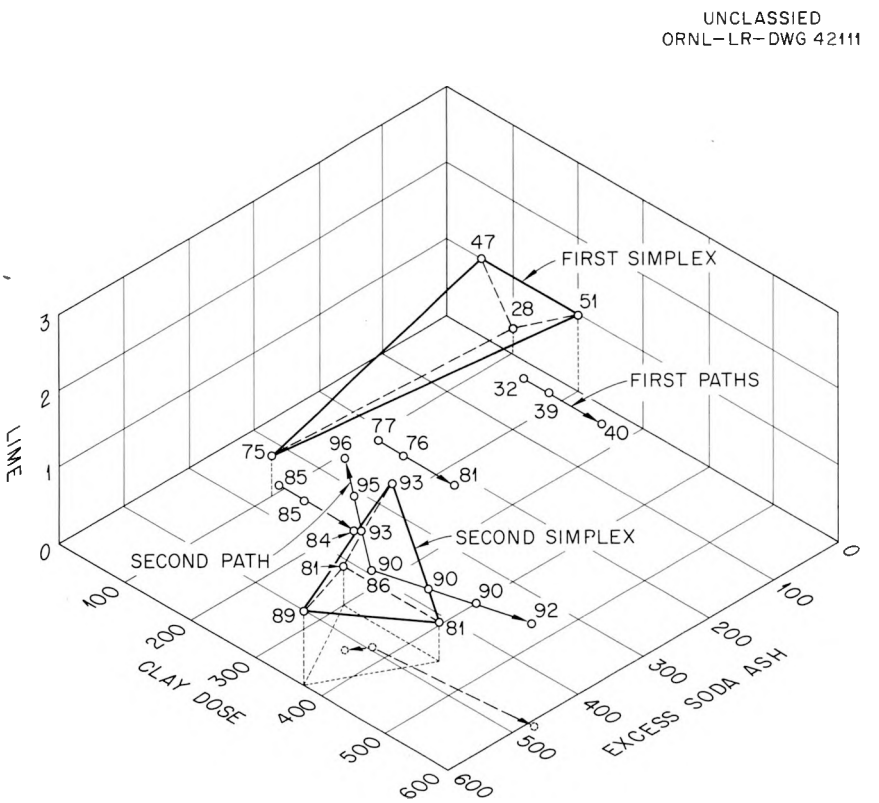

Fig. 1.1. Experimental Points Showing the Per Cent of Strontium Removal.

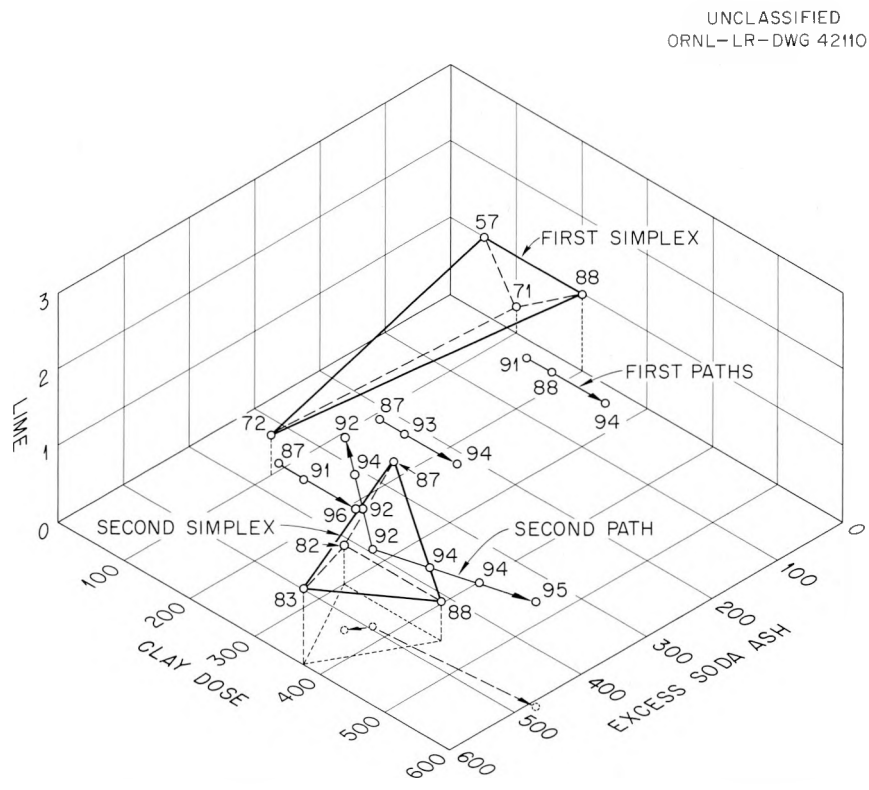

Fig. 1.2. Experimental Points Showing the Per Cent of Cesium Removal.

Fig. 1.2 the results in terms of the percentage of Cs^{137} removed. Otherwise the figures are essentially the same. To make these drawings, the variable particle size of the clay dose was ignored.

The tetrahedron labeled "First Simplex" represents the first phase of the study from which a composite path of steepest ascent (i.e., the path toward higher radionuclide removals) was calculated. This composite path, comprising the second phase of the program, is illustrated by the three arrows labeled "First Paths." The circles on these arrows show the positions of nine trials along the composite path of steepest ascent.

The third phase of the study was an experiment to re-estimate the paths of steepest ascent. This is depicted by the tetrahedron labeled "Second Simplex" in the figures. From this experiment a path of steepest ascent was calculated for Sr^{90} removal, and a separate path of steepest ascent for Cs^{137} removal was also calculated. The path for Sr^{90} removal is labeled "Second Path" in Fig. 1.1, and the path for Cs^{137} removal is

labeled "Second Path" in Fig. 1.2. The fourth phase of the program consisted of trials illustrated by circles on these second paths.

In Fig. 1.1 the arrow points to a removal of Sr^{90} of 96%. This trial consisted of treating the influent with 357 ppm of Grundite clay of 200 to 230 mesh, 520.5 ppm of excess soda ash, and 2.5 times the stoichiometric requirement for lime. In the second figure, the second path points to a removal of 95% of the Cs^{137}. This trial involved treating the influent with 605 ppm of Grundite clay of 200 to 230 mesh, 474 ppm of excess soda ash, and 1.35 times the stoichiometric requirement for lime.

An interesting feature of the study is that at high levels excess soda ash has a detrimental effect on the removal of Cs^{137}. This is seen by the arrow labeled "Second Path" in Fig. 1.2. The direction of this arrow is definitely toward lower levels of excess soda ash.

It is planned to use these data to increase the efficiency of the waste-water-treatment plant. A treatment-plant experiment is being designed in which combinations of the treatment variables, at levels in the vicinity of the greatest Sr^{90} removal found in the laboratory, will be tried.

Use of Coagulant Aids in Lime-Soda Treatment[8]

Investigations of the distribution of radioactivity in the plant effluent showed that approximately 50% of the outgoing activity was associated with suspended solids. If the amount of suspended solids in the effluent could be reduced, it would be possible to increase the efficiency of the treatment plant.

The use of coagulant aids is one approach to the removal of suspended matter in the effluent. The slight increase in the cost of treatment might be justified on the basis of increased efficiency. Accordingly, suitable coagulant aids were selected, and the conditions under which the aids would be most effective were determined. The study was limited to polyelectrolytes only.

---

[8]T. Subbaratnam, K. E. Cowser, and E. G. Struxness, Studies on the Use of Coagulant Aids in the Lime-Soda Treatment of Surge-Volume, Low-Level Radioactive Liquid Waste, ORNL CF-60-7-17 (July 1960).

Several coagulant aids were tested in the laboratory by using conventional jar-test techniques, under varying conditions of coagulant concentration, mode and time of addition, coagulation time, speed sequence, temperature, and the presence of complexing agents. Based on the results of the jar tests, a six-week plant trial with Hagan Aids Nos. 50 and 18 was instituted.

The study of coagulant aids was divided into two main phases, namely: (1) laboratory tests to compare and select the most suitable aid and to evaluate the best possible conditions under which it will work, and (2) plant trials to obtain data on plant performance of the coagulant aid selected.

Laboratory Tests

Samples of a number of coagulant aids were obtained and tested by the conventional jar-test technique.[9] Table 1.1 lists these products by their trade names and manufacturers. Although the chemical composition of the

[9] J. M. Cohen et al., J. Am. Water Works Assoc. 50, 463 (1958).

Table 1.1. Coagulant Aids Tested by the Conventional Jar-Test Technique

Trade Name	Form
Hagan 7[a]	Gray granules
Hagan 11[a]	Gray granules
Hagan 18[a]	Gray granules
Hagan 50[a]	White powder
Hagan X 323[a,b]	
Separan 2610[c]	White powder
Aerofloc 552[d]	Dull yellow powder
Aerofloc 3000[d]	White powder

[a] Hagan Chemicals and Controls, Inc.

[b] Hagan X 323 was supplied as a solution; physical form unknown.

[c] Dow Chemical Co.

[d] American Cyanamid Co.

coagulant aids was not available, three are probably polyanionic electrolytes, possibly polyacylamide. Hagan 7, 11, and 18 are mixtures of a polyampholyte and bentonite clay in varying proportions.[10] The chemical nature of the other aids is unknown.

Since no change in the treatment procedure was contemplated, it was necessary to duplicate plant conditions in the jar tests. Accordingly, the following time and speed sequences were used in the tests: (1) 85-sec flash mixing at 288 rpm, and (2) 21-min coagulation at 81 rpm. These time and speed sequences are typical of those in the flash mixer and three coagulation basins, respectively. At 81 rpm, the stirrer used gave a paddle-tip velocity of 64 fpm. Turbidity measurements were made with a Klett-Summerson photoelectric colorimeter.

A continuous 24-hr sample of plant influent was used in the tests. The concentration of aids in stock solutions ranged from 0.25 to 2.0 g/liter. These concentrations were decided upon after consideration of the dosages suggested by the manufacturers.

Hagan 50, Separan 2610, and Aerofloc 3000 worked better than the other aids tested. Combinations of these aids with Hagan 18 produced even better results. Thus, these combinations were used for detailed study.

Figure 1.3 gives the settling curves obtained for the combination of Hagan 50 and 18 and for Separan 2610. It is seen that an increase in the dosage of Separan 2610 from 2.0 to 3.0 ppm produced very little change in the settling characteristics of the floc and in the final turbidity of the supernatant solution. The same effect is also seen for the combination of Hagan 50 and 18 in spite of the fact that the floc size for 0.75 ppm of Hagan 50 and 5.0 ppm of Hagan 18 was much larger than that for 0.5 ppm of Hagan 50 and 5.0 ppm of Hagan 18. The curves show a wide range of particle-size distribution for coagulation without any aid, and a floc of more or less uniform size with good settling characteristics for coagulation in the presence of an aid. These tests were done at 25°C.

Figure 1.4 shows the settling curves for 0.5 ppm of Hagan 50 and 5.0 ppm of Hagan 18, 2.0 ppm of Separan 2610, and 2.0 ppm of Aerofloc 3000. The performances of Aerofloc and of Separan 2610 were close to each other,

[10] Hagan Chemicals and Controls, Inc., Chemical Products Development Department, Bulletins 1.1PD56 and 6PD57.

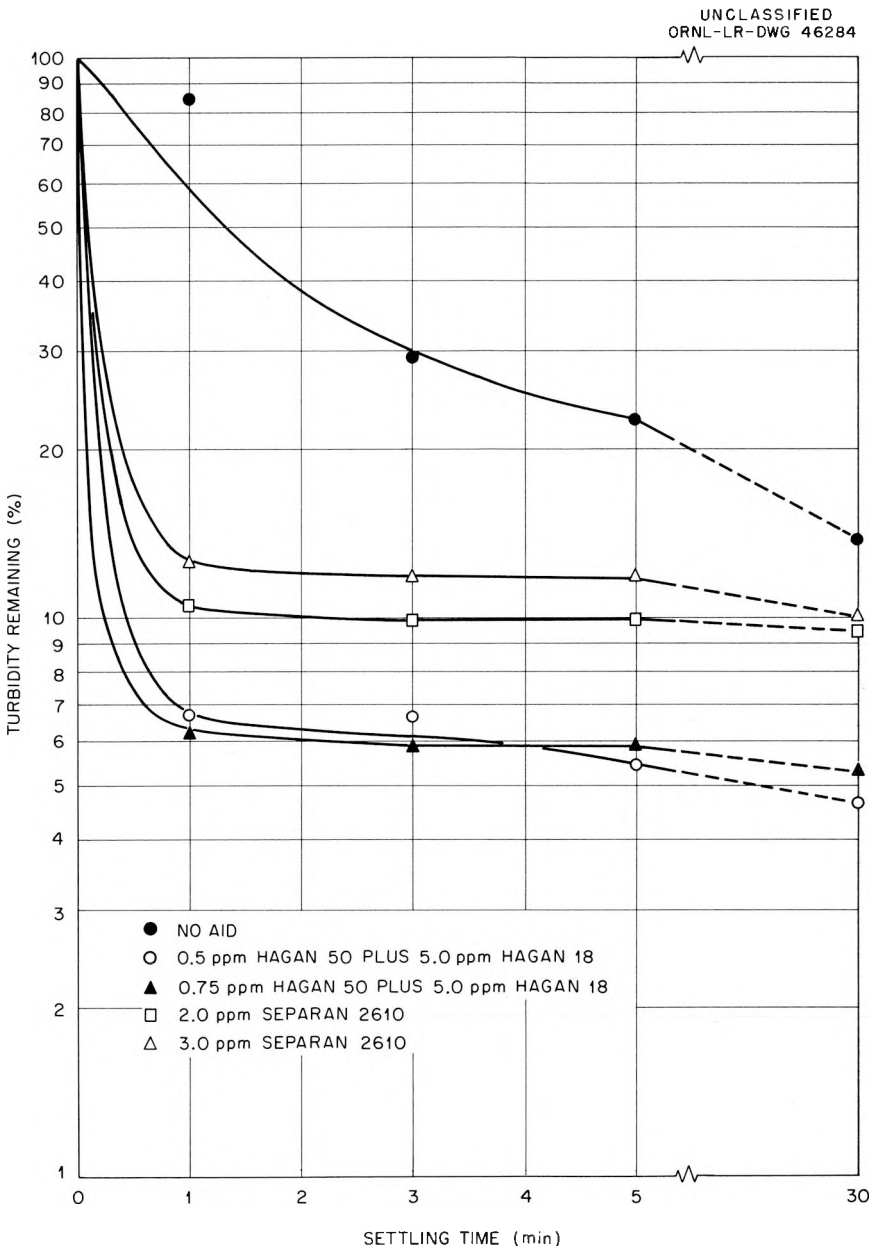

Fig. 1.3. Settling Curves for Hagan 50–Hagan 18 and for Separan 2610.

with the difference that Aerofloc produced a wider range of particle sizes, yielding the sloping curve. Here again, the combination of Hagan 50 and 18 gave somewhat better results than the others.

A slower mix-and-coagulation step gave somewhat higher turbidities in the supernatant than did the time and speed sequence previously mentioned. At low temperatures, 40°F, the aids produced appreciable coagulation. There seemed to be little or no effect on coagulation whether the

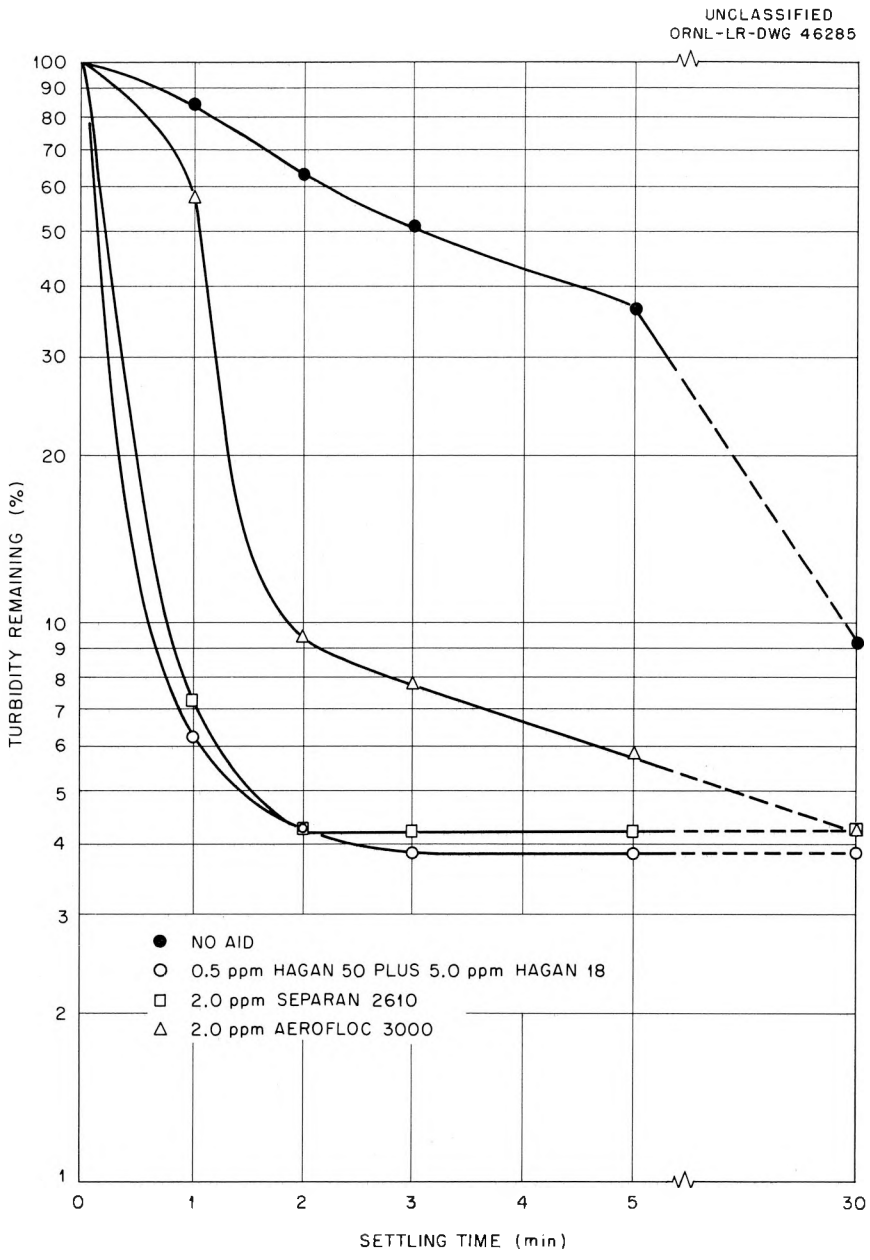

Fig. 1.4. Settling Curves for Hagan 50—Hagan 18, Separan 2610, and Aerofloc 3000.

aids are added before or after chemical treatment; however, additional tests will be required to obtain conclusive results. Complexing agents such as cleansers and compounds used in decontamination operations interfered with coagulation.

The jar tests showed that the use of coagulant aids reduces the turbidity of the treated waste solution and that the combination of Hagan 50 and 18 produced uniformly good results under most conditions encountered.

Since this combination seemed well suited to the conditions existing in the treatment plant, a six-week plant trial was planned for further testing.

Plant Trials

The plant trials showed that it would be possible to obtain, under normal conditions, a good-sized floc of fairly quick settling characteristics by the use of Hagan 50 and 18. There were, however, several features which differentiated the plant trials from the laboratory jar tests. Variation in temperature had a more drastic effect on the size of the floc. The fact that complexing agents were in the system during the plant trials had to be considered in judging the performance of the coagulant aids. Choice of the proper feed concentration for the aid solutions, point and mode of addition of the aids, and careful control of agitation were contributing factors to floc formation. Also, some mechanical modifications were necessary to get the best possible results.

Solutions of Hagan 50 and 18 were made and fed separately into the flash mixer. The following concentrations were used at the start of the plant trials:

Aid No.	Suggested Dosage (ppm)	Dosage Used (ppm)	Feed Solution Concentration (%)	Maximum Suggested Concentration (%)
Hagan 50	0.25 to 1.0	0.5	0.5	0.5 to 2.0
Hagan 18	3.0 to 15	5.0	3.0	3.0

The containers for Hagan 50 were filled once each day, and for Hagan 18 twice a day. After the start of the experiment it was found that a 3.0% solution of Hagan 18 was too viscous. Thereafter, the concentration was reduced to 2.0%, with three fillings per day. To prepare the solutions, the drums were partially filled with water, and the aids were added with the agitators "On." Shortly thereafter the remaining volume of water was added. Hagan 50 dissolved completely in about 1 hr, and no further agitation was required; Hagan 18 required constant agitation.

In the beginning, the aids were fed independently into the flash mixer. After some time it was evident that this point of introduction

was not the most effective, and so Hagan 50 was split into two portions, one going to the flash mixer and the other to the third coagulator basin. Hagan 18 was fed into the flash mixer only.

The results were apparent 48 hr after the initial feeding. There was a marked floc production in the coagulation basins. At the outset the floc size did not improve in the second and third basins but appeared to break up. To prevent this, the speed of the agitators was progressively reduced to 50 rpm in the second basin and to 30 rpm in the third. This amounted to paddle-tip velocities of 393 and 245 fpm, respectively. Also, the floc particles that came to the surface in the settling basin were much smaller than those in the third coagulation basin. To rectify this, the Transite baffles were interchanged with wooden baffles having 7-in. slots instead of 6-in. holes. This reduced the velocity of flow through the baffles from 10.7 fpm to 4.5 fpm.

Conditions in the plant were not uniform and normal during the trials. During very cold days, there was a marked decrease in the floc size and an increase in the amount of carry-over of solids in the effluent. Increasing the dosage of Hagan 50 from 0.5 ppm to 0.75 ppm and splitting the aid solution by feeding part of it into the flash mixer and the rest into the third basin helped to overcome the effect of temperature somewhat.

During the plant trials it was noted that waste solutions containing Turco, a proprietary product used in decontamination operations elsewhere in the Laboratory, were let into the equalization basin and finally into the treatment plant. Analysis of the influent for phosphates showed amounts ranging from 10 to 25 ppm. During continuous operation of the plant it was rather difficult to estimate exactly when these phosphates were coming into the plant. The poor performance of the aids is believed to be due to the influx of Turco into the plant, and this would be expected, based on the results observed in the jar tests.

Mechanical modifications of the plant produced some undesirable results. Slowing the agitation in the coagulators progressively, so that the velocity through the wooden baffles separating the third basin and the settling basin was reduced, resulted in a considerable sludge build-up in the third basin. Since the settled sludge was closely packed,

washing the basin with a water jet provided no improvement. The agitation speed was increased for about 30 min to stir up the sludge once again, and this destroyed the floc already formed. Also, the horizontal slots in the wooden baffles short-circuited the sludge back into the third basin. Circular holes, larger than those in use previously, might help to overcome this effect.

There was a significant reduction in the turbidity of the effluent as a result of coagulation with an aid. That the aids do produce a good floc of fairly uniform size and quick settling characteristics, even at low temperatures, was very evident. Analytical data on several weekly samples confirmed the beneficial effects of the aid. However, results were inconsistent, probably due to the uncontrollable factors described previously. A much longer observation period, including work with equipment to study the particle-size distribution, is necessary to evaluate properly the effect of coagulant aids on the removal of radioactivity from low-level liquid wastes.

Aluminum Phosphate Coagulation

The aim of this study was to evaluate the technical applicability of aluminum phosphate coagulation to the treatment of low-level wastes. First, it was necessary to have information concerning its effectiveness in the removal of radioactivity and, second, its settling behavior.

The study, using conventional jar-test methods, was performed by measuring the removal of radioactive Sr^{85} from distilled water by an aluminum phosphate floc. The floc was formed under various conditions of mixing aluminum nitrate and trisodium phosphate. Measurements of turbidity and of the mass of floc gave information about the settling behavior.

The results of this study are being prepared for publication as an ORNL report[11] and only the conclusions are summarized in this section.

---

[11] K. Eschle, A Study of Aluminum-Phosphate Coagulation with Special Consideration of Strontium Removal from Water, ORNL report (to be published).

With respect to the removal of Sr^{85} from distilled water, the following results were obtained:

1. The most important factor which influences the behavior of the aluminum phosphate floc is pH, as has been found for other water-treatment methods. This refers to a final pH after adjustment with either NaOH or HNO_3.

2. To simulate waste-treatment-plant conditions, samples were taken after 2 hr of settling. In addition, the supernate was filtered and centrifuged. In general, the results of filtration and centrifugation were the same; however, the results of centrifugation were more reproducible and, therefore, more reliable.

3. The greatest strontium removal was found at pH 6.5 to 7 in the samples taken after 2 hr of settling. At pH higher than 7 there was a stable sol which did not settle at all.

4. A steadily increasing strontium removal after filtration or centrifugation was observed until a pH of 10 was reached. Increasing strontium removal at the higher pH can be explained by assuming an increase in the specific sorption capacity of the floc due to changes in its chemical composition. The analyses of both the remaining liquid and the floc itself showed an increasing consumption of water molecules over the phosphate molecules. A floc formed by aluminum nitrate and sodium hydroxide gave an optimum strontium removal at pH 9.

5. The turbidity and the total weight (mass) of the floc reached maximum values at pH 6.5 to 7. To obtain efficient removal, it is essential to have complete and rapid settling. The settling rate is indicated by the clarification, which is defined as the difference between the initial turbidity and the turbidity after 30 min of settling, assuming the initial turbidity to be 100%. Thus it is observed that with aluminum phosphate coagulation there is a stable nonsettleable floc at low and at high pH. In a jar-test experiment a good water-treatment method should give practically 100% clarification after 30 min of settling. Floc produced with a PO_4:Al ratio of 1:5 settled absolutely clearly and rapidly, but did not give the excellent efficiency of strontium removal as did the floc produced with the inverse ratio (PO_4:Al = 5:1).

6. With respect to the concentration of the chemicals, increasing the concentration increased the removal of strontium due to the greater absorbing surface. Efficiencies of 95 to 98% were found with 0.05 N solutions of both chemicals. Additional increases above this concentration would not have produced further increases of efficiency.

7. Regarding the ratio of chemicals, a higher phosphate such as an $Al:PO_4$ ratio of 1:5 content produces better removal; a lower concentration of $Al(NO_3)_3$ may be used to produce the same efficiency as found for a PO_4:Al ratio of 1:1.

The second part of the investigation dealt with improvement of the settling behavior. The following observations were made:

1. A high-potential field up to 30 kv applied to the beakers did not influence the settling rate. Thus, it was deduced that the floc was neutral. No trials to charge the floc were undertaken.

2. The use of large, negatively charged molecules such as salicylic acid, which were supposed to replace some of the phosphate anions, did not show any significant effect.

3. The use of Hagan aids 18 and/or 50 did not give beneficial results, as were obtained in studies of the lime-soda softening process. On the contrary, the settling behavior was worse.

4. A high salt concentration, such as 20 g of NaCl per liter, produced complete settling due to a simple salting-out effect.

In a third part of the investigation, aluminum phosphate coagulation was compared with calcium phosphate coagulation; the applicability of both to a real waste was checked:

1. The calcium phosphate floc settles clearly and rapidly at any pH.

2. Calcium phosphate coagulation gives the best strontium removal at a pH of 10 or greater, as was found by Lauderdale.[12]

3. Aluminum phosphate and calcium phosphate, when applied to low-level waste as encountered in the ORNL waste-treatment plant, have a remarkably lower efficiency of removal than for the removal of strontium from distilled water, as shown in Fig. 1.5. However, aluminum phosphate

---

[12]R. A. Lauderdale, Ind. Eng. Chem. 43, 1538 (1951).

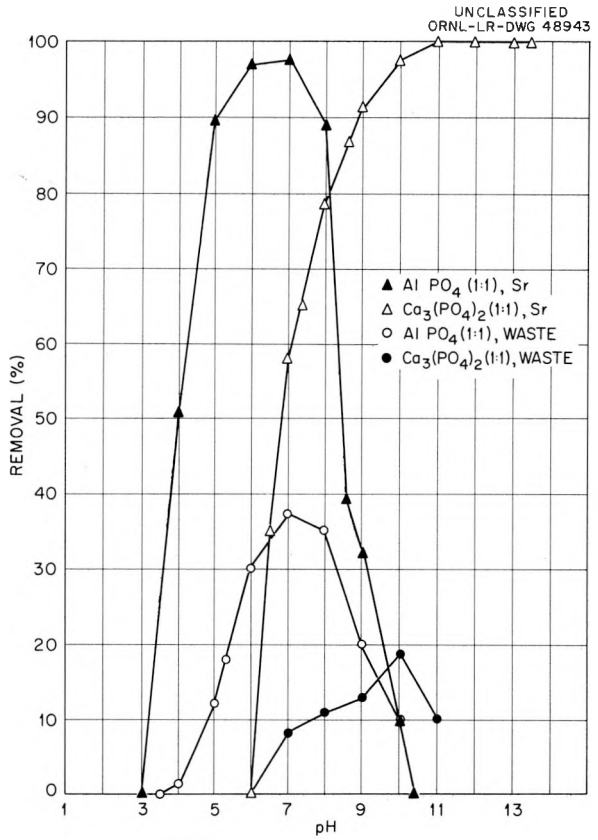

Fig. 1.5. Efficiency of Aluminum and Calcium Phosphates on the Removal of Strontium and Low-Level Activity from ORNL Waste.

was the better of the two treatments. In each case, the optimum pH was shown to be near 7 and 10, respectively.

4. This poor removal efficiency with a real waste was thought to be due to the presence of considerable amounts of cesium. An investigation of the removal of different ions, namely, Sr^{85}, Cs^{137}, Ce^{144}, Zr^{95}-Nb^{95}, Ru^{106}, and Co^{60}, showed that cesium was sorbed only up to 5% by calcium phosphate floc and up to 35% by aluminum phosphate floc, while all the other ions were removed with an efficiency of 90% or more.

5. Aluminum phosphate coagulation may be considered to be as valuable and applicable to waste treatment as calcium phosphate if specific conditions prevail, for example, favorable pH or initial presence of aluminum in the waste, or a low calcium content or intermediate pH.

DISPOSAL OF ORNL WASTES

K. E. Cowser W. de Laguna
D. G. Jacobs T. F. Lomenick
T. Tamura R. L. Bradshaw
H. J. Wyrick R. M. Richardson[13]

Waste Pits 2, 3, and 4

The detailed study of ORNL waste pits 2, 3, and 4, via well sampling, well logging, and the budgeting of liquids, bulk chemicals, and fission products in the pits and in the seeps below them, discussed at some length in previous progress reports,[14,15] was discontinued during the period of this report, and a final report is now in preparation.[16] Meanwhile, their use for the disposal of intermediate-level liquid wastes has been limited, waste pit 4 having been taken out of service, filled and covered, and routine long-range monitoring procedures have been initiated.

A number of factors contributed to the cessation of this study, and it may be of some interest to enumerate the more important ones here. First, although these pits were serving a useful purpose and operating with apparent safety, pit disposal of intermediate-level liquid wastes was not looked upon as a satisfactory method of ground disposal in the long-range view.[17] Consequently, from a research-and-development point of view, continuing the study was unjustified. Second, while a reasonably accurate inventory of radioactive fission products and bulk chemicals released to the pits was possible, the sampling and radiologging of over 50 wells in the pit area did not give sufficiently accurate information on the quality and extent of fission product movement underground to predict,

---

[13]U.S. Geological Survey.

[14]E. G. Struxness et al., H-P Ann. Prog. Rep. July 31, 1958, ORNL-2590, p 6–26.

[15]E. G. Struxness et al., H-P Ann. Prog. Rep. July 31, 1959, ORNL-2806, p 7–13.

[16]K. E. Cowser, W. de Laguna, and F. L. Parker, Soil Disposal of Radioactive Liquid Wastes at ORNL, ORNL report (to be published).

[17]The Disposal of Radioactive Wastes on Land, Report of the Committee on Waste Disposal of the Division of Earth Sciences, National Academy of Sciences–National Research Council, Publication 519 (September 1957).

with the degree of safety required, when the disposal operation should cease. Relying on such information involved considerable risk. The greatest handicap was the lack of detailed information needed to describe the rate and direction of liquid movement through the weathered shale. Finally, it was concluded that soil-column disposal or disposal by hydro-fracturing were attractive possibilities for the disposal of ORNL intermediate-level wastes which should be developed as alternatives to pit disposal.[18]

It is unfortunate that a series of incidents, occurring shortly after the study was concluded, led to circumstances which caused the pits to be "overloaded." Thus, to maintain continuity with waste pit operations previously reported, it is of interest to update the account of the waste pit operation during this period.

From June 1952 through December 1959, 1.53×10^7 gal of waste, containing about 432,000 curies of beta activity, were pumped to the pits. The quantity of specific radionuclides released is summarized in Table 1.2. As shown, there was a significant increase in the quantity released during 1959. Of special note is the approximately 20,000 curies of Ru^{103}, 197,000 curies of Ru^{106}, and 25,000 curies of Sr^{90}. The increase was attributed to the experimental processing of short-time-cooled reactor fuel in the Hot Pilot Plant.[19]

As a result of the increased release to the pits, the amount of Ru^{106} which seeped to the bed of White Oak Lake in 1959 was estimated to be 1300 curies. This is to be compared with the estimated 160 curies of Ru^{106} released in 1958. The concentration of Ru^{106} in several batches of waste pumped to the pits in September 1959 was about 90 $\mu c/ml$, or 3.6 times greater than the calculated upper limit of discharge over extended periods of time without exceeding the MPC_w to the Clinch River.[20] Subsequent discharge of Ru^{106} to the pits was sharply curtailed, and, to reduce the amount of ruthenium leaving the pit area, seepage from the east side of

---

[18]E. G. Struxness et al., "Waste Disposal Research and Development in the U.S.A.," Proceedings of the International Scientific Conference on the Disposal of Radioactive Wastes, Monaco (1960).

[19]F. N. Browder, Description of ORNL Liquid Waste System, Hazard Evaluation – Vol. 3, ORNL CF-60-5-28, p 18 (May 20, 1960).

[20]K. E. Cowser, Potential Hazard of Ruthenium in the ORNL Waste-Pit System, ORNL CF-60-3-93 (Mar. 11, 1960).

Table 1.2. Inventory of Waste-Pit System

	Volume (gal)	Curies										
		Ru^{103}[a]	Ru^{106}	Cs^{134}[a]	Cs^{137}	Zr[a]	Nb[a]	Sr^{89}	Sr^{90}	TRE[b]	Year Total	Gross Beta[c]
	$\times 10^3$											
June 1952 through 1955	432[d]		5,000		11,000							11,600
	2,433		4,400		28,000							25,700
1956	2,779		5,500		18,500			730	1,830	5,400	31,960	33,500
1957	2,902		4,500		10,500			110	420	4,000	19,530	41,800
1958	3,156		2,800		17,000			500	9,800	9,000	39,100	45,400
1959	3,590	19,500	197,400	14,800	65,500	9200	12,600	3300	24,700	52,900	399,900	273,900
Total	15,292	19,500	219,600	14,800	150,500	9200	12,600	4640	36,750	71,300		431,900

[a] Accounted for after Aug. 20, 1959.

[b] Exclusive of Y^{90}.

[c] Based on a counting efficiency of 12.6%, employed by Operations Division.

[d] Evaporator concentrate released to pit 2.

pit 4 was intercepted and pumped back into the pit. Also, to increase the sorption of ruthenium in waste seeping from pit 4, waste in the pit was treated with a reducing agent. Pit 4 was later taken out of operation and filled with Conasauga shale.

About a third of the ruthenium discharged to the bed of White Oak Lake in 1959 moved into the Clinch River. Although the contribution of ruthenium to the river increased, the amount of strontium entering the river from all ORNL operations decreased, and, consequently, the total discharge consumed only 26% of MPC_w (continuous nonoccupational exposure) for the Clinch River during 1959.[21]

Recent samples collected from observation wells in the pit area showed detectable quantities of Cs^{137} in only two wells, both near pit 2. Cesium-137 concentrations of about 5×10^{-6} μc/ml were found in well 54 (50 ft east) and 3×10^{-7} μc/ml in well 52 (35 ft west). Underground movement of Sr^{90} was somewhat more extensive. Wells within 50 ft of pits 2 and 3 (wells 52, 54, 55, and 56) showed concentrations of Sr^{90} up to 2×10^{-5} μc/ml. Beyond these wells and in wells around pit 4, measurable concentrations of Sr^{90} were detected, but generally in concentrations less than 10^{-6} μc/ml.

Soil and liquid samples were also withdrawn from wells in the immediate vicinity of pit 2. Well 201 was drilled (October 28, 1959) on a 30° angle below the SW corner of the pit, about 10 ft from the side wall. The well extended into the ground 19 ft, or about 9 ft below ground surface. Concentrations of about 5×10^{-6} μc/ml of Cs^{137} and 2.4×10^{-5} μc/ml of Sr^{90} were detected in liquid samples from the well. The average amount of Cs^{137} sorbed per gram of soil was 1×10^{-2} μc/g, and of Sr^{90} sorbed, 3.4×10^{-4} μc/g. This cesium loading is considerably less than the saturation capacity of Conasauga shale shown by laboratory studies.[15]

New Waste-Disposal Pit 5

In 1956 the Waste Disposal Research Section test-drilled two possible pit sites and selected one just east of the old pit area (Fig. 16 in ref

---

[21]H. H. Abee, unpublished correspondence.

14). Recommendations for changes in the design of the pit were published in 1958.[22] These were based primarily on the inference that the present pits seeped laterally along the bedding planes of the shale, that is, along the strike of the formation, and that little liquid left the pits in a direction at right angles to the bedding, or out the bottom of the pits.

For a pit oriented at right angles to the strike, the rate of seepage would be determined by the length and depth of the pit, which determine the side area and the head available. The width of the pit is a secondary factor. This meant that the pit could be made narrower without sacrificing disposal capacity, and that this in turn would make it economically feasible to fill the pit with coarse, crushed rock and cover it with dirt.

There are several advantages to such a design. The narrower pit makes it possible to leave more shale in place along the sides, and also makes it easier to adjust the excavation to existing topography. The earth cover provides shielding and reduces the radiation field around the pit. The cover also makes the pit independent to both rainfall and evaporation, an operating advantage in that, in this area, rainfall exceeds evaporation, and also because this greatly simplifies the problem of determining seepage rates. A final obvious advantage is that the pit can be abandoned, when the time comes, by simply shutting a valve.

A possible advantage, which has not yet been evaluated, is the potential usefulness of the rock fill as a decontamination medium. In this area the most convenient source of rock is a neighboring limestone quarry, and it has been shown[23] that, in the presence of phosphate, limestone will react with a waste solution to form calcium phosphate, somewhat similar to the mineral apatite, into which strontium will be incorporated. This mechanism holds promise of effective and permanent fixation of the radioactive strontium in the waste by the rock fill of the pit itself, and, together with related methods of supplementing or accelerating the natural ion exchange properties of the soil, is being investigated by Rimshaw and

---

[22]W. de Laguna et al., Proc. U.N. Intern. Conf. Peaceful Uses Atomic Energy, 2nd, Geneva, 1958 18, p 101-15 (1959).

[23]L. L. Ames, Jr., et al., Proc. U.N. Intern. Conf. Peaceful Uses Atomic Energy, 2nd, Geneva, 1958 18, p 76-81 (1959).

Winkley of the ORNL Operations Division.[24] These favorable factors, actual and potential, plus the fact that the new site was selected with a clearer idea of the problem and the requirements than was previously possible, were considered when pit 4 had to be abandoned.

The ORNL Operations Division began construction of pit 5 in the spring of 1960, and the first test liquid was run into it on May 20, and the first actual waste on June 13. The site, orientation, and general design were those suggested by this Division, but the details of construction were determined by the Operations Division, which has responsibility for the pit and its operation. The pit was 10 ft wide at the top and 4 ft wide at the bottom, and the rock fill, and therefore the maximum operating difference in liquid level, was only 9 ft (see Fig. 1.6). This reduced the cost of the pit, but also reduced its storage capacity, so that it will be necessary to pump waste into it frequently in small batches. The seepage rate of the pit when filled is about 8000 gal/day, but decreases as the stage falls, so that the average operating seepage rate will be somewhat less. It is too early to draw any firm conclusions, but so far the pit has been operating satisfactorily and it appears to be, as expected, a substantial improvement over the earlier design.

The new design does virtually nothing to develop an understanding of the basic problems and defects of seepage pits. The question still remains: how do the radioactive materials disperse into the environment? The shielding provided by the earth cover will make it possible to work for extended periods near the pits, and so more test drilling and water sampling will be possible, but it seems unlikely that, in this hydrologically complex environment, it will ever be possible to feel confident about any seepage pit.

Solid Waste Burial

Burial Ground 4

Burial ground 4 is situated in Melton Valley approximately 0.5 mile southwest of the ORNL plant site. The area was opened in February 1951

---

[24] S. J. Rimshaw and D. C. Winkley, Removal of Cs^{137}, Sr^{90}, and Ru^{106} from ORNL Plant Wastes by Sorption on Various Minerals, ORNL CF-60-4-17 (Apr. 18, 1960).

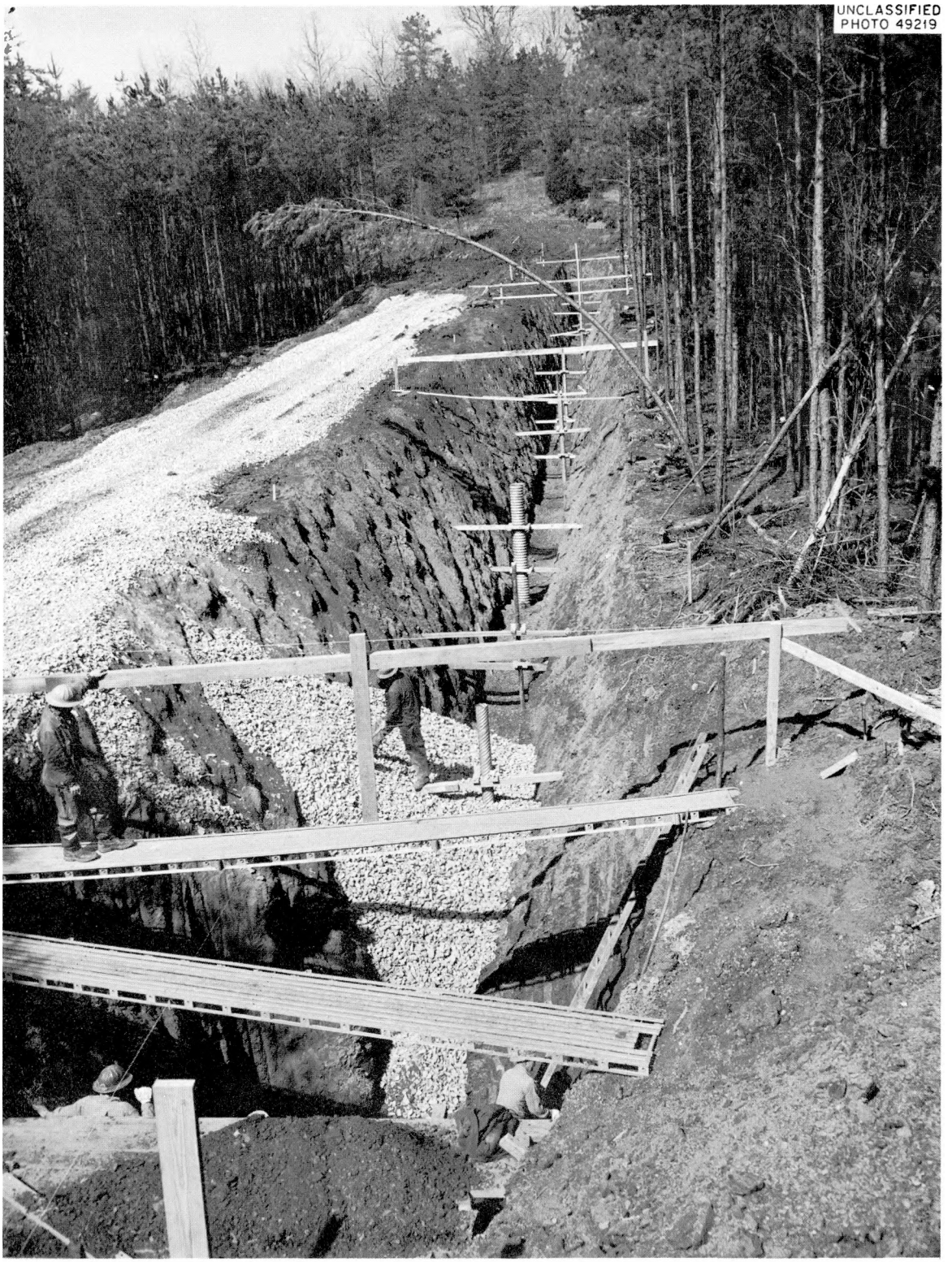

Fig. 1.6. Waste Pit 5 Under Construction.

and closed to routine burial operations in July 1959. It is currently used for special burials, such as potentially explosive waste and high-level waste, and as a stand-by burial ground. In addition, a trench for burning noncontaminated material is operated within the area. Much of the site, especially the northeastern section, has been covered with rock and dirt from building excavations at ORNL. In some places as much as 20 ft of this material overlies the buried waste. The site encompasses an area of about 23 acres. The burial rate during its 8.5 years of operation was a little over 2.5 acres/yr.

The burial procedure consisted of excavating trenches in the weathered shale, dumping the contaminated waste into the excavation, and then covering with the original soil. In the case of some alpha-contaminated wastes, a layer of concrete was poured over the trench. However, no special area of the burial ground was set aside for this material. Auger holes, 1 to 2 ft in diameter and approximately 15 ft deep, were used to dispose of high-level waste. About 50 of these holes are located in the upper part of the burial ground along Lagoon Road. The size and shape of the trenches vary greatly. They range from 50 to 400 ft in length, 8 to 30 ft in width, and 8 to 14 ft in depth. Trench alignment is not confined to any one direction, but varies throughout the burial ground. Burial was limited to higher sections of the burial ground during the wet periods, while the low sections were used during the dry summer months.

A wide variety of contaminated waste has been disposed of at burial ground 4. Included are such things as absorbent paper, glassware, scrap metal, dirt, filters, portions of fuel rods, lumber, irradiated piston rings, oils, powders, wire, depleted uranium, and animal carcasses. A few large pieces of equipment and a small metal building that could not be economically salvaged by decontamination methods were buried at the site. Some waste material was buried in metal, wood, plastic, fiber, and concrete containers, and some was simply dumped loose into the trenches. In many cases the waste was packed into the trenches by back-hoe and bulldozer, which caused many containers to rupture.

[4] The exact amount of waste in burial ground 4 is not known. However, the volume buried in 1957 and 1958 was approximately 255,000 ft^3 and 337,000 ft^3, respectively. During these years ORNL produced about 50% of the waste,

while other Oak Ridge installations and off-site establishments contributed the remainder. Argonne, Knolls, and Mound Laboratories and the General Electric Company of Evendale, Ohio, were the principal off-site shippers, but more than 50 agencies used it. A summary of the waste disposed in 1957 and 1958 is shown in Table 1.3.

Since no records were kept of the amount of activity transferred to the burial ground from the Oak Ridge facilities and since the curie content of off-site waste was frequently incomplete or omitted from the required identification form, it was not possible to determine exactly the amount

Table 1.3. Solid-Waste Burials for 1957 and 1958

Agency	1957		1958	
	Volume (ft^3)	Percentage	Volume (ft^3)	Percentage
ORNL	142,300	55.9	158,000	47.0
Y-12	9,500	3.7	14,800	4.4
U.T. Agricultural Experimental Station	4,100	1.6	4,200	1.3
ORINS	1,300	0.5	1,300	0.4
Oak Ridge Processing Co.	5,700	2.2	16,100	4.8
Knoxville Iron Co.	4,300	1.7	10,700	3.2
K-25	4,100	1.6		
Off-Site Shippers				
KAPL	25,400	10.0	52,100	15.5
ANL	28,900	11.4	33,600	10.0
GE	6,700	2.6	19,000	5.7
Mound Laboratory	13,800	5.4	10,800	3.2
Radiological Service Co.	3,800	1.5	4,400	1.3
BMI			4,200	1.2
Others	4,800	1.9	7,300	2.2
Totals	254,700	100.0	336,500	100.0

of activity disposed of at the burial ground. For 1958, 57,000 curies representing approximately 15,000 ft^3, or 4.5% of that buried, was reported. Most of this activity was associated with shipments from Battelle Memorial Institute. Each 55-gal container shipped by Battelle was reported to have less than 300 curies of activity in it, while each 5-gal container was reported to have less than 2.7. For estimating purposes, the large drums were given values of 100 curies each and the small drums assigned values of 1 curie each. Thus, it can be seen that there may be considerable error in the curie total mentioned above.

Burial ground 4 is underlain by the Conasauga shale of Cambrian age. The formation here consists mostly of dark maroon-to-brown, noncalcareous shales, interbedded with gray, slightly calcareous shales, and thin, gray-blue, silty limestones. A few relatively pure thin limestone lenses are present along with an occasional fine-grained, green, silt-stone bed. Red and brown shales predominate in the northwest part of the area, but in the southeast portion gray shales and interbedded silty limestones are most prevalent. In the higher areas, weathered material extends down 15 or 16 ft, whereas in the lower elevations, fresh rock is encountered within 4 or 5 ft of the surface."

Dip measurements made in and around the burial ground range from vertical to 27° to the southeast. Strike measurements varied from N 85° E to N 15° E. The wide range in dip and strike indicates that many small structures are present within the site.

" All drainage from burial ground 4 is into White Oak Creek. Most of the surface and ground water from the area flows to the northeast. However, because of the low-topographic divide that exists along the southwest boundary of the site, there is some drainage southwestward. White Oak Creek discharges into the Clinch River about 2 miles below the burial ground. "

In order to define more fully the geologic and hydrologic conditions at the site, a series of 21 auger holes, ranging in depth from 5 to 20 ft, were dug. Water-level measurements, taken about once each week since August 1959 at these wells, indicate that the water table fluctuates between 1 and 2 ft below the surface in low areas and 10 to 14 ft beneath it at higher elevations. Hydrographs for wells 182 and 185, the former located

in high topography and the latter in a low elevation, illustrate these fluctuations (Fig. 1.7). Thus, waste buried in the low areas is in contact with the water table at all times, but in the higher areas ground water intersects the material only during the wet season. The depth-to-water contour map of December 24, 1959 (Fig. 1.8), represents typical wet-weather conditions. It is quite probable that the water level may rise even nearer to the surface during times of unusually heavy rainfall.

Water-table contour maps of the area show that the water table is essentially a subdued replica of the topography (Fig. 1.9). From previous work it is known that ground-water movement in the Conasauga shale is greatest along the strike of the formation.[25] However, due to the disturbed nature of the shale, which was a result of trench excavation, the regular

[25]W. de Laguna et al., Proc. U.N. Intern. Conf. Peaceful Uses Atomic Energy, 2nd, Geneva, 1958 18, p 101–15 (1959).

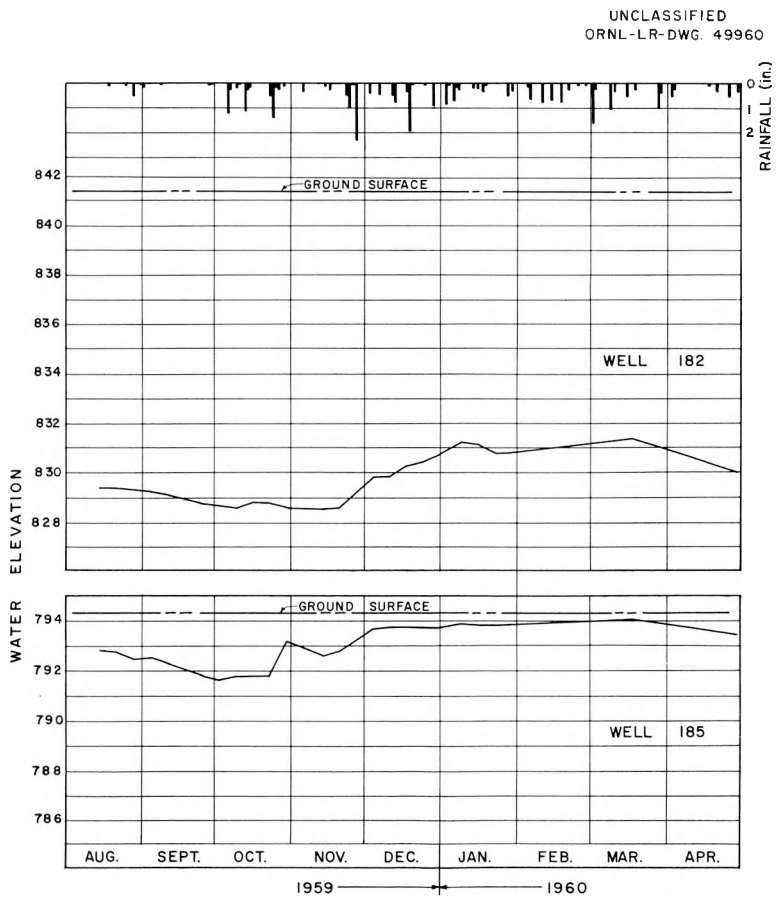

Fig. 1.7. Comparison of Hydrographs for Two Wells at Different Elevations.

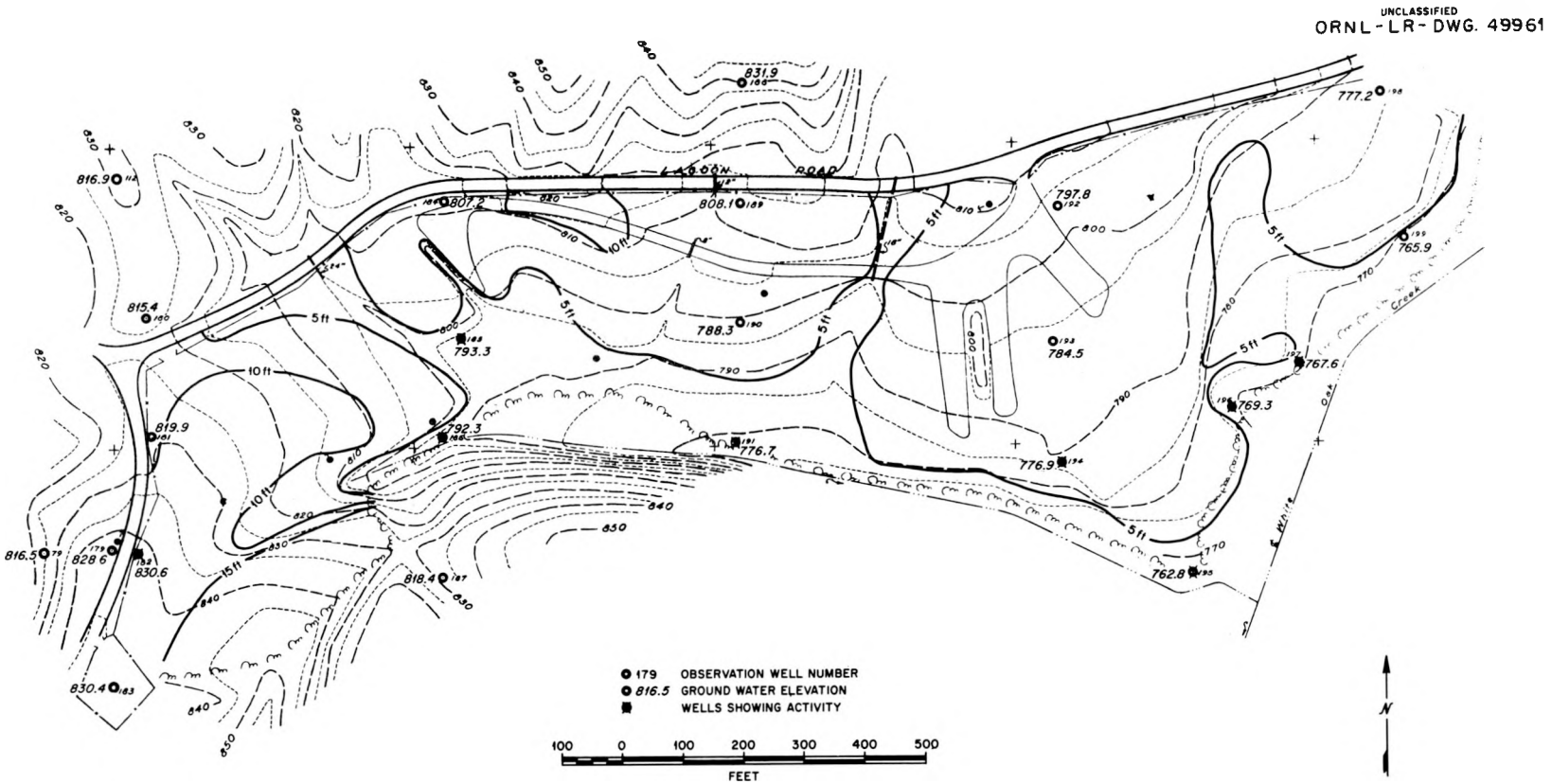

Fig. 1.8. Depth-to-Water Contours at Burial Ground 4, December 24, 1959.

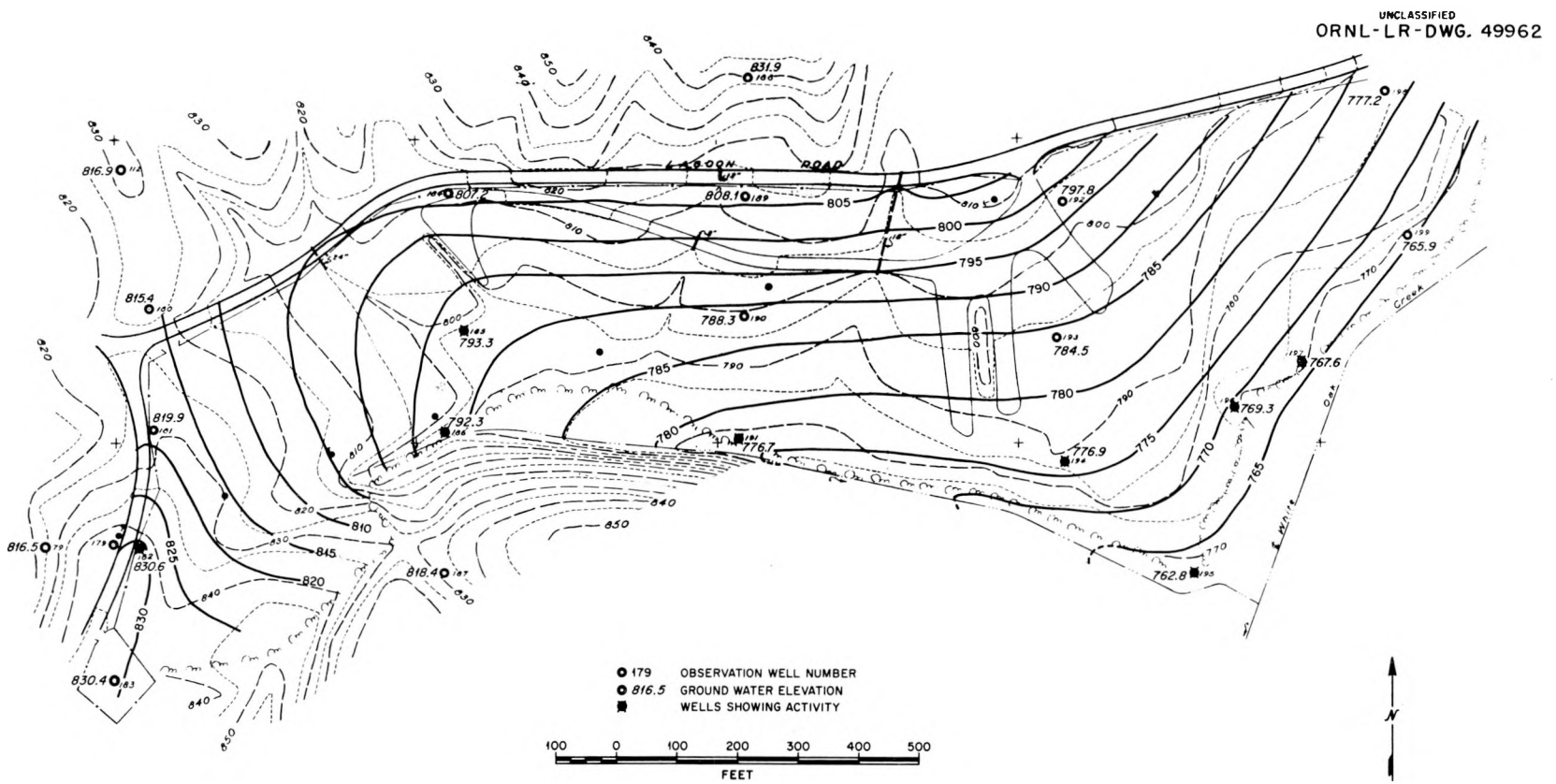

Fig. 1.9. Water-Table Contours at Burial Ground 4, December 24, 1959.

pattern of water movement has probably been disrupted, especially in the uppermost part of the shale. Thus, the principal movement is probably in directions normal to the contour lines in the disturbed part of the shale and is probably along the strike at depths.

The rate of ground-water flow in the area is not known. However, the slow recovery of water levels in the auger wells after pumping suggests that the movement of water in the upper portion of the shale is relatively slow.

Activity has been detected in eight of the sixteen wells located within the burial ground. Beta-gamma contamination was observed in all eight wells, but only two, wells 185 and 186, showed any detectable amounts of alpha activity. With the exception of well 182, all wells showing activity are located in areas where the water table is relatively near the surface. By radiologging with a scintillation probe, it was found that the activity in wells located in low topography was most concentrated within a few feet of the ground surface. In the case of well 182, the maximum radiation was observed at a depth of about 12 ft. Thus, in general, it appears that most activity is entering the wells near the ground-water contact in the weathered portion of the shale.

Radionuclides have been detected in numerous seeps that occur throughout the area, especially during the wet season. Many of the seeps seem to be emerging from the downslope end of covered trenches. These trenches are probably rapidly filled by downward percolating rainfall, and, since the trench is quite porous and its shale walls are rather impervious, water tends to collect in the lower portion. When the trench is filled, water will flow from the lower end. One of these seeps is shown in Fig. 1.10.

Activity has been noted also in the intermittent stream that flows from the area into White Oak Creek. In addition to that contributed by surface seeps, some activity is being transported by ground water through the weathered soil to points of discharge in or near surface streams. This is particularly noticeable in the vicinity of well 185. Here contaminated water was observed to be seeping into the intermittent stream that flows through the area. The activity is believed to be coming from a covered trench located about 5 ft from the stream.

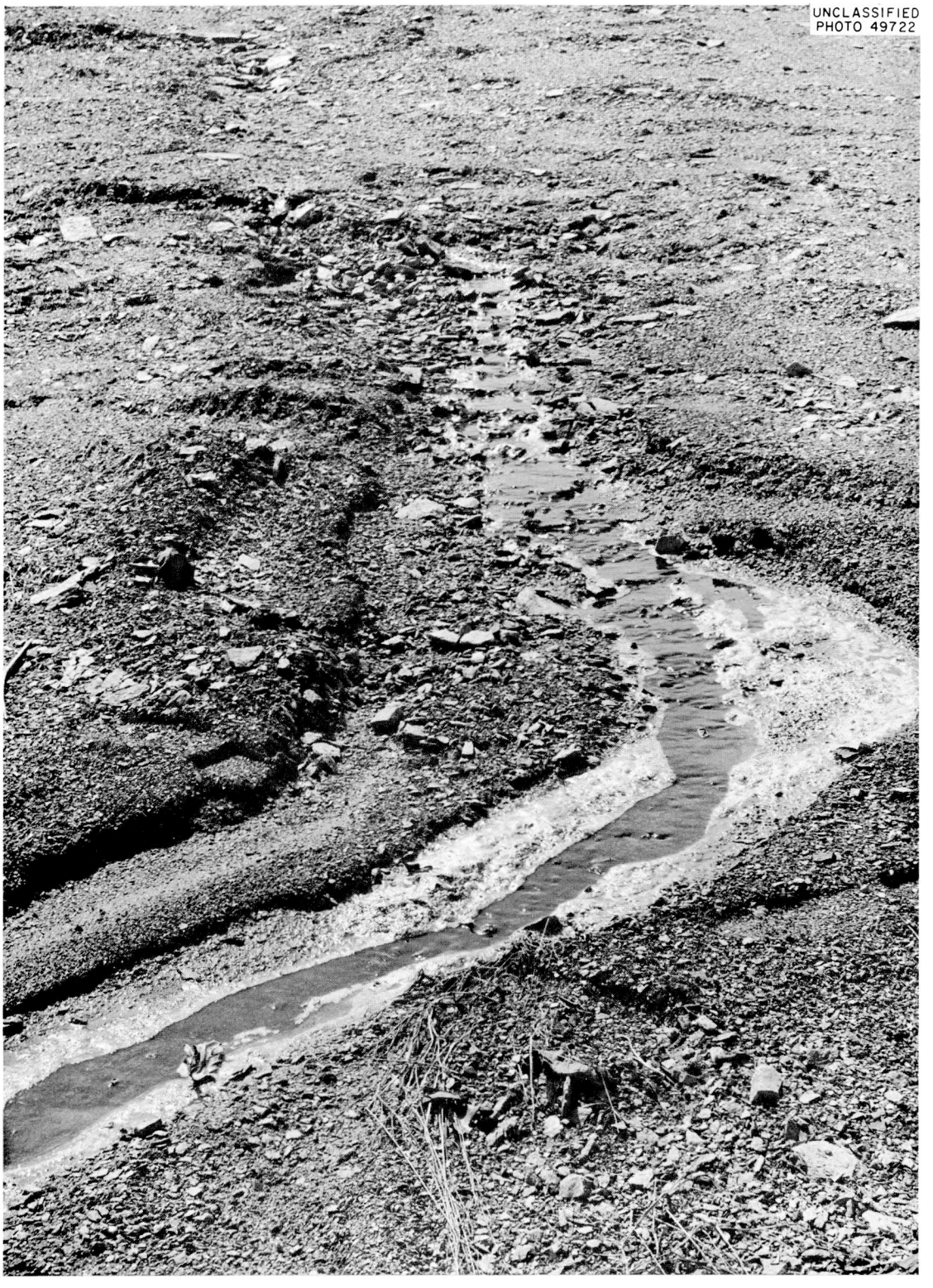

Fig. 1.10. Seep Emerging from Covered Trench.

A summary of the activity occurring in the wells, seeps, and streams at the site is presented in Table 1.4.

Since White Oak Creek is contaminated by water from the Process Waste Treatment Plant and the Settling Basin before it flows past the burial ground, it was necessary to install temporary monitoring stations along the creek immediately above and below the site to determine the amount, if any, of activity contributed by the burial ground to the creek. Water was pumped continuously from the creek at each station, and once each day a liter sample was taken from the collecting container and the remainder discarded. These daily samples were composited, usually in intervals of one week, and then chemically and radiochemically analyzed.

In order to determine the difference in stream flow between the two sampling points, periodic discharge measurements were made with a Price pygmy meter at both sites. Of the six measurements, five showed increases, ranging from 8.7 to 0.8%, at the downstream station, while the sixth showed a decrease of 1.42% in the discharge at the station below the burial ground. By plotting the six measured discharges (cfs) made at the upper station against those made at the downstream station, and then constructing a trend line by the least-squares method, it was possible to estimate the discharge for any period at the upstream station by knowing the discharge at the lower station (see Fig. 1.11). The total volume of water transported past the downstream monitoring station during sampling periods was obtained from the records of a permanent gaging station at this location operated by the Surface Water Branch of the U.S. Geological Survey. The influence of water added to the creek by the Process Waste Water Treatment Plant, the Laundry and Sewage Treatment Plant, and the loss of water by transpiration and ground-water recharge, especially during low flows and hot, dry periods, between the monitoring stations affect the flow of the creek between monitoring stations and may cause some error in computing the flow at the upper station. The distance between the two monitoring points was about 0.5 mile.

The analyses of creek-water samples, taken in a period between February 16, 1960, and May 25, 1960, for total rare earths, cobalt, ruthenium, cesium, zirconium-niobium, and gross alpha contaminants, showed less activity in the stream below the burial ground than above the site. There

Table 1.4. Radioactivity in Wells, Seeps, and Streams at Burial Ground 4

	Maximum Radioactivity (counts min^{-1} ml^{-1})		Radionuclides	Concentration (disintegrations min^{-1} ml^{-1})
	Gross β (~ 8% geometry)	Gross α (~ 47% geometry)		
Wells	25	< 5	Sr^{90} (well 196)	50
			TRE (well 196)	60
Seeps	375	250	Co^{60}	200
			Cs^{137}	2×10^3
			Sr^{90}	294
			$Ru^{103-106}$	55
			Zr^{95}-Nb^{95}	Trace
			TRE	332
			Po^{210}	Trace
Streams	20	92	$Ru^{103-106}$	Trace
			Co^{60}	Trace
			Po^{210}	Trace

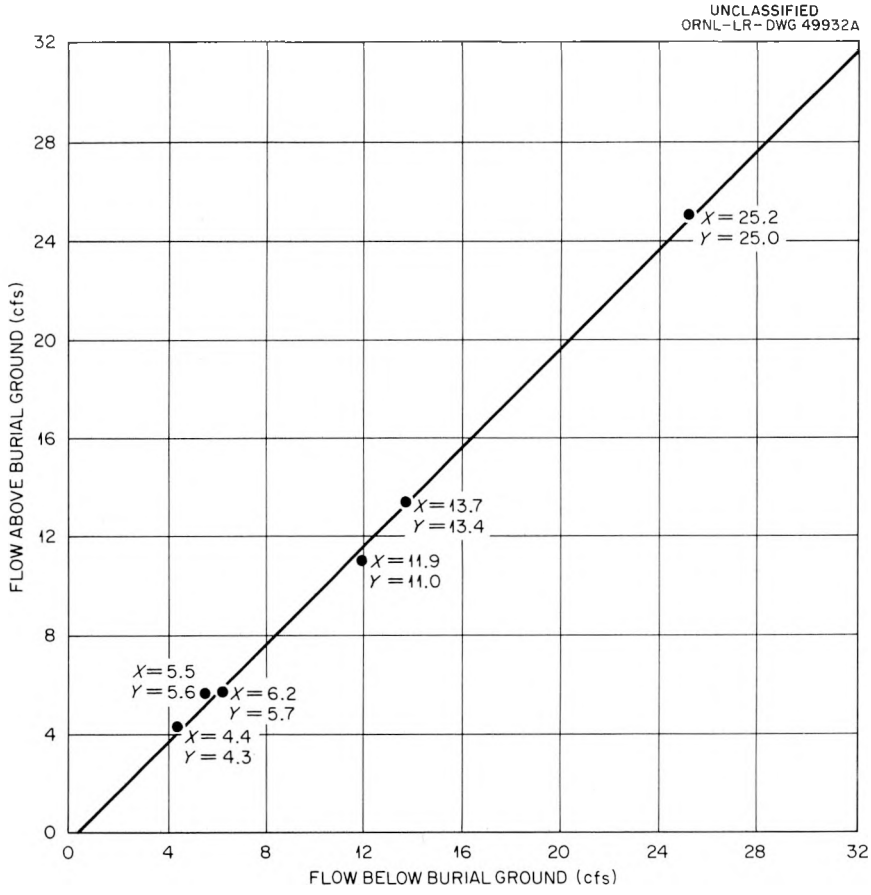

Fig. 1.11. Regression Line for Estimating Flow Above Burial Ground.

was a slight increase in the concentration of Sr^{90} below the burial ground. A summary of the radiochemical analyses of creek water is presented in Table 1.5. It is seen that burial ground 4 contributed activity to White Oak Creek in quantities so small as to be undetectable during this sampling period.

Burial Ground 5

Five deep wells were dug in burial ground 5 to define in greater detail the geology and hydrology of this new burial site. Weathered shale persisted to depths of 35 to 40 ft in areas of high elevation, whereas in low topography fresh rock was found within a few feet of the surface. Hydrographs were made of the wells as an aid in evaluating water-table fluctuations. As shown in Fig. 1.12, the water level in all wells rises

Table 1.5. Radioactivity Measured at Monitoring Stations on White Oak Creek

Composite Date	Volume Discharge (gal)	Activity (mc)						
		Gross α	Sr	Ru	Cs	Zr-Nb	Co	TRE
Upstream from Burial Ground 4								
	× 10^3							
Feb. 16–19, 1960	60,495	10	309	206	206	21	206	980
Feb. 25–Mar. 2, 1960	44,726	30	829	358	229	69	47	1,518
Mar. 8–14, 1960	45,824	16	359	367	305	172	164	1,055
Mar. 22–28, 1960	39,296	40	1173	3819	737	670	170	10,420
Mar. 29–Apr. 3, 1960	66,571	22	568	454	227	227	114	1,873
Apr. 6–12, 1960	33,867	23	92	0	0	0	0	364
Apr. 19–25, 1960	22,686	15	116	182	85	0	553	236
Apr. 25–May 3, 1960	26,433	9	586	234	423	0	252	1,050
May 12–18, 1960	17,127	3	67	79	35	0	129	158
May 19–25, 1960	19,517	8	131	174	218	12	83	449
Totals	376,542	176	4230	5873	2465	1171	1718	18,153
Downstream from Burial Ground 4								
Feb. 16–19, 1960	61,400	10	419	314	314	105	209	1,362
Feb. 26–Mar. 2, 1960	46,405	32	1108	364	190	32	47	1,194
Mar. 8–14, 1960	47,181	16	418	378	322	145	161	869
Mar. 22–28, 1960	40,524	42	1037	3039	553	553	207	6,626
Mar. 29–Apr. 3, 1960	67,863	12	579	810	347	231	116	1,793
Apr. 6–12, 1960	35,094	12	156	0	0	0	0	377
Apr. 19–25, 1960	23,398	16	160	136	60	0	535	287
Apr. 25–May 3, 1960	27,984	10	573	229	253	0	229	1,026
May 12–18, 1960	18,485	3	95	79	28	0	139	199
May 19–25, 1960	21,876	7	444	160	160	22	67	545
Totals	390,210	160	4989	5509	2227	1088	1710	14,238

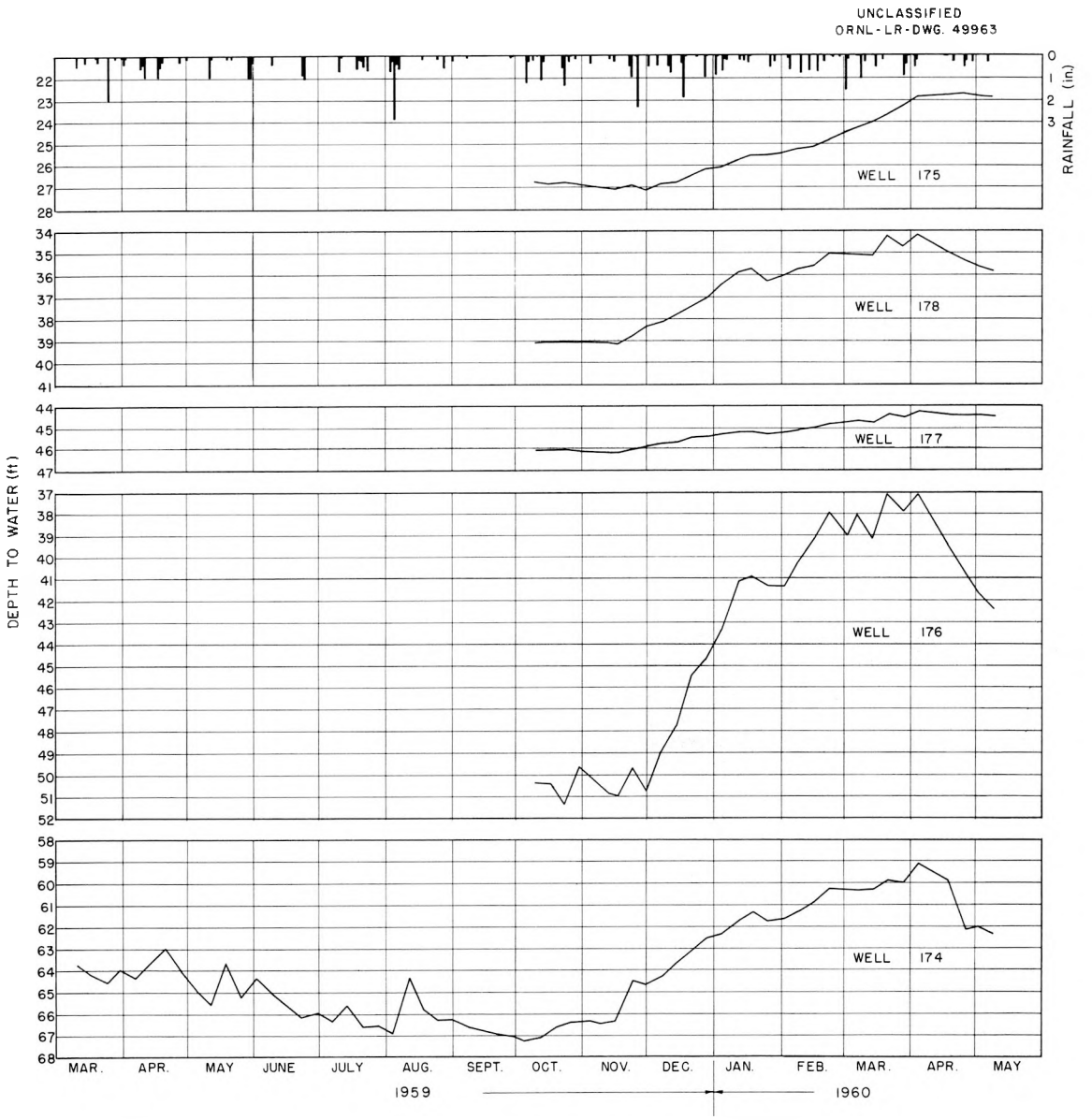

Fig. 1.12. Hydrographs for Deep Wells in Burial Ground No. 5.

during the wet winter months and falls during the summer months when evaporation and transpiration are greater and rainfall is less. However, there is a wide range in water-level fluctuations between the wells. The maximum fluctuation observed from October 1959 to May 1960 was 14 ft in well 176, while the minimum change of 1.5 ft occurred in well 177 over the same period. The reasons for these differences are not clear; however, it is believed that the topographic location of the wells, the permeability of the rock in the immediate vicinity of the holes, and possibly the nearby

perched water-table conditions, in the case of wells 174 and 176, all influence water-level fluctuations.

The circulation of water at depth was determined by pressure testing several churn wells located within the site. This method consists of expanding a rubber packer against the side walls of the well and pumping water under pressure into that portion of the well below the packer. Since the wells were cased down to fresh rock, the permeability of the weathered shale was not tested. From Fig. 1.13 it can be observed that the acceptance rates are in general greater near the top of the fresh shale. Thus, the most permeable zones or fractures occur within the first 100 ft. The wide range in acceptance rates of the different wells and the diversity of leakage at various depths within the wells suggest that the rock underlying the burial site is not homogeneous.

To simplify and improve monitoring, a new trench design was adopted for the disposal of a special solid waste; two trenches have been completed. The waste in both is contained in metal drums and consists mostly

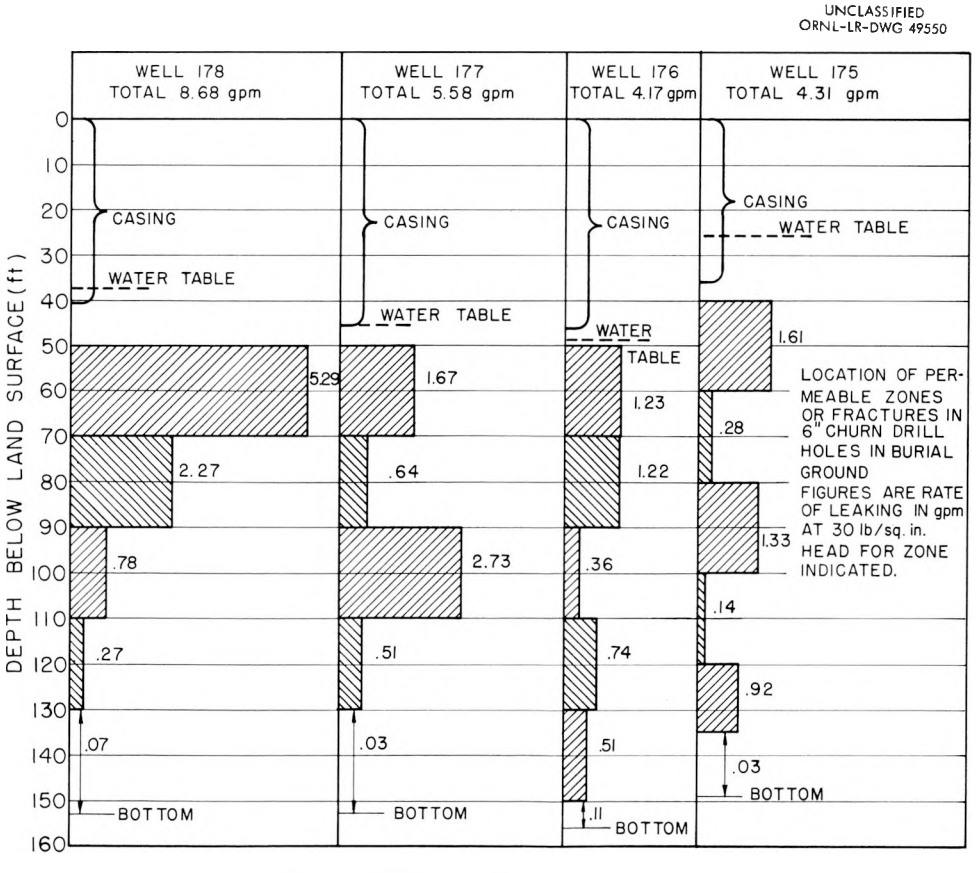

Fig. 1.13. Pressure Testing of Wells in Burial Ground No. 5.

of alpha-contaminated material. Water has been observed in the collecting sumps of the trenches after heavy rainfall and extended wet periods. It is believed that the water is seeping into the trenches from the unlined side walls, since the trenches are situated above the water table and the asphalt cover should prevent direct overhead percolation. Samples taken from the sumps showed gross alpha activity as high as 12.08 ± 0.75 and gross beta activity of 3.02 ± 0.65 counts min^{-1} ml^{-1}. In order to determine the relation, if any, of container integrity to ground-water leaching, the drums in trench 1 were placed in an upright position, while in trench 2 they were simply dumped at random. To date, monitoring data indicate that any damage to the container incurred in dumping does not cause an increase in the activity leached from the waste. However, the material has been buried only since February 1959.

The cost incurred for the construction and operation of trench 1 was $1000. This includes $200 for excavation and filling; $200 for construction of the sump, well, gravel underdrain, and asphalt cover; and $600 for placement of the waste containers in the trench. The excavation and filling expense does not add to the operating cost, since this would be done in any trench disposal. The trench is about 70 ft long, 10 ft wide, and 12 ft deep, comprising a volume of 8400 ft^3. Thus, the additional cost of the sump, well, gravel underdrain, and asphalt cover is about $0.024 per ft^3 of trench space. The cost of protecting the drums by careful placement in the trench is $0.069 per ft^3 of trench space.

EVALUATION OF CONSEQUENCES OF DISPOSAL TO ORNL ENVIRONS

E. G. Struxness

W. J. Boegly, Jr. R. L. Bradshaw K. E. Cowser
W. de Laguna D. G. Jacobs T. F. Lomenick
R. J. Morton F. L. Parker T. Tamura

J. S. Olson[26] R. M. Richardson[27]

As a part of an over-all evaluation of the hazards associated with ORNL operations,[28] the consequences of purposeful or accidental releases

[26]Member of Health Physics Division, Ecology Section.

[27]U.S. Geological Survey.

[28]F. L. Culler (ed.), Summary Report of Hazards Evaluation — Hazards Evaluation, vol 1, ORNL-2956 (in press).

of radioactive material to the immediate environs of ORNL were evaluated. Factual data on the atmosphere, hydrosphere, lithosphere, and biosphere[29] were examined and related to releases of radioactivity which have occurred or might occur under certain circumstances.[30] The ORNL waste-disposal facilities and operations, particularly the ground-disposal operations, were examined and their effectiveness assessed in terms of fission-product movement out of White Oak Creek drainage area into the Clinch River.[31] For the most part, existing data were analyzed, but some additional data were obtained for use in the study.

Environmental Factors

Meteorological computations for estimating the environmental buildup of radioactivity due to fallout from stacks have been compared with data on foilage-contamination at a series of stations radiating in several directions from ORNL.[32] Distributions correspond in a general way with the generalization that southwesterly and northeasterly winds are most important on an average annual basis. For estimating consequences of individual major incidents, long-term wind averages are approximate only for relative probabilistic estimates of the chance that a certain area might be contaminated above some specified level. Calculations for individual meteorological situations are needed to make an estimate of the pattern of contamination as a function of location for individual accidents.[33]

Whereas stack effluents are injected into the air stream, other kinds of radioactive dispersal by wind, such as blowing of dust, can be controlled to a considerable degree by providing adequate vegetation cover.

---

[29]Biological factors are not discussed in this section but will be found in the Ecology section.

[30]E. G. Struxness, General Description of Oak Ridge Site and Surrounding Areas — Hazards Evaluation, vol 2, ORNL CF-60-5-27 (May 31, 1960).

[31]E. G. Struxness, Detailed Assessment of Solid and Liquid Waste System — Hazards Evaluation, vol 4, ORNL CF-60-5-29 (May 31, 1960).

[32]J. S. Olson, "Fallout of Gamma Emitting Isotopes on Tree Foilage of Oak Ridge," (in manuscript).

[33]US Weather Bureau, Meteorology and Atomic Energy; see also Meteorology of the Oak Ridge Area, ORO-99 (1953).

It has been Laboratory policy for several years to provide such cover on areas bared by construction.

Conasauga shale, the soil of White Oak Lake bed, and the Clinch River sediments show moderate-to-high specificities for nearly all fission products, thus providing a safety factor in the case of an accidental release of radioactive materials. In addition, these sediments provide effective decontamination of liquid-waste effluents before they flow into the Clinch River, and the fresh sediments encountered in the river after discharge continue to remove fission products from solution. This is an important factor for downstream water users; the mechanical filtering of sediments from the water in a water-treatment plant could be expected to further remove substantial percentages of activity from the water. On the other hand, the decontamination processes result in contaminated sediments and soils, which may be subsequently leached over long periods of time or may move due to erosional processes into surface drainageways and be transported as sediment in the rivers. The contaminated sediments, whether they remain in place or move into the river, may lead to local accumulation of fission products by living organisms.

The Conasauga shale formation, in which the intermediate-level waste pits are excavated, is an extensive formation which is quite heterogeneous in structure and relatively low in permeability.[34] The depth and extensiveness of the formation provides a large capacity for decontamination of the intermediate-level waste stream, and the slow rate of percolation improves the efficiency of decontamination of the waste stream by ion exchange and radioactive decay. On the debit side, the heterogeneity of the formation makes difficult the prediction of exact patterns and rates of the movement of water and, hence, the fission products contained therein. It has been noted, however, that most of the seepage is along bedding planes parallel to the strike.

There is very little probability of ground-water contamination in areas removed from the ORNL site, and there are no developed ground-water resources in the area. The lack of ground-water resources is due to the

[34]P. B. Stockdale, Geologic Conditions at the Oak Ridge National Laboratory (X-10) Area Relevant to the Disposal of Radioactive Waste, ORO-58 (Aug. 1, 1951).

fact that formations present are, for the most part, too impermeable to hold or transmit economically valuable quantities of water. This means that surface runoff is rapid.

The above discussion indicates three serious shortcomings in the natural environment of ORNL: (1) the high rainfall results in marked leaching of adsorbed activity, (2) the surface runoff leads to erosion and sediment transport, and (3) the heterogeneity of ground-water movement patterns makes monitoring procedures difficult.

Activity Released to Clinch River

Monitoring of Wastes Released to White Oak Creek and Clinch River

Virtually all radioactivity reaching the Clinch River comes through White Oak Creek (see Fig. 1.14). The creek constitutes a direct continuation of the process waste water flow. It also receives contamination released by seepage from the liquid-waste pits and the burial grounds. In addition, drainage from the various reactor facilities located in Melton Valley, as well as cooling water from the LITR and ORR and the laundry waste, are directly discharged to streams leading to White Oak Creek. Erosion of White Oak Lake bed and the Intermediate Pond also contributes activity to the creek.

The original monitoring system was instituted with the primary objective of ensuring that the concentration of mixed fission products in the Clinch River at downstream points of use does not exceed the MPC values recommended by NCRP and ICRP. This objective is being met.[35] However, the original monitoring system, even with subsequent improvements, was not designed for a detailed study of the fate of radionuclides released to the creek.

The process waste is continuously monitored for gross activity and the Process Waste Treatment Plant and settling-basin effluents are proportionally sampled. Most of the other contributing sources are grab-sampled only, and it is not possible to arrive at accurate figures for the total inflow of a particular radionuclide to White Oak Creek.

---

[35] F. N. Browder (ed.), Radioactive Waste Management at ORNL, ORNL-2601 (Apr. 17, 1954).

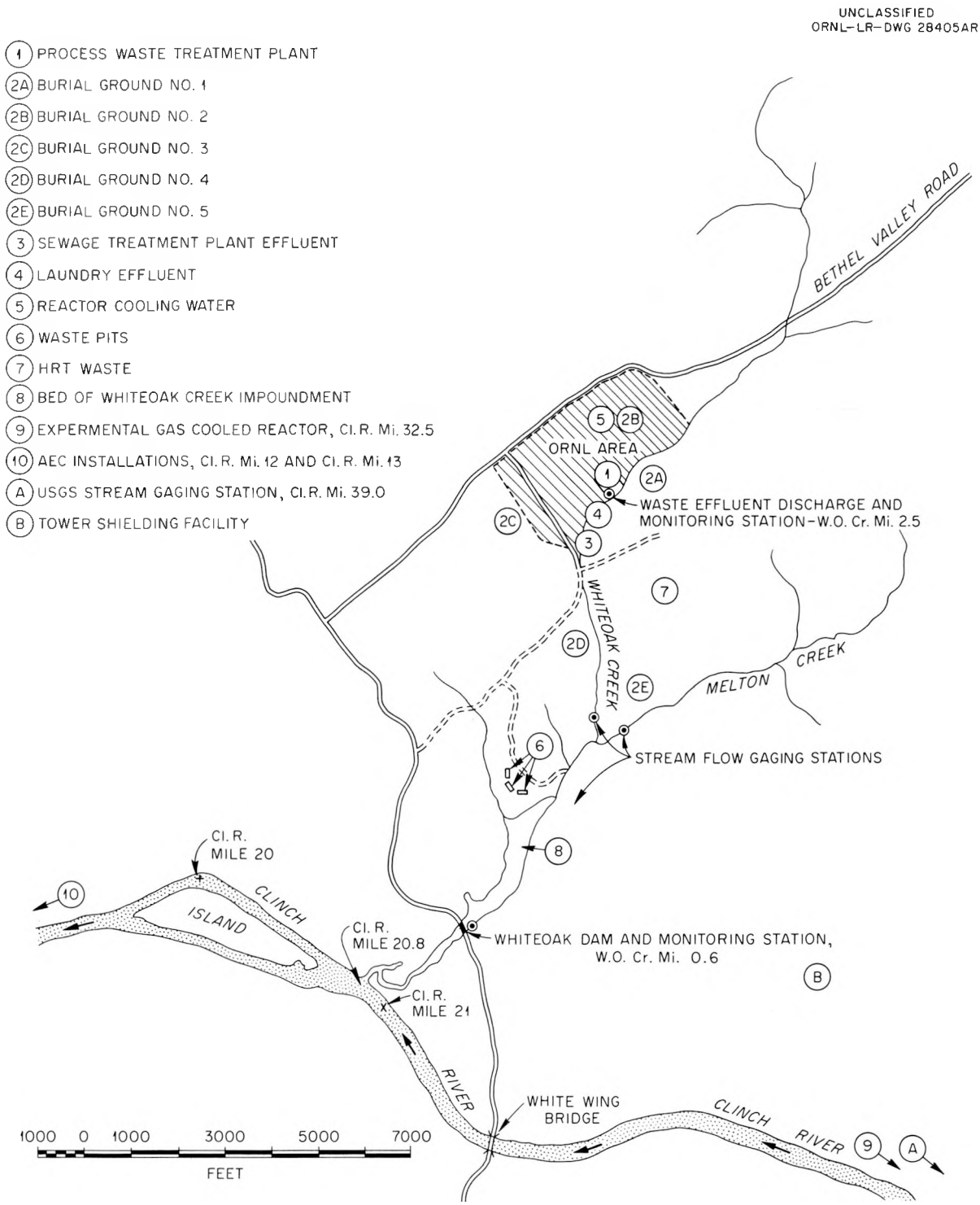

Fig. 1.14. Sources of Radioactive Contamination in the ORNL Environment.

Liquid-Waste Pits

Pits dug in the earth to receive liquid radioactive waste for disposal may function either as storage basisns or as ion exchange columns, as explained by Struxness, Morton, and Straub when they reported on the early experience with waste-disposal pits at Oak Ridge.[36] The concept of the pit as a tank has been largely abandoned, for few, if any, earth materials are sufficiently impermeable. The three waste-disposal pits now in use at Oak Ridge are of value not for their storage capacity but for the ability of the soil around them to trap and hold the radioactive constituents in the waste as it seeps out.[37] The waste pits at Oak Ridge have advantages that they provide secure storage, for the waste cannot be released suddenly from the clay as it could be from a ruptured tank, and the cost is much less than for tank storage. The disadvantage is the inability to determine just what is happening to the waste or how its component elements may disperse.

Ruthenium is not retained completely by the waste-pit system, and, consequently, some of this material finds its way into the Clinch River after passing through White Oak Creek. The estimated release of Ru^{106} from the pit area to White Oak Creek during 1957, 1958, and 1959, was 200, 160, and approximately 1300 curies, respectively (the large increase in 1960 was due to a greatly increased ruthenium inventory in the pits). Considering the concentration of Ru^{106} in the waste and in the liquid seeping to the streams, the decrease in Ru^{106}, due to dilution, decay, and sorption, is calculated to have been 97.7% in 1957 and 97.5% in 1958.

With the waste-pit system acting as the primary source of Ru^{106} discharged to the river, it was estimated by Cowser[38] that the upper limit of Ru^{106} concentration in waste released to the pit system should not exceed 25 $\mu c/ml$; this amounts to 350,000 curies of Ru^{106} in 3,700,000 gal of waste each year. Special treatment of the waste to enhance the removal

[36]E. G. Struxness, R. J. Morton, and C. P. Straub, Proc. Intern. Conf. Peaceful Uses Atomic Energy, Geneva, 1955 9, 684 (1956).

[37]The Disposal of Radioactive Waste on Land, report of the Committee on Waste Disposal of the Division of Earth Sciences, National Academy of Sciences—National Research Council, Publication 519 (September 1957).

[38]K. E. Cowser, Potential Hazard of Ruthenium in the ORNL Waste-Pit System, ORNL CF-60-3-93 (Mar. 11, 1960).

of Ru^{106} was not considered in the calculations. The concentration of ruthenium in waste released to the pits in September 1959 was 3.6 times greater than this estimated upper limit, and a continued discharge at this level could create a potential hazard in the river.

The establishment of the Low-Level Analytical Laboratory in the Analytical Chemistry Division (ORNL) in May 1959 made possible precision analyses of small concentrations of fission products in samples grossly contaminated with Ru^{106}. As a result of more recent work, about 5×10^{-6} μc of Cs^{137} per milliliter was detected in one well (well 52 located 50 ft east of pit 2). Underground movement of Sr^{90} has been somewhat more extensive. Wells within 50 ft of pits 2 and 3 have shown concentrations of Sr^{90} up to 2×10^{-5} μc/ml. Beyond these points and adjacent to pit 4, Sr^{90} has been detected in some wells but generally in concentrations less than 10^{-6} μc/ml. Also, when Sr^{90} was detected in the streams east and west of the pits, it was in concentrations less than 10^{-6} μc/ml. These two small streams receive surface drainage from about 150 acres. By assuming that all the rain falling on the drainage area will pass the monitoring weirs (about 200,000,000 gal/year at 4 ft of rain per year) and that 10^{-6} μc of Sr^{90} per milliliter was present in the liquid passing the weirs, less than 1 curie per year of Sr^{90} would have been contributed to White Oak Creek.

Burial Grounds

The burial grounds are special areas which serve as repositories for packaged and unpackaged solid radioactive wastes from the Oak Ridge plants and off-site installations. Stream and well sampling have indicated that the burial grounds contribute minor amounts of radioactivity to White Oak Creek. Details will be found in the section on Solid-Waste Burial.

White Oak Lake Bed and Intermediate-Pond Sediments

A dike was constructed across the White Oak Creek in the spring of 1944 at Mile 2.0, which created the Intermediate Pond. In a flood on September 29, 1944, this dike failed. The dam at WOC Mile 0.6, constructed in the fall of 1943, is still in existence. The formation of White Oak Lake in 1943 resulted in the deposition and accumulation of sediments on the bottom of the lake. In 1955 White Oak Lake was drained, and the area

now comprises an ecological study preserve. Surveys were made of White Oak Lake bed in 1956, 1958, 1959, and 1960, and of the Intermediate Pond in 1960. From the 1958, 1959, and 1960 surveys, it is estimated that 11.2 curies of Sr^{90}, 477 curies of Cs^{137}, and 58.2 curies of Co^{60} are present in the total lake bed sediment. It is estimated that 3.7 curies of Sr^{90}, 17.0 curies of total rare earths, 113.6 curies of Cs^{137}, and 12.6 curies of Co^{60} are present in the pond sediments.

Since the Sr^{90} concentration is the limiting factor, it is interesting to compare the Sr^{90} value for 1956 with that of 1958–60. Data show that 14.9 curies of Sr^{90} is presently distributed in the sediments of the lake bed and Intermediate Pond. The available data for 1956 do not include Sr^{90} concentrations in portions of the lake bed and the Intermediate Pond sediment. To get an estimate of the Sr^{90} concentration in these sections, the missing values were calculated, assuming a factor of 3.3 greater concentration in 1956 than in 1958–60 (this factor determined from the values of 1956 and 1958–60). The total Sr^{90} budget estimate for 1956 in the lake bed and Intermediate Pond was 47.8 curies.

In order to estimate the losses of Sr^{90} from the White Oak Lake bed by solution transport, surface samples (6-in. depth) of contaminated soil were obtained from the upper lake bed area and subjected to leaching in the laboratory. Sixty-two-gram portions of oven-dried soil (equivalent to a cylinder 1 in. in diameter and 6 in. deep) were leached with several leaching solutions. The average ratio (K_d) of the amount of strontium per gram of sediment to the amount in 1 ml of solution was 1650, a value which agrees very closely with that obtained for Clinch River sediments. Though the simple laboratory leaching experiments do not accurately describe the leaching behavior of Sr^{90} from the lake bed, they serve as a guide.

If White Oak Lake bed is being leached in a manner similar to the leaching of an ion exchange column, that is, if water starts percolating at the higher elevations of the lake bed and moves laterally through the bed, the upper areas would be depleted in Sr^{90} first, and the apparent loss would be greater than that calculated from the K_d values. The percolating solution would contain equilibrium amounts of Sr^{90} before it reached the lower elevations of the lake bed, and in this lower region the loss of Sr^{90} would be much less. Nearly constant annual losses of Sr^{90} at

the dam would be expected. The amount contributed by this source would begin to decline when the Sr^{90} content of the sediment in the region of the dam was depleted. It seems unrealistic to assume that more than 10% of the Sr^{90} would leave the lake bed in any year. Using the Sr^{90} budget for the year 1956, the loss of this element by leaching would amount to approximately 5 curies/year.

Radionuclides can leave the lake bed area as ions dissolved in water or sorbed on particles. From information on the mineralogical character of the sediment, the specific radionuclide affinity of minerals, and the total radionuclide activity discharged to the river, it is possible to infer the form in which radionuclides are leaving the area. Discharge of Cs^{137} and Sr^{90} to the Clinch River is evaluated in terms of the form in which these elements leave the drainage area.

Discharge data from White Oak Creek during 1954–58 (ref 39) show that approximately 25 curies of Cs-Ba^{137} was discharged in 1954 and 1955; in 1956, 160 curies; in 1957, 105 curies; and 1958, 55 curies. The Sr^{90} discharges show a gradually decreasing trend, from approximately 120 curies in 1954 to about 70 in 1958.

While cesium discharge may be due primarily to suspended particle transport, strontium movement as a dissolved ion is suggested. The strontium K_d is 1/50 that of the cesium K_d for lake bed sediment; this means then that the sediment will remove much smaller concentrations of strontium. The recorded discharges suggest that by 1954 most of the strontium was in an ionic state when it left White Oak Lake. If sediment transport played a dominant role in removing strontium from the lake bed, an increase in strontium discharge in 1956 would have been expected, similar to the discharge pattern observed for cesium. However, a decrease in strontium discharge is recorded for 1956, which indicates that very little strontium was sorbed on the sediment relative to the amount normally discharged.

Since the recorded discharges in the year after 1956 show a decrease in cesium discharge, strontium discharge by sediment transport would be expected to decrease proportionately. From these data it may be concluded

---

[39]W. D. Cottrell, Radioactivity in Silt of the Clinch and Tennessee Rivers, ORNL-2847 (Dec. 7, 1959).

that cesium movement from White Oak Lake bed is primarily by sediment transport and strontium movement is primarily by solution transport. The strontium contribution from lake bed sediments to the total strontium discharged at White Oak Dam was less than 10 curies/year in 1956 and more nearly 5 curies/year in 1959.

CLINCH RIVER STUDIES

F. L. Parker

E. G. Struxness
T. Tamura
G. Bruscia[40]
R. J. Morton
E. R. Eastwood
A. Sorathesn[41]

A comprehensive study of the Clinch River downstream from the Oak Ridge area has been started in cooperation with seven state and Federal agencies. The agencies are the U.S. Atomic Energy Commission, U.S. Public Health Service, U.S. Geological Survey, Tennessee Valley Authority, Tennessee Stream Pollution Control Board, Tennessee State Health Department, and the Tennessee Game and Fish Commission.

The purpose of the study of the Clinch River below Oak Ridge National Laboratory is to obtain fundamental information on the physical, chemical, and biological dynamics of a flowing, fresh-water ecosystem which is receiving large volumes of low-level radioactive wastes. Information from a broad fundamental and applied program will have important implications for two major world-wide problems resulting from large-scale environmental contamination. The problems are:

1. What is the over-all diluent capacity of fresh-water environments for an increasing continuous input of large volumes of low-level radioactive wastes?

2. What is the long-term indirect impact of radioactive contamination of such environments?

This program has four general objectives, namely:

1. to determine the fate of radioactive materials currently being discharged to the river,

---

[40]Alien Guest from Italy.

[41]Alien Guest from Thailand.

2. to determine and understand the mechanisms of dispersion of radionuclides released to the river,
3. to evaluate the direct and indirect health hazard aspects of the current river-disposal practices, and
4. to evaluate the over-all usefulness of the Clinch and similar rivers for radioactive waste-disposal purposes.

Hydrology

The Clinch River, a component of the Tennessee River Valley System, rises near Tazewell, Virginia, and flows southwest to join the Tennessee River near Kingston, Tennessee. The Clinch River is over 300 miles long and drains an area of approximately 4400 square miles. Below Norris Dam, at Clinch River Mile (CRM) 79.8, the river is highly regulated by the flow from the dam and by the flow from and the elevation of the water at Watts Bar Dam, located 46 miles downstream from the confluence of the Clinch and Tennessee Rivers. White Oak Creek, which drains the site of the Oak Ridge National Laboratory, joins the Clinch River at Mile 20.8. The backwater pool from Watts Bar Dam extends upstream past White Oak Creek to CRM 28 during the nonflooding season, May to September, and to White Oak Creek during minimum pool elevation. The average flow in the river above White Oak Creek is 4500 cfs with a maximum recorded flow of 42,900 cfs and a minimum of 130 cfs.

The time for water or a wave to move from Norris Dam to CRM 20.8 is variable, depending upon conditions in the river. One turbine operating at full gate at Norris Dam, would discharge 3800 to 4500 cfs, depending upon the head. The electrical output is tied into the TVA power system, and because of the integrated use of water and steam, the flow at Norris Dam through the turbines might be 0, 4500, or 9000 cfs. If the flow were zero prior to startup, then a solitary wave would be generated when the turbine gates were opened. This would also be true if two turbines were operating prior to shutting down one. The velocity of the wave depends in part upon the depth of water in the river and so would vary, depending upon the water elevation at Watts Bar Dam.

The time of travel of water from Norris Dam to CRM 20.8 is about twice the time for the wave to travel. In the summer, backwaters from

Watts Bar Dam are warmer than the Clinch River water released from Norris Dam and cause the Norris water to flow under the pooled water, forming a stratified flow. The "duck under point" varies, depending upon conditions in the river, from CRM 4.4 to CRM 15 to 17. Under the proper conditions it is even possible for Clinch River water to reach the Harriman water supply intake at Emory River Mile 14.7. It is evident that the Clinch River is a highly complex hydraulic system.

The Clinch River is used for fishing, swimming, water skiing, irrigation, drinking water, and industrial cooling. It is also used for navigation, primarily coal barges, up to the Gaseous Diffusion Plant's steam plant at CRM 13. The use of the river will be materially increased if the proposed Melton Hill Dam at CRM 23.1 is constructed. This project would entail important channel changes at the mouth of White Oak Creek and increased velocities and lower temperatures in the river for some distance below the dam.

Water Samples

Water sampling stations have been established at the Oak Ridge Water Treatment Plant, CRM 41.5; Gaseous Diffusion Plant's water-treatment plant, CRM 14.5; and the Kingston Steam Plant, CRM 3.8. The purpose of the routine sampling is to determine the radionuclides and their percentages carried on the suspended silt vs those carried in solution as a function of distance downstream. Preliminary results from the data of the Applied Health Physics Section indicate that at the mouth of the Clinch River over 40% of the total activity carried downstream is Sr^{90}, and that the percentages for Ru^{106}, Ce^{144}, Cs^{137}, Co^{60}, and Zr-Nb^{95} are 23, 13, 13, 7, and 3%, respectively. Close to 70% of the cesium is associated with the suspended sediment, while only 5, 14, 22, 25, and 29% of Sr^{90}, Ru^{106}, Ce^{144}, Co^{60}, and Zr-Nb^{95}, respectively, are associated with sediment. Based on the average suspended sediment load of 27 ppm at CRM 41.5, the percentage of each isotope associated with suspended silt agrees quite well with the values predicted from the laboratory studies reported in this section.

Clay Mineral Testing

The minerals used in this test included Fithian illite (API No. 35), Macon kaolinite (API No. 2), Clay Spur montmorillonite (API No. 26), and Traveler's Rest vermiculite. With the exception of vermiculite, the clays are well characterized minerals. The vermiculite, which was donated by the Zonolite Company, is only 50% vermiculite, the remainder being biotite. The isotopes used were carrier-free Cs^{137}, Zr-Nb^{95} (activity ratio 4.2 to 6.8), Co^{60} (13.6 mc/mg), and Sr^{85} (8.09 mc/mg). Master solutions were made by mixing each of these isotopes separately with distilled water in such amounts that the activity in each master solution was between 15,000 and 30,000 counts min^{-1} ml^{-1}. The solutions were counted in a gamma scintillation-well counter at approximately 25% geometry.

The test consisted in adding a known weight of clay to a known volume of master solution. Following adjustment to pH 6 or 9, and after 1 hr of contact time, the sample was centrifuged and an aliquot taken for counting. The pH was measured again and adjusted if necessary. After three days and seven days this sampling procedure was repeated. A detailed discussion on the selection of the concentration, temperature, pH, sampling time, and sampling procedure has been described elsewhere.[42]

The affinity of the clays for the radionuclide can be expressed in terms of the distribution coefficient, K_d:

$$K_d = \frac{f_c/M}{f_s/V} \quad , \tag{1}$$

where

f_c = fraction of activity sorbed by the clay,
f_s = fraction of activity remaining in solution,
M = weight of clay in grams,
V = volume of solution used in milliliters.

---

[42] A. Sorathesn et al., Mineral and Sediment Affinity for Radionuclides, ORNL CF-60-6-93 (to be published).

Clay Mineral Reactions

In discussing the results, frequent mention is made of the capacity, position, and accessibility of the ion exchange sites of clays. In Table 1.6 a list of these properties is shown for the several minerals. In addition, the interlayer condition of the plate-like minerals (whether separation exists between the plates when stacked) and the thickness of the "unit cell" (c axis) are given. These properties are mentioned frequently in discussing the sorption results shown in Tables 1.7–1.10.

Cesium-137. – An outstanding feature of cesium is its extremely high affinity for illite (see Table 1.7). The relatively high affinity for cesium by the vermiculite sample may be due to the biotite impurity; biotite has a structure almost identical to that of illite. The high specificity for cesium by illitic minerals has been investigated earlier.[43] The internal exchange sites of the illite mineral are not readily accessible because of the closed gap between the layers. In this condition cesium ions can best satisfy the charge requirement of the clay. However, if the gap between the layers is open, then the ionic size of cesium is no longer ideal for that interlayer configuration, and the replacement of other ions is reduced. The expanded or "open" layer condition exists for montmorillonite and vermiculite. This theory also helps to explain the positive time dependence of the illite and vermiculite samples, but the negative time dependence of kaolinite and montmorillonite samples is difficult to explain.

Cobalt-60. – The sorptive capacity of illite and vermiculite for cobalt increases with time, but cobalt sorption decreases with time when contacted with kaolinite and montmorillonite (see Table 1.8). The lower removal at the high pH and the behavior of the master solution when centrifuged suggest that colloid formation may be responsible for the observed behavior.[42]

Strontium-85. – Whereas cesium was sorbed very effectively by illite, strontium sorption is striking because of the low sorption by this mineral (see Table 1.9). Equally surprising is the observation that the mineral with the lowest exchange capacity (kaolinite) exhibits the highest affinity for strontium. An explanation of this relationship is not offered at

[43] T. Tamura and D. G. Jacobs, Health Phys. 2, 391 (1960).

Table 1.6. Ion Exchange and Structural Properties of Some Common Clay Materials in Water

Clay	Ion Exchange Capacity (meq/100 g)	Position of Exchange Site	Accessibility of Internal Site	Interlayer Condition	C-Axis Spacing (A)
Illite	30	Edges and internal	Difficult	Closed	10
Kaolinite	12	Edge		Closed	7
Montmorillonite	90	Edge and internal	Easy	Open	15
Vermiculite*	120	Edge and internal	Easy	Open	14
Vermiculite 50%					
Biotite 50%	5	Edge and internal	Difficult	Closed	10

*The vermiculite sample's purity is only 50%; the two components are mixed at the atomic level and do not occur as discrete particles of vermiculite and biotite.

Table 1.7. Cesium Sorption by Clays, and Calculated K_d

Standard Clays	Contact Time	Activity Sorbed (%)		K_d		Ratio of Clay to Master Solution
		pH 6	pH 9	pH 6	pH 9	
Illite	1 hr	89.99 ± 0.25	90.48 ± 0.25	26,965	28,522	0.1 g/300 ml
	3 days	97.92 ± 0.23	98.60 ± 0.23	141,010	217,815	
	7 days	98.39 ± 0.23	98.56 ± 0.23	183,402	205,014	
Kaolinite	1 hr	74.23 ± 0.28	93.19 ± 0.28	2,880	13,691	0.1 g/100 ml
	3 days	73.96 ± 0.25	62.35 ± 0.27	2,840	1,656	
	7 days	68.47 ± 0.25	51.20 ± 0.44	2,171	1,049	
Montmorillonite	1 hr	61.20 ± 0.34	58.26 ± 0.35	1,577	1,396	0.1 g/100 ml
	3 days	55.14 ± 0.34	56.16 ± 0.35	1,229	1,281	
	7 days	49.95 ± 0.45	50.54 ± 0.45	998	1,022	
Vermiculite	1 hr	96.63 ± 0.25	95.77 ± 0.42	1,433	1,132	1 g/50 ml
	2 days	99.41 ± 0.24	99.64 ± 0.24	8,432	14,087	
	8 days	99.60 ± 0.24	99.76 ± 0.24	12,423	21,155	

Table 1.8. Cobalt-60 Sorption by Clays, and Calculated K_d

Standard Clays	Contact Time	Activity Sorbed (%)		K_d		Ratio of Clay to Master Solution
		pH 6	pH 9	pH 6	pH 9	
	1 hr	28.98 ± 0.52	78.04 ± 0.19	408	3,554	0.1 g/100 ml
Illite	3 days	85.49 ± 0.37	94.65 ± 0.35	5891	17,706	
	7 days	86.43 ± 0.37	95.94 ± 0.35	6372	23,624	
	1 hr	63.91 ± 0.24	69.17 ± 0.22	3541	4,486	0.1 g/300 ml
Kaolinite	3 days	71.54 ± 0.21	51.51 ± 0.29	5028	2,124	
	7 days	60.92 ± 0.25	46.58 ± 0.32	3117	1,744	
	1 hr	69.70 ± 0.21	56.38 ± 0.26	2301	1,293	0.1 g/100 ml
Montmorillonite	3 days	63.91 ± 0.46	45.68 ± 0.60	1771	841	
	7 days	62.36 ± 0.46	45.37 ± 0.60	1657	831	
	1 hr	70.63 ± 0.21	72.87 ± 0.21	120	134	1 g/50 ml
Vermiculite	2 days	98.63 ± 0.16	84.62 ± 0.18	3606	275	
	8 days	98.96 ± 0.16	89.80 ± 0.18	4737	440	

Table 1.9. Strontium-85 Sorption by Clays, and Calculated K_d

Standard Clays	Contact Time	Activity Sorbed (%)		K_d		Ratio of Clay to Master Solution
		pH 6	pH 9	pH 6	pH 9	
Illite	1 hr	23.42 ± 0.62	31.67 ± 0.45	306	316	0.1 g/100 ml
	3 days	26.69 ± 0.54	41.05 ± 0.34	364	696	
	7 days	26.88 ± 0.54	43.17 ± 0.33	368	760	
Kaolinite	1 hr	62.77 ± 0.25	71.24 ± 0.22	3372	4954	0.1 g/200 ml
	3 days	67.49 ± 0.23	68.55 ± 0.23	4152	4358	
	7 days	66.44 ± 0.24	66.28 ± 0.24	3959	3930	
Montmorillonite	1 hr	70.85 ± 0.20	71.88 ± 0.20	2430	2555	0.1 g/100 ml
	3 days	66.88 ± 0.21	68.65 ± 0.21	2019	2189	
	7 days	67.21 ± 0.21	68.67 ± 0.21	2059	2163	
Vermiculite	1 hr	77.45 ± 0.22	67.14 ± 0.26	172	102	1 g/50 ml
	2 days	96.95 ± 0.19	96.46 ± 0.19	1590	1364	
	8 days	97.33 ± 0.19	98.73 ± 0.19	1821	3874	

this time except to point out that kaolinite's exchange capacity is almost exclusively at the edge of the crystal. More work is planned for this phase of the study.

Zirconium-Niobium-95. — In tests performed on the master solution it was obvious that the nuclides were behaving as colloids. The results in Table 1.10 may be interpreted in terms of the negatively charged colloid and negatively charged clays. Since the negative charges on both colloid and clay would cause repulsion of particles, it would be expected that the clay of highest exchange capacity (montmorillonite) would repel most intensely and thus would result in the removal of the least amount of activity when centrifuged. Kaolinite would induce the least repulsion and thus permit the colloidal particles to settle. Unlike the cesium and strontium response, there is an increase in removal with all the clays with time.

Sediment Removal of Radionuclides

Samples from three different uncontaminated locations along the Clinch River were composited; a portion of the composite was saved for mineral identification tests, and the remainder was used for the sorption experiments. The results reported in Table 1.11 are intended to show the usefulness of the mineral and sediment data for an understanding of accumulation and transport in the river.

Mineral Composition of Sediment

X-ray diffraction studies were made for the sediment sample, using the oriented sample technique. Both glycerolated and nonglycerolated specimens were prepared and x rayed with the Norelco x-ray diffractometer. These tests showed that illite, kaolinite, vermiculite, and quartz are the main constituents; quantitative estimates allocated approximately 60, 15, 10 to 15, and 10 to 15%, respectively.

Sediment Reactions with Radionuclides

The high illite content of the sediment is responsible for much of the cesium being associated with sediment in the Clinch River (see Table 1.11). Strontium sorption by the sediment is relatively high, considering the mineralogical composition. Several factors may be responsible: The

Table 1.10. Zirconium-Niobium-95 Sorption by Clays, and Calculated K_d*

Standard Clays	Contact Time	Activity Sorbed (%)		K_d		Ratio of Clay to Master Solution
		pH 6	pH 9	pH 6	pH 9	
Illite	1 hr	83.62 ± 0.25	75.99 ± 0.27	15,310	9,497	0.1 g/300 ml
	3 days	90.39 ± 0.23	83.92 ± 0.30	28,241	15,659	
	7 days	94.05 ± 0.22	89.08 ± 0.23	47,437	24,470	
Kaolinite	1 hr	89.18 ± 0.23	81.73 ± 0.25	24,735	13,423	0.1 g/300 ml
	3 days	94.00 ± 0.22	87.03 ± 0.24	46,973	20,121	
	7 days	94.93 ± 0.22	85.82 ± 0.24	56,158	18,161	
Montmorillonite	1 hr	14.45 ± 1.16	26.28 ± 0.63	169	356	0.1 g/100 ml
	3 days	28.74 ± 0.57	37.90 ± 0.43	403	610	
	7 days	35.24 ± 0.46	42.07 ± 0.39	544	726	

*The above results were calculated from counts/ml of $Zr\text{-}Nb^{95}$. The master solution was well mixed and stirred but not centrifuged.

Table 1.11. Uptake of Radionuclides by Clinch River Sediment

Element	Contact Time	Activity Sorbed (%)		K_d		Ratio of Clay to Master Solution
		pH 6	pH 9	pH 6	pH 9	
	1 hr	53.76 ± 0.42	61.31 ± 0.37	2,326	3,169	0.1 g/200 ml
Cs	3 days	96.17 ± 0.25	96.16 ± 0.25	50,152	50,152	
	7 days	97.78 ± 0.24	97.64 ± 0.24	88,048	82,769	
	1 hr	46.44 ± 0.33	71.91 ± 0.22	1,734	5,120	0.1 g/200 ml
Co^{60}	3 days	93.34 ± 0.17	82.38 ± 0.19	28,017	9,354	
	7 days	97.28 ± 0.17	85.12 ± 0.18	71,567	11,445	
	1 hr	21.42 ± 0.78	24.79 ± 0.67	545	659	0.1 g/200 ml
Sr^{85}	3 days	45.79 ± 0.36	63.87 ± 0.36	1,690	3,537	
	7 days	41.83 ± 0.39	66.80 ± 0.25	1,438	4,024	
	1 hr	62.83 ± 0.32	54.37 ± 0.37	3,380	2,383	0.1 g/200 ml
$Zr\text{-}Nb^{95}$	3 days	82.69 ± 0.25	75.55 ± 0.27	9,554	6,181	
	7 days	86.56 ± 0.24	79.94 ± 0.25	12,886	7,970	

vermiculite in the sediment may, by its smaller particle size, be more effective than the 20 to 30 mesh vermiculite which was used for the strontium test. Also, the sediment may contain organic matter whose affinity for strontium is greater than that of the clay minerals.

The influence of organic matter is suspected from the results of the sorption of cobalt. Though illite is partly responsible for the high K_d for cobalt by the sediment, the higher removal at pH 6 than at 9, and the much higher removal by the sediment, suggest the presence of organic matter.

From the K_d values for the river sediment, the distribution of radionuclide between the sediment and the liquid phases can be calculated over a range of sediment concentrations. In Fig. 1.15 the percentage of the radionuclide on the sediment as a function of the sediment concentration (ppm) and pH is shown. Note that cesium is insensitive to changes in pH;

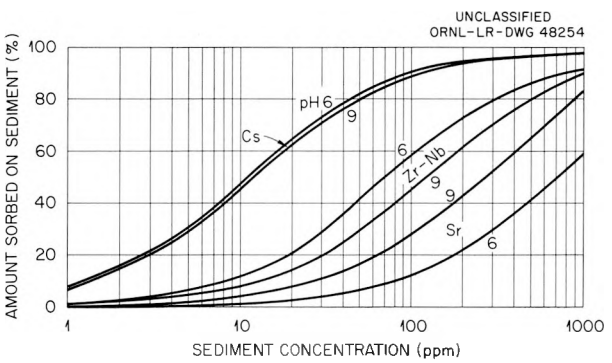

Fig. 1.15. Radionuclide Distribution on Sediments as a Function of the Sediment Load in the River Under Different pH Conditions.

strontium sorption is favorably influenced by increasing pH. If the Clinch River, for example, contains 30 ppm of sediment of the type used here, over 70% of the cesium would be associated with the sediment, but only about 5% of the strontium would be sorbed. These preliminary results appear promising and justify further research on K_d determinations of the sediments collected at different points along the Clinch and Tennessee Rivers.

SORPTION AND RETENTION BY MINERALS AND COMPOUNDS

T. Tamura D. G. Jacobs
F. S. Brinkley D. Catron
O. M. Sealand

Structural Relationships in Cesium Sorption

Treatments which convert the expanded c spacing of clay minerals to the unexpanded 10-A spacing have demonstrated improved cesium sorption from waste solutions.[44,45] The complexities associated with the x-ray diffraction method of analysis do not allow definitive resolution of the exact spacing and changes induced by treatment. Hence, interpretations involving changes in structure have been based largely on known behavior of the clay minerals when treated with chemicals and heat. Ion exchange relationships derived for clay minerals using cesium have also been based on the structure of the materials.[46]

Mineral Sorption of Cesium

Cesium sorption curves obtained for Grundite (Fig. 1.16), a commercial material rich in illite which is used in the process waste-water-treatment plant, show a response nearly identical to that of Fithian illite. As expected, the cesium sorptive properties of illite are dominant over the sorptive properties of the impurities in the material. The sorption curves indicate the multifunctional nature of the exchange reaction and edge fixation.

Cesium sorption by clinoptilolite (Fig. 1.17), which is not a layer-lattice clay mineral but a three-dimensional zeolite, shows that it can be described by simple mass action over the entire range of cesium concentrations employed. The points represent experimental data; the curves are the responses calculated for a system in which the cation exchange capacity

---

[44]T. Tamura and D. G. Jacobs, Health Phys. 2, 391 (1960).

[45]T. Tamura and D. G. Jacobs, "Improving Cesium Selectivity of Bentonites by Heat Treatment," submitted to Health Phys.

[46]D. G. Jacobs and T. Tamura, "The Mechanism of Ion Fixation Using Radio-Isotope Technique," presented at the 7th International Congress of Soil Science, Aug. 14–24, 1960, Madison, Wisconsin.

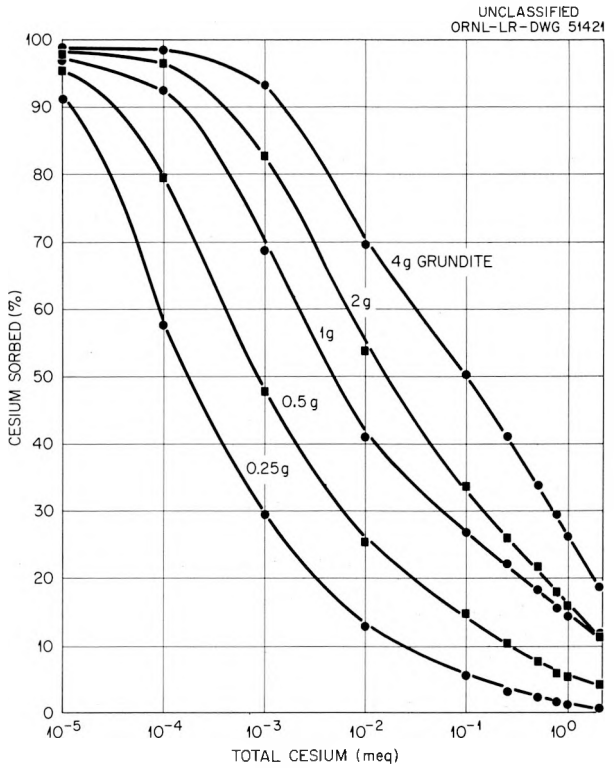

Fig. 1.16. Sorption of Cesium from 0.1 M $NaNO_3$ by Grundite.

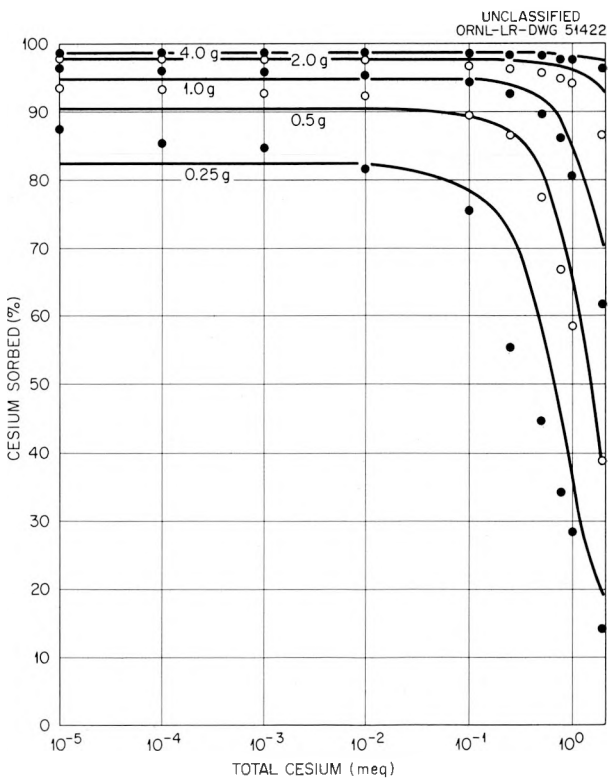

Fig. 1.17. Sorption of Cesium from 0.1 M $NaNO_3$ by Clinoptilolite.

is 167 meq per 100 g and the mass-action coefficient is 112. This response implies that there is no lattice fixation of cesium and that desorption would be a reversal of the sorption process. In cases where lattice fixation occurs, desorption of nonfixed exchangeable cesium would occur readily, but the fixed cesium would be removed only with great difficulty. Thus, clinoptilolite would be very good for sorbing cesium from a waste stream, but the reversibility of sorption would require that saturated clinoptilolite be protected from leaching.

Heat Treatment of Sorbent

Considerable progress was made with studies of cesium sorption by bentonites heated to different temperatures. Expanded Wyoming bentonite gave sorption curves which could be described by a single equilibrium coefficient; after the bentonite was heated to 600 or 700°C, it gave sorption curves which could best be described as a multifunctional exchange reaction. This multifunctional curve was also obtained for illite, which is an unexpanded clay mineral, and for potassium-saturated vermiculite, which is a collapsed (unexpanded) clay mineral. Figure 1.18 shows the cesium sorption curves for oven-dried calcium bentonite (montmorillonite) and for calcium bentonite after being heated to 600°C and cooled. These curves also support the thesis that the unexpanded lattice favors cesium sorption.

The curves in Fig. 1.18 were obtained after heating the bentonite for 3 hr at the designated temperature to ensure complete dehydration and consequent collapse. To test the influence of the time of heating, time was varied from 15 min to 360 min at 600°C. The results are shown in Table 1.12; 1 hr of heating at 700°C and oven-drying overnight are also reported for comparison. These data help to explain why the samples heated for 3 hr require considerable time to reach equilibrium.[45] The data show that short heating is sufficient to collapse the lattice; longer heating tends to reduce the initial sorption response (probably due to crystal edge decomposition), but, as the solution-solid contact time increases, the sorption increases until equilibrium is reached. The x-ray diffraction patterns show that there is a gradual reduction in the c spacing as heating duration and temperature increase; however, the changes in intensity and

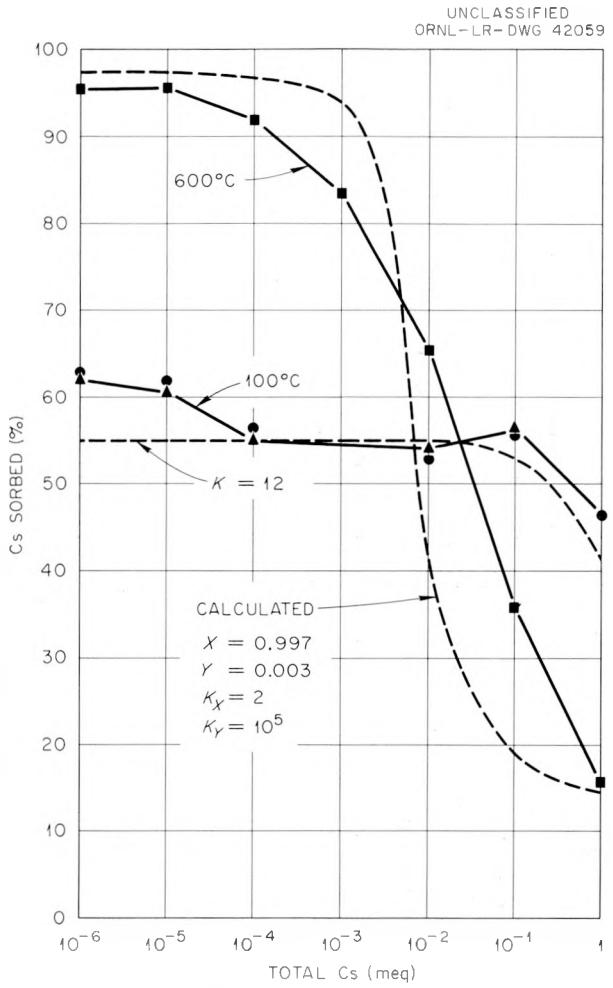

Fig. 1.18. Description of Cesium Sorption by Calcium Bentonite from 0.1 M NaCl Based on Mass Action.

shape of the maxima suggest that the reactions are more complex than simple reduction in spacing.

There was evidence of beneficial influence of heat on the cesium sorption capacity of several bentonites, as shown in Table 1.13. These data re-emphasize the importance of the saturating cation as well as the heat treatment. It is interesting that both dioctahedral and trioctahedral bentonites show improved cesium sorption upon heating. The Wyoming and Arizona bentonites are dioctahedral minerals; the hectorite sample is trioctahedral. The metabentonite is actually an interstratified illite-montmorillonite clay.

Table 1.12. Influence of Heating Duration on Cesium Sorption, 001 Spacing and Weight Loss of Wyoming Bentonite

Heating		Per Cent Sorption* in Contact Times Shown					X-Ray Diffraction Data			
Temperature (°C)	Duration (min)	1 hr	21 hr	75 hr	167 hr	237 hr	001 Maximum (A)	Intensity	Peak Shape	Weight Loss (%)
100		34.5	32.4	31.4	31.5	29.9	12.6	Very strong	Sharp	0
600	15	35.5	47.3	51.1	48.8	49.1	12.6	Very strong	Sharp	4.32
600	30	31.4	46.0	50.4	48.6	50.1	12.6	Strong	Sharp	5.12
600	60	26.6	43.5	51.0	50.6	51.4	12.3	Medium	Sharp	9.78
600	180	24.8	41.1	50.6	52.4	53.8	12.3	Weak	Broad	9.81
600	360	22.6	40.4	49.2	52.6	54.1	11.5	Weak	Broad	10.51
700	60	13.1	27.7	37.5	43.5	45.9	9.93	Weak	Broad	13.58

*1.0 mg of cesium per gram of clay = 100% sorption.

Table 1.13. Influence of Heating on the Sorption of Cesium from 6 M $NaNO_3$ by Several Bentonites

Samples heated for 1 hr at designated temperature; sorption determined at various times and expressed as per cent sorption with 100% = 1.0 mg cesium per gram of clay

Contact Time (hr)	Metabentonite Tazewell, Virginia			Bentonite Chambers, Arizona					Hectorite Hector, California	
	Natural*			Natural		Potassium-Saturated			Natural	
	22°C	600°C	700°C	22°C	700°C	22°C	600°C	700°C	22°C	700°C
1	21.03	24.78	28.11	31.58	18.63	69.10	80.34	84.61	19.36	26.95
24	26.59	35.71	44.06	31.08	29.11	69.84	78.44	85.21	21.28	35.69
74	25.81	42.51	46.05	30.73	33.60	69.73	78.20	83.99	21.82	35.69
145	27.09	42.75	47.06	30.09	34.89	69.73	77.31	83.24	21.21	36.66
241	25.66	42.69	46.25	30.27	35.10	69.19	77.05	82.36	19.19	35.25

*In its natural state of cation saturation.

Chemical Treatment of Sorbent

As the structure of vermiculite differs with changing cation saturation, a series of cesium sorption studies were made using vermiculite treated with various cations. Saturation of the exchange complex with Ca^{++}, Mg^{++}, or Sr^{++} yielded sorption curves nearly identical to those obtained when Na^{+} was the saturating cation (see Fig. 1.19). Pretreatment of the vermiculite with 0.01 M HNO_3 resulted in a slightly different response, that is, in the dilute cesium range no edge fixation was observed. The amount of interlayer fixation was also considerably reduced and a greater degree of cesium saturation was required to induce interlayer fixation.

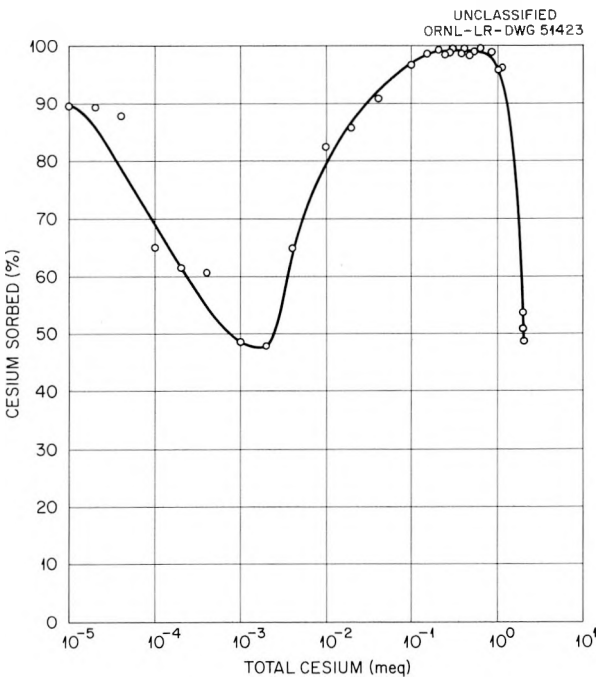

Fig. 1.19. Sorption of Cesium from 0.1 M $NaNO_3$ by 2 g of Calcium Vermiculite.

Rubidium treatment of the vermiculite resulted in a response similar to that observed for potassium treatment (see Fig. 1.20). The most noticeable difference is that sorption is less for the rubidium-treated than for the potassium-treated vermiculite. This is an indication that it is more difficult for cesium to replace rubidium than to replace potassium from the exchange sites. This is in accordance with observations made with

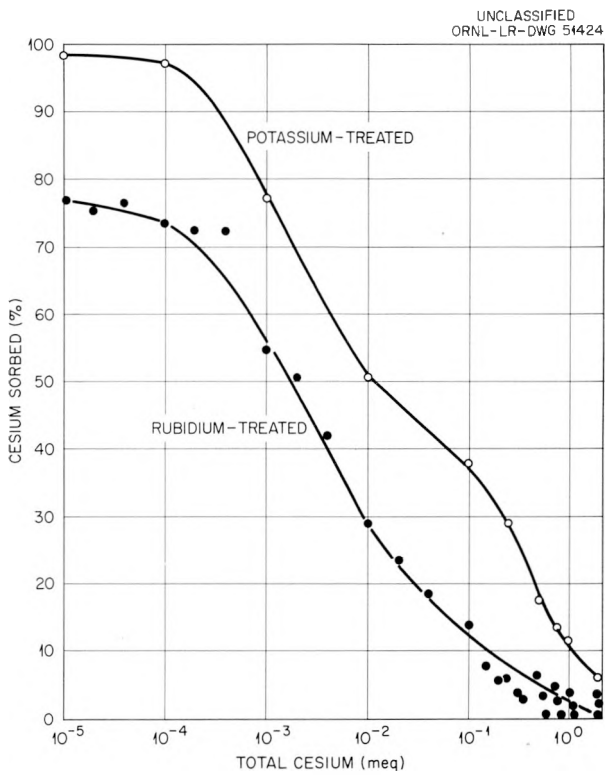

Fig. 1.20. Sorption of Cesium from 0.1 M $NaNO_3$ by 2 g of Vermiculite.

Conasauga shale in which rubidium offers more competition to cesium sorption than does potassium.[47]

In the development of soils under acid leaching conditions, aluminum moves from the lattice framework of the clay minerals into basal exchange positions. The interlayer aluminum may then prevent collapse of the layer lattice and thus inhibit interlayer cation fixation.[48-50] Although it would be impossible to reproduce these soil-forming conditions in the laboratory, time being an important parameter in soil development, an attempt was made to simulate the weathering product. Vermiculite was treated with 0.1 M $Al(NO_3)_3$ in 0.001 M HNO_3 to produce aluminum saturation of the exchange complex. The excess salt was removed with ethanol (95%), and the

---

[47] E. G. Struxness et al., H-P Ann. Prog. Rep. July 31, 1958, ORNL-2590, p 6-26.

[48] G. Brown, Clay Minerals Bull. 2, 54 (1953).

[49] C. I. Rich and S. S. Obenshain, Soil Sci. Soc. Am. Proc. 19, 334 (1955).

[50] T. Tamura, J. Soil Sci. 9, 141 (1958).

pH of the suspension was raised to 10 with NaOH to precipitate aluminum in the basal spacing. The excess salts were again removed with ethanol (95%).

The cesium sorption curves obtained for this aluminum-treated vermiculite are shown in Fig. 1.21. The response differs from that of the rubidium-treated vermiculite in that some interlayer exchange sites are available to the cesium. Thus, there is greater sorption of cesium in the range of higher cesium concentration. The presence of the interlayer aluminum hydroxide seems to prevent interlayer fixation, the aluminum hydroxide presumably preventing structural collapse. This response indicates that weathered vermiculites existing in natural soil formations may resist collapse with cesium treatment. The resistance to lattice collapse and to interlayer fixation may then be a means for studying the degree of alumination resulting from soil development processes.

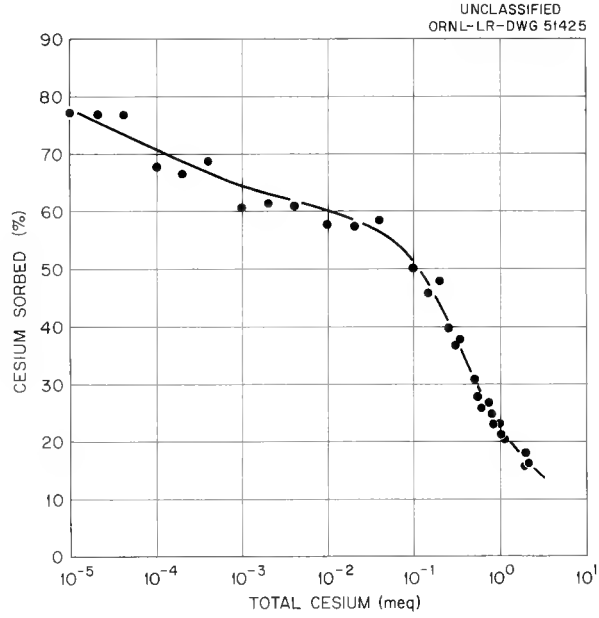

Fig. 1.21. Cesium Sorption from 0.1 M $NaNO_3$ by 2 g of Aluminum-Treated Vermiculite.

Desorption Studies

From consideration of structure in cesium sorption reactions, it appears that there are three types of sorbed cesium in the collapsed lattice systems: (1) easily exchangeable cesium (cesium retained by illite at high levels of cesium saturation), (2) cesium fixed at lattice edges

(cesium retained by illite, micas, potassium-treated vermiculite, and heat-treated bentonites at extremely low levels of cesium saturation), and (3) cesium fixed by entrapment during lattice collapse (cesium trapped by vermiculite at high levels of cesium saturation). The easily exchangeable cesium would be readily removed by a leaching cation, while cesium fixed at lattice edges would be displaced only by another ion having steric favorability for such an exchange site. On the other hand, entrapped ions would be liberated by those cations which would permit lattice expansion.[51] Desorption data (Table 1.14) show this to be true. Stable cesium is slightly more effective than hydrogen ions in the removal of easily exchangeable cesium from illite (column 2, Table 1.14), but is markedly more effective for removing the cesium fixed at the lattice edges of illite

[51] I. Barshad, Am. Mineralogist 33, 655 (1948).

Table 1.14. Desorption of Cesium from Vermiculite and Illite

Amount of Leaching Ion (meq)	Cesium Leached (%)			
	Illite		Vermiculite	
	a	b	c	d
		HCl		
1	27.8 ± 0.9	0.15 ± 0.05	0.15 ± 0.05	1.1 ± 0.1
5	66.4 ± 1.6	0.8 ± 0.2	0.5 ± 0.3	3.8 ± 0.4
10	82.2 ± 1.5	1.1 ± 0.3	1.0 ± 0.5	7.3 ± 0.7
50	91.9 ± 1.3	2.9 ± 0.5	2.4 ± 0.8	27.2 ± 1.5
100	94.0 ± 0.8	4.4 ± 0.7	3.7 ± 1.1	42.4 ± 2.0
500	96.6 ± 0.1	18.6 ± 0.8	12.0 ± 1.8	76.0 ± 3.2
		$CsNO_3$		
1	53.8 ± 1.4	4.1 ± 0.1	0.07 ± 0.03	2.6 ± 0.1
5	86.8 ± 0.8	9.8 ± 0.4	0.19 ± 0.11	3.1 ± 0.3
10	90.0 ± 0.4	15.6 ± 0.7	0.33 ± 0.23	3.6 ± 0.4

[a] Four-gram sample containing 0.272 meq cesium.

[b] Four-gram sample containing 0.990×10^{-5} meq cesium.

[c] Two-gram sample containing 0.518 meq cesium.

[d] Two-gram sample containing 0.618×10^{-5} meq cesium.

(column 3, Table 1.14). Hydrogen ions appear to be more efficient in effecting removal of cesium from vermiculite, though very little of the entrapped cesium can be removed unless the lattice is destroyed (column 4, Table 1.14). The inability of cesium to undergo isotopic exchange within the 1-hr contact time allowed attests to the tenacity with which these interlayer-fixed cations are held. Stable cesium may be less effective than hydrogen ions in desorbing cesium fixed at lattices edges in vermiculite (column 5, Table 1.14), because the addition of stable cesium for desorption would induce further collapse of the vermiculite lattices.

Cesium Sorption as Mineral Identification Technique

With the exception of vermiculite, the clays used in this work were assumed to be monomineralic. This assumption was justified, since the tests were designed to evaluate the influence of major structural differences. Since the cesium sorption reaction appears to be a sensitive indicator of the structural condition of the clay, it is thought that this method could be used to estimate the purity or monomineralic nature of clay minerals. Particularly suspect of heterogeneity is illite. According to Yoder and Engster,[52] Fithian illite which was used in these tests is a mixed-layer structure containing mica and montmorillonite. By using the heat treatment described above for bentonites, it was believed that the existence of the expanded lattice mineral (montmorillonite) could be demonstrated. Figure 1.22 shows the results for Fithian illite compared with several other minerals. The synthetic potassium fluorophlogopite did not show any increase in cesium sorption with heating; this response suggests that no further collapse of the fluorophlogopite lattice occurred. Indeed, the unheated fluorophlogopite did show a very sharp, well-defined, intense 10-A maximum when x rayed; this was in marked contrast to the diffuse, low-intensity 10-A maximum of unheated illite. The increase in cesium sorption after heating to 600°C is supporting evidence for the existence of expanded montmorillonite in illite samples.

These studies have further application than merely improving cesium sorption for application to waste disposal. The techniques help in the

[52]H. S. Yoder and H. P. Engster, Geochem. et Cosmochim. Acta 8, 225 (1955).

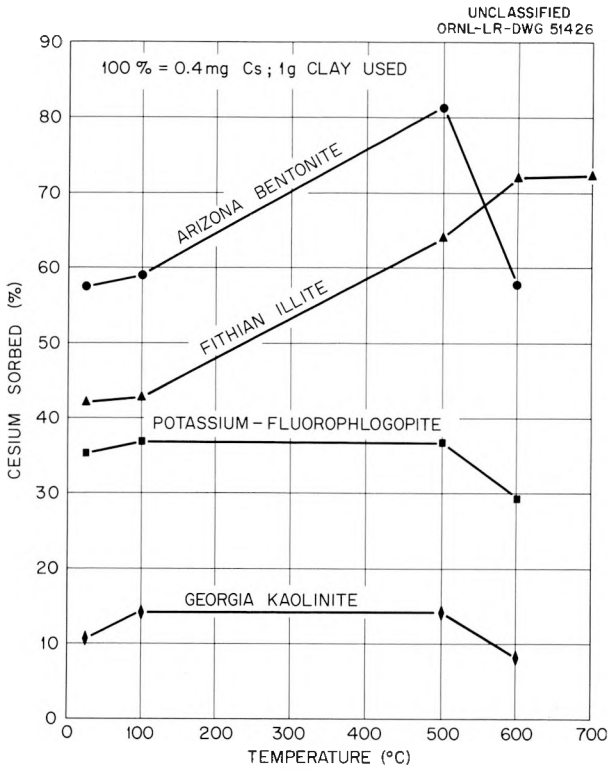

Fig. 1.22. Sorption of Cesium from 1.5 M $NaNO_3$ by Several Clays Previously Heated.

identification of complex mixed-layer systems of clay minerals such as illite. It also shows that ion exchange studies with clay minerals cannot neglect the structural aspects for complete characterization of the reaction. Further work is proceeding on a more exact determination of lattice collapse by use of x-ray diffraction techniques with careful control of temperature, humidity, and time.

Strontium Removal Using Phosphates

Clay minerals normally do not exhibit an outstanding affinity for strontium; hence, waste treatment or disposal techniques cannot depend upon these clay minerals for effective removal of strontium. In order to identify and develop materials suitable for strontium decontamination of wastes, several approaches were taken. One material found to be suitable was apatite (rock phosphate); another promising mineral found to have a relatively high affinity for strontium was variscite. The use of rock phosphates in column applications was an attractive possibility,

since they are commercially available at reasonable cost; studies more directly related to column technique are described in a separate section. Also, the extension of phosphatic coagulation methods for strontium removal seemed worthwhile. Aluminum phosphate coagulation appeared particularly promising and much work was done characterizing the system. This work is reported in the section on low-level waste water treatment. The discussion here is limited to general applications and variables which must be considered.

Mineral Phosphate Reactions

The hazard of Sr^{90} is related to its concentration in phosphate portions of the skeletal system. It is natural then that compounds associated with the phosphate anion be considered for applications in waste disposal. Thus, calcium phosphate floc formation was investigated as a method for removing strontium from contaminated water.[53] It has also been reported that calcareous soils are effective for removing strontium from low-level wastes containing dissolved phosphates. The mechanisms proposed include the formation of calcium phosphate (apatite) with strontium substituting isomorphously.[54]

Samples of naturally occurring rock phosphate from Florida (Florida pebble phosphate – 80% apatite) and from Tennessee (Tennessee rock phosphate – 45% apatite) were obtained from the Tennessee Valley Authority. Numerous exploratory tests were made to evaluate these materials. It was found that strontium removal was improved by increasing the pH of the system (see Table 1.15). Particle size and solution-phosphate contact time were found to be significant parameters in removing strontium from waste solutions. Note the strontium removal by Florida pebble phosphate in Fig. 1.23. Finer particles and longer contact times improved strontium removals.

The observation that rock phosphate minerals can remove strontium from wastes suggested the use of variscite. Rock phosphates are hydroxy

[53]R. A. Lauderdale, Ind. Eng. Chem. 43, 1538 (1951).

[54]L. L. Ames, Jr., J. R. McHenry, and J. F. Honstead, Proc. U.N. Intern. Conf. Peaceful Uses Atomic Energy, 2nd, Geneva, 1958 18, 76 (1958).

Table 1.15. Effect of pH on the Removal of Strontium from 1 M $NaNO_3$ Solutions

Solution-mineral contact time: Tennessee, 15 min; Florida, 60 min
Solution: 150 ml, containing 6 mg Sr
Mineral: 1 g, no size segregation

Tennessee Rock Phosphate		Florida Pebble Phosphate	
pH	Removal (%)	pH	Removal (%)
7.0	6.16	7.0	1.59
8.7	10.5	7.9	8.80
10.8	28.4	9.6	61.6
11.7	42.8	11.5	94.6

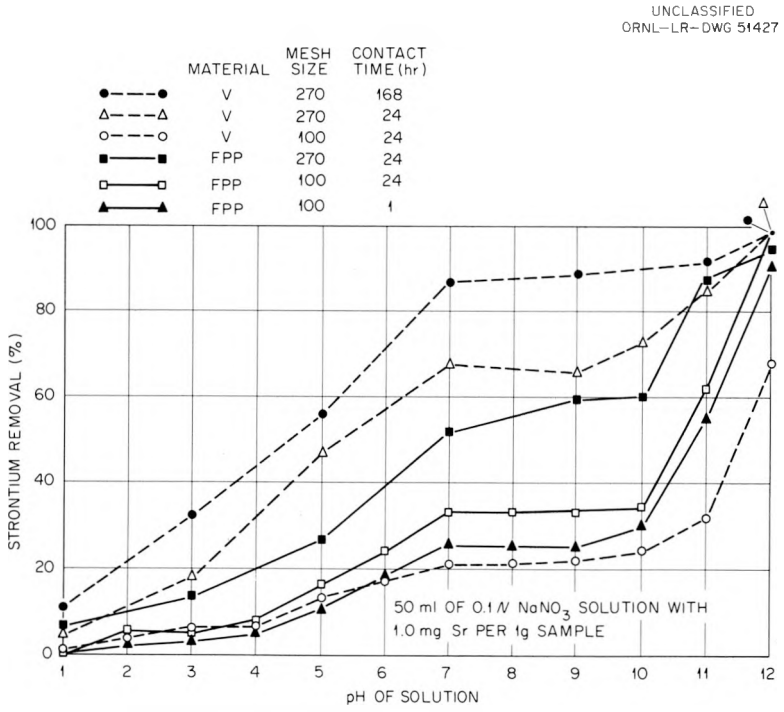

Fig. 1.23. Influence of Particle Size and Solution-Solid Contact Time on Strontium Removal by Variscite (V) and Florida Pebble Phosphate (FPP).

calcium phosphates; variscite is a hydroxy aluminum phosphate. Calcium phosphates are known to be soluble at slightly acid pH; aluminum phosphates are highly insoluble at slightly acid pH. Perhaps even more suggestive is the fact that nature synthesizes aluminum-strontium phosphate (crandallite).

The varisctie used in the experiments was obtained from Ward's Mineral Establishment. It was ground to pass a 100-mesh sieve for use in the slurry tests. Initial testing showed that increased amounts of strontium were sorbed from waste solutions with decreasing particle size (see Fig. 1.23). It was also noted that contact time was important; strontium removal increased with increasing solution-mineral contact time.

In Fig. 1.23, strontium sorption by variscite is compared with sorption by Florida pebble phosphate. The greater removal of strontium by Florida pebble phosphate in the coarser size range is believed to be due to the greater surface area of the more porous particles of the Florida sample. With decreasing particle size the effect of porous structure is nullified; variscite then is more effective than pebble phosphate.

With variscite of 170-mesh size at pH 7.0, a sorption curve was determined at several contact times (see Fig. 1.24). The type of response

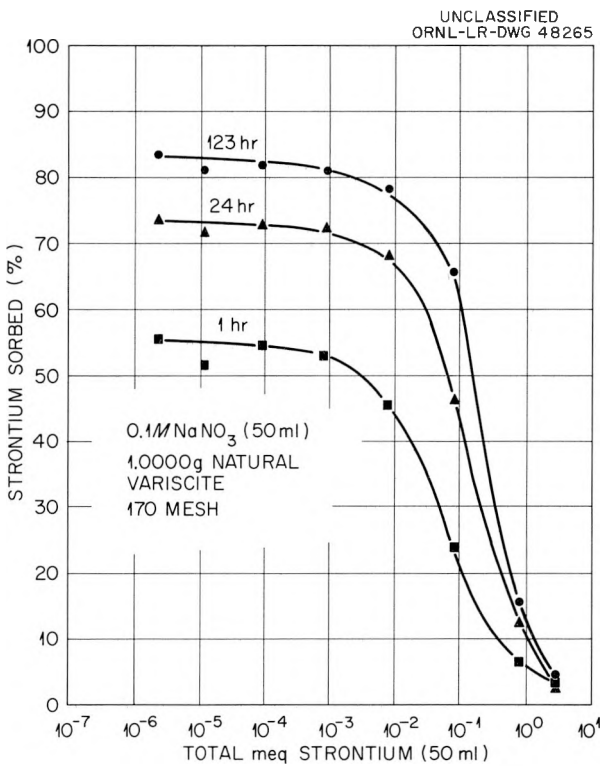

Fig. 1.24. Strontium Sorption by Variscite as a Function of Strontium Concentration and Time.

noted for this reaction is similar to the type observed for cesium-kaolinite.[55] The reaction can be explained on the basis of an ion exchange reaction, assuming a single equilibrium coefficient.

In Fig. 1.25, the removal of strontium as a function of the weight of variscite is shown. Strontium removals by commercially available $AlPO_4$

[55]D. G. Jacobs and T. Tamura, "The Mechanism of Ion Fixation Using Radio-Isotope Technique," presented at the 7th International Congress of Soil Science, Aug. 14–24, 1960, Madison, Wisconsin.

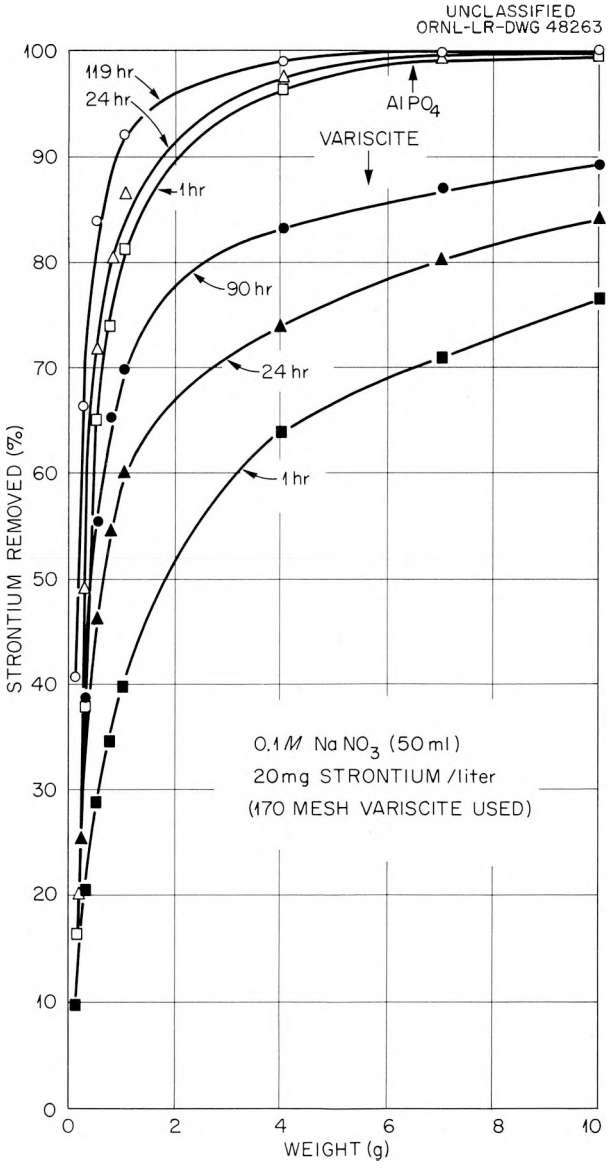

Fig. 1.25. Strontium Sorption – Variscite vs $AlPO_4$.

are also shown. The sorption curves are typical in both cases. Although $AlPO_4$ is more effective per unit weight, this material settles as a flocculent mass in contrast to the granular nonswelling variscite. In both cases, the pH was maintained at neutral.

These results suggest the possible use of variscite and apatites (Florida pebble phosphate or Tennessee rock phosphate) for waste treatment; the behavior of these minerals in actual waste solutions is described elsewhere.

Phosphate Precipitation Reactions

Calcium phosphate precipitation for removing strontium from contaminated water is effective at high pH.[53] For treatment of water for human consumption, this pH is unduly high. The mineral phosphate studies suggested the use of aluminum phosphate precipitation as a method for removing strontium from contaminated water at neutral pH, and it was of interest to compare calcium phosphate precipitation with the aluminum phosphate system.

Precipitation was accomplished by dissolving a known amount of NaH_2PO_4 in a simulated waste water containing 0.1 M $NaNO_3$. For most of the tests, the PO_4^{---} concentration was 0.02 N. Under these conditions a strontium concentration of 1.1×10^{-5} M (i.e., 1 mg/liter) remained in solution up to a pH of 12 for over 40 hr. Higher strontium concentrations at pH 12 would produce strontium phosphate.

The strontium removed by calcium and aluminum phosphate flocs at different pH is shown in Fig. 1.26. At low pH, the aluminum phosphate floc is much superior to the calcium phosphate floc; however, at pH 12, very little strontium was removed by the aluminum phosphate floc. At this pH little or no precipitate was observed in the aluminum phosphate system; obviously the aluminum phosphate is soluble at this pH. At pH 6 the calcium phosphate was soluble and little or no precipitate was observed. Increasing the aluminum or calcium concentration did not improve strontium removal. At pH 9, increasing the calcium concentration from 0.37 meq to 0.67 meq reduced the removal of strontium from 85 to 54%. This reduction

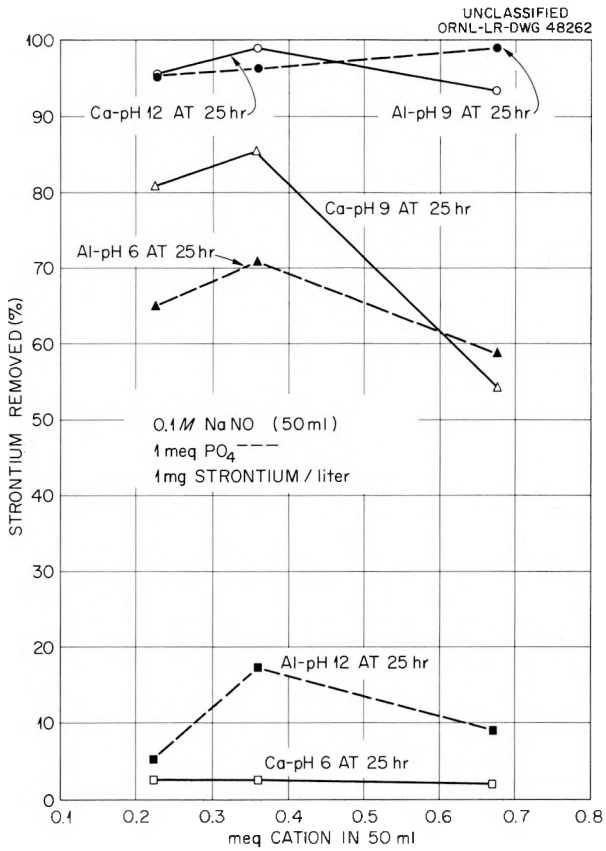

Fig. 1.26. Phosphate Precipitation of Strontium with Ca^{++} and Al^{+++}.

was even more striking since with increasing contact time (95 hr) the 0.23-meq sample removed 95% and the 0.37-meq sample removed 93%, while the 0.67-meq sample continued to remove only 55%.

The reaction involved in the calcium phosphate system is complex and difficult to interpret. Figure 1.27 shows the removal of strontium and calcium as a function of calcium concentration. Although there is a sharp reduction of strontium removal at 0.75-meq calcium concentration (15 mg per 50 ml), the amount of calcium phosphate formed has increased, as evidenced by the continued removal of calcium. This response is difficult to interpret without additional data; studies are now in progress to elucidate the factors responsible. The influences of pH, sodium nitrate concentration, time, and temperature are being investigated along with the complex interaction of aluminum, calcium, and phosphate.

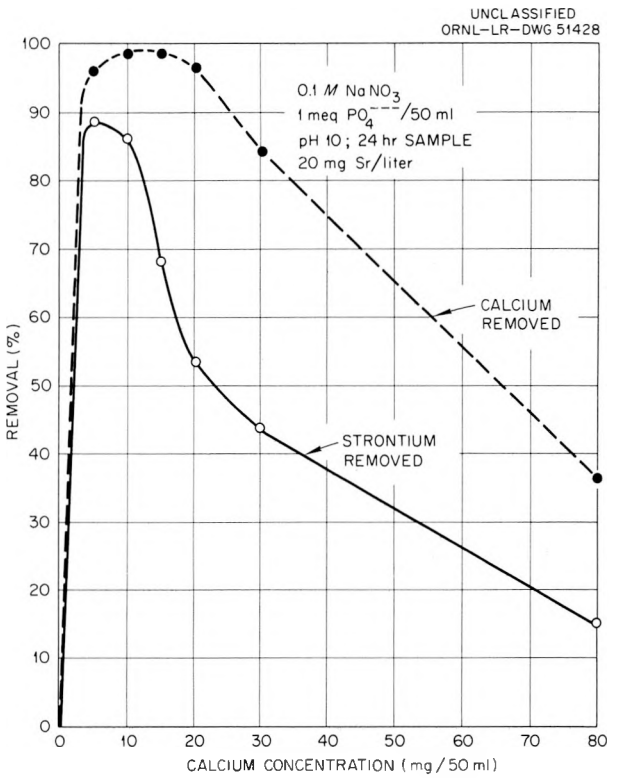

Fig. 1.27. Removal of Calcium and Strontium as a Function of Calcium Concentration.

Alumina and Improved Vermiculite Columns

The phosphate system for strontium removal has been applied in a column study by using mineral apatites and variscite, and in a precipitation technique with dissolved aluminum and phosphate. The possibility of employing precipitation principles in a column was suggested by the studies on aluminum phosphate reactions. The system consisted of powdered alumina (Al_2O_3) packed in a glass column through which the waste solution, containing a known concentration of sodium phosphate, was passed. The waste solution was adjusted to a pH of 7.0.

The comparative responses with equal weights of alumina, iron oxide, and vermiculite are shown in Fig. 1.28. Note the excellent removal of strontium by the alumina column. In Fig. 1.29 is shown the improved strontium removal by the vermiculite column resulting from an increase in phosphate concentration in the waste. Vermiculite is normally saturated with calcium ions, and these ions can be replaced by sodium ions in the waste. By introducing phosphate into the waste solution, it was expected that

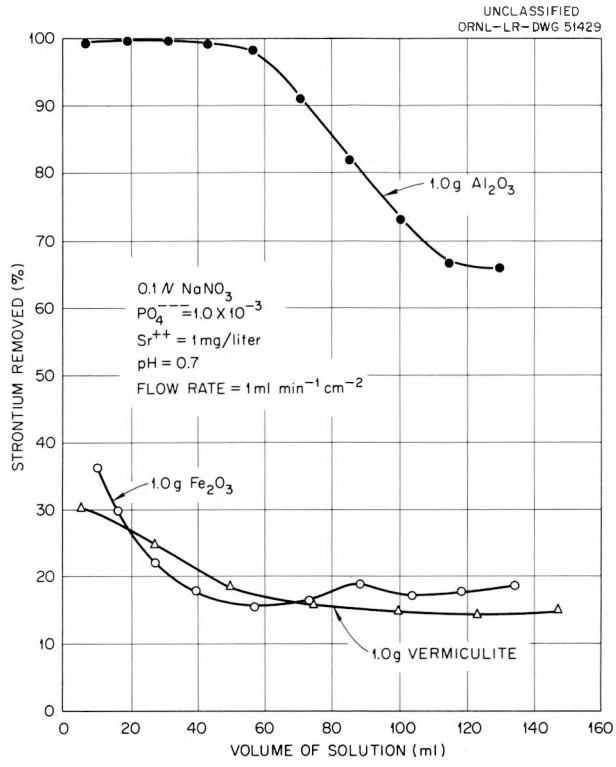

Fig. 1.28. Removal of Strontium by Use of Several Materials.

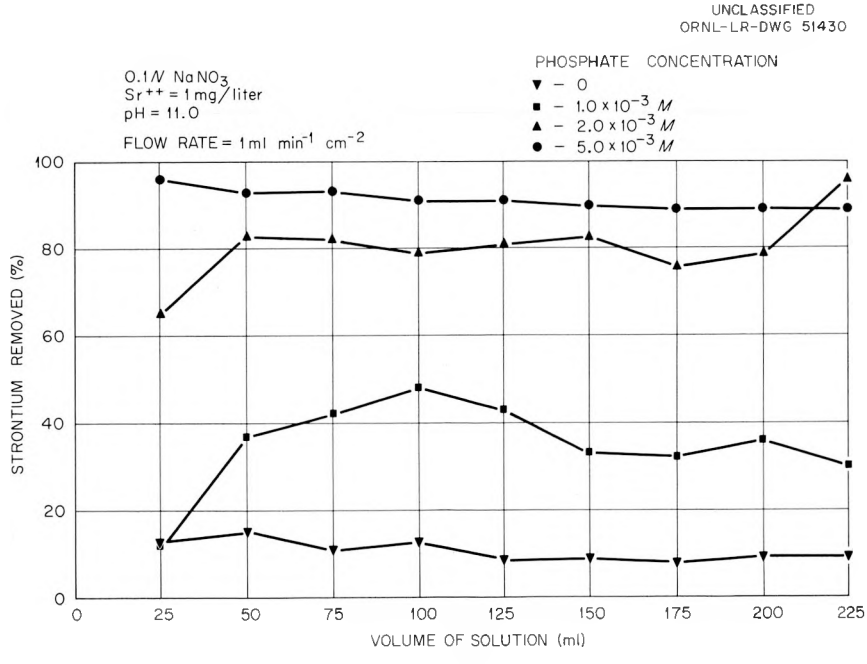

Fig. 1.29. Strontium Removal by Vermiculite as Influenced by Phosphate Concentration.

calcium phosphate would be formed, and at high pH the removal of strontium would be substantially improved. The results show that increasing phosphate concentration does improve strontium removal from waste, but the proposed mechanism of removal is subject to question. Studies will continue with vermiculite in jar tests as well as with columns. In addition to the studies of cesium and strontium, work on the possible removal of ruthenium, cobalt, and zirconium-niobium by clays and other materials will continue.

SOIL COLUMN STUDIES

D. G. Jacobs K. E. Cowser
E. R. Eastwood O. M. Sealand
K. T. Thomas[56]

The study of ion exchange commenced with the study of the reaction observed when manure salts were passed through natural soil. Since that time the ion exchange processes in the soil have been widely studied and documented. It is not surprising, then, that the ion exchanging property of the soil has been used in the decontamination of nuclear waste streams. The major use of the decontaminating ability of the soil at ORNL has been in the disposal of intermediate-level wastes to seepage pits dug in Conasauga shale, though clay minerals have been added in the treatment of process waste water to improve cesium removal.

The seepage pits do a rather effective job in the decontamination of the intermediate-level waste stream before it reaches the surface waterways of White Oak Creek and the Clinch River, but there has been an increasing concern over the lack of control that can be exercised once the wastes have been discharged to the pits. And, although some limits can be estimated, it is not possible to delineate the precise boundaries of the hazardous nuclides in the Conasauga shale. Other objections to the present seepage-pit system are evident and have been noted by de Laguna.[57] The use of a soil or mineral-filled column looks very attractive, as it would eliminate

[56]Alien guest from Atomic Energy Establishment, Trombay, Bombay, India.

[57]W. de Laguna, "Liquid Waste Seepage Pits at ORNL: Disadvantages and Proposed Changes," memorandum to E. G. Struxness, March 1959.

many of the objections to the present seepage-pit system, yet provide an efficient and inexpensive method for waste decontamination. The quality of the effluent could be accurately monitored and controlled, and the exact definition of the boundaries of the sorbed nuclides would be established.

With this in mind, the results of studies on the sorptive behavior of the various clays, clay minerals, and other minerals were scanned to determine which of these materials might be suitable for the decontamination of the intermediate-level waste stream. Two major criteria were considered: (1) the sorptive characteristics of the mineral for cesium and strontium and (2) the physical properties pertaining to stability and transmission of solution. Although ability to transmit water is a limiting property for column application, it is possible to devise schemes for improving the necessary physical properties. Thus, if the sorptive properties of a material are sufficiently high, it would be justifiable to spend some effort in modification of the physical properties.

Cesium Sorption

Cesium-137 presently constitutes the most abundant radionuclide in the intermediate-level waste stream, on the basis of activity. Thus, the operating behavior of a mineral-filled column might be governed primarily by the cesium-breakthrough properties. Previous geochemical studies had revealed that several materials show a high selectivity for cesium compared with sodium, especially those layer-lattice minerals capable of maintaining a collapsed lattice. These cesium-selective materials were considered for column application.

Slurry Studies

The most direct measure of the decontaminating effectiveness of a mineral is the K_d (i.e., the ratio of cesium sorbed per gram of mineral to the cesium remaining unsorbed per milliliter of solution). If the sorption capacity of a column were completely utilized, the weight of the column bed (in grams) multiplied by the K_d would give the volume of solution (in milliliters) that the column was capable of decontaminating. More realistically, the K_d can be used to estimate the 50% break-through volume; the degree of utilization of the column will be measured by the slope of the break-through curve.

Several materials were evaluated for cesium sorption (see Table 1.16). The solution was composed of 0.3 M $NaNO_3$, 0.2 M NaOH, and contained the mass equivalent of approximately 1 μc of Cs^{137} per milliliter. One hundred milliliters of solution was employed, and the weight of mineral ranged from 0.1 to 1.28 g. A 24-hr contact was allowed, and the K_d's were calculated for the solution-solid ratio giving approximately 50% cesium removal.

Table 1.16. The Cesium Decontaminating Ability of Various Minerals

Mineral	K_d (ml/g)
Illite	7000
Conasauge shale	4200
Potassium-treated Arizona bentonite, heated at 600°C for 3 hr	2900
Potassium-treated Wyoming bentonite, heated at 600°C for 3 hr	640
Clinoptilolite	570
Potassium-treated vermiculite	500
Shalite	370
Ammonium-treated vermiculite	90
Natural vermiculite	70
Wyoming bentonite	90
Arizona bentonite	170

There is a hundredfold range in the cesium decontaminating ability of these minerals, but all of them were satisfactory for the decontamination of the intermediate-level waste stream. The collapsed-lattice mineral, illite, and the illite-bearing Conasauga shale ranked very high, as expected. Potassium treatment and heat treatment of the two bentonites to cause lattice collapse markedly improved their capacity for cesium decontamination. Later work[58] revealed that even more pronounced improvement in the response of the bentonites could be realized by controlling the temperature and the

[58]T. Tamura and D. G. Jacobs, "Improving Cesium Selectivity of Bentonite by Heat Treatment," submitted for publication in Health Phys.

time of heating. Potassium treatment of vermiculite to cause collapse of the layer lattice also resulted in an increase in cesium sorption. Surprisingly, ammonium treatment did not result in improved cesium removal. Subsequent studies with exfoliated vermiculite showed that heat treatment improved the cesium sorptive properties of the vermiculite by a factor of 15 to 20. (The vermiculite is subjected to a high temperature for a short time. The rapid escape of steam from the interlayer water of hydration results in an expansion of the vermiculite particles.)

A second parameter investigated according to slurry techniques was the time dependency of the cesium sorption reaction. It is necessary for the reaction to proceed with sufficient rate that the waste stream is decontaminated satisfactorily while passing through the column. Although the vermiculites and the illitic materials showed a time-dependent reaction (Table 1.17), this disadvantage is offset in each case by the fact that selectivity for cesium is greater as the cesium concentration is decreased. The net effect in column operation is that the break-through curve is diffused by the slow reaction but sharpened by the increased selectivity for cesium as cesium concentration is reduced while passing through the column. The cesium content of the initial increments of solution passing through the column would be controlled by a balance of these factors, but the column loading would be governed by the total operating time of the column.

Because of their fine particle size, illite and the bentonites are not especially well suited for direct column application, though further improvement in their physical properties might be possible. Conasauga shale exists in rather large aggregates, but it tends to disintegrate in water. Clinoptilolite has very good physical as well as cesium-sorptive properties, but it is not yet known whether it would be commercially available in quantity. Because of the ability of vermiculite to transmit water readily, and because it is readily available, it was chosen for initial column testing. It was not intended that the other materials would be neglected, but it was felt that the use of vermiculite would reduce the problems of engineering design. If mineral-filled columns work satisfactorily, improvement in the filler material can be made at a later date.

Table 1.17. Time Dependency of the Cesium Sorption Reaction for Various Materials

Time (hr)	K_d (ml/g)							
	Illite	Shalite	Arizona Bentonite (heated)	Wyoming Bentonite (heated)	Clinoptilolite	Conasauga Shale	Potassium Treated Vermiculite	Natural Vermiculite
0.083	1520	65	5900	450	90	900	60	11
0.25	3200	90	7800	1050	350	1620	80	22
0.50	3800	140	6600	940	520	2050	100	27
1.0	4190	135	4900	760	560	2440	120	30
2.0	4440	140	4660	850	520	2900	135	38
5.0	4470	200	4670	865	300	3200	170	44
10	4800	215	4770	890	460	3500	230	51
20	5475	250	4950	930	590	3800	345	66
50	5860	290	5030	940	620	4400	480	94
100	6190	340	5320	1000	620	4900	750	111
200	6590	365	5300	1000	610	5010	1140	144
500	7330	360	5390	900	560	5100	1800	193
1000	7620	355	5990	900	560	5600	2180	220

Column Studies

The saturation capacity of a material is not a complete measure of its decontaminating ability in column operation, because columns are somewhat less than 100% efficient. There are several equations used to describe the S-shaped break-through curve observed for ion exchange columns, but because of its simplicity, the Glueckauf equation[59] was chosen to measure the operating efficiency of the laboratory columns. This equation is written as follows:

$$\frac{C}{C_0} = \frac{1}{2} - A_e\left(\sqrt{N}\,\frac{V - \bar{V}}{\sqrt{V}\,\bar{V}}\right), \qquad (1)$$

where

C = the concentration of activity in the effluent after a given volume has passed through the column (put-through volume),

C_0 = the concentration of activity in the influent,

A_e = the area under the normal curve for the argument in parentheses,

N = the number of theoretical transfer units or plates,

V = the put-through volume,

$\bar{V}$ = the 50% break-through volume.

The slope of the curve obtained when C/C_0 is plotted on a probability scale vs the square root of the volume of solution passed through the column is represented by N. Thus, it is an expression for the slope of the break-through curve and is a measure of the operating efficiency of the column. A higher number of theoretical plates means that a greater percentage of the loading capacity of the column can be utilized before a given break-through is exceeded. The number of theoretical plates in a column can be computed from the break-through data. This is conveniently done by setting the value of the expression in the parentheses in Eq. (1) equal to 1. In this case C/C_0 equals 0.1587, and an expression for N can be written by rearrangement,

$$N = \frac{V\,V'}{(\bar{V} - V')^2}, \qquad (2)$$

[59] E. Glueckauf, Trans. Far. Soc. 51, 34 (1955).

where N and $\bar{V}$ have the same significance as in Eq. (1), and V' is the volume required for 15.87% break-through.

The composition of the simulated waste solution is given in Table 1.18. The more dilute solution (1) was used in initial studies to provide accurate effluent measurements from short vermiculite columns. In later evaluations larger columns were used, and the stable-element composition was increased (solution 2). The use of solutions having two stable-element compositions also makes it possible to extrapolate results in order to consider the effect of increasing or decreasing the total ionic concentration of the waste stream.

Table 1.18. Composition of the Experimental Solutions

Salt	Concentration (M)		
	Solution 1	Solution 2	Solution 3
$NaNO_3$	0.032	0.32	0.32
NaOH	0.022	0.22	0.22
NH_4NO_3	0.0025	0.025	0.025
$Al(NO_3)_3$	0.0022	0.022	0.022
Na_2SO_4	0.0037	0.037	0.037
NaCl	0.0006	0.006	0.006
Cs^{137} mass equivalent	2 μc/ml	2 μc/ml	
Sr^{90} mass equivalent			0.1 μc/ml

Studies were made in order to determine the effect of flow rate, column length, and time of contact on the sorption of cesium by vermiculite ore (BO-4, obtained from the Zonolite Co., Traveler's Rest, South Carolina) was used. The columns were filled by pouring a suspension of the vermiculite into a column half-filled with water. The column was then back-washed to remove fines and air pockets. The results are shown graphically in Figs. 1.30–1.32. Analysis of these data revealed three important points: (1) The break-trhough curves are not symmetric about the 50% break-through point but are sharper at low break-through, becoming more diffuse as the percentage of break-through increases. (2) There is

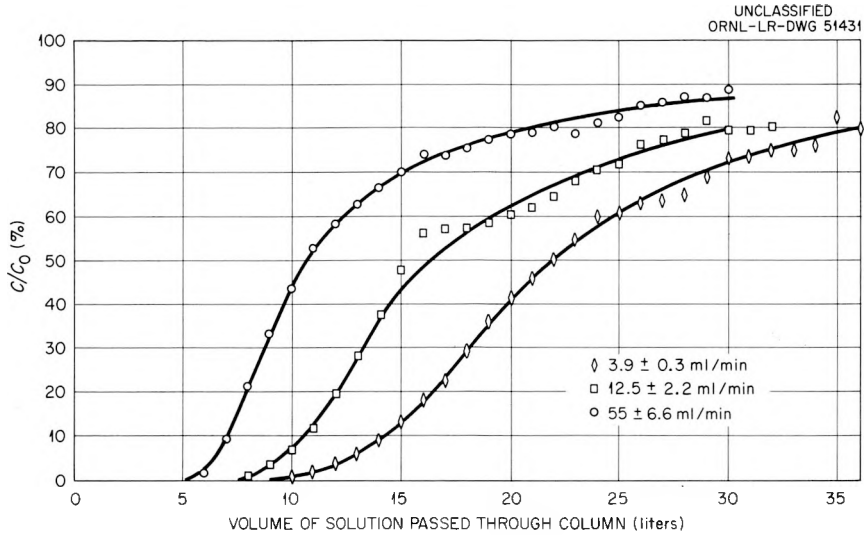

Fig. 1.30. The Effect of Flow Rate on Cesium Sorption by Vermiculite.

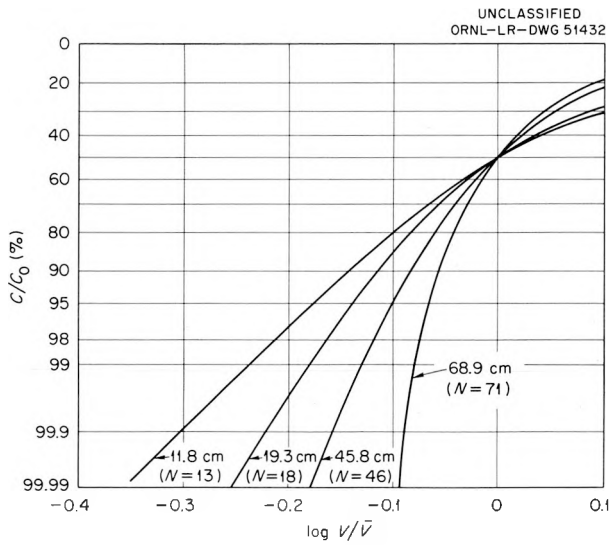

Fig. 1.31. The Effect of Column Length on the Relative Slope of the Cesium Break-Through Curve.

an increase in the cesium loading capacity as contact time increases. (3) The number of theoretical plates, calculated from the 15.87 and 50% break-through volumes, is proportional to the height of the column, the effective height of a theoretical plate (EHTP) being approximately 1 cm.

The asymmetric break-through curves are a result of the slow reaction rate of cesium sorption on vermiculite and are suggestive of particle

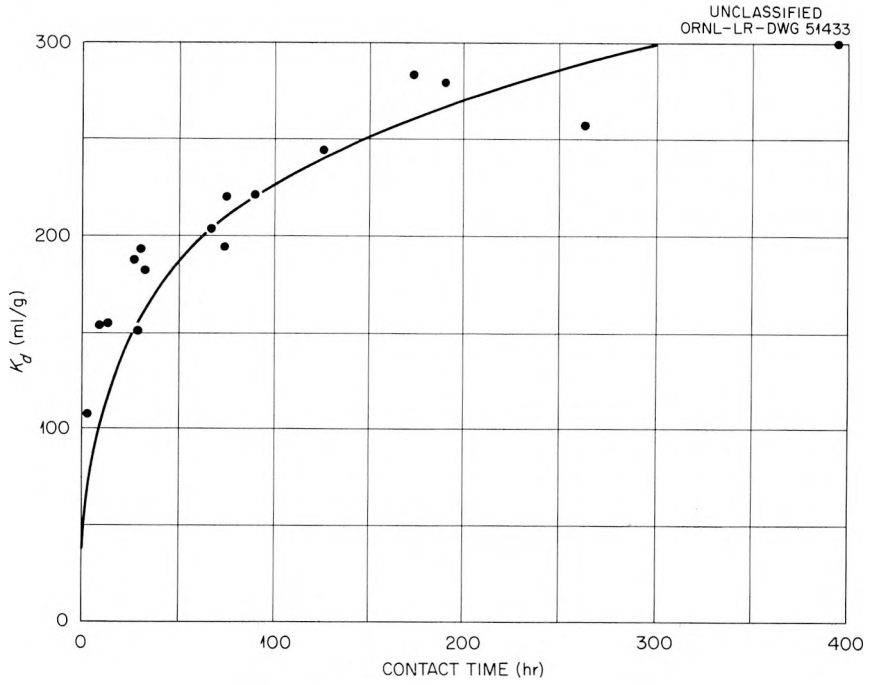

Fig. 1.32. The Effect of Column Operation Time on the Loading Capacity of Vermiculite Columns.

diffusion.[60] It is reasonable to assume such a rate-controlling process because of the layer lattice structure of the vermiculite. The exchange sites lie primarily within the basal spacings of the lattice, and there is some steric impedance as the cesium migrates to these sites. However, from a practical point of view, interest is focused only on rather low break-through percentages so that particle diffusion is primarily of interest in that the time of column operation will markedly affect the cesium loading capacity. The break-through curve is even sharper at low break-through than in the 15.87 to 50% break-through range so that the estimation of the number of theoretical plates is conservative.

The effect of contact time (column operating time) on K_d is shown in Fig. 1.32. The points were obtained experimentally from column studies, and the line represents the shape of the time-dependence curve obtained by slurry studies. The two are not directly comparable because both the

[60] E. Glueckauf, "Principles of Operation of Ion Exchange Columns," in Ion Exchange and Its Applications, Society of Chemical Industry, London, 34-46 (1954).

stable element and the cesium concentration differed, but the general shape of the curves is the same. The slurry studies on time dependence are still being carried on, and K_d is continuing to increase even after six months of contact time; it is reasonable to assume a similar increase would be observed with increased time of column operation. The decreased capacity of the vermiculite columns with increasing flow rate (see Fig. 1.30) can be explained on the basis of the effective contact time.

The stable-element concentration of the simulated waste was increased to the full strength of the intermediate-level waste (solution 2, Table 1.18) for the evaluation of the various commercial grades of vermiculite. Also included in the evaluation were a potassium-treated vermiculite (KBO-4), clinoptilolite, and Florida pebble phosphate. For these tests, a constant flow rate of approximately 1 ml cm^{-2} min^{-1} was used.

When the concentration of competing cations was increased tenfold from the previous experiments, the K_d was reduced by about a factor of 10, as predicted from mass action considerations. The EHTP for particle diffusion controlled exchange is nearly inversely proportional to the K_d (ref 60) so that an increase in K_d is accompanied by a decrease in EHTP. This is shown in Fig. 1.33. The increased concentration of NaOH also resulted in an initial movement of $Mg(OH)_2$ from the column as sodium replaced the native magnesium from the vermiculite.

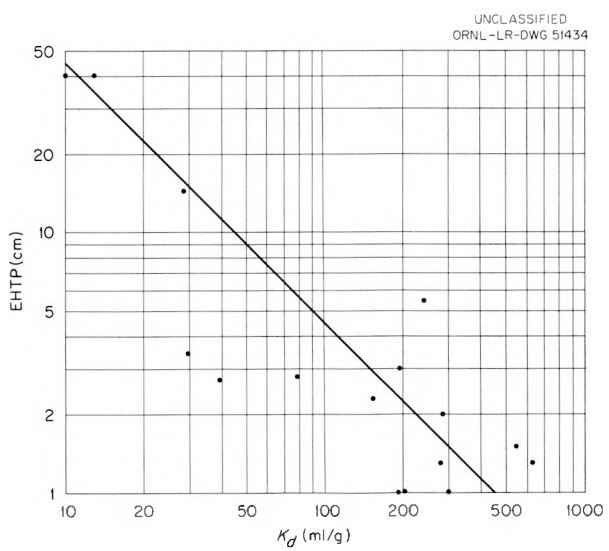

Fig. 1.33. The Relationship Between EHTP and K_d for Vermiculite Columns.

There is a strong dependency of K_d and EHTP on the particle size of the vermiculite ores (BO-series, Table 1.19), the K_d increasing with decreasing effective particle size. Potassium treatment of the vermiculite (KBO-4) to produce a collapsed lattice resulted in a definite increase in K_d, but the effect was not so pronounced as that noticed in the slurry studies. This is probably due to the fact that the solution leaching through the column caused a continuing replacement of interlayer potassium with sodium, permitting re-expansion of the lattice. In this study, no addition of potassium to the solution was made for maintaining a collapsed lattice.

Heat treatment of the vermiculite (BE-3, BGF-23, BGF-35) resulted in a very marked increase in K_d, and particle diffusion was no longer observed. The BE-3 vermiculite also transmitted water much more rapidly than the ores,

Table 1.19. Evaluation of Materials for Removal of Cesium from the Intermediate-Level Waste Stream

Description of Material	Size Range (mesh)	EHTP (cm)	K_d (ml/g)
Vermiculite ore (BO-1), mechanically cleaned	6	40.5	9.9
Vermiculite ore (BO-2), mechanically cleaned	6–12	40.1	12.8
Vermiculite ore (BO-3), mechanically cleaned	8–20	14.5	28.3
Vermiculite ore (BO-4), mechanically cleaned	20–65	3.4	29.6
Vermiculite ore (BO-5), flotation product	40–100	2.7	39.3
Exfoliated vermiculite (BE-3)	6–14	12.4	523
Exfoliated vermiculite, H_2SO_4 treated, ball-milled (BGF-35)	30–50	1.5	547
Exfoliated vermiculite, H_2SO_4 treated, ball-milled (BGF-23)	20–30	1.3	630
Potassium-treated vermiculite (KBO-4)	20–65	2.8	77.6
Florida pebble phosphate		22.6	4.7
Clinoptilolite	20–35	3.9	524

and although hydraulic tests have not yet been made of this material, it seems that the head loss across a column would be less than that observed for the corresponding ore. On the other hand, it was more difficult to pass solution through the ball-milled BGF materials than through the ore.

Clinoptilolite showed the same K_d as the exfoliated vermiculite, but it is a much denser material. This means that on a weight basis the two materials would behave nearly the same, but that the clinoptilolite would be more effective in columns of equal dimensions. Florida pebble phosphate was tested because it is a likely material for use in removing strontium from the waste stream. This material showed little specificity for cesium removal so that including it in a column would result in little improvement in cesium removal, and the expected cesium removal would be governed by the amount and the effective height of the vermiculite of clinoptilolite in the column.

Strontium Sorption

Although the Sr^{90} activity of the intermediate-level waste stream is much less than that of Cs^{137}, it constitutes a greater hazard. The clay minerals selectively remove strontium from highly basic sodium solutions, but the phosphatic minerals have been found to be much more effective.[61] Therefore four materials were investigated for strontium removal; vermiculite, variscite (an aluminum phosphate mineral), Florida pebble phosphate, and Tennessee rock phosphate. The latter two materials are commercial calcium phosphate fertilizers and are readily available.

Slurry Studies

Slurry tests were made to determine the order of magnitude of the sorptive capacities of these materials for strontium from the intermediate-level waste stream (solution 3, Table 1.18). Increments of the material were added to 100 ml of solution tagged with Sr^{85}; they were shaken and allowed to stand overnight. These slurry tests were made with powdered samples, except for vermiculite, in which the BO-4 ore was used. Strontium sorption was estimated by comparing the activity in the supernatant liquid

[61] E. G. Struxness et al., H-P Ann. Prog. Rep. July 31, 1959, ORNL-2806, p 59.

with the initial activity, using a NaI(Tl) scintillation crystal and a binary scaler. The results of these tests (Fig. 1.34) show that the phosphatic minerals are much superior to vermiculite for strontium removal. Values of K_d at 50% strontium removal were as follows: variscite (5000), Tennessee rock phosphate (1000), Florida pebble phosphate (1000), and vermiculite (25). Because powdered samples were used, the results are higher than would be expected for the coarser materials that would be used in columns.

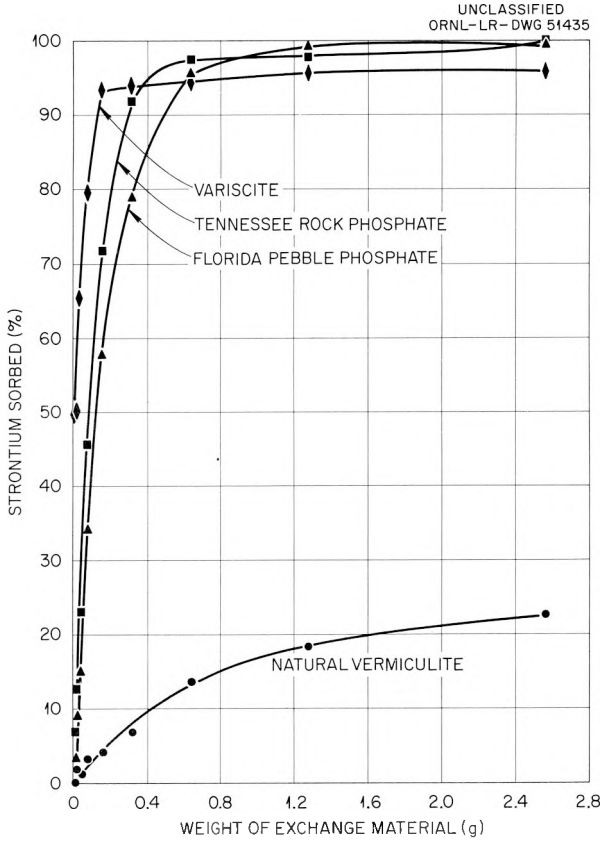

Fig. 1.34. The Sorption of Strontium from Intermediate-Level Wastes by Various Minerals.

Work at HAPO[62,63] suggested that addition of soluble phosphate to the highly basic waste solution would improve strontium removal by vermiculite. Two series of tests were run, one with vermiculite as the sorbent material and a second using vermiculite-limestone. Addition of phosphate resulted

[62]D. W. Rhodes, Soil Sci. Soc. Am. Proc. 21, 389 (1957).

[63]J. R. McHenry, Soil Sci. Soc. Am. Proc. 22, 514 (1958).

in remarkable improvement in strontium removal, 100 ppm PO_4^{---} being a satisfactory concentration (see Fig. 1.35). Addition of limestone improved strontium removal even further.

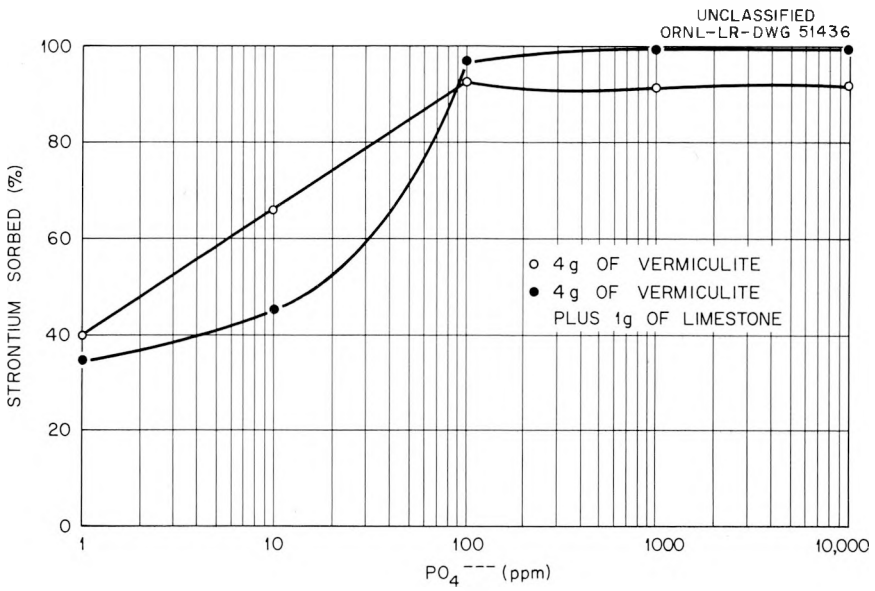

Fig. 1.35. The Effect of Phosphate and Limestone on the Removal of Strontium from Solution by Vermiculite.

Strontium sorption by these materials was adversely affected by decreasing the solution pH. Reducing it to 9 to 10 affected strontium removal by vermiculite to a greater extent than for the phosphates (see Fig. 1.36). At lower pH all materials were ineffective. Figure 1.37 shows the effect of pH on strontium removal by Florida pebble phosphate.

There was a general increase in strontium removal with addition of calcium up to 1000 ppm Ca^{++}, but sodium concentration changes had no effect over a range of 0.22 to 0.52 M Na^{+}. The mass equivalent of Sr^{90} was varied from 0.1 μc/ml to 50 μc/ml, with no apparent effect on the efficiency of strontium removal.

Column Studies

The above materials, plus exfoliated vermiculite (BE-3), were evaluated by column techniques. The materials were used as-received and backwashed for removal of fines before commencing column operations. A flow

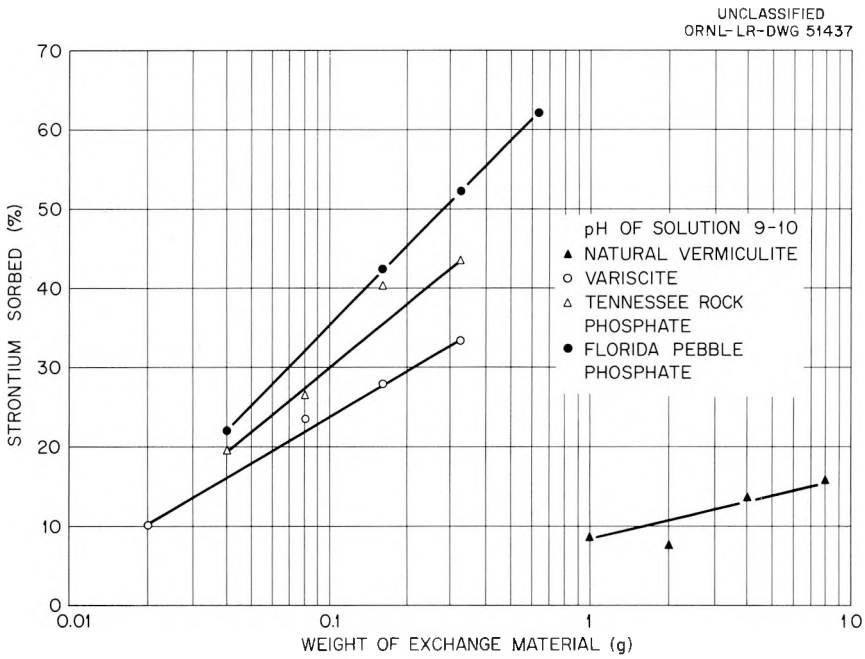

Fig. 1.36. Sorption of Strontium from Waste Solution at pH 9 to 10 by Various Materials.

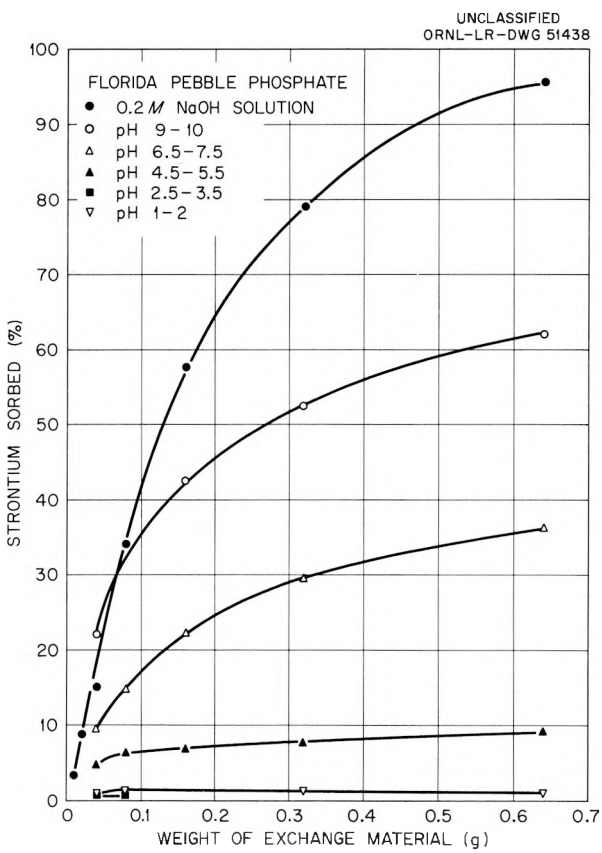

Fig. 1.37. The Effect of pH on the Removal of Strontium from Solution by Florida Pebble Phosphate.

rate of 1 ml cm^{-2} min^{-1} was used. The results are given in Table 1.20. The data obtained with 1-cm-dia columns were suspect, so additional tests were run with 1-in. columns.

Table 1.20. Evaluation of Materials for the Removal of Strontium from Solution

Material	Column Size (diameter)	EHTP (cm)	K_d (ml/g)
Vermiculite (BO-4)	1 in.	14	46
	1 in.	12	36
Tennessee rock phosphate	1 cm	14	100
Florida pebble phosphate	1 cm	1.2	125
	1 in.	12	100
Variscite	1 cm	2	1000
Exfoliated vermiculite (BE-3)	1 in.	18	45

The Florida pebble phosphate was fractionated into various particle sizes, and the saturation capacity doubled as the range of particle size decreased from +2 to −0.5 mm. Exfoliation of the vermiculite did not result in an improvement in strontium sorption over the vermiculite ore. Tennessee rock phosphate tended to break down in the column, but the Florida pebble phosphate maintained excellent physical structure.

Hydraulic Tests

Previous column studies with Conasauga shale indicated that this material was not suitable for use in columns.[64] The physical properties of vermiculite were quite satisfactory and, since cesium sorption by vermiculite was known to be high, hydraulic tests were conducted with this material.

Several columns of vermiculite ore (BO-4) were tested for head loss at various flow rates. The head loss characteristics of two columns, one of 12-in. bed depth before use and the other of 6-in. bed depth after saturation with cesium from solution 2 (Table 1.18), are shown in Fig. 1.38.

[64]E. G. Struxness et al., H-P Ann. Prog. Rep. July 31, 1959, ORNL-2806, p 10–12.

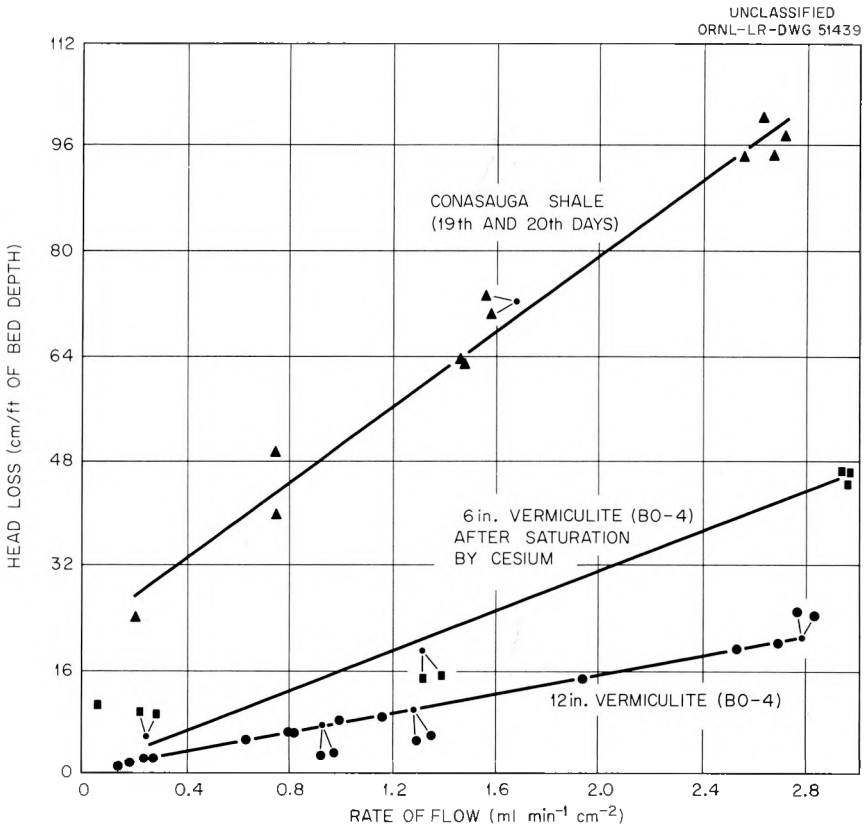

Fig. 1.38. Head-Loss Characteristics of Vermiculite (BO-4) and Conasauga Shale at Various Rates of Flow.

The head loss tests with Conasauge shale are shown for comparison. Head loss is a linear function of flow rate, and the straight line intercepts the origin. The reason for increased impedance in the smaller column is probably due to plugging caused by precipitation of $Mg(OH)_2$ within the column during saturation with cesium. Additional information is being obtained on head loss resulting from compaction due to the greater weight in a longer column. The use of exfoliated vermiculite may reduce head loss considerably.

Future Plans

A laboratory test will be made with a column 10 ft long. Cesium and strontium break-throughs will be determined simultaneously by the use of solutions tagged with Cs^{137} and Sr^{85}. The effluent will be assayed with a NaI(Tl) scintillation crystal and a single-channel analyzer. This test will also serve to check out equipment that may be used later in a field

demonstration. The column will be filled with a mixed bed of exfoliated vermiculite (BE-5) and Florida pebble phosphate. A second column, filled with exfoliated vermiculite, will be tested by using solutions to which 100 ppm PO_4^{---} have been added.

Laboratory investigations will continue in an attempt to devise methods for removing Ru^{106} from waste streams. In addition, an effort will be made to improve the physical properties of bentonites and other select materials so that their use in columns will be feasible.

DISPOSAL IN SALT FORMATIONS

E. G. Struxness F. L. Parker

W. J. Boegly, Jr.
F. M. Empson
T. Tamura
E. R. Eastwood
H. Kubota[65]

R. L. Bradshaw
L. Hemphill
D. G. Catron
O. H. Myers
R. C. Sexton[66]

The problems of radioactive waste disposal in natural salt formations are those of the degree to which the structural properties of salt are affected by chemical interaction, pressure, temperature, and radiation, and of handling any gases which may emanate from the wastes. Previous studies indicated that the effects of radiation on the structural properties of rock salt are minor.[67] Theoretical studies indicate that the temperature of radioactive wastes stored in salt cavities can be kept within acceptable limits by controlling the age of the wastes and the size of the cavity. Because theoretical solutions require a number of simplifying assumptions, and laboratory tests of distrubed geological materials are not conclusive, a number of field tests are required.

Three small, preliminary field tests have been run to get an estimate of the effects of impurities in the salt on temperature rise in the wastes and to "shake down" the equipment and operating procedures for the large tests.

---

[65]Member of Analytical Chemistry Division.

[66]Member of Engineering and Mechanical Division.

[67]F. L. Parker (ed.), Status Report on Waste Disposal in Natural Salt Formations: II, ORNL-2700, p 25 (May 4, 1959).

Two large-scale tests (3000 gal each), one with 7 M acid Purex waste and one with neutralized Purex waste, are now in operation. Plans are for the experiment with neutralized waste to continue indefinitely. This will give additional information on heat dissipation and plastic movement of salt under stress and elevated temperature. It is planned to terminate the experiment using acid waste at approximately 200 days. Evidences of corrosion of the cover have been observed, and it is necessary to avoid possible failure of the cover while the experiment is in operation. Following cooling of the experiments to near ambient temperature, the wastes will be removed and detailed examinations of the cavities made. This will yield information on the effects of Purex waste solutions on the salt-shale-anhydrite structure.

After the current large-scale experiments are terminated, several additional smaller experiments of a different nature are planned. These experiments are designed to yield information on (1) cavity alterations in full and partially full cylindrical cavities completely surrounded by salt, (2) the effect of variation of thermal properties of salt with temperature on temperature rise predicted by summing the contributions from a number of cavities, (3) the effect of shale and anhydrite bands on the temperature rise in long cylindrical cavities, (4) the problems of storage of waste in thin layers in sealed rooms, and (5) the effect of elevation of the temperature of an entire room on the structural stability of the room.

In addition to the field experiments, laboratory work on means of inhibiting gas production, theoretical studies of the effect of heat on the structural stability of salt cavities, and theoretical studies of temperature rises to be expected in an actual mine-disposal operation will continue.

Chemical Laboratory Studies

Chemical Gas Production

The chemical compatibility of simulated 7 M acid Purex solution and salt was studied in the laboratory with equipment designed to closely duplicate the conditions of the field experiment. The solutions were in a glass system in which all vapors issuing from the solution were air-refluxed, permitting noncondensible gases to diffuse out of the system, thus,

maintaining atmospheric pressure over the liquid. One major difference was the application of heat through the walls of the containing vessel, rather than directly into the solution.

A large portion of 7 M acid Purex is HNO_3, and the ions which predominate in the mixed solution are hydrogen, sodium, nitrate, and chloride. This composition suggests that any reaction which might occur would be similar to that between HNO_3 and HCl, the aqua regia reaction. This similarity was verified by laboratory tests using (1) NaCl and HNO_3 and (2) NaCl and simulated 7 M acid Purex waste solution. The identifiable products of both reactions were NOCl and Cl_2. Taking the idealized over-all reaction to be

$$NO_3^- + 3Cl^- + 4H^+ = NOCl + Cl_2 + 2H_2O$$

and noting that both nitrate and chloride are always present in abundance, it was found that the hydrogen ion concentration is the condition that limits the extent of the reaction. There is also a marked temperature effect upon both speed and degree of the reaction. The influence of hydrogen ion concentration and temperature on the reaction is shown in Fig. 1.39. From the stoichiometry of the aqua regia reaction, the gas production is calculated to be 11.2 liters of gas per equivalent of acid consumed. The approximate maximum gas production that could be expected from a 7 M Purex–salt system at different solution temperatures is given in Table 1.21.

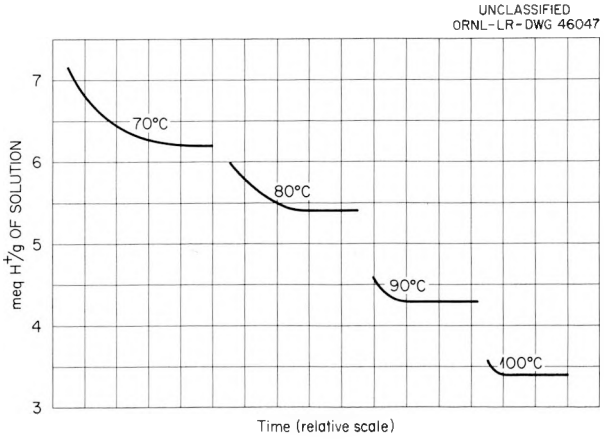

Fig. 1.39. The HNO_3-NaCl Reaction as a Function of Temperature.

Table 1.21. Calculated Maximum Gas Production from 7 M Acid Purex–Salt Solution

Temperature (°C)	Acid Consumed (equivalents/liter)	Volume of Gas Produced, STP (liters per liter of solution)	Volume of Gas Produced, STP (ft^3/gal)
70	< 0.05	Trace	
80	0.5	6	0.6
90	1.8	20	1.9
100	3.2	36	3.5

When the acid molarity at which the rate of reaction becomes imperceptible is plotted against the corresponding temperature, the points describe a line which extrapolates to 4 M (3.2 m) and 60°C. These two intercepts indicate the minimum conditions below which gas production ceases at 1 atm of pressure. Thus, chemical gas production in a 7 M acid Purex–salt solution can be inhibited by decreasing the acidity of the solution through denitration or neutralization, or by cooling the solution. These conclusions were confirmed by laboratory tests.

A thermochemical balance of the chemical reaction shows a net endothermic uptake of 42 kcal for the balanced reaction or about 10 kcal absorbed per equivalent of acid ion consumed. This is equivalent to a 10°C cooling per equivalent of acid consumed.

In order to develop a method for directly measuring the volume of gas produced by heated mixtures of NaCl-saturated synthetic waste solutions, two gas-measurement systems were studied. The first system studied, cold-trap fractionation, used helium gas to sweep the product gases, Cl_2, NOCl, and water vapor, from a heated synthetic waste-salt sample through a series of water, CO_2-methanol, and liquid-nitrogen-cooled condensers. The condensers were arranged in the order listed to selectively remove water in the 0°C water-cooled condenser, NOCl and Cl_2, in the CO_2-methanol condenser, and nitrogen oxides in the liquid-nitrogen-cooled condenser. Following sample collection, a manometric method was used to measure the gas volume of each fraction. Qualitative and quantitative chemical analysis

of the fractions showed that NOCl and Cl_2 gases were produced in equimolar amounts by solution samples of salt-saturated 7 M Purex waste. Accurate quantitative measurement of the gas volumes produced by the salt-saturated sample was not attained, because the waste-salt solution system was sensitive to sweep-gas rates. Another factor which contributed to large variance in the quantitative measurement was the reaction of the product gases, Cl_2 and NOCl, with the water vapor.

The principal feature of the second gas-measurement method was the quantitative displacement of helium by the product gases in the apparatus shown in Fig. 1.40. After introduction of the 50-ml sample, all air in

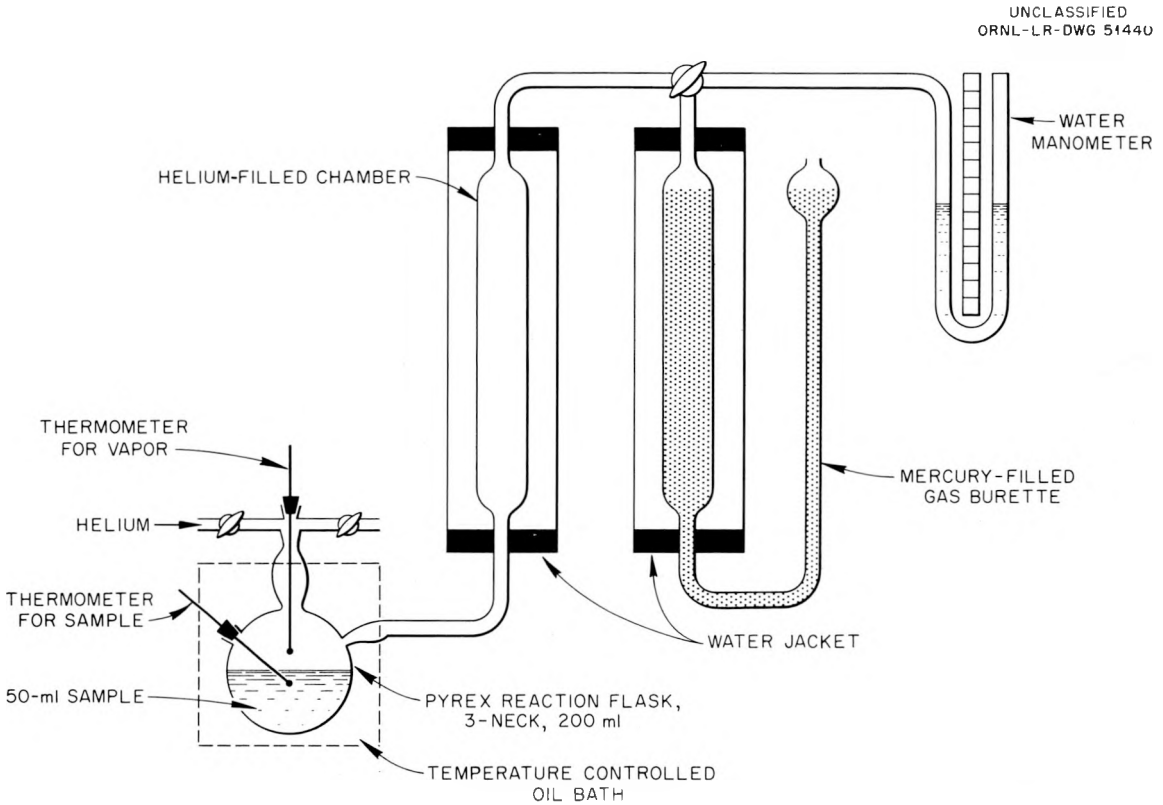

Fig. 1.40. Helium-Displacement Gas-Measuring Apparatus.

the system was displaced by helium, and the apparatus was adjusted to ambient pressure which was maintained during the heating period by manipulating the volume of the gas burette. During the heating period the gases produced by the sample, as well as water vapor, displaced helium into the calibrated gas burette. A number of preliminary experiments established the optimum sample volume, container size, and amount of helium required

to prevent chemical reaction between the product gases and mercury in the gas burette. A calibration curve of the apparatus was prepared by comparing experimentally determined pressures, temperatures, and volumes with calculated values.

Figure 1.41 shows a typical temperature-vapor-volume curve for 50-ml samples of synthetic 7 M Purex waste solution and salt-saturated 7 M Purex waste solution. Below 65°C the salt-saturated waste solution exhibits

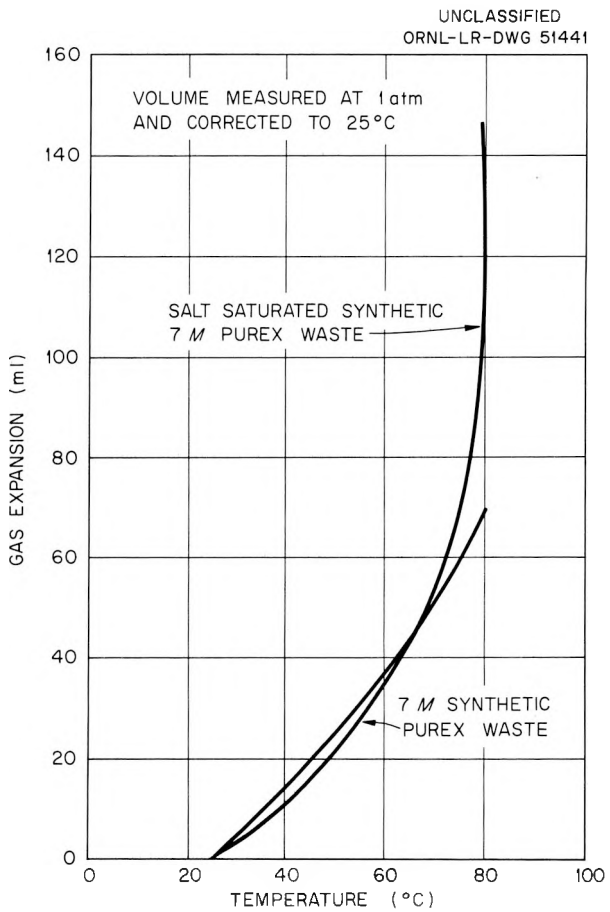

Fig. 1.41. Experimental Determination of Gas Production.

negligible gas production and reduced vapor volume due to an increased concentration of ionized solute as compared with the 7 M Purex waste solution. When the temperature of the solution is increased above 65°C, vapor volume of the salt-saturated sample increases due to the production of NOCl and Cl_2. This action, when plotted, results in an intersection of the two

curves and accounts for the increased slope of the salt-saturated vapor-volume curve at higher temperatures. Analysis of a series of curves similar to the above for separate samples of synthetic waste and salt-saturated samples are summarized in Table 1.22. These values show that the gas volumes predicted by the aqua regia study are in close agreement with the experimentally determined volumes. Also listed in Table 1.22 are the

Table 1.22. Comparison of Calculated (ΔH^+) and Experimental Gas Yield of Synthetic Purex Waste–Salt Solutions

Sample Description	25°C Calculated* Yield (ml of gas per liter of solution)	25°C Experimental Yield (ml of gas per liter of solution)	Temperature (°C)
Salt-saturated 7 M Purex	1200	1560	80
Salt-saturated 7 M Purex	1220	1600	100
Salt-saturated (+10 excess salt) 7 M Purex	1300	1590	100
Salt-saturated NaOH neutral Purex	0	0	100
Salt-saturated 3.5 M Purex	0	0	100

*Gas-yield values calculated on basis of measured acidity change of the sample solution.

vapor volumes for samples of NaOH neutralized and half-neutralized waste solutions with and without salt, which show that gas production by the aqua regia reaction can be minimized by decreasing the acidity.

Radiolytic Gas Production

In view of the high activity predicted for high-level waste solutions, it is necessary to determine whether gas production by radiolysis of the solutions will preclude disposal in liquid form. It is also pertinent to check whether radiolysis can be controlled by altering certain solution conditions.

From the standpoint of radiation chemistry the radiolysis of very pure water produces a cycle of reactions that produce no net change in the system. With the introduction of small amounts of impurities, as found in good grades of distilled water, hydrogen is evolved at the rate of about 0.001 cc per gram of water per 10^6 rad. When nitrate is present, oxygen is evolved at a rate that varies with the pH of the system and the nitrate concentration. The G values for the yields of radiolytic products reported in the literature were determined with practically pure systems and are not generally applicable to this situation; however, they can be taken to approximate maximum yields. Furthermore, should the system be confined, the buildup of product gases may increase the rate of recombination processes to such an extent that a low-yield steady-state condition will be attained.

A study of the radiolytic stability of representative waste solutions was initiated in order to determine the degree of radiolysis, as well as the solution conditions which control radiolysis. The solutions were irradiated in the Co^{60} facility, and the results are limited, therefore, to the effects of gamma radiation from an external source.

The composition of the waste solutions studied are given in Table 1.23. Each solution type was irradiated under three conditions: no salt

Table 1.23. Compsoition of Waste Solution Types Investigated for Radiolytic Stability

Type	Ionic Concentration (equivalents/liter)				
	Free H^+	Fe	Na	NO_3	SO_4
7 M Purex	7.0	1.0	0.3	7.3	1.5
3.5 M Purex	3.5	0.5	0.15	3.65	0.75
Semineutral Purex	3.61	0.87	3.17	6.35	1.30
Neutral Purex	1.23	0.78	4.84	5.68	1.17
Formaldehyde-denitrated Purex*	0.5	2.4	0.9	0.5	4.0

*Also contains 0.7 equivalent of aluminum.

added, salt saturated, and salt saturated plus excess salt. The irradiations were carried out in tubes fashioned after a model furnished by the Chemistry Division. Each tube had a sample capacity of about 4 ml and included a built-in mercury manometer to indicate the internal pressure. A known volume of each solution was put into a tube, the inlet port was sealed, and the tube was irradiated. The pressure within the tube, determined by the height of the mercury column, was recorded as a function of absorbed radiation.

The degree of radiolysis represented by the internal pressure of the irradiation tubes is plotted as a function of absorbed dose for each solution type in Figs. 1.42–1.46. Since the pressure was determined with closed-end manometers, there is a greater uncertainty in the higher pressure readings than the lower pressure readings. Thus, an uncertainty of 4% at 2 atm increases to 5.3% at 4 atm and 9% at 8 atm.

All the systems investigated approached steady-state conditions as the dosage approached 10^9 rad; however, there is no definite pattern which will explain the role of salt both in solution and in a solid phase. In

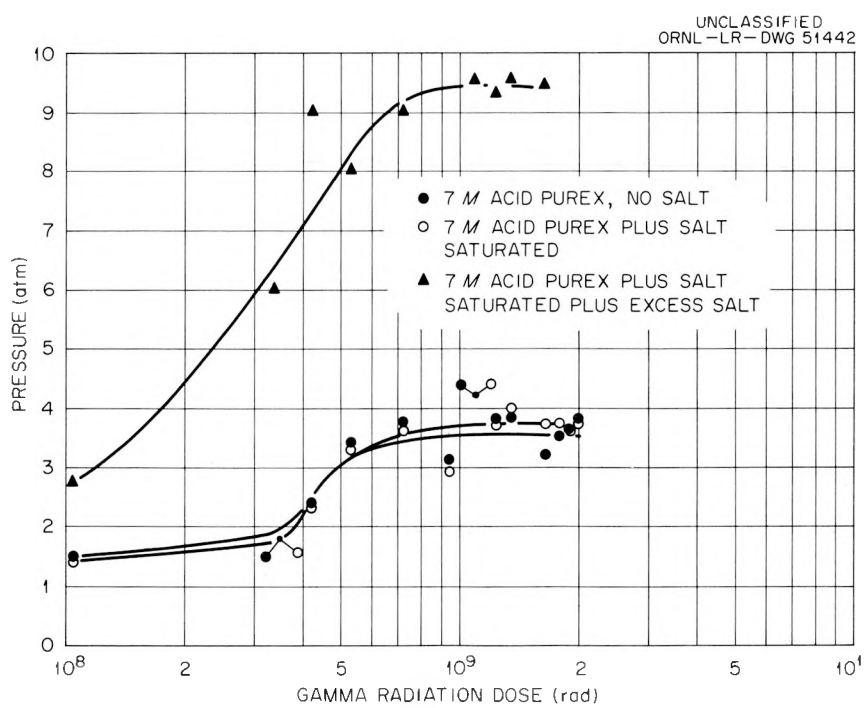

Fig. 1.42. Vapor Pressure of Co^{60}-Irradiated Waste-Salt Samples, 7 M Acid Purex and Salt.

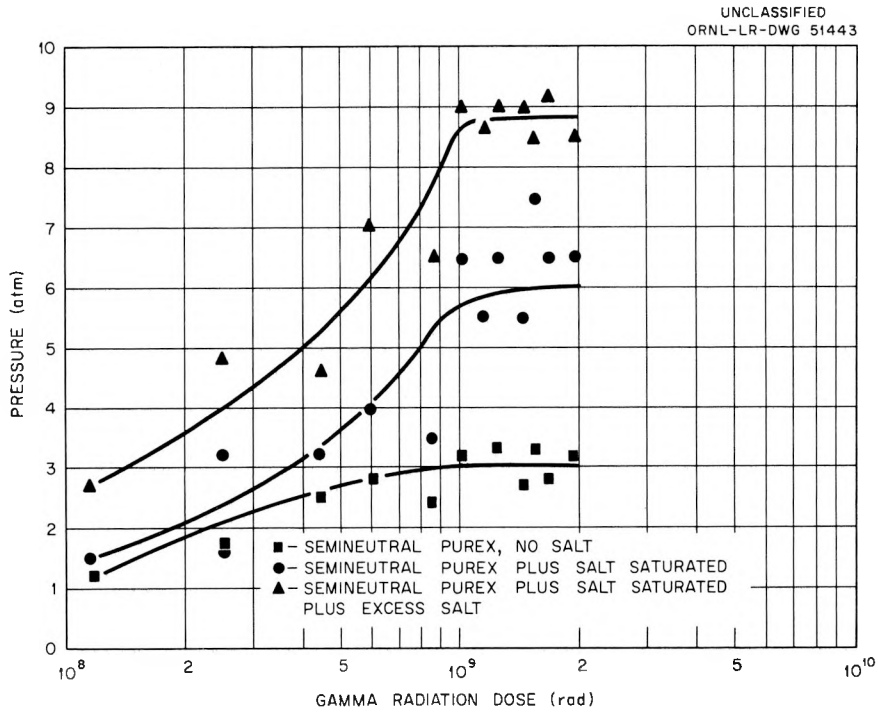

Fig. 1.43. Vapor Pressure of Co^{60}-Irradiated Waste-Salt Samples, Semineutral Purex.

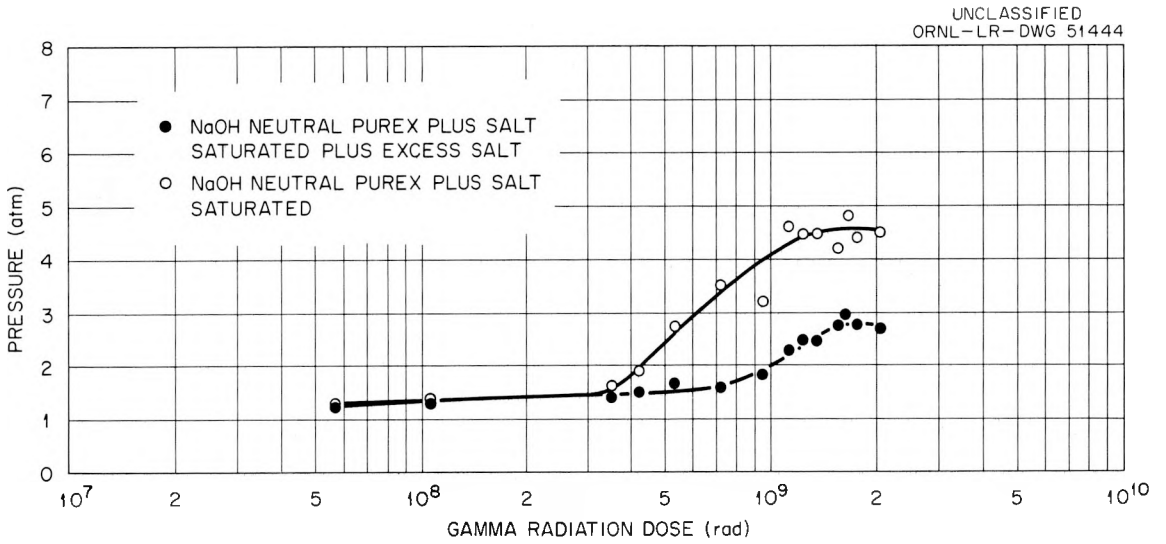

Fig. 1.44. Vapor Pressure of Co^{60}-Irradiated Waste-Salt Samples, Neutralized Purex Salt.

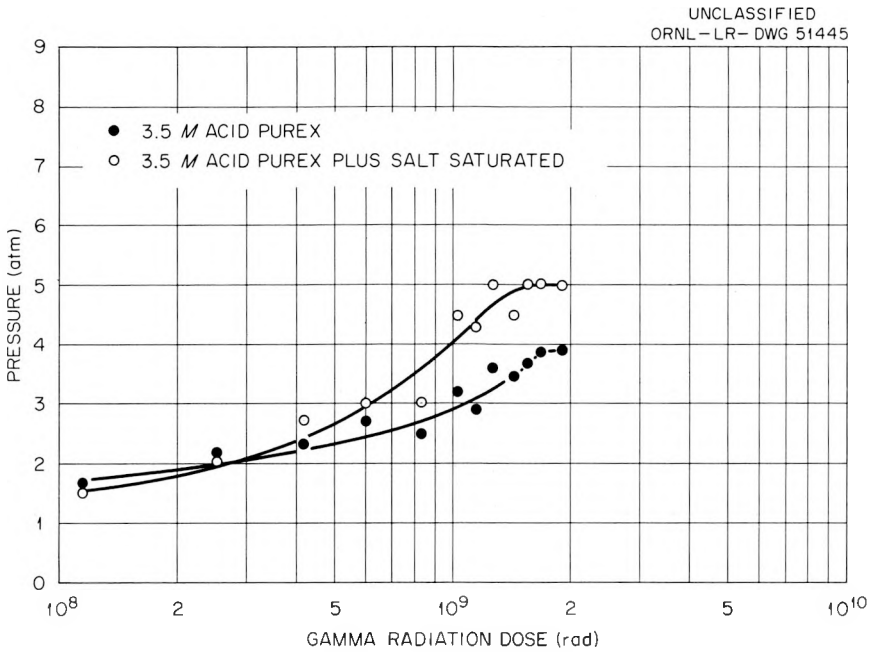

Fig. 1.45. Vapor Pressure of Co^{60}-Irradiated Waste-Salt Samples, 3.5 M Purex.

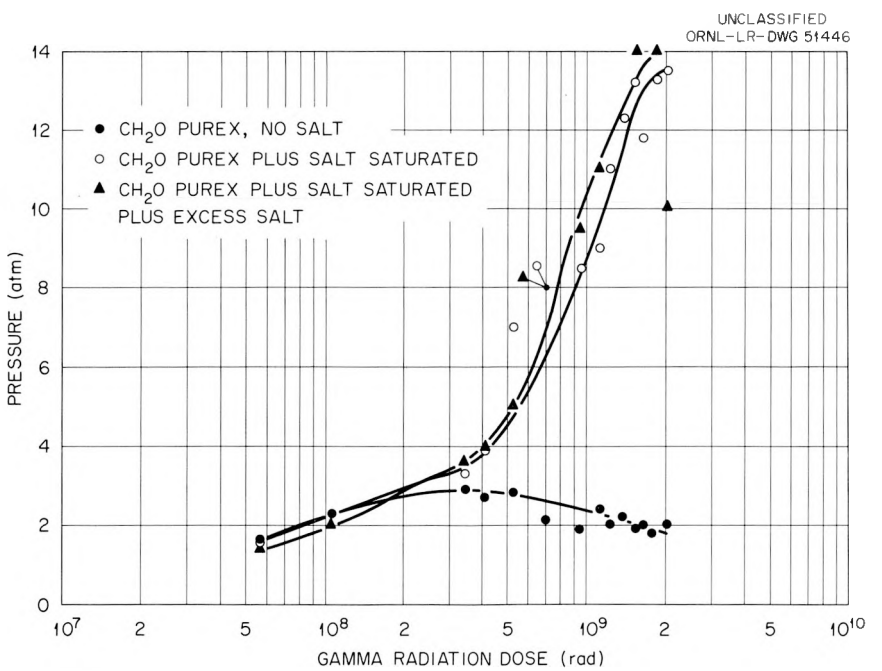

Fig. 1.46. Vapor Pressure of Co^{60}-Irradiated Waste-Salt Samples, Formaldehyde-Denitrated Purex.

general, the degree of radiolysis before steady state sets in is increased by saturating the solution with salt and is even more enhanced by the presence of excess solid salt. The data for the neutral Purex solution is anomalous to the general trend; the minimum steady-state pressure is observed with excess salt present.

It is not known whether the steady-state condition is a function of the total pressure or the partial pressure of individual gases over the solution. The total pressure and the total gas production per milliliter of solution at the steady-state condition are included in Table 1.24. The

Table 1.24. Steady-State Pressures and Total Gas Production

Type	Condition	Steady-State Pressure (atm)	Yield (ml of gas per ml of solution)
7 M Purex	A[a]	3.55	1.44
	B[b]	3.64	1.40
	C[c]	9.4	4.90
3.5 M Purex	A	3.85	1.42
	B	5.01	1.90
	C[d]		
Semineutral Purex	A	2.94	1.02
	B	5.68	2.00
	C	8.88	4.28
Neutral Purex	A[d]		
	B	4.58	1.43
	C	2.68	0.91
Formaldehyde denitrated	A	2.06	0.29
	B	11.9	6.35
	C	11.6	6.62

[a]No salt added.

[b]Salt saturated.

[c]Salt saturated plus excess solid salt.

[d]Original samples damaged – data incomplete.

analysis of gases from an irradiated tube containing synthetic denitrated Purex gave 6 vol % hydrogen, 23 vol % oxygen, and the remainder was nitrogen. Further tests are planned to evaluate the role of the gas-phase composition in radiolytic equilibrium.

A comparison of the steady-state pressures and volumes of gas produced by Co^{60} radiation absorption with the volume of gas produced by chemical interaction indicates that chemical gas production is negligible compared with radiolytic gas production.

Although the experimental results show a wide variation in radiolytic behavior, the minimal steady-state radiolytic gas pressure found in certain instances points to a rate which might allow storage of liquid wastes in salt formations.

Thermal Studies

Field Experiments

The heat-production rate being used in the large-scale (7.5-ft cube) field experiments is equivalent to that of two-year-cooled wastes from fuel irradiated 10,000 Mwd per metric ton of uranium at a specific power of 33 Mw/ton and yielding 800 gal of waste per ton.[68] Interpolation of previous thermal calculations[69] for one- and six-year-cooled wastes indicated that two-year-cooled wastes could be stored in a 10-ft-dia sphere (surface area approximately the same as a 7.5-ft cube) without boiling.

An analytical solution for the time-temperature relationship at the surface of a heated sphere of uniform conductivity in a uniform medium with exponential decay of the heating rate is given by Birch:[70]

$$T(a,t) = \frac{A_0 a^2}{3ck}\left\{3e^{-\alpha t}\int_{a/\sqrt{kt}}^{\infty} e^{\alpha a^2/k\beta^2}\left[\operatorname{erf}\beta - \frac{2}{\beta\sqrt{\pi}}\left(1 - e^{-\beta^2}\right)\right]\frac{d\beta}{\beta^3}\right\} , \quad (1)$$

---

[68]J. O. Blomeke, Status Report on the Disposal of Radioactive Wastes, ORNL CF-57-3-114 (Rev.), p 68 (June 25, 1957).

[69]E. G. Struxness et al., H-P Ann. Prog. Rep. July 31, 1959, ORNL-2806, p 69.

[70]F. Birch, Thermal Considerations in Deep Disposal of Radioactive Wastes, NAS-NRC 588, p 18 (July 1958).

where

A_0 = the initial heating rate per unit volume,

a = the radius of the sphere,

c = the specific heat per unit volume of the medium,

k = thermal diffusivity of the medium,

α = the heating rate decay constant,

t = time,

β = variable of integration.

This equation was solved by numerical integration for the time variation of temperature at the surface of a 10-ft sphere, equivalent to the 7.5-ft-cube field experiments. An analytical solution for the time-space variation of temperatures in the salt medium surrounding the sphere when the heating rate is constant is:[71]

$$T(r,t) = (2Aat/cr)\left[i^2 \operatorname{erfc} \frac{r-a}{\sqrt{4kt}} + i^2 \operatorname{erfc} \frac{r+a}{\sqrt{4kt}} + \right.$$

$$\left. + \frac{\sqrt{4kt}}{a}\left(i^3 \operatorname{erfc} \frac{r+a}{\sqrt{4kt}} - i^3 \operatorname{erfc} \frac{r-a}{\sqrt{4kt}} \right) \right] , \quad (2)$$

where

r = the distance from center of sphere to a point in the medium,

i^2 = second integral,

i^3 = third integral.

The other terms are the same as for Eq. (1).

In the 7.5-ft-cube field experiments the heating rate is almost constant, starting at 1.8 w/gal and falling to 1.7 w/gal after 200 days. Over this period the effect of the decaying heat-production rate is not great, as may be seen from Fig. 1.47. A comparison of the experimental data with the theoretical calculations is made in the section on Field Experiments.

Calculations for the surface temperatures of a sphere equivalent to the 18-in., small-scale experiments were made by utilizing Eq. (1). The results will be found in the section on Field Experiments.

---

[71] Ibid., p 17.

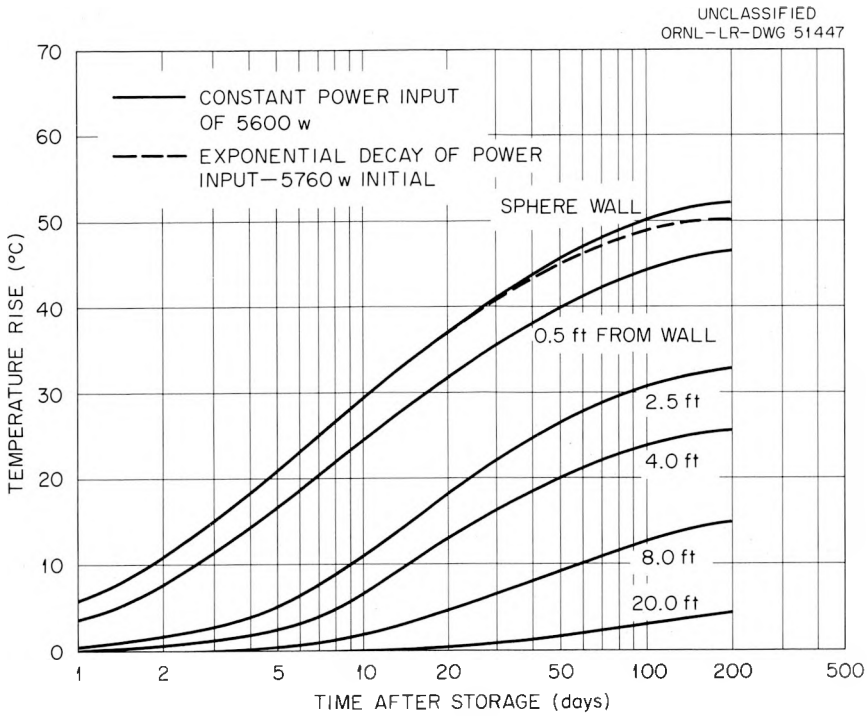

Fig. 1.47. Ten-Foot Sphere — Theoretical Temperature Rise in Infinite Salt Medium.

Mine Disposal

In a mine-disposal operation each cavity will be affected by heat from other cavities, and, thus, it becomes necessary to investigate maximum temperature rises for various sizes and shapes of cavities in various configurations which might be encountered.

A solution is available for the temperature rise in an infinite slab in contact with an infinite medium and with exponential decay of the heating rate.[72] By use of this equation, and approximating the power-decay curve of Blomeke[68] by a series of exponentials, the curve in Fig. 1.48 was calculated. Inherent in these calculations are the assumptions: (1) The heat source is uniformly distributed in a 10-ft-thick layer of salt, extending infinitely in the horizontal plane. (2) The conductivity of the salt in the heat generating layer is infinite, although the heat capacity is the same as that of the infinite salt medium. (3) Thermal properties do not change with temperature.

[72] Ibid., p 4.

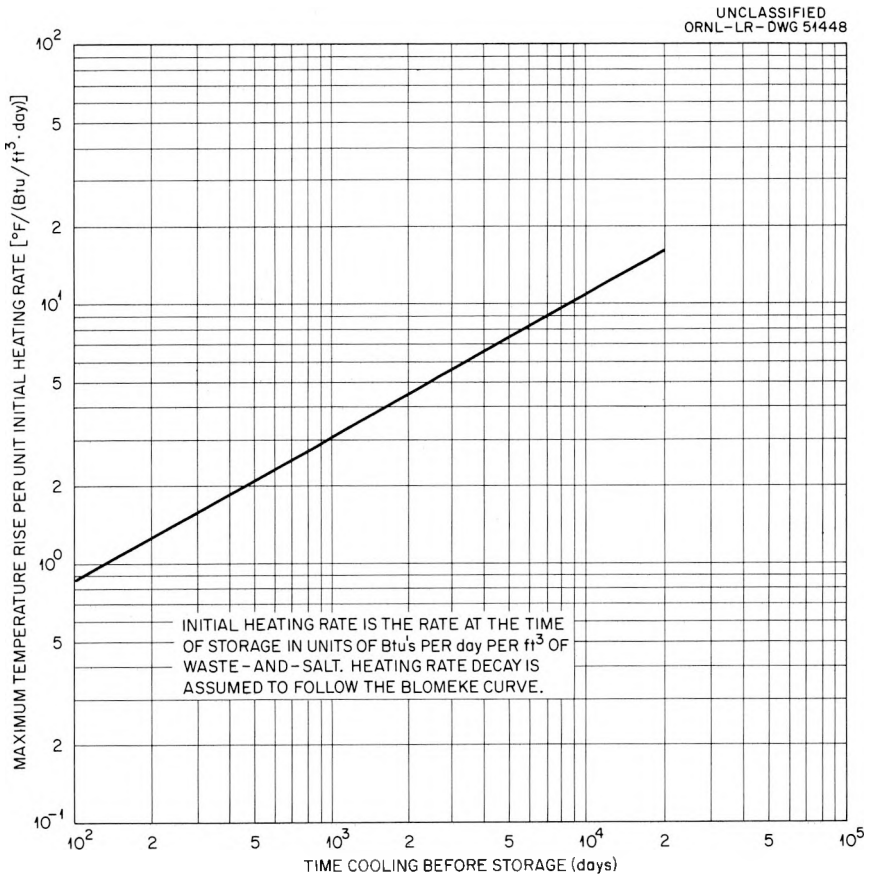

Fig. 1.48. Maximum Temperature Rise in a 10-ft-thick Infinite Slab of Waste and Salt in Infinite Expanse of Salt.

The assumption of the infinite horizontal slab is conservative, since probably no more than 60% of the gross area of a mine would be used for actual waste storage. The assumption of infinite conductivity is approximately true for a layer of freely convecting liquid. The principal thermal advantage gained in dispersing the waste to a finite depth in the salt is the sensible heat of the salt within the layer, and, while this may be important for short-cooled wastes, infinite-slab calculations show that for a fixed quantity of eight-year-cooled waste per unit horizontal area the maximum temperature rise is unaffected by the thickness of the layer (layers thicker than 10 ft were not calculated).

A study is under way to more closely define the limits for various configurations in mine disposal. The problem is being programmed by the

Engineering Research Section of the Reactor Experimental Engineering Division for solution by the method of finite differences, on the IBM 704 computer.[73]

Field Experiments

Small-Scale

Purpose and Operation. — The small-scale tests were designed to determine the effect of impurities in the salt on temperature rise in the wastes and to "shake down" the equipment and operating procedures for the large tests. Two experiments with acid waste were operated, one in pure salt and the second in salt containing about 25% anhydrite and traces of shale. A single experiment with neutralized waste was operated in pure salt. The cavities were 18 × 18 × 25 in. deep, and were one-fifth the scale of the large experiments. Metal covers fabricated of Haynes Alloy No. 25 were used to cover the pits. Figure 1.49 shows the arrangement of the two experiments in pure salt. Heat was applied by impressing an a-c voltage across graphite electrodes inserted through the cover into the synthetic waste solution.

Heat Transfer. — Power was supplied in such a manner as to simulate the energy output of a 10,000-Mwd/ton burnup, 33-Mw/ton specific power, 800-gal/ton waste. For the one-fifth-scale tests, power was supplied at an initial rate of 40 w/gal, which is equivalent to 50 days of cooling, and was decreased daily in accordance with the decay curve for 50-day-old waste. The temperature reached, as well as the predicted temperatures in the neutralized waste in pure salt, are shown in Fig. 1.50. The measured power input, as well as the design power input, are also shown in this figure. The power inputs do not coincide, because large fluctuations in line voltage made it impossible to set the correct power input.

Figure 1.51 shows the temperature of the acid waste in the cavity excavated in pure salt. The power input varied widely until a controlling wattmeter was installed, as the manual controls were not as sensitive as

---

[73]T. B. Fowler and E. R. Volk, Generalized Heat Conduction Code for the IBM-704 Computer, ORNL-2734 (Oct. 16, 1959).

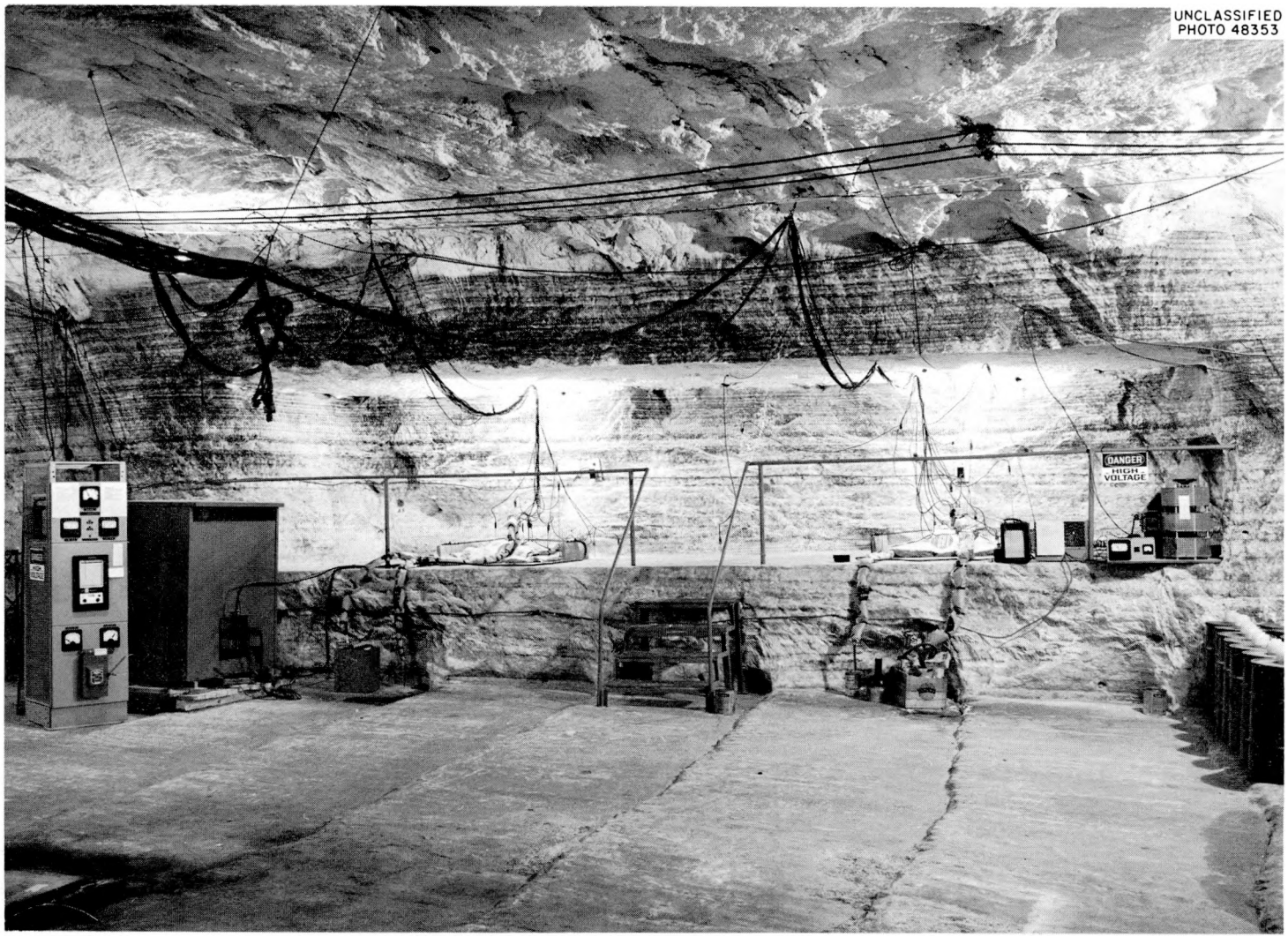

Fig. 1.49. One-Fifth-Scale Experiments in Salt.

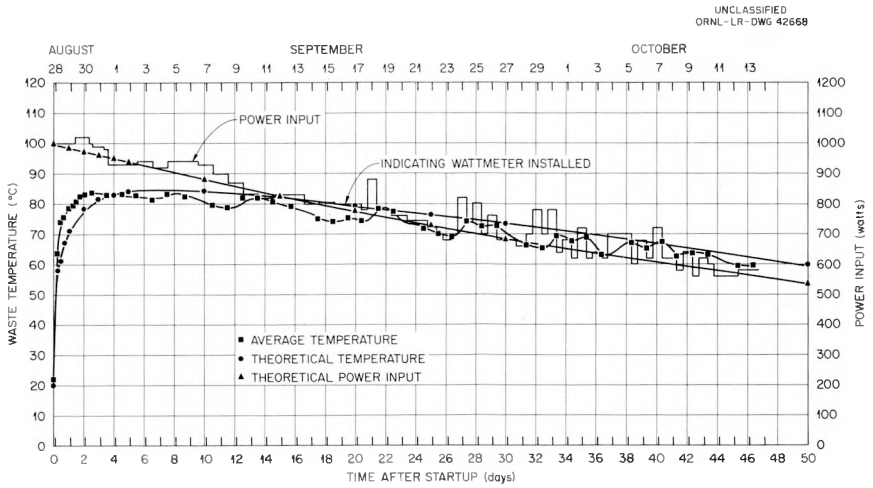

Fig. 1.50. Synthetic Neutralized Purex Waste in 18-in. Cavity in 100% NaCl.

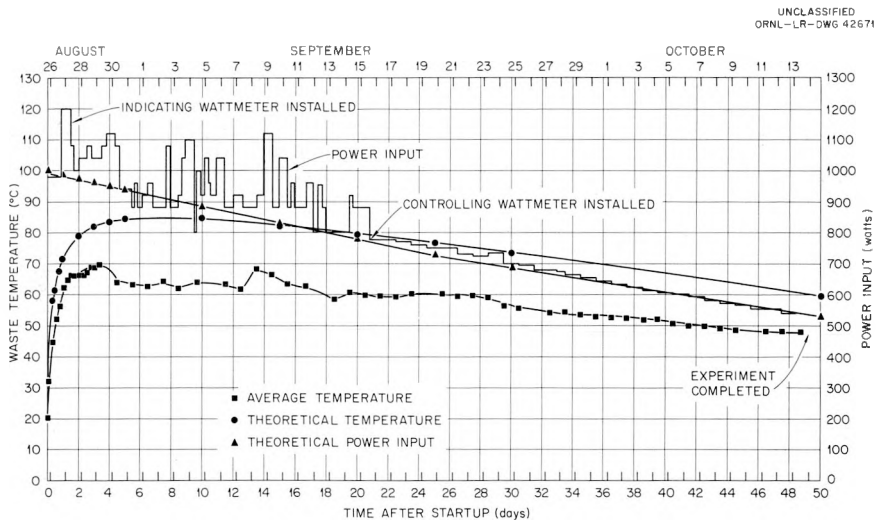

Fig. 1.51. Synthetic Purex Waste in 18-in. Cavity in 100% NaCl.

the variable transformer controls used for the neutralized pit. The maximum temperature reached was approximately 20°C below that predicted or 30% below the predicted temperature rise. Figure 1.52 shows that the maximum temperature of the acid pit in the floor of the mine was also about 20°C below the predicted maximum.

On the basis of these preliminary tests, it was concluded that the anhydrite in the floor of the mine had no major effect on temperature

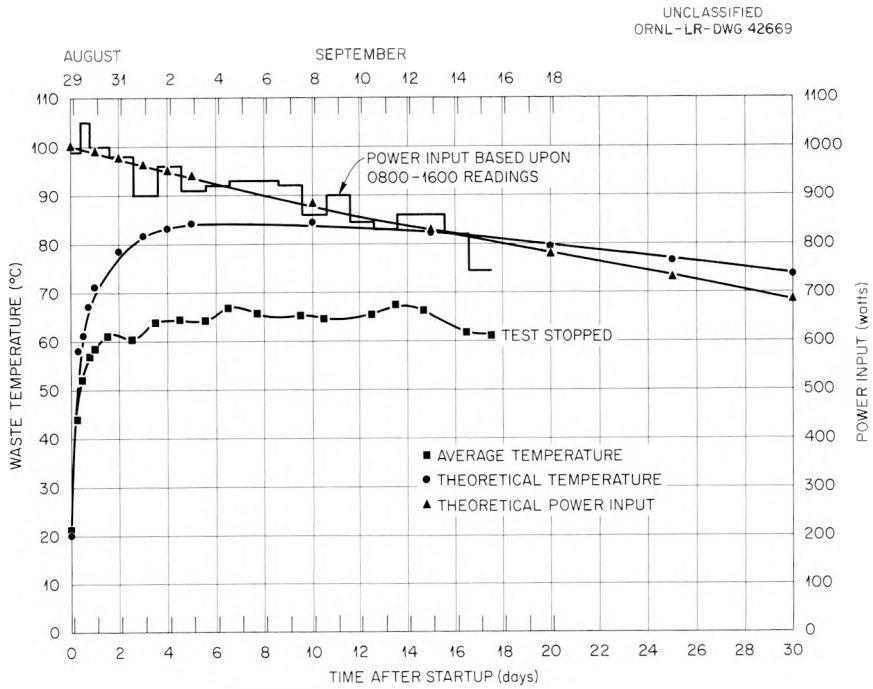

Fig. 1.52. Synthetic Purex Waste in 18-in. Cavity in 75% NaCl, 25% $CaSO_4$.

rise in the waste. Temperature rise in the neutralized waste pit was considerably higher than in the acid-waste pit, probably due to the lower thermal conductivity of the precipitate in the neutralized waste.

Gas Production. — The wastes used in the small field experiments were from the solutions prepared for the large field experiments. These solutions were prepared by an outside vendor, delivered to the experiment site in the Carey Mine, and saturated with salt by agitation in the shipping container (polyethylene carboys for acid waste and steel drums for neutralized waste). The analyses of the synthetic Purex waste, both before and after the experiments, are given in Table 1.25. Note that a change in composition of the waste is produced by saturation with NaCl. The nitrate content is reduced without a change in volume, and the sodium ion concentration is approximately half of the chlorine concentration. This is believed to be due to the precipitation of $NaNO_3$ from the saturated solution.

The contact of synthetic Purex waste with NaCl establishes conditions for the aqua regia reaction discussed earlier. Nitrosyl chloride (NOCl) and other gases are produced, resulting in an off-gas which would be hazardous in the relatively confined atmosphere of a mine. Neutralized Purex

Table 1.25. Field-Waste Solutions — One-Fifth-Scale Experiments

Sample	Cations (equivalents/liter)			Anions (equivalents/liter)			Total		Specific Gravity
	H^+	Na^+	Fe^{+++}	Cl^-	SO_4^{--}	NO_3^-	Cations	Anions	
Initial Composition									
Acid waste composite	7.21	0.25	1.40	0.01	1.55	7.31	8.86	8.87	
Neutralized waste (after saturation with salt)									
Pit 1	0.5 (OH^-)	7.69	0.93	3.05	1.02	4.37	8.62	8.94	1.3823
Acid waste (after saturation with salt)									
Pit 2	7.09	1.72	1.50	3.44	1.48	5.38	10.31	10.30	1.3251
Pit 3	7.22	1.74	1.50	3.55	1.53	5.42	10.46	10.50	1.3262
Final Composition									
Pit 2	5.99	2.08	1.53	3.74	1.42	4.45	9.60	9.61	
Pit 3	5.40	2.21	2.17	3.88	1.60	4.17	9.78	9.65	

waste saturated with salt and heated above 80°C produces only water vapor in air. The gas problem in the disposal of neutralized waste in salt would, therefore, result only from water vapor and the radiolytic decomposition of water.

The experiments with acid waste produced substantial quantities of the end products of the aqua regia reaction. The gases were identified as nitrosyl chloride (NOCl), nitrous oxide (N_2O), chlorine, and carbon dioxide. Semiquantitative analyses of off-gas samples taken during the operation of small-scale field experiments Nos. 2 and 3 are given in Tables 1.26 and 1.27. Analytical data are given only for the small field experiments with acid waste, since no gaseous reaction products were produced in the neutralized experiment.

Samples were collected in three ways: Samples of the gas in the vapor space were obtained by pulling 250 ml from the vapor space of the cavity into an evacuated gas-sample bottle after flushing the sample connection. The bottles were sealed by dipping the stopcock on each end into hot paraffin. To secure large quantities of the gases, freeze traps were

Table 1.26. Off-Gas Composition, One-Fifth-Scale Experiment, Pit 2
Acid waste in pure salt

Temperature Range (°C)	Sampling Method	Gas Concentration (vol %)			
		CO_2	NOCl	Cl_2	N_2O
20–60	Evacuated bottle			< 2	
	CO_2-methanol trap	1.6	60	2	0.8
	Liquid N_2 trap	2.5			0.6
60–70	Evacuated bottle	2.6	17.0	7.8	1.5
	CO_2-methanol trap	1.1	36.4		1.0
	Liquid N_2 trap	17.0		27.9	12.3
66–64	CO_2-methanol trap	0	76	4.8	0
	Liquid N_2 trap	~ 7	~ 18.5	~ 18	~ 2

Table 1.27. Off-Gas Composition, One-Fifth-Scale Experiment, Pit 3

Acid waste in salt and anhydrite

Temperature Range (°C)	Sampling Method	Gas Concentration (vol %)			
		CO_2	NOCl	Cl_2	N_2O
55	Evacuated bottle	4.1	9.5		3.6
20–60	CO_2-methanol trap	40.0	43.7		7.5
20–60	Liquid N_2 trap	64.0			36.0
60–65	Evacuated bottle	25	19.6		6.9
	CO_2-methanol trap	5.8	90.6		1.0
	Liquid N_2 trap	51.0	> 2.0		14.5
65–68	Liquid N_2 trap	48.0	~ 7.0	29.8	3.4
68–75*	Evacuated bottle	3.1	13.9	13.9	1.5
	CO_2-methanol trap	1.9	65.8	11.6	> 0.6
	Liquid N_2 trap	6.7	< 2	~ 12.0	1.4
75–72*	CO_2-methanol trap	5.8	44.2	27.6	Tr
72–77*	CO_2-methanol trap	3.0	55.9	25.4	0.8
	Liquid N_2 trap	9.2	< 2		3.1

*These temperatures were reached after September 15, during intermittent periods of high-power operation, designed to test trench-seal materials.

used. A CO_2 (solid)-in-methanol (–78.5°C) trap was followed by a liquid-nitrogen (–195.8°) trap. Samples were recovered from the freeze traps by allowing the condensed material to evaporate into the evacuated 250-ml gas sample bottles. Composition of the samples represented an average composition of the gas evolved during the period of collection. All reactive components of the gas were condensed and/or frozen by the two cold traps.

The conclusions drawn from these experiments are: (1) Significant quantities of NOCl are produced only after the solution temperature rises above 60°C. (2) The quantity of gas produced by conducting an experiment

in mixed salt and anhydrite was not significantly greater than that produced in a pure salt environment. (3) There was an appreciable amount of shale present in experiment 3, as evidenced by the CO_2 produced at low temperatures.

Large-Scale

Operation. – Equipment design, site description and exploration, and proposed operating procedures were given in the Annual Report for 1959.[74] The procedures outlined at that time were followed. The installation of equipment was completed in early December 1959. The experiment with neutralized waste was placed in operation on January 6, 1960, and the acid-waste experiment on January 18, 1960. Power input is based on an assumed cooling time of two years for 10,000/Mwd/ton burnup, 33-Mw/ton specific power, 800-gal/ton waste. For wastes of this age, the decay curve is relatively flat, and the experiments have operated approximately 200 days with power being reduced only from 5.8 to 5.4 kw. Comprehensive temperature data are being collected by a logger system from approximately 125 thermocouples. Maximum average temperatures which were reached at about 100 days were 73°C for the neutralized-waste experiment and 64°C for the acid-waste experiment. The temperatures, after reaching the peak, have remained essentially constant, except for a 4°C temporary drop due to a 16-hr power failure on June 14, 1960.

Heat Transfer. – Temperature rises in both the acid-waste and neutralized-waste experiments have generally followed those predicted for an equivalent sphere in an infinite salt medium. Perfect agreement would not be expected, since (1) the sphere only approximates the cube, (2) heat transfer from the floor to the mine air would not be the same as for conduction in salt, and (3) there are horizontal shale and anhydrite bands in the cavity walls.

Figures 1.53 and 1.54 show a comparison of experiment temperatures with those calculated for a sphere whose surface area is equal to the area of a 7.5-ft cube. The salt temperatures shown were obtained from thermocouples located at a depth of 6 ft 3 in. below the mine floor, on a horizontal line through the center of the waste solutions.

[74]E. G. Struxness et al., loc. cit., p 85.

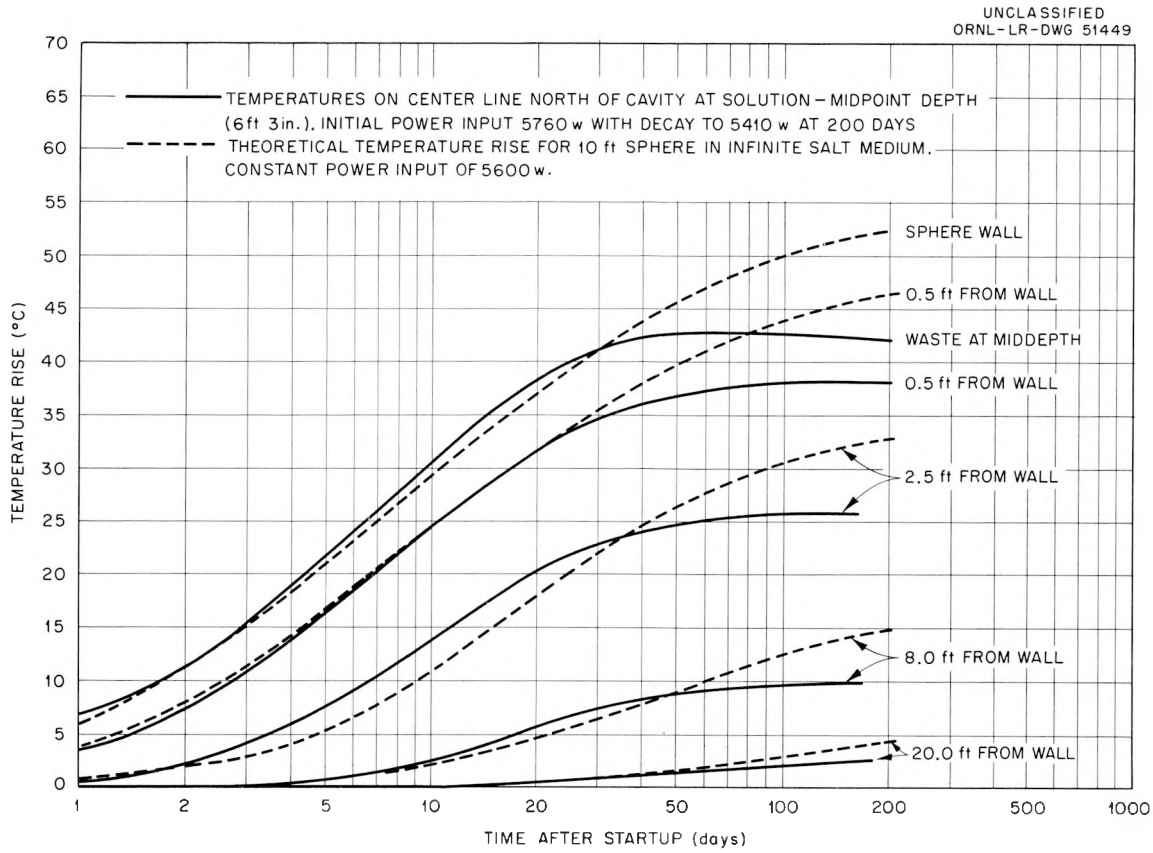

Fig. 1.53. Temperature Rise in 7-1/2-ft Acid-Waste Experiment.

In the acid-waste experiment the temperature in the waste is uniform, both horizontally and vertically, with the exception of the lower foot or so which is several degrees cooler than the upper portions. This results in an average waste temperature 1 to 2°C lower than that shown in Fig. 1.53 for the waste at mid-depth.

In the neutralized waste there is a viscous precipitate which settles to occupy approximately 25% of the solution volume. Heating is essentially confined to this region, since most of the fission products would be scavenged by the precipitate. There is little or no convection in the precipitate, and, consequently, temperatures as high as 120°C were recorded near the center; however, a steep gradient exists, and temperatures at the cavity wall are approximately the same as in the supernatant region. There is free convection in the supernatant, and thereby a uniform temperature distribution.

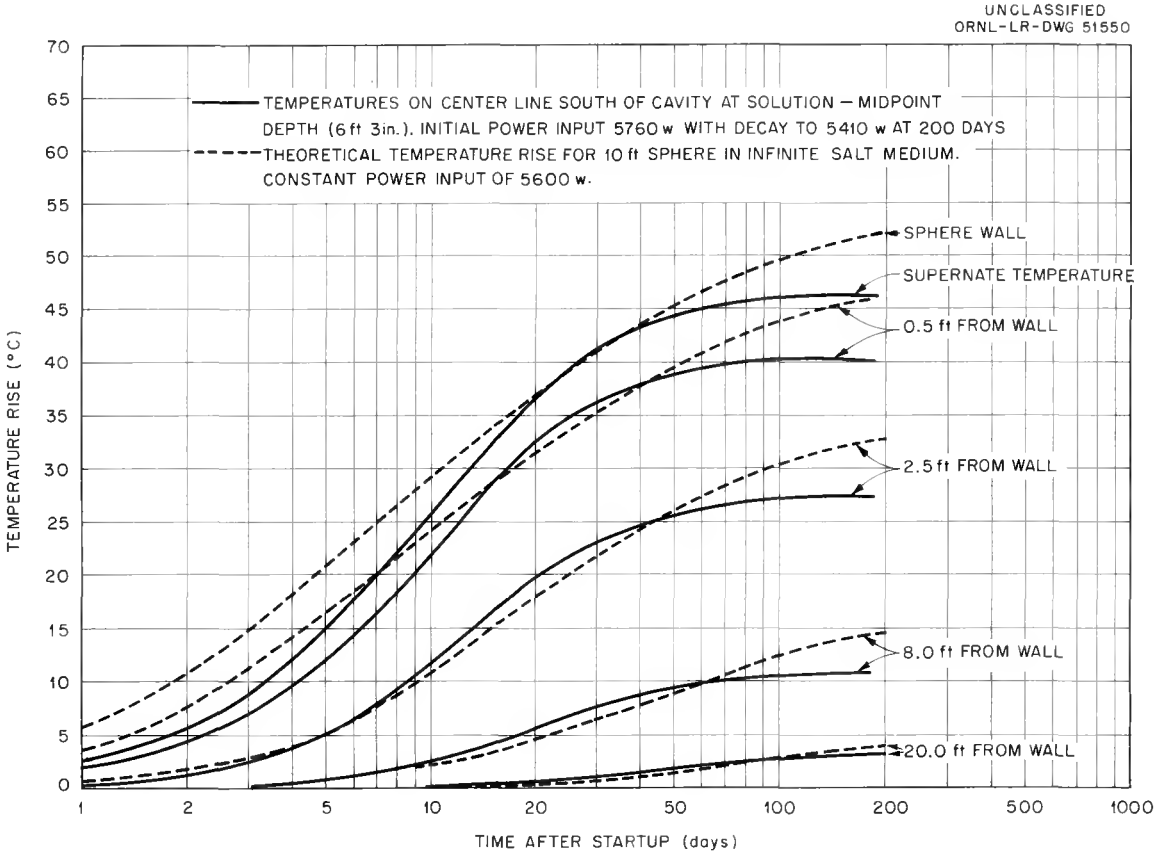

Fig. 1.54. Temperature Rise in 7-1/2-ft Neutralized-Waste Experiment.

Plastic-Flow Studies. – The stresses in a salt formation due to overburden pressure are disturbed during the mining operation, resulting in a process of stress redistribution within the formation. Depending on the volume of salt removed, the stress in the salt pillars supporting the roof can exceed the elastic limit for salt, and plastic flow will result. Plastic flow produces a change in room dimensions, thereby reducing the stresses in the salt surrounding the room and producing a new condition of stability. The size of the plastic zone increases with rising temperature, resulting in an increased plastic flow (creep rate).

Gages have been installed in the Carey Mine to measure the plastic flow in the vicinity of the field experiments. Figure 1.55 shows the gages installed by ORNL around the neutralized-waste cavity. Two types of gages have been installed: dial-gage extensometers, used to measure the linear movement of salt per unit time between two reference points, and strain seismographs, used to determine if the rate of movement has a

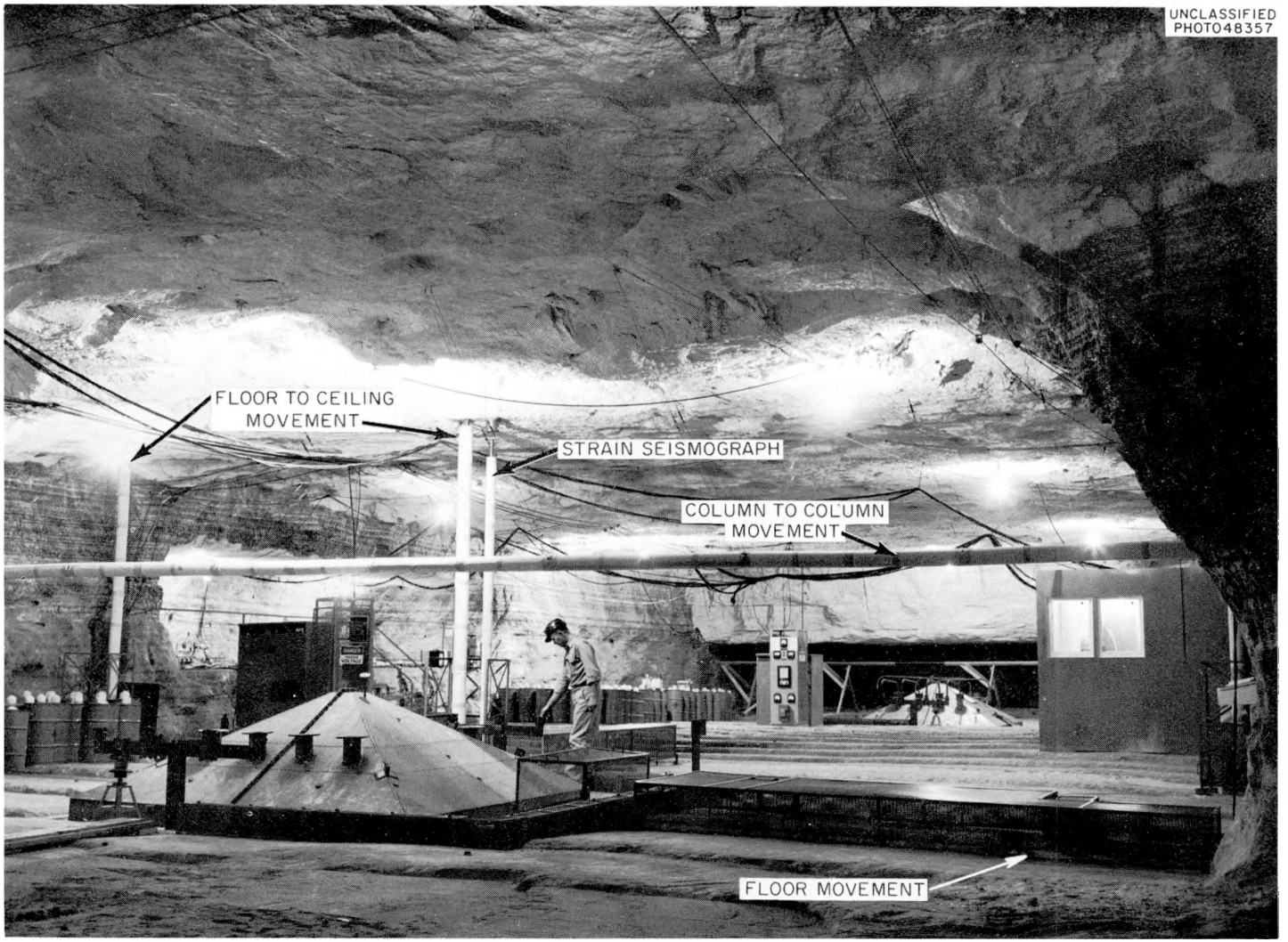

Fig. 1.55. Location of Devices for Measuring Plastic Flow.

constant or a variable velocity. Measurements are being taken of the floor-to-ceiling movement, column-to-column movement, and floor movement. Measurement began before heat was applied to the cavity. Figure 1.56 shows the results obtained from the floor-to-ceiling gages and the column-to-column gages. The data plotted in these curves are not corrected for the thermal expansion of salt or of the measuring rod. The vertical gage located in the center of the room has shown a sixfold increase in creep rate due to a rise in salt temperature of approximately 20°C, whereas the

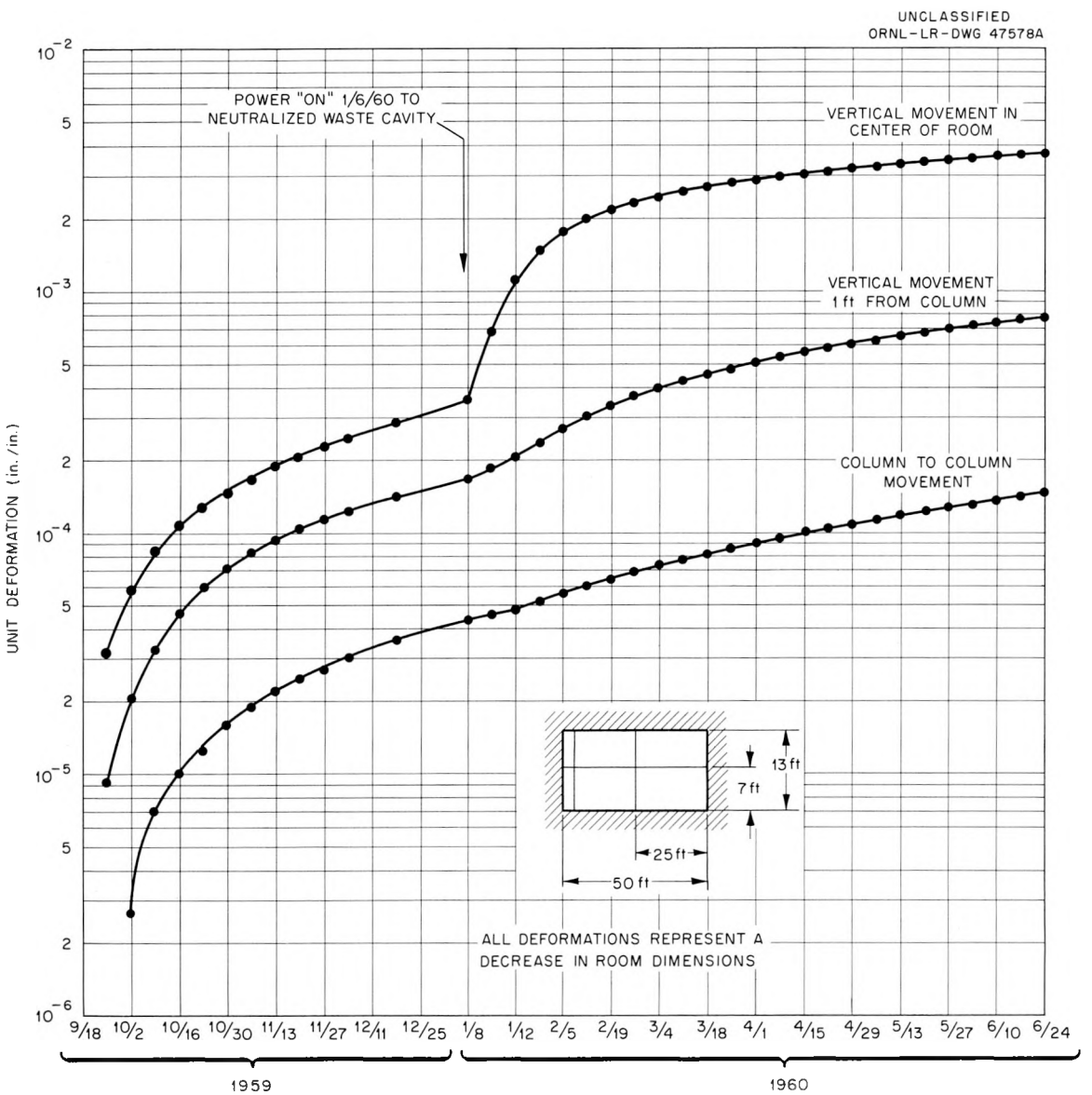

Fig. 1.56. Unit Deformation in Salt Surrounding Neutralized Waste Cavity.

vertical gage near the wall has shown a creep rate increase of about three times the initial rate due to a temperature rise of approximately 3°C. In all cases the creep curves show a slope decreasing with time, which is representative of the creep curve for a cavity approaching a condition of stability by adjusting its dimensions, as predicted by the theory of plasticity. Members of the University of Texas installed gages in the vicinity of the acid-waste cavity, and similar results are recorded.

Measurements of the movement of the floor in the area surrounding the neutralized-waste cavity show a flow of salt toward the cavity. Due to difficulties in attaching these gages to the salt without disturbing the mine floor, the data are not consistent from gage to gage. Strain-measuring devices installed in the mine floor by the Bureau of Mines show similar movement toward the cavity.

Preliminary analysis of the charts from the strain seismographs indicates that the salt may not be moving with constant velocity. More detailed analysis of these charts is required to separate the information on the movement of salt from the background disturbances due to local vibrations and extraneous signals. This work is in progress.

The data collected to date indicate a need for further study of plastic flow and the effect of temperature on the flow rate. By means of a number of measurements under different conditions of temperature, room size, and overburden pressure (depth), it should be possible to determine criteria for the design of a cavity which will be stable for long periods of time.

Gas Production. — The synthetic Purex waste solution used in the large-scale experiments was from the same lot as that used in the small-scale experiments (see Table 1.25). However, the structure in which the large pits are excavated is a complex mixture with salt, shale, and anhydrite present in clearly defined strata. The shale contains oxidizable material which will react with HNO_3 at ambient temperature to produce volatile oxides of nitrogen, and carbonates which will react to liberate CO_2. No interaction has been observed between anhydrite and the acid waste solution. The slight attack of acid Purex waste solution on the Haynes Alloy No. 25 cover of the experimental pit produces small amounts of the oxides of nitrogen.

Samples of the gaseous products were taken at the beginning of the experiment (temperature, 22°C) and at regular intervals up to the maximum temperature reached. Samples were obtained by pulling 250 ml into an evacuated bottle. Table 1.28 contains a summary of the composition of the

Table 1.28. Analysis of Gases from the Acid Pit

Date	Liquid Temperature (°C)	Vapor Temperature (°C)	Sample Port[a]	Gas Found (vol %)			
				N_2O-NO_2	NOCl	Cl_2	CO_2
January 1960							
18	22	22	I	T[b]	*[c]	*	*
			II	T	*	*	*
			III	T	*	*	*
			IV	*	*	*	*
			V	T	*	*	*
23	42.8	42.0	I	T	*	*	*
			II	T	*	*	*
			III	T	*	*	1
			IV	*	*	*	*
			V	T	*	*	*
27	56.3	49.0	I	1	*	*	1
			II	1	*	*	*
			III	1	*	*	*
			IV	*	*	*	*
			V	1	*	*	1
February 1960							
9	59.9	57.4	I	3	5	*	4
			II	3	10	*	4
			III	3	3	*	4
			IV	*	*	*	*
			V	3	5	*	4
March 1960							
31	63.7	60.1	I	10	18.5	*	3
			II	10	20	*	3
			III	8	10	*	3
			IV	*	*	*	*
			V	8	10	*	3

[a]Sample Ports:

I. Under cover, above liquid.
II. Before condenser.
III. After condenser.
IV. After scrubber.
V. Under cover, above seal.

[b]T = trace.

[c]* = not detectable.

off-gas in equilibrium with salt-saturated acid Purex waste at the temperatures listed. No data are given for the neutralized Purex waste, since no gases were produced.

Gas production becomes substantial only between 50 and 60°C. The vapor contained no detectable NOCl at 51°C and had reached 7% (by volume) at 60°C. A further rise in temperature to 63.7°C resulted in an NOCl content of 18%. The storage of acid Purex waste in a salt cavity would be simplified if the facility were designed to prevent the temperature from rising above 50°C. Only the gaseous products of radiolytic decomposition would then be a problem.

Routine analysis of off-gases from the acid pit did not show a positive indication of the presence of chlorine. However, when a sample of the gases was collected in a CO_2-methanol trap, chlorine was present.

The off-gases from the experiments are controlled by a water-cooled condenser followed by a vacuum jet-type scrubber which functions both to provide a flow of gaseous products from the cavity and to absorb the acidic gases by reaction with a 5 M NaOH scrubbing solution. The scrubber functions by pumping the caustic soda solution through the jet (mounted on top of a 55-gal drum), thus pulling gases from the pit into the drum. The drum is vented through an activated-carbon filter to the mine atmosphere. This system has been most effective in the removal of noxious gases, as illustrated in Table 1.28. No measurable concentrations have been found in the off-gas following the scrubber, even without the activated-carbon filter bed.

Laboratory studies have shown that there is a close relationship between the free-acid content of acid Purex waste and gas production. The free-acid content was monitored at two locations during the rising-temperature phase of the experiment and is shown in Table 1.29. Samples were obtained from two points within the pit solution: (1) midway between the two rows of electrodes and about 2 ft from the bottom of the pit, and (2) about a foot from one row and a foot below the surface. The samples were withdrawn into tared polyethylene bottles and returned to the laboratory for analysis. Since the hot solution deposits salt upon cooling, it was necessary to weigh and dilute the entire sample to a known volume before the analysis. Density measurements were made at the start of the run and

Table 1.29. Free Acid of Acid Pit

Sampling Date	Sample	Temperature (°C)	Concentration of Free Acid	
			Molal	Molar
January 1960				
18		21	5.793	7.015
21	I*	35.7	6.417	8.047
	II**	36.7	5.576	7.003
22	I	39.4	5.554	7.020
	II	40.4	5.443	6.902
24	I	39.2	5.446	6.884
	II	40.3	5.755	7.297
27	I	49.7	5.314	6.876
	II	49.7	5.302	6.866
31	I	54.3	5.274	6.893
	II	55.4	5.324	6.974
February 1960				
9	I	60.0	5.169	6.833
	II	60.7	5.212	6.895
March 1960				
31	I	63.4	4.914	6.560
	II	64.3	4.940	6.595

*I = Center of pit, 2 ft from bottom.
**II = One foot from electrodes, 1 ft from surface.

at maximum solution temperature, and values in between were approximated by interpolation. The acid concentrations were converted from the molal to the molar scale by using the density values thus derived.

Cooperative Studies

The Geotechnical Corporation. – W. B. Heroy, Sr., president of the corporation, has served as a consultant to the Laboratory on problems related to disposal of radioactive waste into salt. This has included investigation of sites for the present experiments and for possible future experiments. In addition, the corporation, under contract, designed and

installed instrumentation for the measurement of plastic movement of the salt surrounding the experiments. These data are presented in the section on Plastic Flow.

University of Texas. — The Department of Sanitary Engineering of the University of Texas, under the direction of E. F. Gloyna, is carrying on a study of plastic flow in the area around the waste experiments and also in a remote area of the mine. The data are being collected by ORNL personnel, but will be correlated by the University of Texas.

U.S. Bureau of Mines. — The Applied Physics Laboratory of the U.S. Bureau of Mines, under the direction of L. Obert, is also making strain measurements in the vicinity of one of the experiments. The instruments are read by ORNL personnel, and the data will be correlated and reported by the Bureau of Mines.

The Carey Salt Company. — The field experiments are being carried out in an unused section of the Hutchinson, Kansas, mine of the Carey Salt Co. The company has furnished labor, utilities, and mechanical facilities for operating the field experiments.

New Concepts

Previous experimental studies on disposal in salt have been based on wastes from natural or slightly enriched uranium fuel irradiated to 10,000 Mwd/metric ton at a specific power of 33 Mw/ton, and reprocessed to produce 800 gal of waste per ton.

Recent developments in fuel reprocessing indicate that it is quite feasible to reduce the waste volumes to as little as 60 gal or less per ton; the general trend is in the direction of reduced volumes. After a three-month decay period, wastes from a 60-gal/ton plant would have a heat generation rate (based on the aforementioned irradiation history) of 260 w/gal, and after an eight-year decay, the generation rate would still be 8 w/gal.

An isolated sphere, in an infinite bed of salt, capable of dissipating the heat from eight-year cooled, 60-gal/ton wastes could have a diameter no larger than 5 ft. In an economically feasible operation, waste cavities cannot be spaced so that there is no thermal interaction, and, therefore, the sphere would have to be less than 5 ft in diameter.

Thus, it appears that, for storage of the projected high-specific-activity wastes, numerous closely spaced cavities will be required. In fact, from the standpoint of economics and heat transfer, the best configuration for salt-mine disposal of large quantities of long-cooled, high-level liquid waste would seem to be a single horizontal layer of waste.

The projected thermal capacity of power generating reactors in the United States by 1970 is 33,000 Mw.[75] It is of interest to examine a salt-mine disposal operation to handle the ultimate storage of waste from a plant processing all fuel from these reactors. This plant would process 3.3 tons of fuel, producing 200 gal of waste per day.

Assume tank storage for eight years before disposal in the mine, after which time the specific power would be 8 w/gal or 1600 w per one-day batch. Assume ambient mine temperature of 70°F, and allow a 125°F rise in waste temperature. According to the curve of Fig. 1.48, it is found that, in an infinite slab, 228 Btu ft^{-2} day^{-1} will produce a 125°F rise. Thus, 575 ft^2 of storage area will be required for one day's plant output. On the basis of current salt-mining practice approximately 60% of the gross area of a mine would be available for waste storage. Gross area requirements are then 960 ft^2/day or 8 acres/year. If all rooms and passageways are opened to a height of 7 ft, this would require the removal of an average of 330 tons of salt each day. By comparison, the Carey operation at Hutchinson (a relatively small operation) removes 1000 to 1200 tons a day during the peak season.

Future studies and experiments will be directed toward determining optimum conditions, from the standpoint of heat dissipation, structural integrity, and economics, for a practical mine-disposal operation.

DISPOSAL OF RADIOACTIVE WASTE BY HYDRAULIC FRACTURING

W. de Laguna

B. L. Houser

For several years certain representatives of the petroleum industry, in particular D. A. Shock, Director of the Central Research Division of the Continental Oil Co. (Conoco) have urged the AEC and ORNL to explore

[75] H. R. Zeitlin, E. D. Arnold, and J. W. Ullman, Nucleonics 15(1), p 58–62, 1957.

the possibility of radioactive waste disposal by hydraulic fracturing. Although this method of rock fracturing is now a routine procedure for increasing the flow of sluggish oil wells, the theory of the mechanics by which the fractures are produced, and hence the fracture pattern to be expected, has been the subject of much debate among petroleum engineers.[76,77] This uncertainty has cast doubts on the wisdom of employing the method for waste disposal, an operation for which a high degree of certainty is required. However, the potential advantages of the method are so real, and its potential usefulness for the Oak Ridge area so attractive, that a series of field experiments has been undertaken.

It is not the purpose of these experiments to test any theory or to develop general principles, but rather to determine empirically what type of fracture pattern will develop in the local Conasauga shale and Rome sandstone, the two most suitable formations, at depths to about 1000 ft. There is justification for such an approach because it is generally agreed that down to depths of 1000 to 2000 ft, the chances of producing bedding-plane or horizontal fractures are at their best, and the fracture pattern will be governed largely by the nature of the rock and the residual stresses in it, factors which must be determined for each area.

First Fracturing Experiment

The first experiment was designed to test the testing method, and to give some information on the fracture pattern to be expected at relatively shallow depths. It was not intended to test potentially useful disposal procedures. To this end, the test was carried out in the so-called "Four Acre Site" where earlier work for another project had established the general picture of surface and subsurface geology. A steel casing (3.5-in. OD, J-55 type, high strength) was cemented into an existing 300-ft-deep well, and slotted at a depth of 290 ft with a sand jet,

---

[76] J. M. Cleary, Hydraulic Fracture Theory, Part I, Mechanics of Materials, Part II, Fracture Orientation and Possibility of Fracture Control, Illinois State Geological Survey, Circulars 251 and 252, Urbana, Ill. (1958).

[77] M. K. Hubbert and D. G. Willis, J. Petrol. Technol. IX(6), p 153–66 (1957).

which cut through the casing and out into the shale. Water was then pumped down the well until the shale fractured at a pressure of 2300 psi, after which the pressure dropped. The fracture was extended by continuing to pump at a rate of about 300 gpm and a well-head pressure of 600 psig.

Once it was clear that the well was taking the injected water easily Portland cement and diatomaceous earth in equal amounts by volume were added to the water (see Fig. 1.57), and a small high-pressure metering pump injected a solution of radioactive cesium into the top of the well casing where it mixed with the grout. A total of 20,000 gal of water, 1370 ft^3 of bulk Portland cement, and 1370 ft^3 of Litepoz (diatomaceous earth) were pumped into the well at a rate of 90 gpm and a pressure of 300 psig. The total volume injected was about 26,000 gal, or 3500 ft^3, to which was added 35 curies of Cs^{137} and 8 curies of Ce^{144}.

Just as the operation was completed, the grout mixture started to flow very slowly out of a pre-existing test hole 200 ft deep and located 200 ft NW up-dip from the injection well, showing that the grout had traveled that far at least. Later test drilling showed that the main grout sheet barely intersected the bottom of this well (No. 72) and that a second, thinner sheet passed just below it. Figure 1.58 shows the general relations as developed by the later drilling of core hole 202. More recent drilling penetrated the grout sheet at a depth of 143 ft, 345 ft to the NW along this same line of section. Figure 1.59 shows the core of shale containing the grout obtained from this well. In a test hole drilled 400 ft from the injection well in this same direction, a very thin sheet of grout was found at a depth of 126 ft. As nearly as can be determined, the grout sheet, in moving to the NW up-dip, followed essentially the same bedding plane except where it divided into parallel sheets, probably about halfway between the injection well, 73, and well 72. This separation was probably due to the small fault and narrow zone of overthrust folding observed at the surface, which probably extends down to the horizon of the grout seam.

Test drilling along the strike to the NE showed that the grout extended in this direction at least as far as 275 ft, and that it followed very closely the same horizon (see Fig. 1.60). To the SW the grout has been found by recent drilling to extend only 80 ft, beyond which it was

Fig. 1.57. High-Pressure Pump Truck and Bulk Dry Cement Carrier Used in the First Fracturing Experiment.

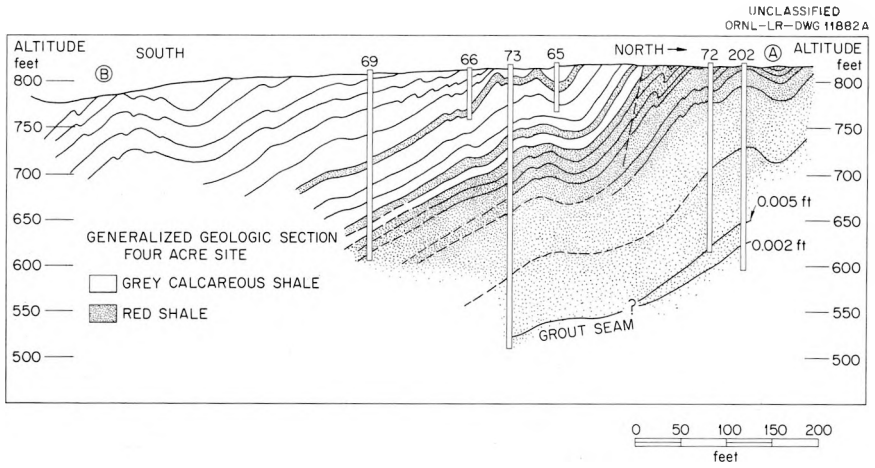

Fig. 1.58. Wells Projected Along Strike to Line of Section.

apparently blocked by a zone of crumpled shale. The thickness of the grout sheet is somewhat variable, ranging from 0.03 to 0.005 ft in the cores so far recovered, but averaging about 0.02 to 0.015 ft.

It is generally agreed that space for a horizontal fracture is created by an uplift of the surface, while the space for a vertical fracture is created by compressing the rock laterally. An attempt to measure the vertical uplift of a group of benchmarks in the area of the first experiment was inconclusive, although there was a strong suggestion that the benchmarks in the NE and NW quadrants underneath which the grout passed were lifted up by about 0.010 ft, roughly the thickness of the grout sheet. The survey of the line of benchmarks to the SW now appears to contain erratic variations, although additional drilling may provide an explanation. No drilling has yet been done to the SE, where the benchmarks show a clear uplift out to but not beyond 75 ft.

The injection and fracturing operations were performed by Dowell, Inc., one of the oil-field service companies specializing in this type of work. Without question, it went easily and almost without incident. The subsequent core drilling provided a clear picture of the location and thickness of the grout sheet, the amount of detail being limited only by the number of holes drilled. The radioactive tracer in the grout made it possible to positively identify the fracture in the cores recovered, or by logging the core hole. Although local irregularities of the geologic structure modified the pattern, the fracture followed by the grout sheet conformed

UNCLASSIFIED
PHOTO 50391

Fig. 1.59. Core Containing Grout Seam from Well 345 ft NW of Injection Well.

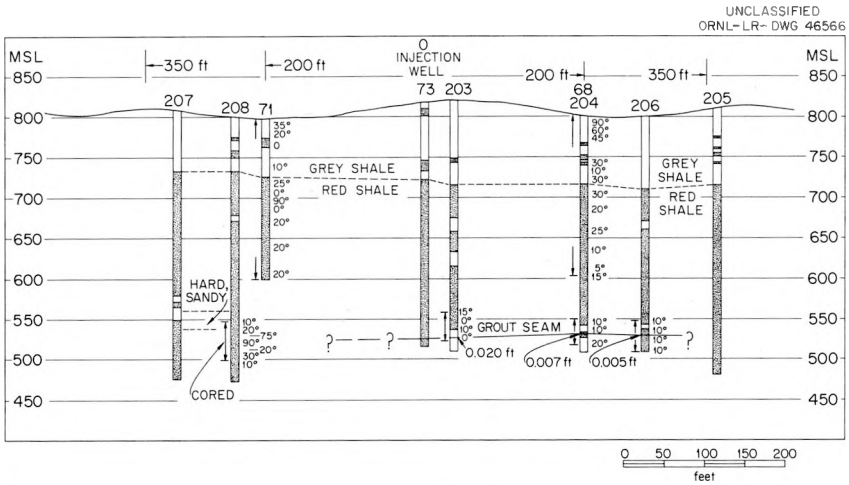

Fig. 1.60. First Hydraulic Fracturing Experiment, Four-Acre Site, Oak Ridge.

closely to a single bedding plane and showed no tendency to cut across the bedding up toward the surface. The grout-filled fracture is highly impermeable, so that leaching of the grout by ground water would appear to be unlikely.

Because all the factors are favorable, and because the test method shows capabilities of furnishing the data required, plans have been made for a second experiment, and the preparatory work is under way. Test drilling at the site of the first experiment to define the shape and extent of the grout sheet is not yet completed, and it is possible that the final delineation will offer some surprises.

Second Fracturing Experiment

The purpose of the second experiment will be to duplicate in scale an actual disposal operation, except that water and a radioactive tracer will be used rather than actual waste. Two separate batches of grout will be injected into the same well, each batch containing 100,000 gal of water; the volume for the two batches will be approximately ten times that injected in the first experiment. The first batch will be injected at a depth of 1000 ft, and the second at a depth of 700. These depths represent, on the one hand, the lower limit of easy test drilling, and on the other, a thickness of cover which would provide that large margin of safety required by disposal operations. If it is possible to inject into the

Conasauga and Rome formations through a single well a series of grout batches, each batch containing 100,000 gal of liquid, then the method has operational possibilities.

The site of the experiment has been chosen in Melton Valley, about 0.5 mile south of the 7500 (experimental reactor) Area, near the top of the Conasauga shale, and where the meager surface indications suggested a minimum of folding. More importantly, perhaps, the site is adjacent to a 4-in. water line and an electric power line. The churn-drill hole which will be used for the fracturing has been completed at a depth of 1050 ft and apparently has penetrated about 200 ft into the top of the Rome sandstone. The neighboring stratigraphic test hole, which is being cored to the same depth, has reached a depth of about 500 ft, and so far shows the rock to have an average dip of about 20° and somewhat less folding and faulting than the rock at the site of the first experiment. Except for the volumes involved, and perhaps for the rate of pumping, the injection and fracturing operation are expected to be much like those of the first experiment. Experience with the cesium tracer has shown that it can be detected easily in even lower concentrations than were used in the first test. It is planned to add 25 curies of Cs^{137} to each of the two batches of grout.

The help of the U.S. Geological Survey has been obtained for a more precise survey of benchmarks at the site of the second experiment, and also for an attempt with special, precise equipment to measure earth tilt during the course of the injection. It would be a matter of some interest to be able to follow the movement of the grout sheet in depth by measurements made at the surface, although to detect a deformation of 0.010 ft at a depth of 1000 ft may be impracticable.

Future Problems

If the mechanics and configuration of hydraulically produced fractures in the local shale and sandstone could be predicted, even empirically, then a potentially useful method of radioactive waste disposal might be realized. Other less critical and less serious problems, however, will have to be solved.

Present well-drilling and test-drilling methods are quite adequate for any proposed disposal operation. The mixing and pumping equipment required are also relatively standard items but will have to be redesigned for remote operation, decontamination, and repair. This question, in turn, is related to the mixes that will be used, for it may well be possible to use even cheaper materials than Portland cement and diatomaceous earth. The questions here are not so much concerned with feasibility as with cost, but they will require careful study. Preliminary tests suggest, however, that even simple, cheap, clay-cement mixtures can be blended with almost any neutralized-liquid waste, including a heavy load of suspended solids, in such a way that they will set up with sufficient strength in depth to immobilize the waste. Also, it appears that heat dissipation from a thin grout sheet is unlikely to be a problem. It is not unreasonable to expect, therefore, that the method may be relatively cheap, for the equipment and raw materials required are simple and inexpensive. Further, the method shows some promise of being able to handle many waste types, regardless of their chemical composition and specific activity. Geologically, the sites are not hard to find. Shale or shaly sandstone are among the most common of sedimentary rocks, and in much of the United States (or the world) they are present in flat-lying beds with much simpler and, therefore, more favorable structure than in the test areas in Oak Ridge.

The operational hazard will come largely from the high pressures required, but the volumes that could be accidentally released at any one time by a single broken pipe would be small, and even this possibility appears remote. The long-term hazard from a thin, solid sheet of grout, firmly cemented in depth into a virtually impermeable shale, well below all moving ground water, would also appear to be minimal.

RELATED COOPERATIVE PROJECTS

E. G. Struxness R. J. Morton

K. E. Cowser
L. C. Emerson
L. Hemphill
F. L. Parker
P. H. Carrigan[78]
R. M. Richardson[78]
W. de Laguna
F. M. Empson
D. G. Jacobs
T. Tamura
B. J. Frederick[78]
E. T. Chanlett[79]

Geologic and Hydrologic Studies by U.S. Geological Survey

To provide for the safe disposal of solid, packaged radioactive wastes generated by AEC licensees, the AEC plans to establish one or more regional burial grounds. One of the sites under consideration is that part of Bear Creek Valley west of the Y-12 Plant and east of White Wing Road.

To determine the suitability of the site for land burial, the U.S. Geological Survey began an investigation in May 1959. Five core holes, 3 in. in diameter and 200 ft deep, and ten churn-drill wells, 6 in. in diameter and 150 ft deep, were drilled to further define the geology and hydrology of the area. The core holes were pressure tested to determine the location of permeable zones and the amount of water they would accept. Fluorescein was injected under pressure in one core hole to determine the rate and direction of ground-water motion. Depth to water in the 15 wells was measured periodically to determine the position and range of fluctuation of the water table. Five stream-gaging stations were established on Bear Creek and tributary springs to determine seasonal variations in flow.

The area is underlain by the Conasauga shale of Cambrian age. Test drilling showed that the bedrock consists predominantly of gray calcareous shale containing lenses of relatively pure limestone. The amount of limestone increases to the SE. The three wells drilled at the base of Chestnut Ridge encountered very little shale. Bedrock is covered by a zone of weathered rock, ranging in thickness from about 20 ft in the lower areas up to about 50 ft at points of higher elevation. The weathered rock is covered by a thin mantle of soil about 1 to 2 ft thick.

---

[78]U.S. Geological Survey.

[79]ORINS research participant, University of North Carolina.

Pressure testing the five core holes indicated that the bedrock is fractured and is capable of transmitting water to depths of about 150 ft. The test drilling indicated a persistent cavernous zone at depths between 60 and 80 ft below land surface in the area adjacent to the base of Chestnut Ridge. Foundation explorations during construction in the Y-12 Plant area indicated that similar conditions exist there, and it is probable that the cavernous zone extends the entire length of the valley.

To determine whether Bear Creek was hydraulically connected with the cavernous zone, a dye test was run on a core hole at the base of Chestnut Ridge and about 25 ft from the creek. A packer was set in the hole 75 ft below land surface. One-half pound of sodium fluorescein and one-half pound of sodium hydroxide were mixed with 2 gal of water and poured into the well through the drill rods supporting the packer. A pump was connected to the drill rods and water was pumped into the well at a rate of about 10 gpm for 4.5 hr. Dye was observed coming from cavities in rock in the creek bed at points about 300 and 1200 ft downstream from the well 3 hr after pumping began. However, the time at which the dye first appeared was not determined.

Water levels in the area are deepest in the elevated areas and shallowest in areas of lower elevation. Depth to water in wells on the top of Pine Ridge ranges from about 25 to 50 ft below land surface. In wells at lower elevation near Bear Creek, the depth to water ranges from about 3 to 10 ft below land surface.

Since April 1959, discharge measurements have been made at monthly intervals at five stations on Bear Creek and at tributary springs. At the station farthest downstream, where Bear Creek crosses State Highway 95, the lowest flow measured was 0.589 cfs on September 9, 1959, and the highest was 10.9 cfs on March 15, 1960. While the low-flow figure is representative of discharge in the fall, it is certain that stream flow was significantly higher than 10.9 cfs many times during the period of record after intense rains on the watershed.

The investigation indicated that solid, packaged radioactive wastes could probably be disposed of safely by burial in trenches excavated along the crest of Pine Ridge. At this location the depth to water is such that

the bottom of the trenches would be above the water table throughout the year. Rainfall percolating downward through the trenches to the water table would move several hundred feet through the weathered shale before being discharged to the surface.

Areas at lower elevation within the site are not as favorable for land burial. The water table is at shallower depth; the travel distance of water movement underground from trench to point of surface discharge is less; and the existence of cavities in the limestones that underlie the areas at lower elevation would permit more rapid ground-water movement and with less chance for fixation of fission products.

The width of the crest of Pine Ridge is generally 300 ft or less. The ridge crest is also dissected by streams about 1000 ft apart. Hence, individual burial sites would comprise only a few acres. It appears that the favorable areas available are not sufficient to warrant consideration of Bear Creek Valley for use as a regional burial ground for solid, radioactive waste.

In addition to the investigation in Bear Creek Valley reported above, preliminary field examinations have been made of a number of sites on federally-owned land in Indiana, Ohio, Pennsylvania, and New York to determine their suitability for possible use as regional burial grounds for solid, packaged radioactive waste.

The Knoxville Office of the Surface Water Branch cooperated with the Clinch River survey groups in making a series of velocity and temperature measurements in Clinch River downstream from White Oak Creek.

Cooperation of Other Agencies in ORNL Studies

Clinch River Study

Several state and federal agencies are cooperating in the Clinch River study described in an earlier section of this report and have contributed substantially in the formulation of plans and in the field and laboratory work to date. TVA has made available its knowledge of the hydraulics of the Clinch River and the techniques used for measuring the various physical parameters of the system. The U.S. Geological Survey

has made available knowledge of diffusion processes and has provided temperature and velocity profiles of the river. The U.S. Public Health Service has contributed by quarterly sampling in the Clinch and Tennessee Rivers and by laboratory analyses and assembly of data. The AEC, Tennessee Game and Fish Commission, Tennessee State Department of Health, and Tennessee Stream Pollution Control Board have provided advice and guidance, based upon their long experience in similar river studies.

Disposal in Salt Formations

Several phases of the program of studies on waste disposal in natural salt formations have been strengthened and supplemented by cooperative work by other agencies. These include the Geotechnical Corp. of Dallas, Texas; The Department of Sanitary Engineering of the University of Texas; the Applied Physics Laboratory of the U.S. Bureau of Mines; and the Carey Salt Co. of Hutchinson, Kansas. The contributions by these agencies are acknowledged, and the results of cooperative work are included in an earlier section of the report, Disposal in Salt Formations.

Disposal in Deep Wells

Following one of the specific suggestions of the American Petroleum Institute Committee, the U.S. Bureau of Mines Laboratory at Bartlesville, Oklahoma, has begun a study of the factors which control the injectability of a liquid waste into a permeable formation. The initial work has been with synthetic Purex-type waste and cores of natural sandstone.

The U.S. Geological Survey is in the course of preparing a series of geologic reports on the stratigraphy of the major sedimentary basins of the United States. It is planned to submit these reports to a committee of the American Association of Petroleum Geologists for amplification. To date the Survey has completed one report, that on the San Juan basin.

A proposal from the Petroleum Research Corporation of Denver, Colorado, concerned with a possible study of the mechanisms that produce apparently anomalous hydraulic gradients in deep artesian aquifers, has cast a fresh light on the problem of dispersing fluid waste into deep permeable formations. As the deep-well-disposal program advances, it is hoped that their ideas and experience can be fully utilized.

Low-Level Waste Treatment – Dorr-Oliver

Members of the staff are assisting the AEC in coordinating work to be performed by Dorr-Oliver, Inc. The studies proposed by Dorr-Oliver and approved by the AEC include an evaluation of the volume and particle-size distribution of suspended solids in low-level waste at ORNL and the relationship of particle size to activity level, and an evaluation of proprietary equipment of Dorr-Oliver for concentrating sludge generated in the waste-water treatment plant.

Visiting Investigators from Abroad

During the year eight engineers and scientists, associated with nuclear energy programs in other countries, worked as members of the research staff of the Radioactive Waste Disposal Section. Each of these assignees, designated in the Laboratory as "Alien Guests," selected a research problem pertinent to the program of his own country and worked under the guidance of one of the project leaders in the section. The results of each investigation are to be made available in an ORNL topical report, and are included in the appropriate project section of this progress report.

The investigator's name and home agency and the approximate length of time for each of the individuals assigned to the section under this cooperative arrangement, the problem selected for study, the section project in which he worked (or is now working), and the section staff member who directed his research are given below.

S. Amarantos (Greece), Democritus Nuclear Center, Greek Atomic Energy Committee, Athens, Greece, approximately 9 months. Problem: Reaction of Naturally Occurring Organic Matter with Radionuclides. Project: "Sorption and Retention by Minerals and Compounds" (Tamura).

G. Bruscia (Sicily), Municipality of Licata, Licata (Ag.), Italy, approximately 5 months. Problem: Radionuclide Uptake by Clinch River Sediments. Project: "Clinch River Studies" (Tamura).

K. Eschle (Switzerland), Reaktor Limited, Würenlingen (AG), Switzerland, approximately 9 months. Problem: Aluminum Phosphate Coagulation for Radiostrontium Removal. Project: "Low-Level Waste Water Treatment" (Tamura).

Y. Feige (Israel), Israel Atomic Energy Commission, Rehovoth, Israel, approximately 8 months. Problem: Analysis of Waste Disposal Practice and Control at ORNL. Project: "Clinch River Studies" (Parker).

Y. Nakayama (Japan), Research Division, Nippon Atomic Industry Group Company, Ltd. (NAIG), Tokoyo, Japan, approximately 12 months. Problem: Removal of Radiostrontium Using Alumina Column Technique. Project: "Sorption and Retention by Minerals and Compounds" (Tamura).

A Sorathesn (Thailand), Sanitary Engineering Department, Chulalongkorn University, Ministry of Education, Bangkok, Thailand, approximately 5 months. Problem: Radionuclide Uptake by Clinch River Sediments. Project: "Clinch River Studies" (Tamura).

T. Subbaratnam (India), Atomic Energy Establishment, Trombay, Bombay, India, approximately 6 months. Problem: Studies on the Use of Coagulant Aids in the Lime-Soda Treatment of Large-Volume, Low-Level Radioactive Liquid Waste. Project: "Low-Level Waste Water Treatment" (Cowser).

K. T. Thomas (India), Atomic Energy Establishment, Trombay, Bombay, India, approximately 6 months. Problem: Radiostrontium Removal Using Natural Mineral Columns. Project: "Soil Column Studies" (Jacobs).

Observations on Aerosol Emissions from High-Level Liquid Wastes During Storage

These studies were made during the summer of 1959 by a research participant from the University of North Carolina. The purpose and early stages of the studies were reported a year ago.[80] Of four things that were done in the investigation, three were attempts to characterize the wastes in tank W-6 which received liquid residues from the Fission Product Pilot Plant (F3P). These consisted in (1) ionic and radiochemical analyses of a single grab sample from tank W-6; (2) study of the unit processes and flow pattern in F3P; and (3) scanning of the operational records of F3P, which included certain analytical data. These efforts to describe quantitatively the contents of tank W-6 were not successful, and, therefore, an actual waste composition could not be simulated for study.

[80] E. G. Struxness et al., H-P Ann. Prog. Rep. July 31, 1959, ORNL-2806, p 119.

The fourth thing done was laboratory-batch heating of simulated Purex waste at selected temperatures and with or without air sweeping over the liquid surface to determine whether entrainment and aerosol emission occurred. A topical report will give details of these laboratory experiments and the results obtained.[81]

Twenty-two experimental runs were made, in each of which a 1500-ml portion of simulated waste solution was heated in a 3000-ml flask by means of upper and lower electric mantles. The controlled variable included pH of waste solution, temperature and time of heating, and volume of air sweep through the flask (liters per minute per square foot of liquid surface). The determinations made included: volume of condensate collected in the ice bath (0°C) and freeze-out trap (−75°C), chemical determinations of iron and nitrate in the condensate, and radioactivity carry-over in three runs that were spiked with a mixture of Fe^{55} and Fe^{59}.

This investigation was exploratory, and the data obtained were not sufficient for extensive interpretation. Observations of particular interest include the following:

1. The initial measurable condensate was collected in the ice bath at a flask temperature of about 90°C. At temperatures of around 90°C without air sweeping, the condensate yield was less than 1.0 ml/hr. Condensate volumes rose rapidly with temperature increases from 90°C to boiling (above 100°C).

2. Air sweeping the 100°C runs at a flow rate of 1.5 liters per minute per square foot of liquid surface increased condensate recovery in milliliters per hour tenfold, compared with similar runs without air sweeping.

3. Iron concentrations in the condensate decreased with temperature increases and with condensate volume increases. Furthermore, the amount of iron recovered in the condensate decreased with increasing temperature. This suggests that the carry-over of iron, and presumably of other nonvolatile ions, is associated mainly with aerosol emission, rather than with the gaseous vapors which would be expected to increase at the higher temperatures.

[81] E. T. Chanlett, Preliminary Observations on Aerosol Emissions from High-Level Liquid Wastes During Tank Storage, ORNL report (to be published).

Nuclear Safety Review

Two members of the section served on the editorial staff of Nuclear Safety. During the year several individuals in the section contributed review articles on the subject of radioactivity release and its consequences.

Committee Work

American Standards Association Committees

Three of the staff have served on ASA committees as representatives of professional organizations and of the Laboratory. Two have continued as members and have participated in the work of ASA Sectional Committee N5, "Chemical Engineering for the Nuclear Field," and of its Subcommittee N5.2 on "Radioactive Waste Disposal." One has continued as a member of Sectional Committee Z54, "Industrial Use of Radiation," and of its Subcommittee Z54.9 on "Contamination Levels of Industrial Materials." Participation of these three members includes attendance at committee meetings, and work assignments to explore the need and feasibility of standardization on particular problems; and one serves as secretary for Subcommittee N5.2.

American Public Health Association Committee on Radiological Health

One member of the section has continued to serve on the APHA Program Area Committee on Radiological Health and has attended two meetings of this committee during the year. A revised statement of "Public Health Policy on Radiological Health" has been completed by the Committee and approved by the APHA as a guide to public health agencies in their programs of radiation control. Other problems on which this Committee is working directly or by coordination include procurement, graduate education, and in-service training of public health personnel in radiological health; inclusion of information about ionizing radiation in public health education programs; analysis of and advice regarding proposed or enacted legislation; and review of resolutions concerning ionizing radiation proposed for adoption by the APHA.

Expert Committee V of International Commission on Radiological Protection

The section leader was recently appointed a member of Committee V on "Handling of Radioactive Isotopes and Disposal of Radioactive Wastes," one of several expert committees of the ICRP.

ORNL Committees and Special Working Groups

One member of the staff was designated to provide liaison with several Laboratory groups and to make information available to them as necessary.

Information was assembled and furnished to the Office of Radiation Safety and Control regarding vermiculite for further treatment of the effluent from the waste-water treatment plant. This was requested by the ORSC in connection with an engineering study to evaluate the present waste handling, treatment, and disposal system at ORNL and to recommend improvements. The designated representative of the section upon request has attended several meetings and participated in discussions by the ORNL Waste Effluents Committee. In cooperation with a working group of the Engineering and Mechanical Division, plans for testing reduced pressure principle back-flow preventers with radioactive tracers have been developed, and technical criteria for such tests have been formulated.

Participation in Educational Programs

In the program of the Oak Ridge School of Reactor Technology for a group of foreign students, six members of the section gave seven lectures on radioactive waste problems and waste-disposal studies at ORNL. Also, the course in physical geology, reported for a previous foreign group,[82] was given again for this group.

Three members of the section gave a total of four lectures in the AEC Fellowship course in radiological physics, conducted by the Education, Training, and Consultation Section of the Division, at Vanderbilt University.

---

[82] E. G. Struxness et al., H-P Ann. Prog. Rep. July 31, 1959, ORNL-2806, p 120.

Three lectures by two members of the section were given as part of the course for personnel of public health agencies conducted by the Health Physics Division at ORNL.

Four lectures and a field tour of the Laboratory's waste-disposal facilities and research activities were provided at ORNL as part of the course conducted by the U.S. Public Health Service on "Reactor Environmental Health Problems."

One staff member gave two lectures on "Radiation Problems Related to Public Health" at the University of Tennessee for the College of Education's course in public health education.

2. ECOLOGICAL RESEARCH

WHITE OAK LAKE BED STUDIES

S. I. Auerbach

D. A. Crosley, Jr.
P. B. Dunaway
G. L. Plummer[1]
S. V. Kaye
R. M. Anderson
M. P. Hoglund
V. I. Dodson
J. H. Schnell[2]

Ecological research in this area takes advantage of the radioactive contamination present to obtain needed information on the movement, distribution, and biological cycling of mixed fission products under field conditions. The size of the area (about 35 acres) provides sufficient space for a number of basic and applied studies including movement in soil, uptake by plants, rates of transfer through food chains, and investigations on the effect of chronic radiation on a variety of organisms. Essentially this area is a large-scale field tracer experiment in which the contained radioactive isotopes also are being used for obtaining fundamental knowledge on the relations between organisms and their environment.

Soils

Knowledge of the movements and changes in distribution of radionuclides in soils under field conditions is important for predicting the fate of contaminants released to the environment. In restricted areas such as the lake bed, data on the budget of fission products in the soil are necessary for planning and control of waste effluent releases, especially when the bed is part of an over-all waste-disposal system. Last year (FY 1960) studies were begun on the yearly changes and movement of fission products in the lake-bed soils.[3] Changes in Sr^{90} concentrations in the upper 6 in. of soil were determined for 1956–58, and budgets for these years were calculated. These data suggested a 50% loss from the

---

[1]Research participant.

[2]Summer employee.

[3]S. I. Auerbach et al., H-P Ann. Prog. Rep. July 31, 1959, ORNL-2806, p 18–20.

upper soil in 1.25 years. Soil samples taken during 1956–58 were analyzed during the past year for total radiocesium and radiocobalt. In 1959, 200 soil cores were taken from the lower part of the lake bed, and composite samples were radioanalyzed. Fixed sampling points also were established for continuing studies, and samples were taken at various depths in the soil profile down to the water table. The results of these analyses have been reported elsewhere.[4] Of particular interest is the fact that the mean concentration of Sr^{90} for 1959 (0.040 μc/100 g) is practically unchanged from 1958 (0.045 μc/100 g). This indication of little further loss of Sr^{90} from the upper 6-in. layer suggests that the rate of loss may be decreasing to a point where there will be a reservoir of Sr^{90} above fallout levels available for biological uptake for a long time. The concentrations of Cs^{137} and Co^{60} in the upper soil have remained almost the same (except for decay) since the lake was drained. From the 1958–59 data it is estimated the current Cs^{137} concentration in the lake bed is approximately 12 curies/acre.

Plants

An analysis was made of two species of plants (sedges) which have been resident on the lake bed for four years and which have been exposed continuously, both internally and externally, to radiation during this period.[5] The lengths of the pistils were analyzed as indicators of growth response to site quality and to ionizing radiation. Samples were taken from areas with 0, 10, 20, and 40 mr/hr dose rates. Lengths of the pistils varied with does rate but are believed to be independent of the ionizing radiation and more closely associated with other soil factors. Further studies are under way to delineate the soil factors affecting the plant response.

Much of the work that has been done on soil-plant relationships involving radiostrontium and radiocesium has treated these radionuclides

---

[4]E. G. Struxness et al., Detailed Assessment of Solid and Liquid Waste Systems – Hazards Evaluation Vol 4, ORNL CF-60-5-29, p 35–39 (May 31, 1960).

[5]G. L. Plummer, Biometric Analysis of a Growth Response of Two Plant Species in a Radioactive Waste Area, ORNL-2903 (Apr. 11, 1960).

independently even though they frequently occur together, as in fallout. The presence of both these isotopes in the lake-bed soil provides an opportunity for considering them together in matters involving soil-plant relationships, plant composition, and the subsequent transfer of radionuclides to animals.

During the summer of 1959, yield-harvests (total standing crop per square meter) of smartweed (Polygonum sp.) were taken every four weeks beginning in June. This species has been abundant on the lake bed since draining, and grows in stands which facilitate yield-harvesting. The differences in uptake between radiostrontium and radiocesium by this crop during the growing season are summarized in Table 2.1. In the leaves, the concentration ($\mu c/g$) of radiostrontium is reduced during the growing season by approximately 30%, whereas the concentration of radiocesium increased by approximately 76%. The stems show the same pattern (Sr^{90}, -57% vs Cs^{137}, -4%) between the first and third harvests. For both leaves and stems the percentage increase of Cs^{137} per square meter between the first and last harvests is greater (leaves, +441%; stems, +513%) than the percentage increase in yield (g/m^2) (leaves, +229%; stems, +456%). While there is also an increase in total Sr^{90} per square meter (leaves, +130%; stems, +155%) during the growing season, the increase is less than the percentage increase in yield.

The reduction in Sr^{90} uptake in proportion to yield-increase in contrast to the uptake of Cs^{137} may reflect a change in the availability of this radionuclide as well as some dilution by increased production of cellulose. However, the data indicate that some uptake occurred throughout the season because yield-increase ($\mu c/m^2$) exceeded the reduction in unit weight concentration.

The evidence that increase in yield occurred without proportionate increase in radionuclide content in native vegetation raises two questions: (1) Can the same phenomenon occur in crop plants, especially forage species? (2) If so, is it possible to use soil treatments which would accelerate yield without increasing uptake? To this end, field-plot and greenhouse experiments have been started, testing the effect of phosphate fertilizer on the uptake of mixed fission products from White Oak Lake soils by two species of crop plants.

Table 2.1. Uptake and Accumulation of Sr^{90} and Cs^{137} by Smartweed (Polygonum sp.) in Relation to Growth (Yield)

Each value represents the average of two samples

	Harvest			Percentage Change*
	6/23/59	7/20/59	8/20/59	
		Leaves		
Sr^{90} ($\mu c \times 10^{-3}/g$)	1.27	1.30	0.89	−30
Cs^{137} ($\mu c \times 10^{-3}/g$)	0.28	0.24	0.50	+76
Yield (g/m^2)	72.4	92.4	238.2	+229
Sr^{90} ($\mu c \times 10^{-3}/m^2$)	92.0	119.7	212.0	+130
Cs^{137} ($\mu c \times 10^{-3}/m^2$)	20.6	21.9	111.5	+441
		Stems		
Sr^{90} ($\mu c \times 10^{-3}/g$)	1.09	0.67	0.47	−57
Cs^{137} ($\mu c \times 10^{-3}/g$)	0.054	0.047	0.052	−4
Yield (g/m^2)	114.0	218.6	633.4	+456
Sr^{90} ($\mu c \times 10^{-3}/m^2$)	125.0	146.0	319.3	+155
Cs^{137} ($\mu c \times 10^{-3}/m^2$)	6.1	10.3	37.4	+513

*Percentage change between first and third harvests.

Insect Studies

Investigations on the role of the insects in the biological cycling of fission products have continued to receive the major emphasis in the insect studies. Both field and laboratory data are utilized as follows: Samples of insects and plants from White Oak Lake bed are taken in order to estimate the equilibria of radioisotope concentrations in plant and

insect tissues. Laboratory experiments are performed on the rates of elimination of the radioisotopes by insects. These field and laboratory data, in combination with field observations and measurements on feeding habits of the insects, and the densities of insects and plants, are providing information on the quantities of fission products which pass through insects in the food chain.[6] Also, the isotopes provide estimates of the amount of the plants eaten by the insects, which are of importance in tracing the transfer of energy through ecological systems.

Laboratory Studies

Pilot studies on the accumulation and elimination of Cs^{137} by the eastern lubber grasshopper (Romalea microptera Beauv.) have been reported.[7] Two grasshopper residents of White Oak Lake bed have been the subjects of similar studies. The differential grasshopper (Melanoplus differentialis Thomas) and the red-legged grasshopper [Melanoplus femur-rubrum (DeGeer)] have been used in investigations on the comparitive elimination of radiostrontium and radiocesium by insects.

The method was as follows: Radioisotopes were smeared on grass leaves and allowed to dry. Insects were permitted to feed upon the contaminated leaves and were counted immediately for gamma radioactivity so that subsequent counts could be expressed as a percentage of the original count. Subsequent feedings were uncontaminated. A model 810 Baird-Atomic gamma scintillation detector with a 2 × 2 in. well crystal was used.

Results of the experiments with Sr^{85} and Cs^{137} in the differential grasshopper showed that strontium was eliminated much more rapidly than cesium. Figure 2.1 illustrates the elimination of Cs^{137} by this grasshopper species; these data suggest a biological half life of about two days. Strontium-85 was eliminated with a biological half life of only about 12 hr (see Fig. 2.2). Similarly, for the red-legged grasshopper, biological half lives were approximately 30 hr for Cs^{137} and 10 hr for Sr^{85} (see Fig. 2.3).

---

[6]D. A. Crossley, Jr., and H. F. Howden, Insect-Vegetation Relationships in an Area Contaminated by Radioactive Wastes (in manuscript).

[7]S. I. Auerbach et al., H-P Ann. Prog. Rep. July 31, 1959, ORNL-2806, p 30.

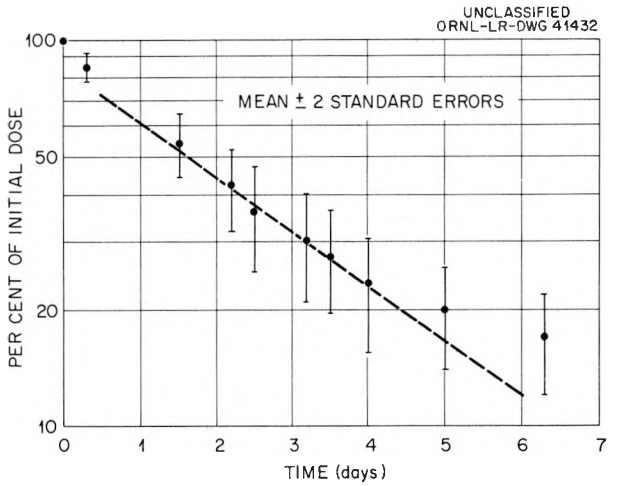

Fig. 2.1. Elimination of Cs^{137} by the Differential Grasshopper (Melanoplus differentialis Thomas).

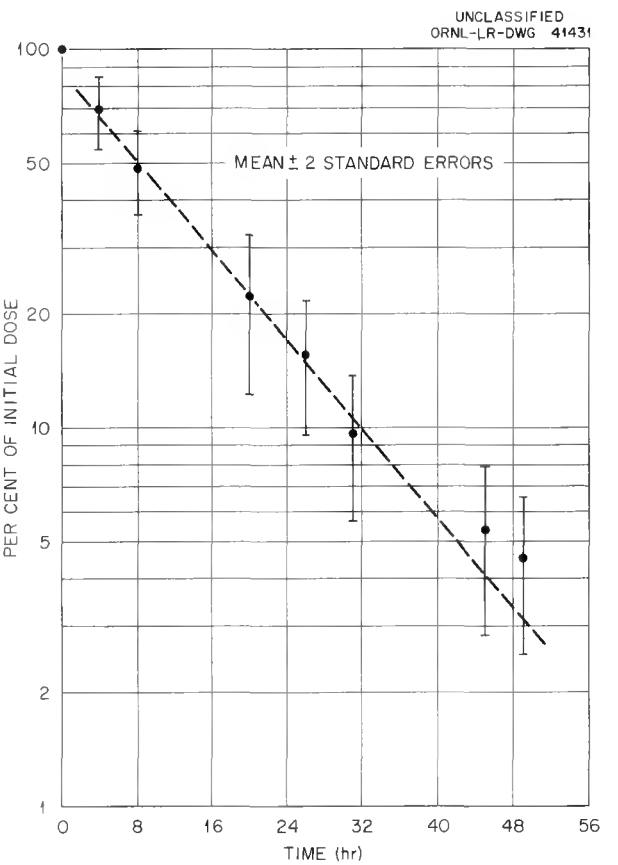

Fig. 2.2. Elimination of Sr^{85} by the Differential Grasshopper (Melanoplus differentialis Thomas).

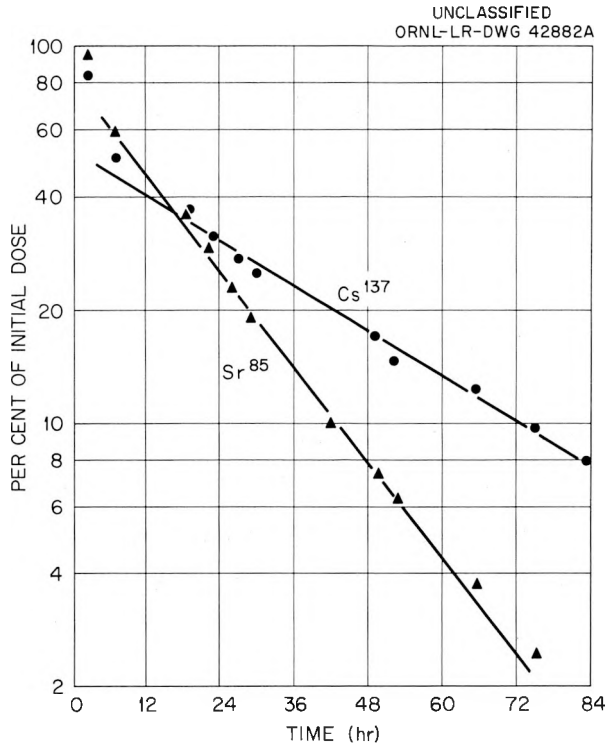

Fig. 2.3. Elimination of Cs^{137} and Sr^{85} by the Red-Legged Grasshopper [Melanoplus femur-rubrum (DeGeer)]. Values shown are means for 6 to 8 specimens.

The data also suggest that size of the insect may be a useful criterion for a rough estimation of elimination rates in field situations. The smaller insect (the red-legged grasshopper) eliminated both isotopes more rapidly than the larger one did (the differential grasshopper). The eastern lubber grasshopper is larger than both of these species and had a still longer (4 to 5 day) biological half life for Cs^{137}. Additional work will be done to quantify the relationship between size of insect and rate of elimination, both for different insect species and for individuals of the same species.

The last points on the curves in Figs. 2.1–2.3 fall above the line, suggesting that a longer component elimination rate is present. For the purposes of comparing the two isotopes, and without elimination data for longer periods of time, it is adequate to use a single exponential. For studies involving equilibration with isotope concentrations in food materials, equations using more than one exponential may be necessary.

Field Studies

The insects resident on White Oak Lake bed accumulate fission products from their plant food. Work reported previously[8] has dealt with the numbers of insect species, their densities, their relations to vegetation types, and their general levels of radionuclide content. The present report deals with the role of the insects in the biological cycling of Sr^{90} and Cs^{137}.

Table 2.2 shows the concentrations of Sr^{90} and Cs^{137} in the soil and in three trophic levels (plants, herbivores, and carnivores) on per-unit-weight and per-unit-area bases. Unit-weight concentrations show some reduction in movement through the food chain, but Sr^{90} still constitutes about 25% of its concentration in the soil; Cs^{137} concentrations are about 1% of the soil concentrations. In the Sr^{90} chain, the major reduction in concentration occurs at the plant-insect transfer; in the Cs^{137} chain, this reduction occurs at the soil-plant transfer. Reduction does not necessarily occur at each transfer; plant leaves have higher

[8] Ibid., p 29.

Table 2.2. Concentrations of Sr^{90} and Cs^{137} in Soil and Trophic Levels of the White Oak Lake Bed System

	Sr^{90}	Cs^{137}
Concentrations per Unit Weight (μc/100 g of dry wt)		
Soils	0.036	0.73
Plants (leaves)	0.12	0.018
Insects:		
Herbivores	0.0091	0.0087
Predators	0.0081	0.0097
Concentrations per Unit Area (μc/m^2)		
Soils	60	1.2×10^{3}
Plants (total)	3.3×10^{-1}	5.5×10^{-2}
Insects:		
Herbivores	2.1×10^{-5}	2.2×10^{-5}
Predators	3.1×10^{-6}	3.7×10^{-6}

Sr^{90} concentrations than the soil has. Expressed as per-unit-weight concentrations, the transfer of Sr^{90} and Cs^{137} is relatively efficient.

When the concentrations of radionuclides are expressed on a per-unit-area basis (bottom of Table 2.2), significant reduction in amount occurs at each transfer. Of course this is due to the decreasing bulk of material in higher trophic levels: plant biomass is less than the soil mass, and insect biomass is less than the plant biomass. Between soils and insects, reductions of several orders of magnitude are involved.

Accordingly (see Table 2.2), it appears obvious that the data could include drastic errors, even of orders of magnitude, without affecting the conclusion that the insects contain only a small portion of the total Sr^{90} and Cs^{137} in the system. However, the data in Table 2.2 are not an adequate measure of the turnover of radioisotopes by insects, since the concentration in insects at any time is a balance between intake and elimination. Although the concentration does not change with time, a continuous intake representing consumption of plants must occur in order to maintain the equilibrium.

An estimate of the insect consumption of radioisotopes (and plant material) may be obtained from the relationship

$$ra = \lambda Q_e \quad , \tag{1}$$

where r is the rate of feeding, a is the proportion of the ingested material assimilated, λ is 0.693 divided by the biological half life, and Q_e is the radioisotope concentration in the insects at equilibrium. For Cs^{137}, conservative estimates are as follows: a = 1 and λ = 0.17 (based on the laboratory studies on Romalea microptera). Equilibrium concentrations for isotopes in insects are those listed in Table 2.2. By substituting these values in Eq. (1), r is estimated to be 0.15×10^{-4} $\mu c/g$ of insect per day. This would amount to 0.7% of the plant biomass.

Table 2.3 presents the percentage consumption of the plant biomass by insects as a function of varying a and λ. The insects represented a population of mixed species, and undoubtedly have a combination of high and low elimination rates and assimilation coefficients. For such a mixed population, the most reasonable estimates would involve higher

Table 2.3. Percentage of Plant Biomass Consumed by Herbivorous Insects, as Estimated with Different a and λ for Cs^{137}

λ = elimination constant
a = proportion of ingested material assimilated
T_b = biological half life

a	λ = 0.173 (T_b = 4 days)	λ = 0.346 (T_b = 2 days)	λ = 0.693 (T_b = 1 day)	λ = 1.39 (T_b = 0.5 day)
1.0	0.7	1.4	2.7	5.5
0.75	0.9	1.9	3.6	7.4
0.50	1.4	2.8	5.4	10.9
0.25	2.7	5.4	10.9	21.8

estimates of a (between 0.75 and 1.0) and a biological half life of about one day (λ = 0.693); under these conditions, insect consumption of plants (and of Cs^{137}) would amount to about 3% of the plant biomass.

Small-Mammal Program

The small-mammal program is concerned with (1) the accumulation of radionuclides by natural populations of small mammals in areas contaminated by radioactive wastes and (2) the effects on the mammals of chronic, low-level radiation from the contaminated environments and the internally deposited emitters.

The first phase of the long-term population studies begun in December 1957 (refs 9 and 10) was completed in July 1960. This phase of the studies dealt with population phenomena such as succession, fluctuations, structures, and home ranges in order to obtain baseline data.

In future studies, such aspects as longevity, litter size, histopathology, and age distribution will be examined more closely. Trapping will continue, although less frequently, to follow successional trends and to keep abreast of changes in population dynamics.

Studies were initiated in February 1960 to determine the body burden of radionuclides in the mammals living in contaminated areas. Preliminary

[9] S. I. Auerbach et al., H-P Ann. Prog. Rep. July 31, 1958, ORNL-2590, p 41.

[10] S. I. Auerbach et al., H-P Ann. Prog. Rep. July 31, 1959, ORNL-2806, p 33.

sampling was done in several areas contaminated with various levels of activity to determine the radionuclides present, organ and tissues in which the radioisotopes are located, and the levels of activity. These radioanalyses are an integral part of those studies concerned with biological cycling and internal dose.

Population Studies

The methods employed and the study areas used for the long-term mammal studies were described previously.[9,10] In brief, these studies are made by utilizing a capture-recapture procedure by systematic live-trapping in a contaminated and in an uncontaminated area.

Data from two years of detailed studies and two years of preliminary observations have been accumulated and are stored on IBM cards, from which information is being extracted for publication. Data are available for 13 species of small mammals. More than 4300 examinations were made on over 1400 different individuals in the study areas. Many additional examinations have been made on individuals in other areas and in the laboratory.

The main small-mammal species in lake-bed area 3 (WOL-3) during the past year were cotton rats (Sigmodon hispidus), rice rats (Oryzomys palustris), white-footed mice (Peromyscus leucopus), harvest mice (Reithrodontomys humulis), and pine mice (Pitymys pinetorum). In the old-field area 1 (OF-1) pine mice, harvest mice, cotton rats, white-footed mice, and least shrews (Cryptotis parva) were the main species. A few resident and several wandering individuals of other species were caught in each area. The appearance of the harvest mice and pine mice in WOL-3 and cotton rats in OF-1 were the chief successional events. In the following discussion of populations much of the information will pertain to cotton rats and pine mice, the dominant species of the WOL-3 and OF-1 areas, respectively.

Population densities of mammals are the result of the influences of the environment upon the inherent capabilities of increase of the species. Within the span of time covered by these studies, season fluctuations have occurred in the populations. Relative numbers of pine mice and cotton rats are shown in Fig. 2.4 by a population index, "number of

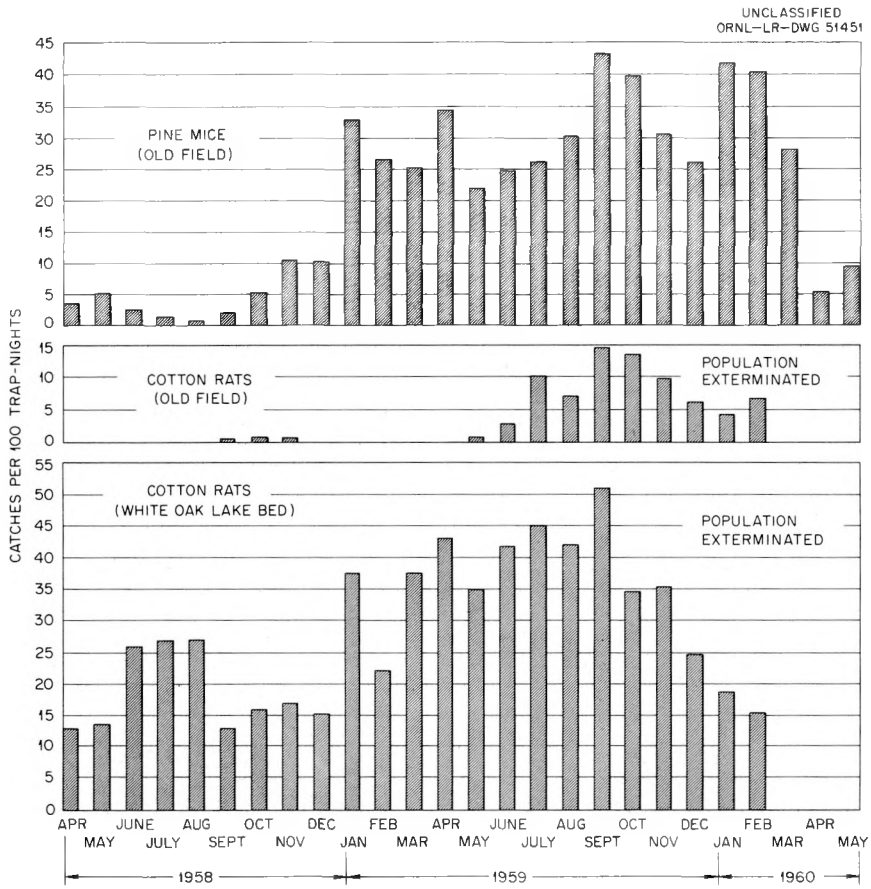

Fig. 2.4. Population Fluctuations of Cotton Rats and Pine Mice.

captures per 100 trap nights." A "trap night" is one trap set for one night. This population index will hereinafter be referred to as "index number."

Populations of cotton rats in the WOL-3 and OF-1 areas and of pine mice in the OF-1 area during 1959 were higher than the comparable populations in 1958 (see Fig. 2.4). For cotton rats the average index number in 1958 was 4; in 1959, 30. The average index number for pine mice in 1958 was 19; in 1959, 38. Also, the numbers of all species combined (not shown) were higher during the later successional stages than during the earlier stages. For instance, in the lake bed the average index numbers for 1956–59 were 6, 13, 34, and 57, respectively. The increases of populations are probably related to the increasing complexity and coverage of vegetation in these areas.

The winter of 1959–60 was severe for this region. The Oak Ridge Weather Bureau report for February states, "greatest monthly and seasonal snowfall of record." The report for March noted, "coldest March, heaviest monthly snowfall on record." During the early part of March 1960 the cotton rat populations were completely exterminated from both study areas. Direct observations of mortality were made during this period. Four dead cotton rats were discovered in a nest box on March 8, 1960, in the WOL-3 area (see Fig. 2.5), and remains of other cotton rats were found later in both the WOL-3 and OF-1 areas.[11] The pine mice, on the other hand, did not show a sharp drop in numbers until April and were

[11]P. B. Dunaway and S. V. Kaye, Cotton Rat Mortality During Unusually Severe Winter in Tennessee (in manuscript).

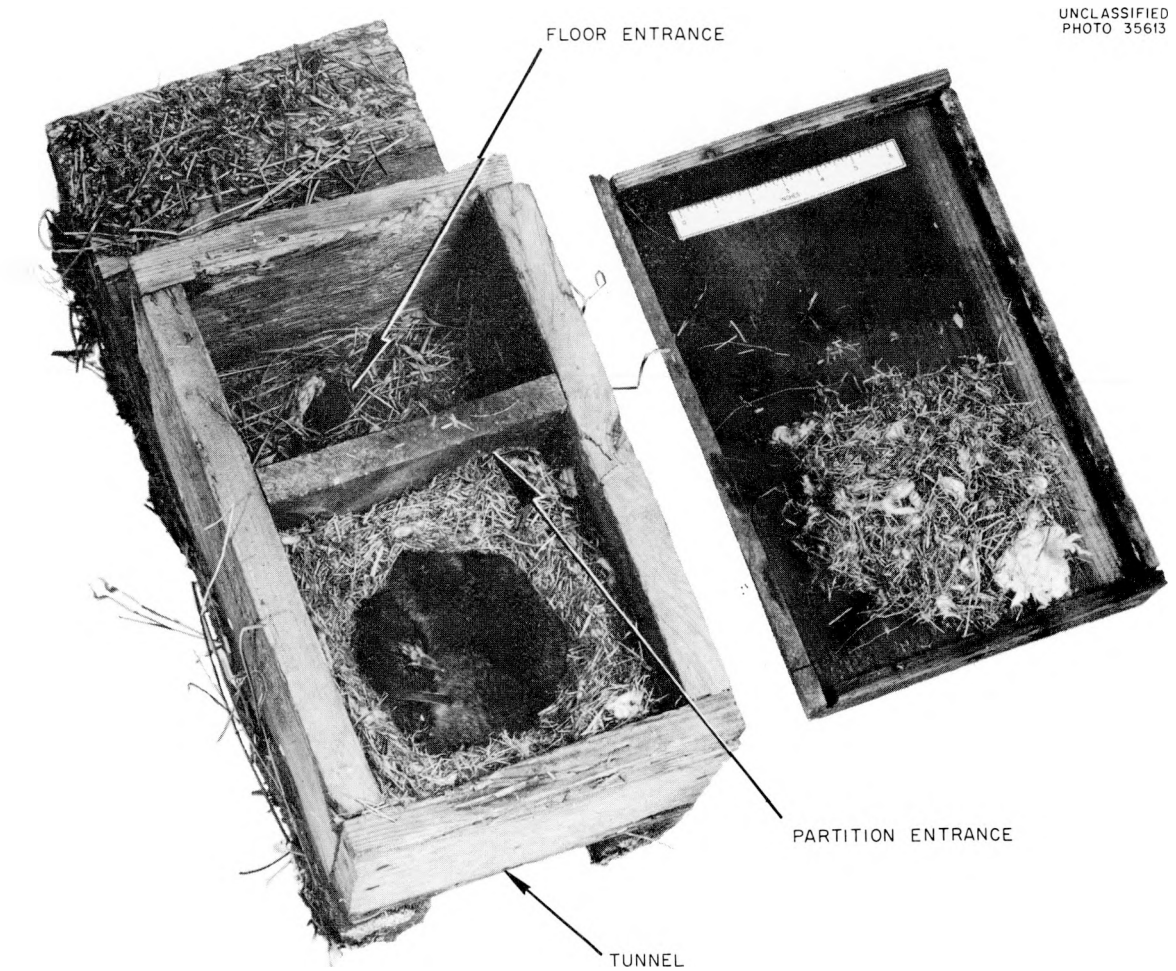

Fig. 2.5. Four Dead Cotton Rats in Nest Box.

not exterminated from the old field. Other species of importance, excluding the white-footed mice at WOL-3, also suffered sharp drops in population during the late winter and early spring of 1960.

The sex ratios of most of the populations tended to be nearly equal, but, depending on the species and season of year, one sex was slightly more numerous than the other for periods of several months. Female cotton rats were more numerous than males from July or August to November or December (see Fig. 2.6); however, it can be seen that male rice rats were consistently more numerous than females.

Data on weights of the mammals have shown significant facts about the populations. In Fig. 2.7, note that the heaviest weight class of cotton rats decreased steadily in percentage from May (88.8% in 1958, 97.2% in 1959) until by February of the next year there were more individuals of the 51- to 100-g class (1959, 55.8%; 1960, 68.7%). The persistence of the 51- to 100-g class during late winter and early spring was not due to recruitment from the 0- to 50-g class but to slow weight gain by the 51- to 100-g class and recruitment from the 101+ g class because of the great weight losses of members of this class during cold weather. Some rats lost as much as 25% of weight in a month. Apparently, weights cannot be employed as an index to age during cold weather.

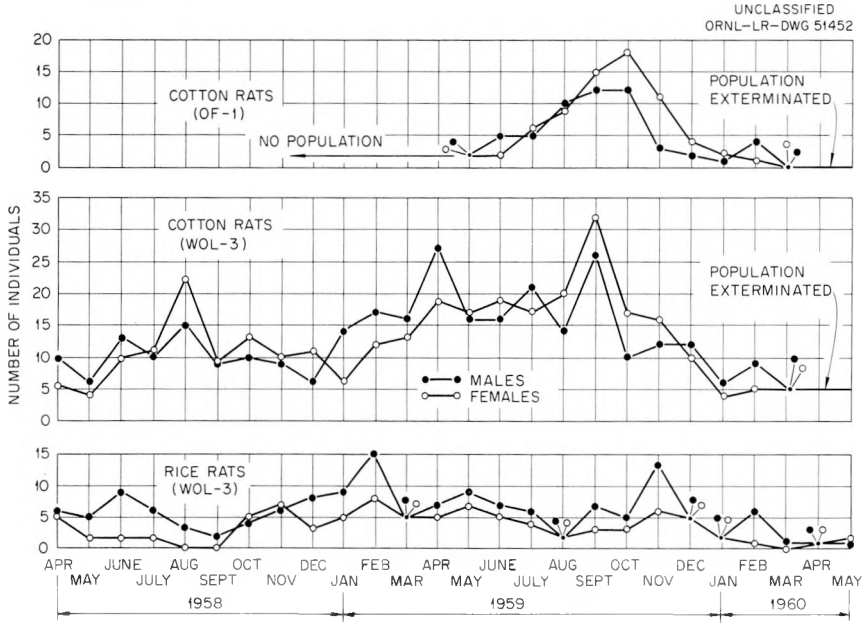

Fig. 2.6. Number of Female and Male Cotton Rats and Rice Rats Present per Month.

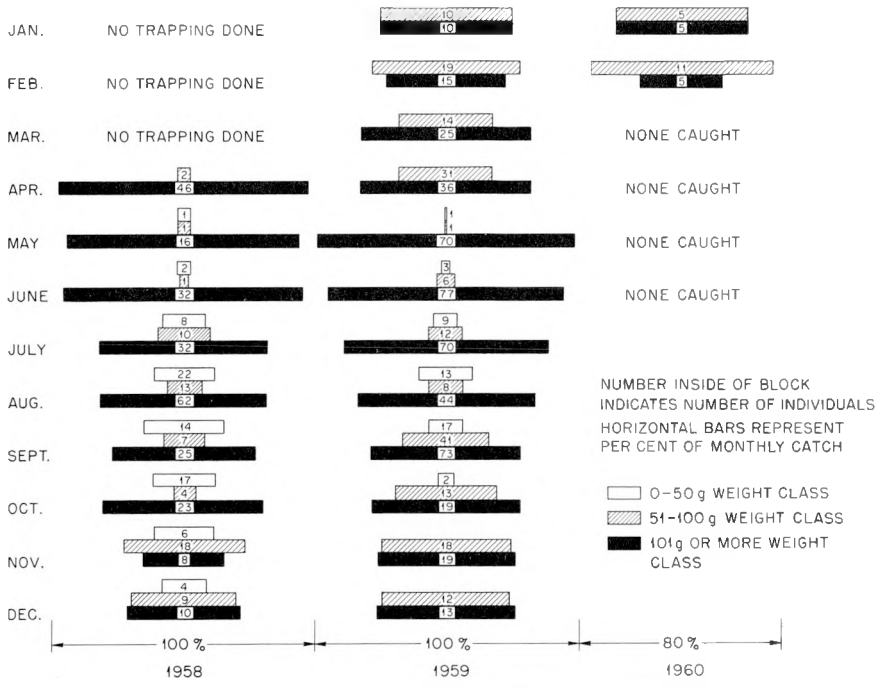

Fig. 2.7. Weight Classes of Cotton Rats — Percentages per Month.

The young group of rats (0 to 50 g) was smaller in 1959 than in 1958 (see Fig. 2.7). In 1958, this group averaged 17.6% of the population per month from May through October; in 1959, the average was 8.8% per month. Also, young did not appear in November and December of 1959, as they did in 1958. This smaller percentage of young in the population is probably attributable in part to the larger populations existing in 1959 (see Fig. 2.7) and to the increased pressures that usually accompany higher densities.[12]

Populations of 12.3 terrestrial small mammals per acre on the WOL-3 area and 23.3 per acre on the OF-1 area were computed for July 1959, a month of uniformly high populations for all species. The formula was that used by Tanaka (ref 13), $y = (x/P)^{\beta}$, where x is the number of marked animals previously handled at any given time, y is the proportion of the total previously marked which are handled, P is the calculated population, and β is an index determined by the frequency of replacement of marked animals and probability of capture of all animals.

---

[12]P. L. Errington, Quart. Rev. Biol. 21, 144–77 (1946).

[13]R. Tanaka, J. Mammalogy 32, 450–58 (1951).

The biomass of small mammals in the WOL-3 and OF-1 areas in July 1959 was calculated to be 1250 g/acre and 760 g/acre, respectively. Although the population density of the OF-1 area was greater (23.3 per acre) than that of the WOL-3 area (12.3 per acre), the biomass of the WOL-3 area was greater because more individuals of the heaviest species were present.

Radioassay Studies of Small Mammals

Work on the movement of radionuclides through the soil, plant, insect, and bird compartments of the lake-bed ecosystem has been reported.[14-16] Population densities, spatial relationships, species succession, and other aspects of the species ecology of the small mammals have been characterized during the past two years.[14,17] Interpretation of bioaccumulation by small mammals in habitats contaminated with mixed fission products required detailed knowledge of the ecology of the populations. Since this information on population ecology is now available, emphasis is being shifted to work on the bioaccumulation of radionuclides in order to evaluate the role of mammals in the movement and cycling of radioactive isotopes.

During the late winter and spring of 1960, 29 small mammals of eight different species were processed for gamma spectrometric analyses and alpha and beta radiochemical analyses.[18] Organs and tissues analyzed ranged from 3 to 20 samples per animal to provide estimates of the kinds and quantities of radionuclides in each organ. Such data are a prerequisite for design of detailed studies. Vacuum-oven drying was used exclusively for preparing tissues, and the low operating temperature (40 ± 2°C) serves to minimize loss of volatile radionuclides.

---

[14]S. I. Auerbach *et al.*, *H-P Ann. Prog. Rep. July 31, 1959*, ORNL-2806, p 18.

[15]D. A. Crossley, Jr., and H. F. Howden, *Insect-Vegetation Relationships in an Area Contaminated by Radioactive Wastes* (in manuscript).

[16]W. K. Willard, *Science* 132, 148-50 (1960).

[17]S. I. Auerbach *et al.*, *H-P Ann. Prog. Rep. July 31, 1958*, ORNL-2590, p 41.

[18]All counting and radiochemical analyses performed by Low-Level Radioanalytical Laboratory of the Analytical Chemistry Division.

White Oak Lake Bed. – Concentrations of abundant radionuclides in stomach contents for three species from the lake bed are shown in Table 2.4. The muskrat had the highest concentrations of Ru^{106}, Cs^{137}, and Sr^{90}, while the cotton rats had the highest average concentration of Co^{60}. In all animals except the muskrat, the stomach contents have a higher concentration of gamma emitters than does the critical organ for the particular isotope, whereas the concentration of Sr^{90} is higher in the critical organ (femur) than in the stomach contents. The higher concentrations in the muskrat can be attributed to its living and feeding in White Oak Creek, which receives low-level radioactive waste effluents.

A preliminary estimate of the quantity of radionuclides in the terrestrial small mammals of the WOL-3 area can be calculated by using the biomass data obtained in the population studies and applying them to the radioassay data. Concentrations of different radionuclides per acre and square meter are shown in Table 2.5. These estimates were obtained by assuming that the concentrations in the sample of four cotton rats are representative of the terrestrial small-mammal population. A comparison with other trophic levels of the lake bed (Table 2.2) reveals that the per-unit-area concentrations of Cs^{137} in insect and mammal herbivores are almost equal, but Sr^{90} in the mammals is three times greater. The

Table 2.4. Results of Radioanalyses of Lake-Bed Mammals

No. in Sample	Species	Sample	Concentration of Radionuclide ($\mu c \times 10^{-4}$/g dry weight)			
			Ru^{106}	Cs^{137}	Co^{60}	Sr^{90}
1	Muskrat	Stomach contents	19.7	13.3	1.3	7.1
		Critical organ*	40.2	4.0	1.0	94.3
4	Rabbit	Stomach contents	11.6	3.7	0.6	2.9
		Critical organ*	1.9	0.5	0.4	7.7
4	Cotton rat	Stomach contents	4.5	7.0	3.2	1.3
		Critical organ*	0.0	1.0	2.3	16.8

*Isotope and critical organ: Ru^{106}, kidneys; Cs^{137}, muscle; Co^{60}, liver; Sr^{90}, femur.

Table 2.5. Concentrations of Radionuclides in Cotton Rats of White Oak Lake Bed Area 3

Radionuclide	Whole-Body Concentrations ($\mu c \times 10^{-4}$/g dry weight)				Average	Concentration per Unit Area	
	Rat 1	Rat 2	Rat 3	Rat 4		$\mu c \times 10^{-4}$/acre	$\mu c \times 10^{-4}/m^2$
Ru^{106}	1.63	2.20	1.07	1.75	1.66	693	0.17
Cs^{137}	1.47	1.11	1.11	1.36	1.26	492	0.13
Co^{60}	1.07	0.98	0.54	1.09	0.92	383	0.09
Sr^{90}	5.99	5.38	6.45	6.28	6.03	2513	0.63

concentrations of radioisotopes reported by Willard[16] for the birds of the lake bed are considerably lower than for the mammals: mammals have 35 times more Sr^{90} and 3 times more Cs^{137}. These differences may be a reflection of different feeding habits; however, Sr^{90} concentrations in mammals may be expected to be higher because of their being more bone per gram of animal.

Waste Pit Area. — One cotton rat, three golden mice, and two white-footed mice were trapped from the last seepage area of the liquid-waste pit system. Pelt, GI tract and contents, and residual carcass were analyzed separately. In addition, the liver, kidneys, and femurs of the cotton rat were radioassayed. A considerable quantity of Ru^{106} is incorporated into the vegetation and soil of this area because of seepage from the waste pits and is reflected in the tissues of the resident mammals as shown below.

	Ru^{106} concentration ($\mu c \times 10^{-4}$)/g dry weight		
	Kidneys	GI tract and contents	Carcass
Cotton rat	44.7	242	12.4
Golden mouse		158	3.9
White-footed mouse		261	19.4

Significant quantities of Sr^{90}, Cs^{137}, Co^{60}, and Zr-Nb^{95} (0.15 to 22.6 $\times$ 10^{-4} μc per gram of dry weight) were found in all animals, suggesting that these radionuclides are being incorporated into the habitats around the pits.

White Oak Creek and Burial Grounds. — Five white-footed mice and one pine mouse were taken from both sides of White Oak Creek about 200 yd upstream from the lake bed and above any source of waste-pit effluents. Strontium-90 activity appears to be less than that for animals from the lake bed but is greater than the concentrations in animals around the waste-pit seeps.

Animals also were collected from the creek banks at the 7500-Area road bridge and from the east side of the solid-waste burial grounds (burial ground 4) near monitoring well 195. The gross beta and gross alpha activities are shown in Table 2.6. Alpha activity of the white-footed mice is comparable for the two areas, whereas beta activity was

somewhat greater in animals from the burial-ground area. Gross beta and alpha activities of the shrew were higher than those of the mice of both areas. The strikingly greater alpha activity may result from the fact that shrews have quite different food habits than mice or rats. Such differences emphasize once again the need for detailed studies of natural food chains.

Table 2.6. Gross Alpha and Beta Radioactivity in Small Mammals from Solid Burial Ground 4 and 7500-Road Bridge Area

Species	Sample	Counts min^{-1} g^{-1}, Dry Weight	
		Gross Alpha	Gross Beta
	7500-Road Bridge Area		
White-footed mouse	Pelt	19	6
	GI tract and contents	4	68
	Residual carcass	*	11
White-footed mouse	Pelt	2	20
	GI tract and contents	6	20
	Residual carcass	*	35
	Solid Burial Grounds		
White-footed mouse	Pelt	*	6
	GI tract and contents ·	7	53
	Residual carcass	4	170
White-footed mouse	Pelt	10	2
	GI tract and contents	20	30
	Residual carcass	2	140
Short-tailed shrew	Pelt	280	67
	GI tract and contents	1600	380
	Residual carcass	340	190

*None detected.

FOREST STUDIES

J. S. Olson

W. C. Cate
D. A. Crossley
M. P. Hoglund
R. B. Neel
H. D. Waller
M. Witkamp
J. P. Witherspoon
J. A. Wolfe

Diverse coniferous and deciduous forests on contrasting soils of the Oak Ridge Reservation provide favorable opportunities for controlled tracer experiments and other studies concerned with the movement of chemical elements from soil to plants and from plants back to soil (see Fig. 2.8). This natural circulation of nutrient elements has fundamental importance for the successional development of ecological systems (ecosystems), and for maintaining their productivity — their efficiency in capturing and transforming solar energy biologically.

Better understanding of the mechanisms which determine the movement of normal chemical elements in ecosystems will aid in predicting the move-

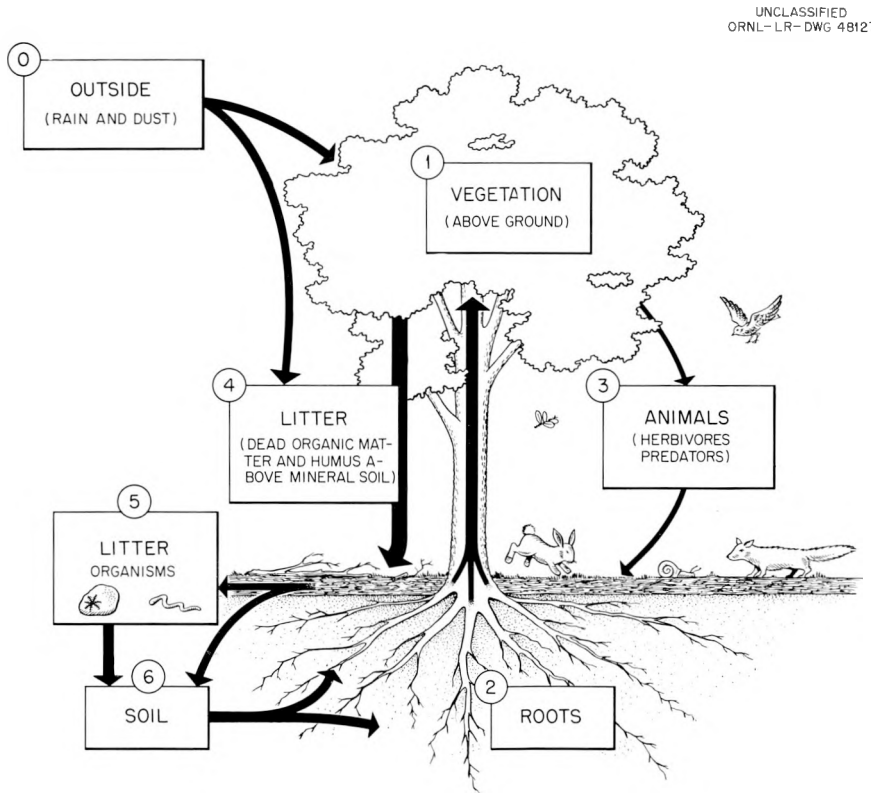

Fig. 2.8. Diagram of a Forest Ecosystem, with Arrows Showing Major Pathways of Transfer of Mineral Nutrients and Radioactive Isotopes Between Compartments.

ment of radioactive contamination in the environment. Case studies of contamination provide some guide as to what might happen as a result of future contamination elsewhere. But to make predictions for conditions of contamination which have not yet occurred, it is necessary to develop and test quantitative models which have general application. Field studies can then aim to evaluate parameters of ecosystems which may vary systematically from place to place. Such combination of theoretical and field research is one objective of the program outlined below.

Development of Theoretical Ecological Models

Pathways of Circulation of Chemical Elements

Arrows in Fig. 2.8 illustrate how mineral nutrient elements and most fission products would move through a terrestrial ecosystem — from air (in the case of fallout) or soil to vegetation, to litter (partly by way of animals), to soil (partly through soil organisms), and eventually to roots and above-ground parts of vegetation. Carbon and C^{14} and fallout contamination could move directly from above-ground vegetation to roots and soils. Last year[19-21] it was pointed out how the net change in quantity of an element or radioisotope in any compartment of the system might be considered as the balance of income and losses for that compartment, and illustrations were provided for the case of carbon in the litter compartment which is emphasized in several of our field studies. This year, the approach was generalized to differential equations including transfers from and to all ecologically relevant compartments; analog computers (Donner 3400, RCAF-X10) were used[22] to solve these equations and simulate the actual flow of C or C^{14} through computer circuits which are direct analogs of the circuits which carbon traverses in nature.

---

[19] S. I. Auerbach et al., H-P Ann. Prog. Rep. July 31, 1959, ORNL-2806, p 41-45.

[20] J. S. Olson, Proc. Intern. Botan. Congr., 9th Congr., 2, 287 (1959).

[21] J. S. Olson, "Energy Storage and the Balance of Producers and Reducers," Symposium: Energy Flow in Ecosystems, Proc., p 3 (1959).

[22] R. B. Neel, Use of Analog Computers for Simulating the Movement of Isotopes in Ecological Systems. Manuscript for M. S. Thesis, Vanderbilt University, April 1960.

The Use of Analog Computers to Simulate Ecosystems

Whereas last year's model for litter accumulation considered only the extreme cases of continuous leaf production and fall, and of instantaneous autumn litter fall, one convenient feature of the analog-computer circuit is the ease of including continuous oscillations (to simulate seasonal production), and gradual trends from year to year (to simulate gradual improvement or gradual deterioration in productivity), as shown in input function of Fig. 2.9. A second feature is the possibility of connecting a whole series of summer-integrator circuits in a network that simulates the accumulation in many compartments simultaneously. Figure 2.10 illustrates the changes for a simple circuit that result from the input which is illustrated in Fig. 2.9, assuming boundary conditions of zero initial content of organic carbon in the system. These conditions might simulate ecological succession on a barren, initially sterile soil. Changes well

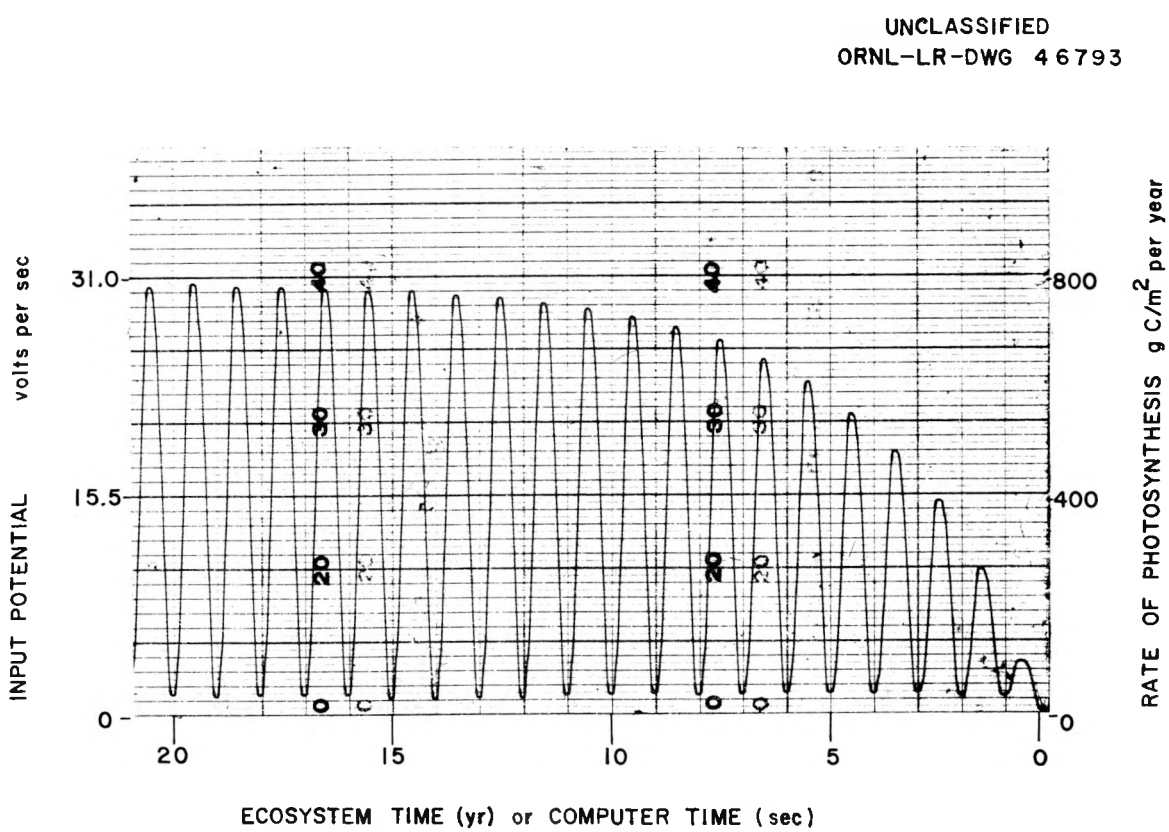

Fig. 2.9. Analog Computer Input to Simulate Photosynthetic Production of Vegetation, with Annual Seasonal Cycle Superimposed on Transient Increase Toward Steady Mean Production.

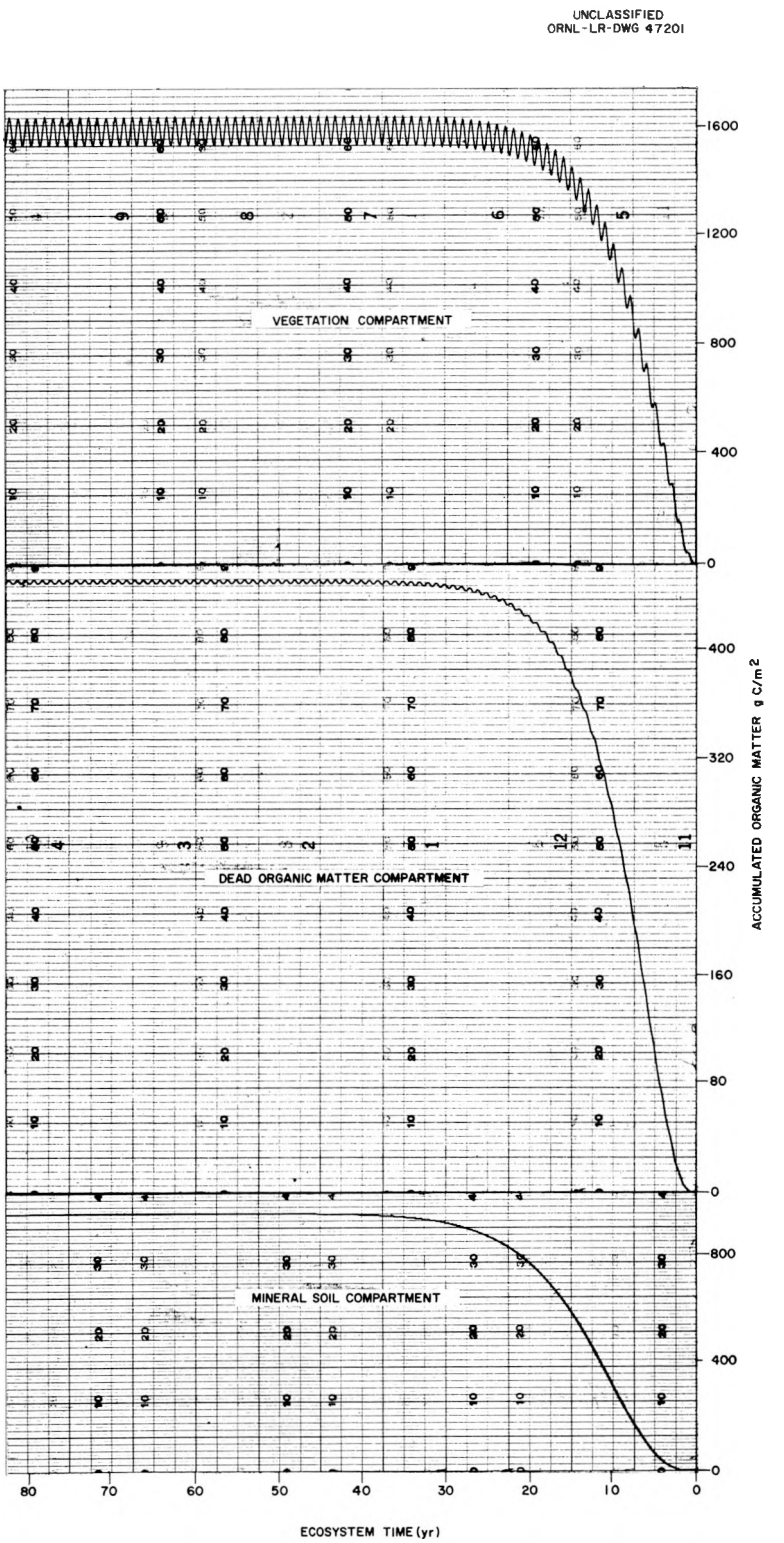

Fig. 2.10. Analog Computer Output, Schematically Simulating Accumulated Organic Carbon in Vegetation, Dead Organic Litter, and Mineral Soil — Each Compartment Showing a Linear Lag Behind Its Source Compartment, and a Corresponding Damping of Annual Oscillations.

illustrate a series of linear lags shown by compartments which are successively more remote from the source of carbon input, and pronounced damping of the annual oscillations at each of these steps. The consequences of feedback were considered in relation to local circulation of C^{14}.

A number of combinations of parameters were readily explored by changing the time constants ("decay" parameters) for individual summer integrators. Much more remains to be done with this approach in order to simulate a variety of real and hypothetical ecological conditions. A larger number of compartments and subcompartments (corresponding to various plant and animal species and various organs of these species) can be added on large computers such as the RCAF-X10. Whereas carbon provided a logical choice for illustrating changes related to the total quantities of organic matter present, the computer will be able to simulate changes in many other elements and isotopes when field data provide appropriate values for choice of the relevant parameters for the circuit.

Movement of Tracer Isotopes in Trees

Discrimination Between Sr^{85} and Ca^{45} in Dogwood Trees

Rapid uptake of K^{42} and the slower uptake of Sr^{85} and Ca^{45} within a young flowering dogwood tree were reported last year.[23] More extensive analyses of Sr^{85} by gamma scintillation spectrometry and of Ca^{45} by beta liquid-scintillation spectrometry[24] were made for several collections of leaves from this tree and four others, growing on several geologic formations. Both isotopes continued to move upward from the source (a hole in the trunk of the tree) through the first growing season, but slower movement by strontium is shown by ratios of Sr^{85}/Ca^{45}, which are consistently below the ratio that would be expected from the initial ratios

---

[23]S. I. Auerbach *et al.*, *op cit.*, p 46–49.

[24]G. D. Novelli of the Biology Division kindly provided the use of the beta scintillation spectrometer.

of activities, corrected for radioactive decay, as shown below:

Ratio of Sr^{85}/Ca^{45} injected	1.09	
Ratio of Sr^{85}/Ca^{45} detected	July 2	August 26
Tree 1 (Conasauga shale)	0.159	0.136
Tree 2 (Rome formation)	0.196	0.140
Tree 3 (Knox dolomite)	0.198	0.122
Tree 4 (Knox dolomite)	0.183	0.132
Mean	0.184	0.132
Ratio expected from decay, assuming no discrimination	0.69	0.49
Observed ratio/expected ratio	0.27	0.27

This tendency for discrimination against strontium emphasizes limitations on the widespread use of Sr^{90}/Ca ratios for interpreting the movement of contamination, and the need for evaluating the chemistry and ecology of each element that modifies the movement of a given isotope.

Tagged leaves produced in this and other tracer experiments were used in studies of litter breakdown described in the following section.

Rapid Movement of Cs^{134} and K^{42} in White Oak Forests

New experiments with Cs^{134} indicate that cesium is likely to be more mobile than the alkaline earths in contaminated forests (White Oak Lake bed, White Oak Creek floodplain, liquid-waste-pit areas).

Table 2.7 shows how Cs^{134} and K^{42} applied together both move rapidly to the tops of small white oak trees, as K^{42} did in dogwood. Potassium appears to be preferentially taken into new buds (Table 2.7, bottom), and this might in part explain a tendency for the K^{42}/Cs^{134} ratio in leaves to be depleted below that expected from the initial ratio of the two isotopes (1.89). Rainfall samples (0.8 in.) collected under the tree during the night following inoculation also showed a tendency for enrichment of the K^{42}/Cs^{134} ratio [4.05, based on 75 dis/min (Cs^{134}) per milliliter].

While rates of movement of cesium are thus not identical with those of potassium, they were high in 12 inoculated trees, growing in four contrasting locations (potassium-rich Conasauga shale soil, both wet and dry; potassium-poor Knox dolomite soil, wet and dry). Radioactivity of leaves increased about fivefold between 7 and 30 days, when they frequently

Table 2.7. Gamma Activity in White Oak (Quercus alba)

Original quantity of tracer introduced:
K^{42}, 3.78 mc; Cs^{134}, 2.00 mc
K^{42}/Cs^{134} ratio: 1.89

Part Sampled and Designation	Height Above Inoculation (m)	Gamma Activity (dis min^{-1} g^{-1}) and K/Cs Ratios			
		1.5 hr After Inoculation		21.5 hr After Inoculation	
		Cs^{134}	K/Cs*	Cs^{134}	K/Cs*
		$\times 10^4$		$\times 10^4$	
Leaves					
N	0.2	177.41	1.59	298.94	1.53
N	0.6	5.77	1.31	3.96	1.19
S	0.6	0.007	1.49	0.15	2.15
E	0.6	1.13	1.25	1.94	1.05
E	1.7	16.70	1.77	105.97	1.27
N	2.5	7.61	1.36	7.48	1.01
W	2.5	41.39	1.68	59.91	1.28
E	2.5	0.86	1.68	1.01	1.21
Top A	3.5	6.06	0.90	11.07	0.87
Top B	3.5	6.93	0.98	8.86	1.28
Stem					
Top A	3.5	7.69	1.03		
Top B	3.5	3.02	1.68		
Buds					
Top	3.5	15.84	4.13	22.19	3.99

*Corrected for decay to the ratio as of the time of inoculation.

reached as high as 1 μc/g, dry weight. Tentative estimates of leaf numbers suggest that 50 to 70% of the 2 mc inoculated in each tree might have moved to the leaves after only 30 days.

Further measurements of Cs^{134} leached in rainfall, and preliminary estimates of amounts already contaminating the litter under the trees, agree in suggesting that after 70 days almost 2% of the inoculated activity had already moved to the litter compartment of the forest (see Fig. 2.11); further transfer by rain is expected before the main movement of Cs^{134} to the litter during leaf fall. Small amounts of Cs^{134} are already moving into the undergrowth below the inoculated trees (10^2 to 10^4 dis min^{-1} g^{-1}) after 70 days. The beginning of movement from plucked leaves

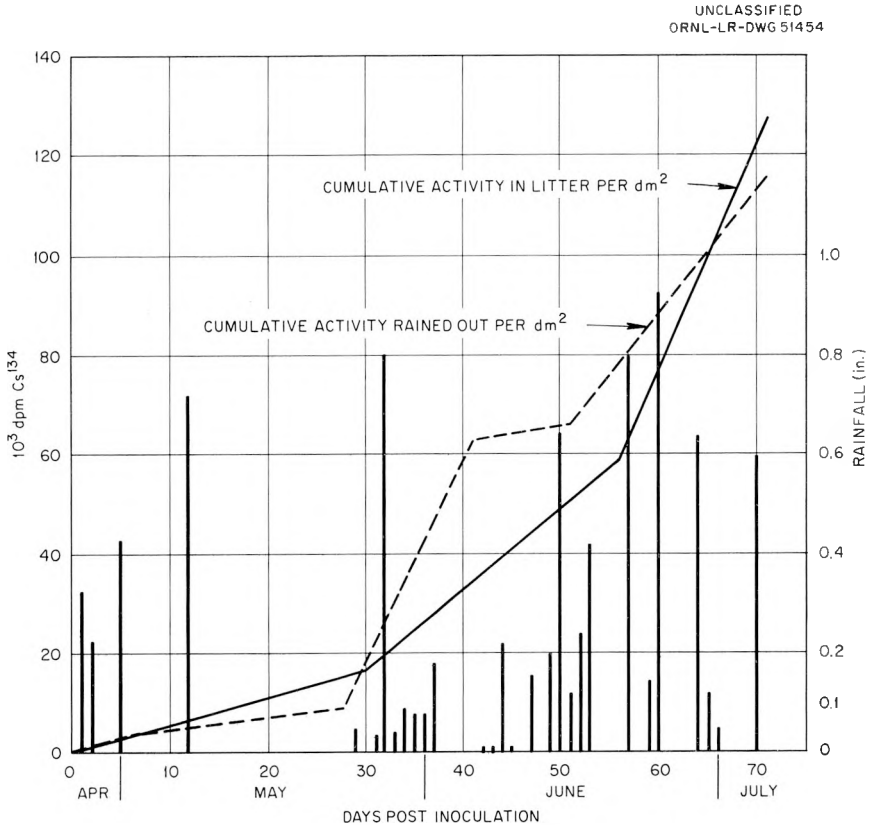

Fig. 2.11. Cesium-134 Leached Out of White Oak by Rain, as Measured in Rainfall and by Activity Detected in Litter Below Tree Crowns.

(10^6 dis min^{-1} g^{-1}) to surface soil and to ten 1-m saplings of white oak was also prompt (23 to 206 dis min^{-1} g^{-1} after 6 days with 1.73 in. of rain, and 279 to 388 dis min^{-1} g^{-1} after 18 more days with 3.16 in. of rain). Thus a complete ecological cycle from plants to litter and back to plants can be completed by a small fraction of the radiocesium contamination (and presumably by potassium nutrient) in a brief portion of a single growing season, without waiting for the normal processes of leaf fall and decay.

Breakdown of Organic Litter and Transfer of Radioactive Isotopes

A continuing cooperative study with R. E. Shanks of the University of Tennessee showed that differences in weight loss of leaf litter in nylon net bags at Oak Ridge and at two elevations in the Great Smoky Mountains

reported previously[25] are even greater and more systematic at the end of the first full year (see Table 2.8). Mulberry leaves not only showed more weight loss than four other species, but the remaining material had already transformed into humus within the litter bags; other leaves showed lesser degrees of discoloration by fungi and fragmentation by animals — approximately proportional to the weight losses shown in Table 2.8.

Evaluation of the role of leaf species, forest cover, and climate has been expanded to include microclimatic contrasts of north and south slopes at each of the six conditions listed in Table 2.8. The following studies are evaluating both the release of radioactive isotopes during the processes of breakdown and the role of the microfauna and microflora in these processes.

Role of Bacteria and Fungi in Litter Decay

In June 1960, the microflora of litter bags in Oak Ridge and the Great Smoky Mountains showed bacterial counts 30 times as high in mulberry leaves as in other species listed in Table 2.8; this helps to explain mulberry's faster weight loss and transformation into humus. Lowest numbers of bacteria were found in white oak and beech, but white oak had higher counts of fungi. Mean counts of bacteria were twice as high in hardwood stands as in the same litter placed in conifer stands, but did not differ consistently between north and south slopes.

Periodic characterization of the soil microflora and its activity at Oak Ridge was started in April 1960. Two mesophytic forests yielded more bacteria and fewer fungi than drier oak and pine stands; oak had more bacteria and fungi than pine, but neither forest showed differences between north and south slopes. A new counting method was developed and tested for measuring the development of mycelium in soil. Soil respiration increased rapidly after rain, and was higher in an oak forest than in pine.

Respiration studies and subsequent counts of samples from the Lockheed Aircraft Reactor site at Dawsonville, Georgia, in June 1960, indicated slightly higher respiration and microbial concentration in samples

[25] S. I. Auerbach et al., op. cit., p 53–54.

Table 2.8. First-Year Weight Losses of Deciduous Leaf Litter from Nylon Net Bags in Deciduous and Conifer Forests at Three Elevations (Percentage of Original Weight)

Species of Leaves	Deciduous Forests				Conifer Forests				Grand Mean
	White Oak, 850 ft	Cove Hardwoods, 3400 ft	Beech, 5200 ft	Mean	Pine, 850 ft	Hemlock, 3400 ft	Spruce-Fir, 5200 ft	Mean	
Red mulberry	67	72	59	66	68	58	58	61	64
White oak	47	36	36	40	38	33	22	31	35
Shumard oak	46	35	29	37	35	31	31	32	34.5
Sugar maple	40	36	31	36	31	32	21	28	32
Beech	29	22	22	24	26	19	12	19	21
Mean	46	40	35	40	40	34	29	34	37

near the reactor. This might be due to partial sterilization of the soil surface and subsequent redevelopment of the ephemeral soil microbiota from underneath.

Arthropods Associated with Litter Breakdown and Release of Radioactive Isotopes

A preliminary report on the numbers of microarthropods resident in pine forest litter has been completed.[26] New experiments are evaluating (1) the numbers of arthropods associated with slow, medium, and rapid litter breakdown, (2) the effects of environmental factors, principally temperature and moisture, on numbers of arthropods in litter, and (3) the ecology of the species in the soil fauna which invade freshly fallen litter and thus are important in litter breakdown.

Small litter bags (about 1 dm square) containing pine, oak, or dogwood leaves were placed in pine or oak stations during November. Each week subsequently, a replicate bag for each leaf type at each station was brought into the laboratory and the arthropods extracted with Tullgren funnels. Since the leaves were from trees inoculated with radioisotopes (Sr^{85}, Ru^{106}, Co^{60}, and Ca^{45}), the bags were also counted for gamma radioactivity.

During the winter and spring of 1960 the arthropod fauna in the litter bags was composed of few species, although core samples of the F and H layers at the stations showed that a rich and varied arthropod fauna was present. Numbers of arthropods in litter bags during this period are illustrated in Fig. 2.12b. Peaks of numbers in winter were due to influxes of tydeid mites and podurid collembolans. Only in the late spring did many of the soil-inhabiting species appear in the litter.

Moisture contents of about 100% of the dry weights of the litter were the most favorable for arthropods; under these conditions numbers per litter bag were 100 to 200. Higher moisture contents (in excess of 200% of dry weight) and lower ones (below 30%) produced much smaller samples of arthropods.

---

[26] D. A. Crossley, Jr., and K. K. Bohnsack, "The Orbatid Mite Fauna in Pine Litter," Ecology (1960) (in press).

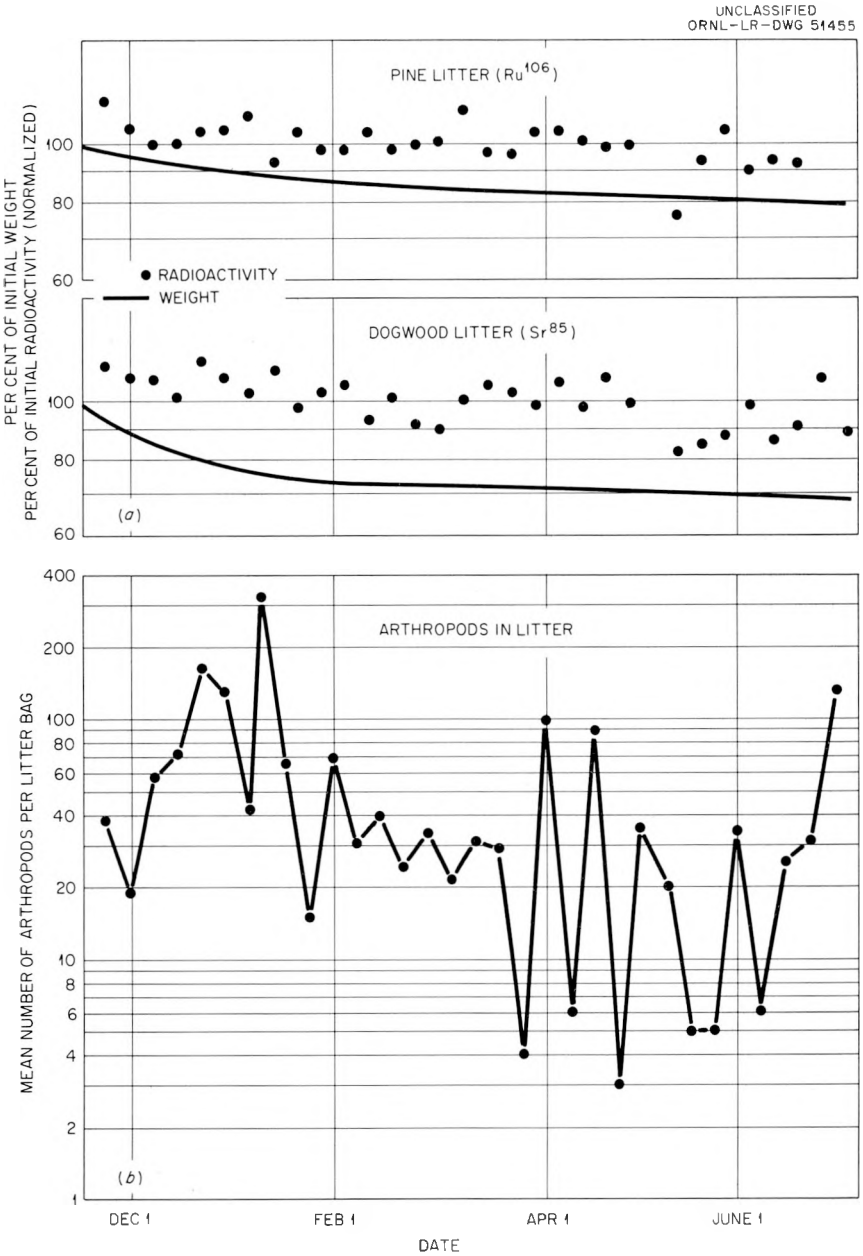

Fig. 2.12. (a) Breakdown of Pine and Dogwood Litter (Solid Line) with Release of Radioactive Isotopes (Points). (b) Mean Numbers of Arthropods in Litter Bags.

Physical breakdown of the litter was measured by weekly weighings of the litter bags, and is illustrated by solid lines in Fig. 2.12a for pine and dogwood litter. Weight loss was rapid for about the first six weeks in the field, probably due to the loss of readily soluble compounds. After the first six weeks, weight loss proceeded at a slower rate. Also included in Fig. 2.12a are losses of incorporated radioisotopes due to

litter breakdown. The counts of radioactivity have been normalized to percentages of the initial count. Due to changes in counting geometry caused by settling of the litter under field conditions, most of the early counts exceeded 100% of the initial count. Rate of loss of radioisotopes from litter closely parallels the loss of weight due to litter breakdown, although difficulties with repeated counting at similar geometries have induced considerable variation in the estimates of loss of radioactivity.

Where Cs^{134} leaches rapidly from litter and is quickly available for absorption by undergrowth, most Sr^{85} and Ru^{106} remain bound to the decaying litter and their release is approximately proportional to total loss of weight.

Sources of Radioactive Contamination of the Environment of Oak Ridge

Ecologists contributed a review of "Biological Contamination and Dispersal of Radioactive Wastes,"[27] substantial sections on the "Significance of Environmental Factors" for the hazards evaluation of waste disposal at Oak Ridge National Laboratory,[28] and several studies of the origin of radioactive contamination near Oak Ridge. Such contamination, well above trace levels, is indicative of the kind of localized sources that might initiate ecological cycling of isotopes in the environment of future nuclear installations.

White Oak Creek Floodplain

In April 1960, sediment cores were collected in the forested floodplain upstream from White Oak Lake bed (the Intermediate Pond area). Analyses tabulated elsewhere indicate approximately 330 μμc/g in the surface 15 cm and an average of 15 μμc/g from 15 to 105 cm for Sr^{90}, and larger concentrations of Cs^{137} (15,500 and 7200 μμc/g respectively).[29]

---

[27] J. S. Olson and S. I. Auerbach, Nuclear Safety: A Quarterly Tech. Prog. Review 1(3), 62–65 (1960).

[28] E. G. Struxness et al., General Description of Oak Ridge Site and Surrounding Areas – Hazards Evaluation Vol 2, ORNL CF-60-5-27, p 23–28 (May 31, 1960).

[29] E. G. Struxness et al., Detailed Assessment of Solid and Liquid Waste Systems – Hazards Evaluation Vol 4, ORNL CF-60-5-29, p 35–38 (May 31, 1960).

The area therefore provides a favorable situation for research on redistribution of long-lived isotopes in forests, and for predicting some features of the future development of White Oak Lake bed as it becomes increasingly covered by trees.

Additional Isotopes in Trees near Waste Pits

To supplement earlier analyses of $Ru\text{-}Rh^{106}$, Co^{60}, $Zr\text{-}Nb^{95}$, and traces of Cs^{137} in trees around liquid-waste pits,[30] gamma spectrometric analyses were made using standard complement subtraction.[31] This sensitive method detected Cs^{134} and Zn^{65} not reported earlier. A comparison of walnuts and walnut hulls from tree 19 on the east seep[32] was chosen because the walnuts had been completely protected from direct exposure to air contamination, which had been considered as the main pathway of contamination by radiocesium. Results given below show that $Zr\text{-}Nb^{95}$ was below the limits of detection in the nuts (< 0.4 μμc/g), while the hulls had 3.5 μμc/g – a quantity which can reasonably be attributed to weapons fallout. For all five other isotopes, hulls had 2 to 4 times as much isotopes per gram of air-dried hulls as had the nuts themselves, but all five were detected in the nuts and were presumably contributed in part from local waste disposal. It is not certain whether all the nut contamination could have resulted from translocation from the hulls, or whether traces of cesium are now beginning to become available in ground waters around the waste pits in spite of the strong tendency for the illite minerals in Conasauga shale to fix most of the waste cesium in the immediate margin of the pits. The table below shows the distribution of radioisotopes in nuts and hulls.

Radioisotope	Nuts (μμc/g)	Hulls (μμc/g)
Ru^{106}	31	117
Co^{60}	5	11
Cs^{137}	6	22
Cs^{134}	1.35	5.86
$Zr\text{-}Nb^{95}$	< 0.04	3.38
Zn^{65}	0.01	0.02

[30] S. I. Auerbach et al., H-P Ann. Prog. Rep. July 31, 1958, ORNL-2590, p 46–47.

[31] L. C. Bate and G. W. Leddicotte, personal communication, Mar. 23, 1960.

[32] S. I. Auerbach et al., H-P Ann. Prog. Rep. July 31, 1957, ORNL-2384, p 31.

Pattern of Stack Fallout of I^{131} and Other Isotopes

After last year's report[33] indicated the presence of several radioisotopes on tree foliage outside the areas affected by waste processing, a pattern of sampling points for dogwood leaves was laid out in late September 1959, in four directions from the ORNL stacks to see whether there was a gradient in contamination which could reasonably be attributed to these stacks. Culkowski's predicted pattern of environmental buildup of radioactivity was used in choosing directions and distances of these stations, and his computational procedure[34] was programmed on the IBM 610 computer to use local wind records for predicting theoretical pattern of fallout expected according to Sutton's theory of atmospheric turbulence.

Iodine-131 decreased regularly with distance from ORNL (see Fig. 2.13a), and was below limits of detection in dogwood leaf collections NE of the Oak Ridge Reservation. Observed concentrations were consistent with meteorological prediction that greatest deposition should be found in an area NE to N of the Laboratory because of frequent winds from SW to S in September (see Fig. 2.13b). Frequent winds from NE, the opposite direction along the valley and ridge topography, account for secondary maximum readings SW of the Laboratory. Lower concentrations were found to the NW, and lowest of all in the SE, as expected from the low frequency of winds blowing in these directions. Five other gamma emitters apparently did not exceed levels expected from weapons fallout over most of the Oak Ridge Reservation, but did exceed these levels over small areas

---

[33]S. I. Auerbach et al., H-P Ann. Prog. Rep. July 31, 1959, ORNL-2806, p 51–52.

[34]W. M. Culkowski, Estimates of Accumulated Exposures and Environmental Buildup of Radioactivity, 6th AEC Air Cleaning Conf., Idaho Falls, Idaho, July 7–9, 1959.

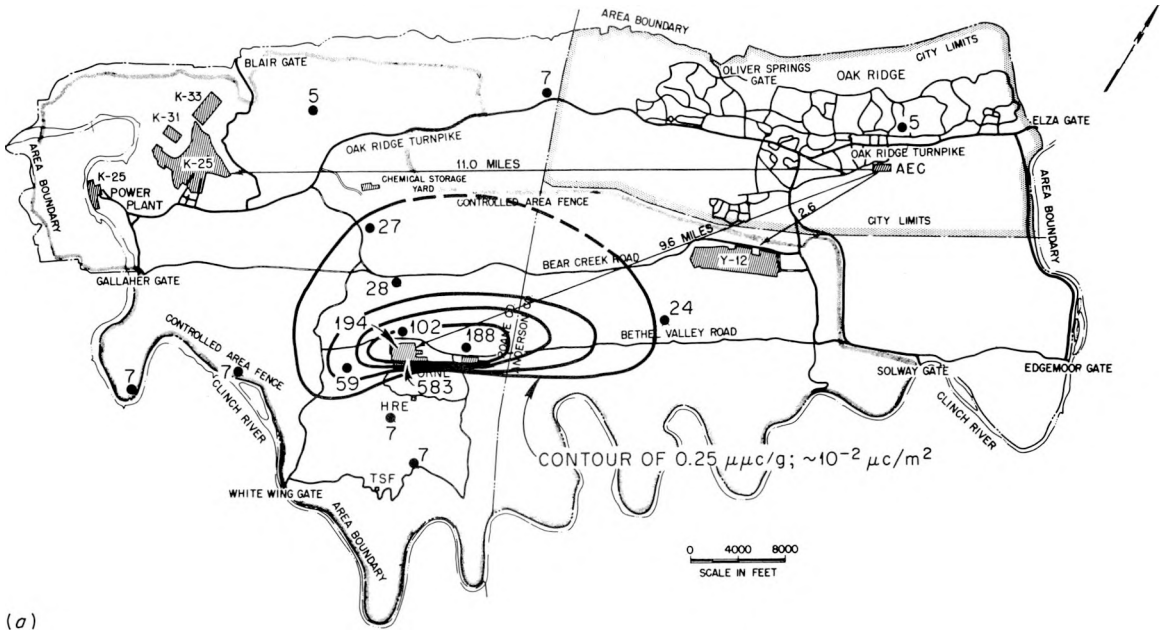

(a)

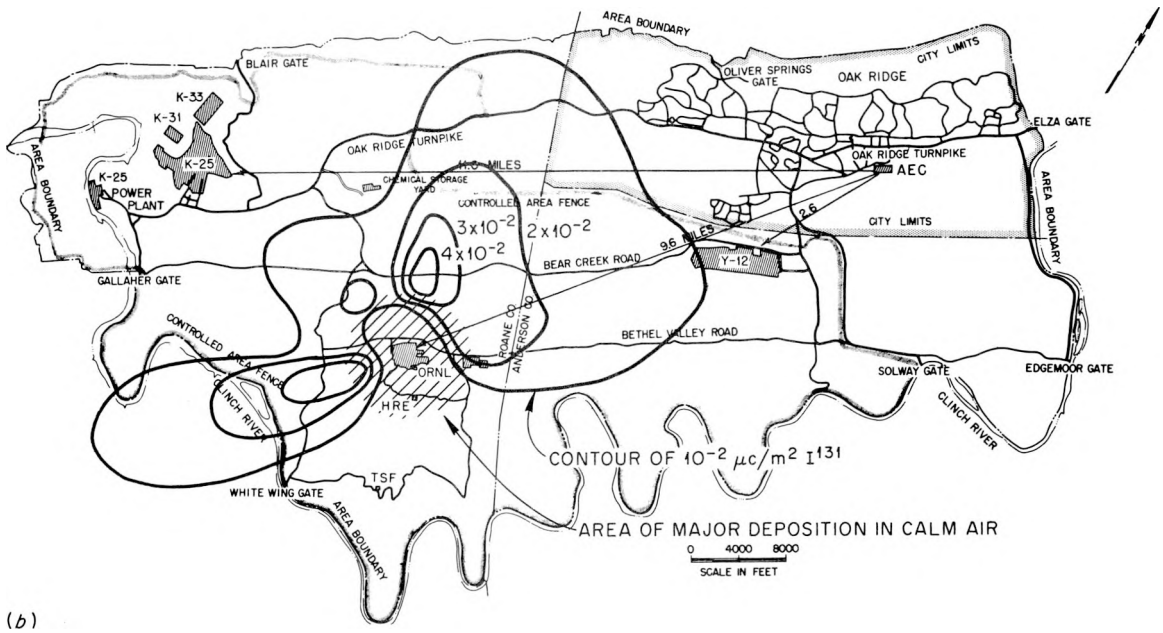

(b)

Fig. 2.13. Dispersal of I^{131} Around Oak Ridge, September 1959: (a) Observed on Sampling of Foliage of Dogwood Trees; (b) Predicted from Wind Distribution.

near ORNL,[35] as shown below:

Isotope	Local Deposition			Distant Deposition (up to 32 miles)
	Distance (miles)	Prevalent Direction	Amount ($\mu\mu c/g$)	Amounts in Any Direction ($\mu\mu c/g$)
I^{131}	0–8	NE–SW	0–583	0
$Ru\text{-}Rh^{106}$	0–2	SW–NE	12–113	2–9
$Cs\text{-}Ba^{137}$	0–1	SE	4–22	1–3
$Zr\text{-}Nb^{95}$	< 0.5	SW	7–68	4–8
$Ce\text{-}Pr^{144}$	< 1	NE–SW	30–214(?)	12–20(?)
Co^{60}	< 0.5	SW	2.6–5.5	< 1

For $Zr\text{-}Nb^{95}$, even the local high values, up to 68 $\mu\mu c/g$, are below the estimates of 7 to 190 and 170 to 400 $\mu\mu c/g$ for June 1959 and November 1958.[36]

Biological Contamination near Isotope Processing Areas[37]

An isolated example of highly localized biological contamination in the Laboratory Isotopes Area is provided by the following data for a silver poplar tree (Populus alba):

	In Tree Trunks	In Fallen Leaves
Co^{60} 10^{-3} $\mu c/g$	8.2–12.7	209
Cs^{137} 10^{-3} $\mu c/g$	0.64–1.27	None detected
Sr^{90} 10^{-3} $\mu c/g$	8.2–17.3	86
Gross beta 10^3 counts min^{-1} g^{-1}	3.8–7.6	41
Gross gamma 10^3 counts min^{-1} g^{-1}	12–22	205

The tree was removed to the solid-waste burial ground at the time of sample collection (December 1959), and contaminated soil around the tree was subsequently replaced. If such concentrations had been present in leaves

---

[35]The aid of C. L. Burros in scheduling samples for prompt analysis of gamma spectra for I^{131} and other isotopes was indispensible for obtaining the present results.

[36]S. I. Auerbach et al., op. cit., Table 19; Table 18, corrected for radioactive decay.

[37]The aid of H. A. Parker and J. H. Cooper in providing analyses is gratefully acknowledged.

whose wind dispersal was considered in last year's report, average contamination would have reached 2 to approximately 30 μc of Co^{60} and 0.86 to 14 μc of Sr^{90} per square meter, over an elliptical area of approximately 20 × 50 m — levels of contamination well above those expected from fallout or from foliage uptake in the White Oak Lake bed area.

Another study was made of isotopes distributed on grass and soil across the street south of Building 3019, following the ruthenium fallout incident and the plutonium explosion incident of November 1959. Values up to 34 $\mu c/m^2$ for Ru^{106}, 1.6 $\mu c/m^2$ for Ru^{103}, and 16 $\mu c/m^2$ for $Zr\text{-}Nb^{95}$ on ground surface debris may have been related to the localized particulate fallout. Maximum counts of Pu^{239} were 7.2×10^4 counts min^{-1} m^{-2} (counting leachates at 51% geometry). Soil from these areas was also removed during decontamination.

Analysis of Oak Ridge Forests

Soil Profiles

To aid the selection of research sites, soil associations have been mapped in the X-10 area, and 15 profiles have been collected for analysis. Contrasts between residual and colluvial profiles over the same geologic belt are important for rates of ecological succession and forest growth and for the cycling of nutrients and isotopes of the site.

Forest Mapping

With the aid of the TVA Forest Development Branch, forests of much of the Oak Ridge Reservation have been mapped. Reference sheets provide coded information on topographic and age condition as well as forest type and degree of cover for the present and for 1935. These records show major changes in the landscape in the past 25 years, which are being considered in the planning of future research use and management of the area. The maps provide a first step in the quantitative sampling of the forests by plot records.

Biomass and Productivity of Forests

Data on standing crop of forests (including foliage, branches, and some data on roots) and annual productivity are being evaluated by harvest methods illustrated last year.[38] Work still emphasizes shortleaf pine, recently harvested during clearing at the High Flux Reactor site.

Chemical Analyses[39]

Analyses of tree harvests, other plant samples, and soils include routine measurements of Sr, Ca, Mg, K, Na, and Mn by flame photometry (with special attention to interference problems), of P, Fe, and Al by colorimetry, of Si by HF fuming and weighing, of C by CO_2 adsorption, and of N by Kjeldahl digestion and titration. Activation analysis appears to offer promising increases in sensitivity for several elements, using nondestructive techniques. Results will be reported elsewhere.

IBM Data Processing

Progress has been made toward incorporating numerous calculations in forest mensuration, counting data, and chemical analyses into a system of IBM computing programs and punch-card records for convenience in sorting data for a variety of purposes.

---

[38] S. I. Auerbach et. al., op. cit., p 45–47.

[39] The aid and interest of T. C. Raines, L. J. Brady, G. W. Leddicotte, and others of the Analytical Chemistry Division is much appreciated.

CLINCH RIVER STUDIES

D. J. Nelson

R. C. Early
C. W. Wiser[40]
R. L. Herman[41]
M. N. Stamper[40]
J. M. Schurr[41]

Oak Ridge National Laboratory has been releasing long-lived radioactive waste materials into the Clinch River by way of the White Oak Creek drainage system. The release of radioisotopes is continuing, and it is known that these radioisotopes are concentrated by organisms and bottom sediments. A knowledge of the distribution and fate of the radioactive materials in the Clinch River is essential in order to evaluate the potential hazard and the effects of the continuous releases to the river. The experience gained in related work on other rivers has shown that the resolution of this problem can be achieved only by a study of the biological and closely related chemical and physical processes which affect the distribution and fate of radioactive materials in the river system. Especially important is information on the densities of biological populations present, their ability to concentrate radioactive materials from the river water, and the role of these populations in effecting redistribution of hazardous long-lived radioisotopes downstream. In this, the initial year for the Clinch River investigations, preliminary studies have been conducted to define more clearly the problems associated with the release of radioactive isotopes to the Clinch River.

This study is part of a joint river study program which includes these cooperating agencies: U.S. Atomic Energy Commission, Oak Ridge National Laboratory, U.S. Public Health Service, U.S. Geological Survey, Tennessee Game and Fish Commission, Tennessee Valley Authority, Tennessee State Health Department, and Tennessee Stream Pollution Control Board.

Bottom Organism Studies

The bottom sediments of the Clinch River were sampled at intervals of approximately 1 mile, from Clinch River Mile (CRM) 23 to CRM 0, to provide a qualitative evaluation of the kinds and relative abundance of organisms present. The tubificid worms, Tubifex and Limnodrilus, were the

[40]Research participant.
[41]Summer employee.

most abundant organisms in the river bottom. Preliminary estimates of abundance indicate about 1000 individuals per square meter. The worms were counted for gross gamma activity after they had defecated the radioactive mud in their intestines. These worms did not contain amounts of radioactivity significantly different from background; however, in all instances samples of less than 0.3 g wet weight were counted for short periods. An improved design[42] has been obtained for a device to wash organisms from bottom sediments. With this equipment it should be possible to obtain larger quantities of bottom organisms for more accurate radioanalyses.

Diptera larvae, primarily chironomids (midges), were also common in the bottom samples. The total of all species was about 600 individuals per square meter. Species found were Chironomus tentans, Cryptochironomus fulvus, Polypedilum flavus, Endochironomus dimorphus, Calopsectra sp., and Anatopynia sp. As was the instance with tubificids, no large quantity of Diptera biomass was accumulated at any one time and no significant gamma activity was detected.

Other bottom organisms found less frequently included round worms (Nematoda), Cladocera (Ilyocryptus), isopods (Lirceus fontinalis), mayfly nymphs (Hexagenia limbata), biting midges (Heleidae), phantom midges (Chaoborus), and beetle larvae (Elmidae).

The fauna living in the bottom of the Clinch River is similar to that found in other large, warm-water streams in the eastern United States. Therefore, the basic information concerning radioactive contamination of the Clinch River will find general application to a much larger geographic area.

Worm Studies

Laboratory experiments are being conducted on feeding rates of the tubificid worms. These worms feed with their head end in the bottom sediments and their tail in the overlying water. In this way they continually bring bottom mud into the water as they feed and defecate. If water currents are present, one would expect a downstream transport of worm feces as they fall back to the surface of the bottom sediments. In reaches of

[42]G. H. Lauff, University of Michigan, personal communication.

the Clinch River where there is significant current, turbulence created by the current would be expected to play a much more important role in the downstream transport of sediment. In the Watts Bar embayment portion of the Clinch River, currents are not sufficiently great to creat turbulence and pick up bottom sediments. In these areas density currents do exist close to the bottom, and velocities up to 2 cm/sec may be found. In such an instance the action of the worm and the weak current operate together and could result in the downstream transport of radioactive bottom sediment. With long-lived fission products such as Cs^{137}, the worms may cause a significant dispersal of radioactive meterials. The movement of bottom sediments by worms and weak density currents can be evaluated by a mathematical model which is being developed.[43]

Diptera Studies

One of the species of Diptera present, Chironomus tentans, is widely distributed in North America and Europe. The salivary gland chromosomes of this species have been the subject of research[44,45] to determine the frequency of naturally occurring mutations in wild populations. The population of Chironomus tentans in White Oak Creek and the Clinch River downstream from White Oak Creek has been exposed to low-level chronic radiation from waste fission products since the time of the first releases of radioactive materials from Oak Ridge National Laboratory in 1943. Therefore, with cytogenetic and population genetics techniques it may be possible to detect radiation effects. Such a study has been started with the cooperation of D. L. Lindsley, Biology Division. Chromosomes found in the salivary glands of Chironomus tentans larvae collected from the Clinch River downstream from and at the mouth of White Oak Creek have been examined and contain chromosomal aberrations which have not been described previously. The populations are being compared with nearby populations not subject to radiation from waste fission products.

---

[43]The assistance of M. A. Kastenbaum, Mathematics Panel, is gratefully acknowledged.

[44]W. Beerman, Chromosoma 7, 198–259 (1955).

[45]A. B. Acton, Proc. Roy. Soc. (London) B151, 277–96 (1959).

Crayfish Studies

Strontium Uptake. -- The crayfish, Cambarus longulus longerostris Ort., was used to study the uptake of strontium.[46] The uptake of strontium by crayfish as a function of time may be approximated by this equation:

$$Sr_{acc}(t) = Sr_{eq}(1 - e^{-kt}) \quad ,$$

where $Sr_{acc}(t)$ is accumulated strontium at time t, Sr_{eq} is the equilibrium level, and k is a positive constant. When the logarithm of

$$\frac{Sr_{eq} - Sr_{acc}}{Sr_{eq}}$$

is plotted as a function of time, the slopes of the resulting straight lines estimate the values of k. These values decrease (0.608, 0.536, 0.382, 0.358 per day) with increasing length (32, 38, 42, 72 mm) of the crayfish. The corresponding biological half times for accumulation are 1.1, 1.3, 1.8, and 1.9 days. These differences in relation to size are consistent with differences expected due to metabolic rates as a function of size.[47]

Cobalt Uptake. -- Studies of crayfish with cobalt are designed to determine uptake and excretion rates, the effect of size upon uptake and excretion, the effect of different levels of concentration of cobalt upon equilibrium values, and the mode of uptake.

The total accumulation or equilibrium concentration of Co^{60} in the crayfish was found to be a function of the type $y = ax^b$ of the Co^{60} concentration in the solution, within the range of concentrations used (10 to 10^5 dis min^{-1} ml^{-1}). The approximate equilibrium concentration in crayfish varied from 35 to 650 times the concentration in solution.

Uptake in all cases is rapid in the first 4 hr and as much as 30% of the equilibrium concentration is attained within this time. Since uptake by freshly killed crayfish is similar in the initial stages, and the equilibrium level is reached within five to six days, it appears that adsorption accounts for the rapid initial uptake.

---

[46] J. M. Schurr and M. N. Stamper, A Model for the Accumulation of Strontium and Calcium by Recently Molted Crayfish (Cambarus longulus longerostris Ort.) (to be published).

[47] E. Zeuthen, Quart. Rev. Biol. 28, 1–12 (1953).

When the contaminated crayfish are placed in uncontaminated water, up to 10% of the activity is lost within 4 hr. Thereafter, the loss is slow and no extensive loss occurs until molting. The tremendous loss of Co^{60} at the time of molting (95 to 98%) demonstrates that the exoskeleton is the site of greatest accumulation.

3. RADIATION PHYSICS AND DOSIMETRY

G. S. Hurst[1]

R. H. Ritchie[2] R. D. Birkhoff[2]

THEORETICAL PHYSICS OF DOSIMETRY

J. Neufeld

P. H. Doyle[3] J. S. Mendell[4]
H. B. Eldridge R. H. Ritchie
P. R. Flusser[4] W. S. Snyder

Estimates of Energy Dissipation by Heavy Charged Particles in Tissue

In a recent publication Snyder and Neufeld[5] have computed the stopping power of various ions in tissue by use of a method suggested by Knipp and Teller[6] in which the LET is represented as a product of two factors, the average square charge of an ion, and the "specific energy loss." These calculations were based on experimental data that have since been superceded by more exact values. A new paper[7] revises these calculations and is based on extensive new measurements. The average charge of a moving ion has been determined on the basis of data summarized by Neufeld,[8] and the average square charge has been calculated by taking into account several recent measurements on the equilibrium charge distribution of heavy ions as a function of energy in the range from 6 to 26 Mev. The specific energy loss has been determined by means of recent measurements on the stopping power of protons in the energy range 20 to 250 kev and the experimental data on the average charge of a proton for various velocities. The LET for tissue has been represented as a summation of terms representing individual contributions of the LET values corresponding to various

---

[1]Section chief.

[2]Assistant section chief.

[3]Consultant.

[4]Summer employee.

[5]W. S. Snyder and J. Neufeld, Rad. Res. 6, 67 (1957).

[6]J. Knipp and E. Teller, Phys. Rev. 59, 659 (1941).

[7]J. Neufeld and W. S. Snyder, Estimates of Energy Dissipation by Heavy Charged Particles in Tissue (to be published).

[8]J. Neufeld, Health Phys. 1, 315 (1958).

components of tissue. The new values indicate higher LET values for heavy charged particles than those indicated in the earlier calculation.

Radiation Produced by an Electron Beam Passing Through a Dielectric Medium

An electron beam passing through a dielectric medium may produce an instability that is associated with the growth of longitudinal waves having a velocity close to that of the beam. For a transparent dielectric medium this instability occurs if the frequency ω of these waves satisfies the following conditions:

$$\omega_1^2 < \omega^2 < \omega_1^2 + \omega_0^2 \quad ,$$

where

ω_1 = the frequency of bound oscillators in the dielectric medium,

$\omega_0 = (4\pi ne^2/m)^{1/2}$, where n is the electron density.

If inhomogeneities are present, these longitudinal waves may be converted into transverse waves and radiated into space. Thus, there is a possibility of a luminous effect at "Bohr frequencies" that differ from the Vavilov-Cerenkov frequencies.

Slowing Down of Electrons in a Fermi-Dirac Electron Gas

The processes by which electrons having energies of the order of tens to hundreds of volts lose energy in metals are of considerable interest in connection with the phenomenon of secondary electron emission, and with observations of electron energy distributions in media bombarded by x rays.[9] A theoretical treatment of the cascade process in a free electron gas has been made by Wolff.[10] He considered only binary collisions between an incident electron and electrons in the Fermi sea, assumed only a screened Coulomb interaction, and neglected coherent excitations of the electron gas.

---

[9]R. A. Finston et al., Measurement of Electron Flux in Irradiated Media by AC Methods, ORNL-2732 (Aug. 31, 1959); D. R. Nelson et al., Measurement of Electron Flux in Media Bombarded by X Rays (to be published).

[10]P. A. Wolff, Phys. Rev. 95, 56 (1954).

Cross sections for both individual electron-electron and coherent excitation processes have been derived by using a consistent perturbation treatment of the many-body problem[11] in a free electron gas and are being employed in a systematic treatment of the slowing-down problem. The space-and-angle independent Boltzmann equation describing n(x), the electron flux per unit energy interval with energy x, may be written

$$n(x) \int_0^{x-1} \{\tau_1(x,t) + \tau_2(x,t)\}\, dt$$

$$= \int_x^{\infty} n(t)\{\tau_1(t,t-x) + \tau_2(t,t-x)\}\, dt +$$

$$+ \int_x^{\infty} n(t)\, \tau_s(x,t)\, dt + S(x) \quad ,$$

where

$$\tau_2(x,t) = \int_{t-1}^{t} T_2(x,t,w)\, dw \quad ,$$

$$\tau_s(x,t) = \int_{w-1}^{w} T_2(x,t,w)\, dt \quad ,$$

and $T_2(x,t,w)$ is the reciprocal mean free path for energy loss t by an incident electron of energy x and the simultaneous creation of a secondary electron of energy w. All energies are measured in units of the Fermi energy for the electron gas being considered. The quantity $\tau_1(x,t)$ is the reciprocal mean free path for energy loss to plasma oscillations. The source term is S(x), which represents the number of electrons introduced at energy x per second.

A machine code for numerical solution of the integral equation has been written and tested, and routines for computation of the various cross sections are nearly complete.

Gaseous Electronics Theory

The experimental program in gaseous electronics pursued by the Radiation Physics and Dosimetry Section is devoted mainly to the study of the

---

[11] R. H. Ritchie, Phys. Rev. 114, 644 (1959).

behavior of electron swarms in particular gases and their interaction with controlled amounts of contaminant gases. By these means measurements of attachment coefficients, drift velocities, and agitation energies may be carried out with considerable accuracy even though the quantities measured are swarm averages.

In order to infer the actual energy dependence of a given quantity, say $\alpha(\epsilon)$, from measured values of its average over the energy distribution of electrons in a swarm, $f(\epsilon,\bar{\epsilon})$, it is necessary to solve the following integral equation:

$$\alpha_0(\bar{\epsilon}) = \int_0^\infty \alpha(\epsilon)\, f(\epsilon,\bar{\epsilon})\, d\epsilon \quad , \tag{1}$$

where $\bar{\epsilon}$ is the average swarm energy and depends explicitly on the electric field applied to the chamber containing the gas and contaminant.

It is felt that reasonably good estimates of the electron distribution function $f(\epsilon,\bar{\epsilon})$ may be made for the noble gases at energies ϵ well below the first excitation potential.[12]

The solution of the given integral equation may be attempted by an iterative scheme in which $\alpha_1(\epsilon)$, the first approximation to $\alpha(\epsilon)$, is

$$\alpha_1(\epsilon) = \alpha_0(\epsilon) - \left[\int_0^\infty \alpha_0(\epsilon')\, f(\epsilon',\epsilon) - \alpha_0(\epsilon) \right] \quad , \tag{2}$$

or, if one defines the operator $K\{\ \}$ to be

$$K\{\ \} = \int_0^\infty f(\epsilon',\epsilon)\{\ \}\, d\epsilon' \quad , \tag{3}$$

the nth approximation α_n is

$$\alpha_n = \alpha_{n-1} - [K(\alpha_{n-1}) - \alpha_0] \quad , \tag{4}$$

while the original integral equation may be rewritten as

$$\alpha_0 = K\alpha \quad , \tag{5}$$

---

[12] T. Holstein, Phys. Rev. 70, 367 (1946); J. C. Bowe, Phys. Rev. 117, 1416 (1960).

with symbolic solution

$$\alpha = \frac{1}{K}\,\alpha_0 \quad . \tag{6}$$

The iterative scheme defined by Eq. (4) has been used with excellent results by several workers in the correction of data for smearing effects introduced by experimental apparatus.[13] The justification for the use of this procedure does not seem to have been given but follows easily from Eq. (4). By repeated substitution, Eq. (4) may be written as follows:

$$\alpha_n = [(1 - K)^n + (1 - K)^{n-1} + \ldots + 1]\,\alpha_0 \quad ,$$

and in the limit as $n \longrightarrow \infty$, one may write symbolically

$$\lim_{n \longrightarrow \infty} \alpha_n = \sum_{n=0}^{\infty} (1 - K)^n\,\alpha_0 = \left[\frac{1}{1 - (1 - K)}\right]\alpha_0 = \frac{1}{K}\,\alpha_0 \quad ,$$

which is identical with Eq. (6) and shows that the scheme is just the Neumann series solution of the integral equation written in the form,

$$\alpha = \alpha_0 + (1 - K)\,\alpha = \sum_{n=0}^{\infty} (1 - K)^n\,\alpha_0 \quad .$$

Machine routines have been written and tested for the computation of the kernel $f(\epsilon,\bar{\epsilon})$ and the evaluation of integrals of the form

$$\int_0^{\infty} f(\epsilon,\bar{\epsilon})\,\alpha(\epsilon)\,d\epsilon \quad .$$

A code is being written for obtaining the nth iterate of α according to Eq. (4), together with error estimates for the solution.

---

[13] G. E. Owen and H. Primakoff, Phys. Rev. 74, 1406 (1948); M. S. Freedman et al., Rev. Sci. Instr. 27, 716 (1956); J. C. Villforth, R. D. Birkhoff, and H. H. Hubbell, Jr., Comparison of Theoretical and Experimental Filtered X-Ray Spectra, ORNL-2529 (July 1, 1958).

Radiation Leakage from Bare Critical Assemblies

Methods of calculating the radiation yield of critical nuclear assemblies are of great importance in assessing the amount of ionizing radiation received by persons exposed in criticality accidents. Calculations of the leakage from some assemblies, neglecting scattering of both neutron and gamma rays on walls and objects which might be around the system, have been carried out, using a rather straightforward approach. Such an approach is sufficient for many purposes and gives reasonable accuracy for distances from the reactor which are usually of interest in criticality accident studies.

The method of computing neutron leakage which has been most useful in our work is the multigroup-diffusion approach. An existing criticality code written for the IBM 704 which automatically computes neutron leakage in several energy ranges has been employed.[14] The computing time for this code is quite modest for most systems. Gamma-ray leakage is treated by special IBM 704 codes. The method uses known gamma-ray cross sections and buildup factors to calculate attenuation kernels for the medium under consideration. The radiation field at various points inside or outside the assembly is then computed by summing over source points in the assembly, using best estimates available for the gamma-ray spectra of the various sources. The spatial distribution of fissions in the assembly is obtained from the neutron criticality code and is used as a source distribution in the gamma-leakage program.

Figure 3.1 shows a plot of the quantity EN(E), where N(E) is the number of neutrons escaping per unit energy interval at energy E per core neutron, for three typical bare reactors.

In the dosimetric evaluation of a criticality accident, the amount of activity induced in the bodies of those exposed is of prime importance. The body-fluid activation method of dosimetry has been used alone or in

---

[14] C. L. Davis, J. M. Bookston, and B. E. Smith, A Multigroup One-Dimension-Diffusion Program, GMR-101 (Nov. 12, 1957).

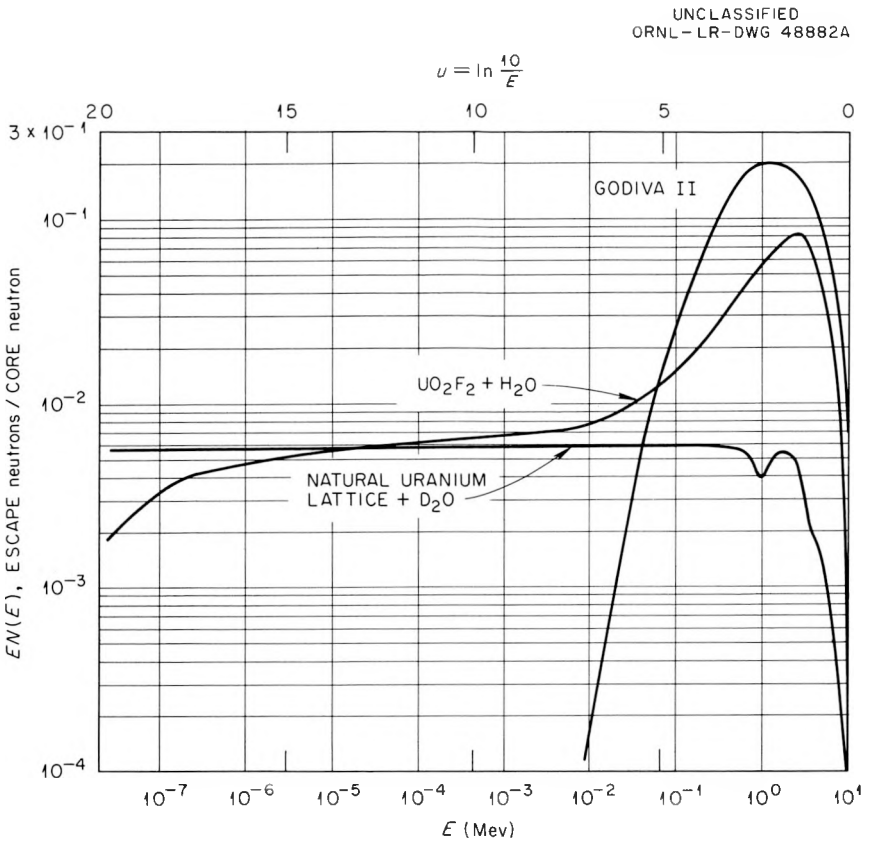

Fig. 3.1. Neutron Escape Spectra for Various Assemblies.

conjunction with other methods in every reported study of accidental criticality.[15] The method depends upon a knowledge of two quantities in addition to the activation level A in the body of an individual. These are D_n/A, the ratio of neutron dose imparted to the body to the activation produced therein, and D_γ/D_n, the ratio of gamma dose received by the individual to the neutron dose received. A knowledge of the activation level A in a person exposed to a nuclear accident then allows one to normalize to his integrated exposure, if both these ratios are constant over the range of distances at which he was exposed.

The basic quantities D_n, D_γ, and A may be calculated for a given nuclear assembly once the leakage of neutrons and gamma rays is computed. Conversion from neutron spectrum to neutron dose is accomplished by using

---

[15] G. S. Hurst and R. H. Ritchie (eds.), Radiation Accidents: Dosimetric Aspects of Neutron and Gamma-Ray Exposures, ORNL-2748A (Nov. 2, 1959).

either first collision data or multiple collision data.[16] The activation A in a phantom may be determined from the spectrum by using values of the neutron capture probability inferred from Snyder's Monte Carlo data,[17] while the leakage routines described above yield the gamma dose directly.

Table 3.1 shows a summary of the results of leakage calculations for four critical assemblies. The results are compared with experimental data obtained by members of the Radiation Physics and Dosimetry Section. In all cases the neutron dose D_n referred to in the table is first collision dose. The quantity Φ_S is the flux of neutrons above the effective sulfur threshold (approximately 2.5 Mev). It is seen that the agreement between theory and experiment is generally good. With few exceptions they agree to within 20% of each other. Thus it seems that ratios of quantities relevant to criticality dosimetry, such as D_n/A and D_γ/D_n, are not sensitive functions of distance from the assembly in the range of distances in which measurements were made (approximately 1 to 4 m). All data refer to unshielded geometries.

The Penetration of Gamma Rays in Inhomogeneous Media

Calculations of the transport of gamma rays and neutrons in infinite homogeneous media have been carried out by various workers using the semi-analytic moments of Spencer and Fano. In many practical situations one needs information relative to particle transport in finite inhomogeneous media. Cases of this sort arise in connection with radiation leakage from critical assemblies, in shielding problems, and in weapons-effect studies. The stochastic method seems to furnish the most flexible and powerful approach to such problems. An IBM 704 code has been written for the purpose of studying the energy-angle distribution of photons in various media.

Figure 3.2 shows the calculated angular dependence of the dose at various distances from an isotropic source of 1.25-Mev photons in an infinite medium of air. Figure 3.3 shows the energy distribution of photons

---

[16] Protection Against Neutron Radiation Up to 30 Million Electron Volts, National Bureau of Standards Handbook 63 (Nov. 22, 1957).

[17] G. S. Hurst, R. H. Ritchie, and L. C. Emerson, Health Phys. 2, 121 (1959).

Table 3.1. Comparison of Leakage Calculations and Experimental Data for Four Types of Critical Assemblies

r_0 = radius of reactor
h = height of reactor
ρ_u = density of U^{235} in solution

Critical Assembly	Description	D_n/A [rads/μc (g of Na^{23})]		$D_n/\phi_S \times 10^8$ (a) (rads cm^2/neutron)		ϕ_i/ϕ_S (b)		$(4\pi R^2 D_n/F) \times 10^9$ (rads cm^2/fission)		D_γ/D_n (r/rad)	
		Experiment	Theory	Experiment	Theory	Experiment	Theory	Experiment	Theory	Experiment	Theory
LASL GODIVA II	Bare U^{235} sphere r_0 = 8.7 cm	491	540	(1.4 ± 0.2)	1.22	1 1.96 2 3.12 3 5.0	1.8 2.3 3.6	4.4 ± 0.4	3.32	0.22	0.09 (c)
Y-12	Aqueous UO_2F_2 solution r_0 = 25.4 cm, h = 38.1 cm, ρ_u = 0.0259 g/cm^3	315	370	1.1	0.89	1 2.16 2 3.56 3 4.09	2.0 2.8 4.0	0.9	1.08	2.8	3.1
ORNL UO_2F_2 Assembly	Aqueous UO_2F_2 solution r_0 = 15.2 cm, h = 29.4 cm, ρ_u = 0.643 g/cm^3	300	400	1.2 ± 0.2	1.00	1 2.0 2 3.1 3 5.0	1.8 2.3 3.6	2.0 ± 0.2	1.82	~ 1.6	1.57
Boris Kidric	Natural U rod, 1 in. dia, in D_2O r_0 = 100 cm, h = 178 cm	67	71	1.6 (d)	1.55 (e)	1 2.1 2 3.8 3 11.3	2.32 3.84 15.6	0.79 (d)	0.77 (e)	4–4.6	3.5–4.2 (f)

(a) ϕ_S is the flux of neutrons having energies above approximately 2.5 Mev.

(b) i = 1 — flux above ~ 1.5 Mev; i = 2 — flux above approximately 0.7 Mev; i = 3 — flux above approximately 0.01 Mev.

(c) Neglecting gamma rays from inelastic scatter.

(d) Radsan dose.

(e) Calculated Radsan dose.

(f) Neglecting gamma rays from neutron capture in walls.

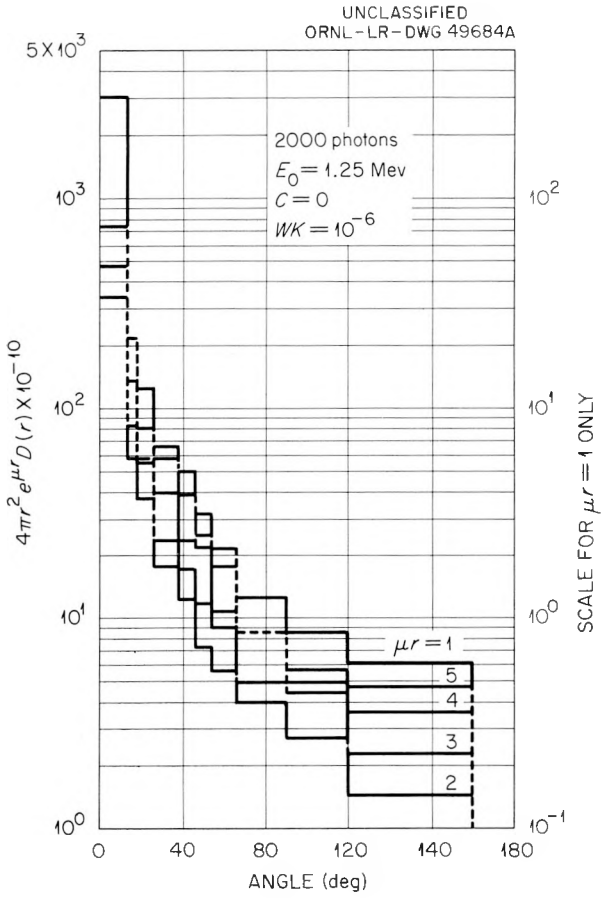

Fig. 3.2. Calculated Angular Dependence of the Dose at Various Distances from an Isotropic Source of 1.25-Mev Photons in an Infinite Medium of Air.

integrated over all angles for the same case. Figure 3.4 shows the joint energy-angle spectrum at 3 mean free paths in air. The solid curves were taken from the measurements of Peelle, Maienschein, and Love[18] of the energy-angle spectrum of photons at 5 mean free paths in H_2O from an isotropic source of Co^{60} gamma rays. The cross sections of air and H_2O (at this energy) are essentially the same except for the density factor. The distributions are comparable, and it seems that an equilibrium is approached at only a few mean free paths from the source. Studies of the

[18] R. Peelle, F. Maienschein, and T. A. Love, Energy and Angular Distribution of Gamma Radiation from a Co^{60} Source After Diffusion Through Many Mean Free Paths of Water, ORNL-2196 (Aug. 12, 1957).

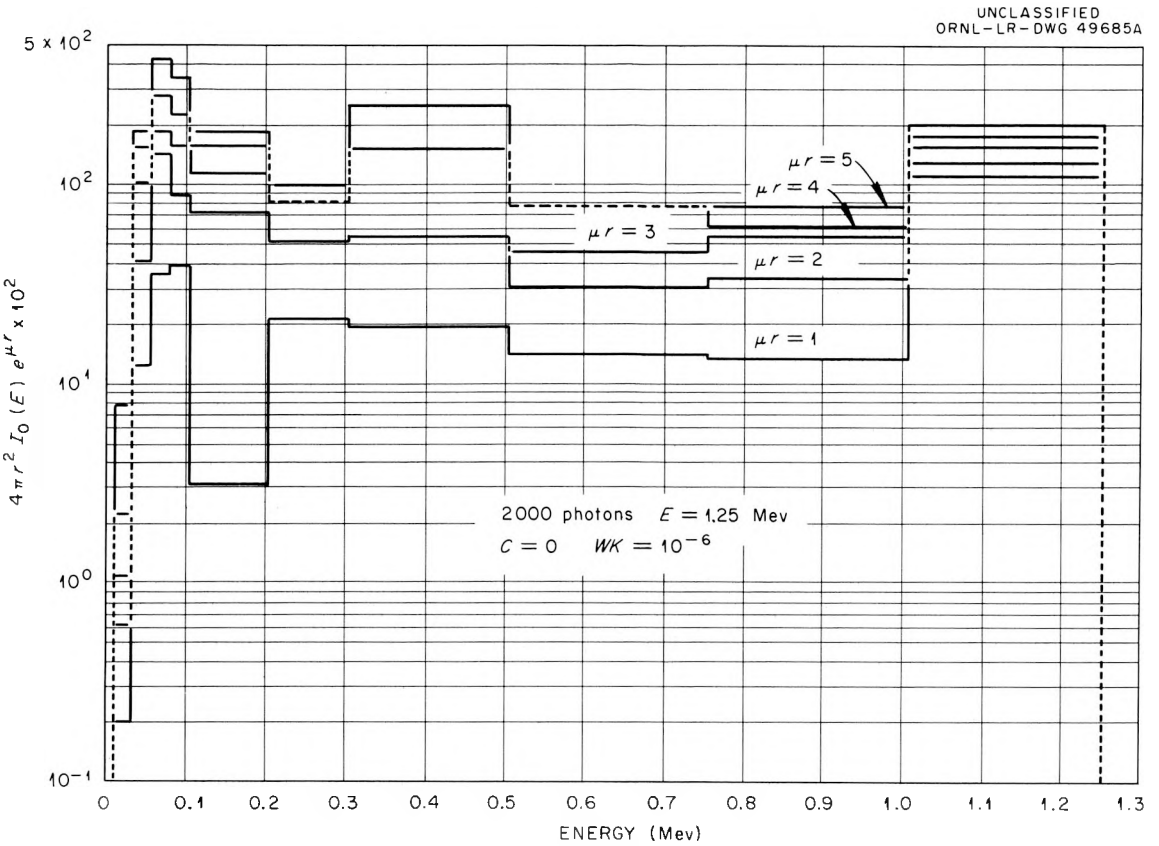

Fig. 3.3. Energy Distribution of Photons Integrated Over All Angles for the Dose at Various Distances from an Isotropic Source of 1.25-Mev Photons in an Infinite Medium of Air.

ratios of doses in spherical media which are finite and infinite, respectively, using correlated sampling techniques, are being carried out. Variance reduction techniques are being tested for use where deep penetration is important.

Neutron Dosimeter Design

For the purpose of theoretical optimization of neutron dosimeters of the count-rate variety[19] and for calculating corrections to the response of the absolute neutron dosimeter,[20] two machine codes have been designed.

---

[19] G. S. Hurst, R. H. Ritchie, and H. N. Wilson, Rev. Sci. Instr. 22, 981 (1951).

[20] G. S. Hurst and R. H. Ritchie, Radiol. 60, 864 (1953).

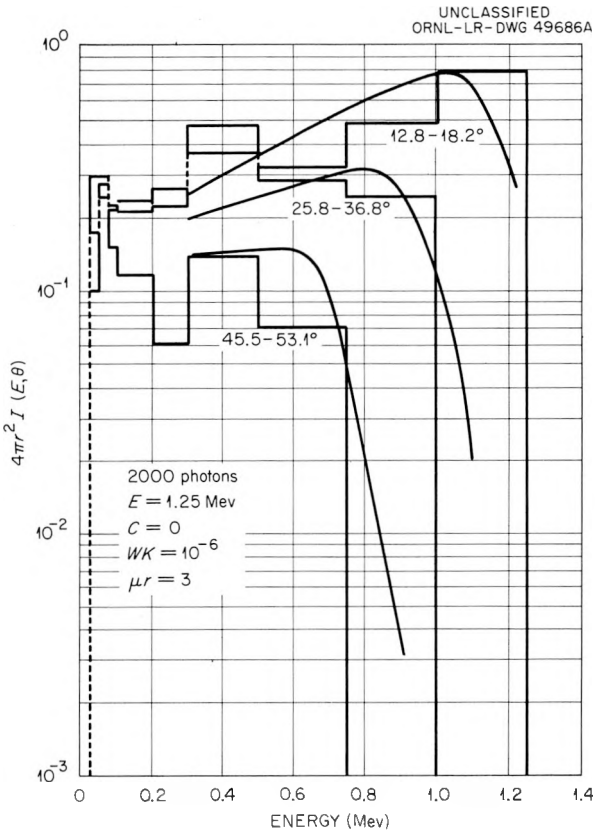

Fig. 3.4. Joint Energy-Angle Spectrum at Three Mean Free Paths in Air for 1.25-Mev Photons in an Infinite Medium of Air.

The first code assumes a plane parallel geometry consisting of hydrogenous gas and radiator, in both of which recoil protons may be generated by incident neutrons.[21] The neutron irradiation may be either normal to the slabs or isotropic in space. The program yields $N(E,\epsilon)\ \Delta\epsilon$, the number of recoils depositing energy between ϵ and $\epsilon + \Delta\epsilon$ in the gas from first collisions with neutrons of energy E occurring in an arbitrary combination of radiators and absorbers. Attenuation of neutrons in the system is neglected but wall losses are considered in detail, using a numerically specified relation between energy and residual range of the recoil protons. The quantity $\epsilon^n N(E,\epsilon)\ \Delta\epsilon$, where n is any integer, is also

[21]This model is identical with that used by R. H. Ritchie, Health Phys. 2, 73 (1959).

calculated. Figure 3.5 shows

$$\int_{\epsilon}^{E} N(E,\epsilon)\, d\epsilon$$

as a function of ϵ for normally incident neutrons of various energies. The wall thickness is greater than the range of the most energetic proton in all the cases plotted.

The second code employs a stochastic approach and treats a more realistic spherical model for the absolute neutron dosimeter. First collisions are required to occur uniformly throughout the wall and gas of the

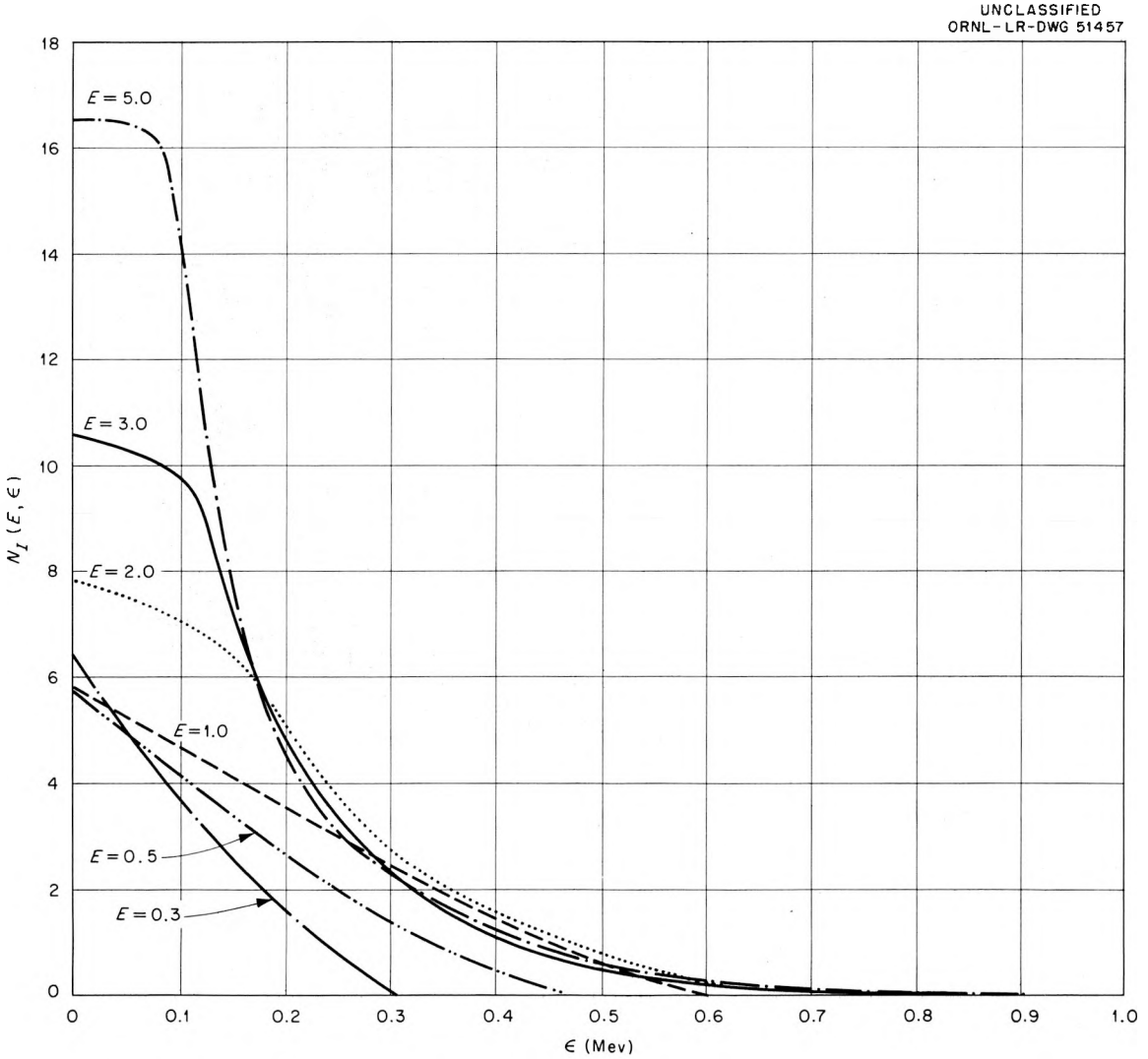

Fig. 3.5. $\int_{\epsilon}^{E} N(E,\epsilon)\, d\epsilon$ as a Function of ϵ for Normally Incident Neutrons of Various Energies.

dosimeter, and attenuation of the uncollided beam is accounted for by applying a weighting factor to the neutron. Collisions may occur with either carbon or hydrogen nuclei, and the energy deposited in the central gas volume by recoils is calculated from energy-residual range relations for the two recoil species and is classified according to its magnitude and the kind of recoil causing it. After undergoing a first collision in the system, a neutron is forced to experience a specified number of subsequent collisions in the system, and the distribution of energy depositions is calculated for these collisions separately from the first collisions. Inelastic collisions with carbon nuclei are included but only the total number of these processes is recorded. The effect of wall losses, inelastic collisions, and wall attenuation of neutrons in the absolute neutron dosimeter will be evaluated by means of this procedure. Much of the work has been done on this code, and some sections are being checked now for errors.

EXPERIMENTAL PHYSICS OF DOSIMETRY

R. D. Birkhoff

E. T. Arakawa
T. E. Bortner[22]
L. W. Cochran[23]
H. H. Hubbell, Jr.
G. S. Hurst
R. M. Johnson
L. B. O'Kelly
T. D. Strickler[22]

Electron Capture in Water Vapor

Electron attachment in mixtures of argon and water vapor and of carbon dioxide and water vapor has been studied by using the method and apparatus described previously.[24] For each case, the quantity determined is α, the probability of electron capture per centimeter of drift in the direction of the applied electric field and per unit (mm Hg) pressure of the attached gas (water vapor).

The mixtures of argon and water vapor were studied over a total pressure range of 400 to 1800 mm Hg, and over an E/P range of 0.05 to 0.9 v/cm

---

[22]Consultant.
[23]Temporary employee.
[24]T. E. Bortner and G. S. Hurst, Health Phys. 1, 39 (1958).

(mm Hg). Higher fields could not be used because of internal arcing in the ion chamber when filled with pure argon. The maximum water vapor concentration used was 11.25 mm Hg in 1800 mm Hg total pressure (0.59%).

Attachment begins at an E/P of approximately 0.3 for small concentrations of water vapor and increases rapidly above this value, suggesting dissociative capture. Since the average electron energy in argon decreases rapidly with the addition of small amounts of impurity, the attachment threshold shifts upward as larger amounts of water vapor are added. Figure 3.6 shows α plotted against water vapor concentration (f_1P/f_2P) for several values of E/P and for total pressures of 1800, 800, and 400 mm Hg. There is essentially no dependence on total pressure, which is consistent with the notion of dissociative attachment.

An analysis of the results of electron capture in mixtures of argon and water vapor has been set up as follows:

$$\bar{\alpha}_0(E/P) = \frac{\text{constant}}{\bar{w}(E/P)} \int_0^\infty u\sigma_c(u)\, f(u,E/P)\, du \quad ,$$

where $\bar{\alpha}_0(E/P)$ is the value of α for $f_1P/f_2P \rightarrow 0$ (Fig. 3.6), $\bar{w}$ is the drift velocity of electrons, u is the kinetic velocity, $\sigma_c(u)$ is the cross section for electron capture at velocity u, and $f(u,E/P)$ is the energy distribution function for pure argon. Experimental values of $\bar{\alpha}_0 \times \bar{w}$ are inserted and the integral equation is solved for $\sigma_c(u)$. The machine code for the IBM 704 for the solution of the above integral equation has been completed where values of $f(u,E/P)$ for argon are based on the approach of Barbiere.[25] From mass spectrographic studies[26] it appears that for the range of electron energies used in this experiment the cross section $\sigma_c(u)$ will correspond to the formation of H^- according to

$$H_2O + e \rightarrow H^- + OH$$

Studies of attachment in carbon dioxide–water vapor mixtures are complicated by the extreme sensitivity of carbon dioxide to oxygen contamination, only a few parts per million of oxygen being necessary to mask the relatively slight attachment in water vapor. To obtain water free from

---

[25]D. Barbiere, Phys. Rev. 84, 653 (1951).

[26]M. Cottin, J. Chim. Phys. 56, 1024 (1959).

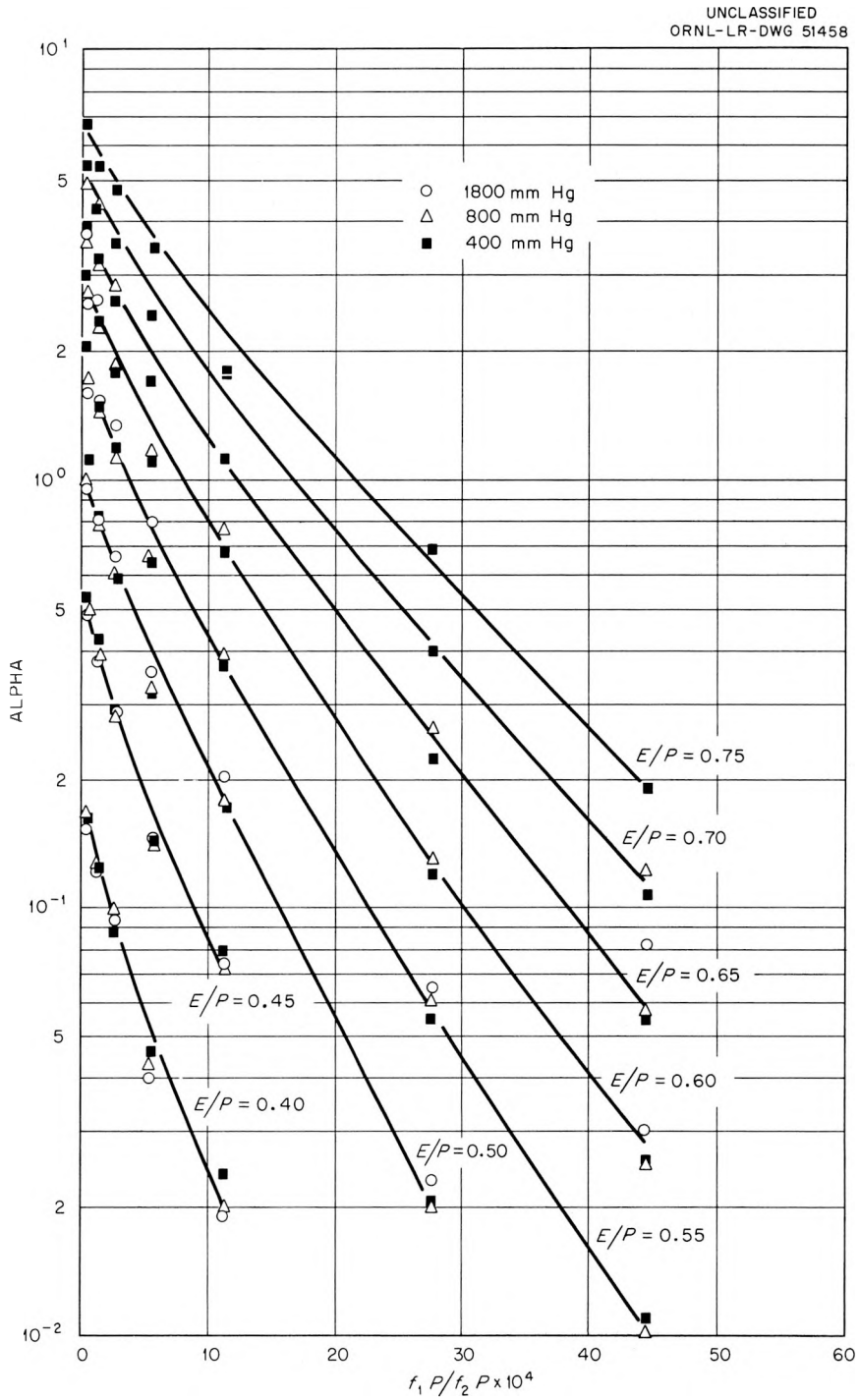

Fig. 3.6. Alpha vs f_1P/f_2P for Water Vapor–Argon Mixtures.

dissolved oxygen it was held in a trap for several days before use and the vapor above it pumped off periodically during this time. This appeared to give water vapor of satisfactory purity. Carbon dioxide–water vapor mixtures were studied over a pressure range of 250 to 800 mm Hg and an E/P range of 0.1 to 3.0 v/cm (mm Hg). The maximum concentration of water vapor was 15 mm Hg in 250 mm Hg total pressure (6%). Attachment was found to increase with a given mixture as total pressure increased and to decrease as E/P increased. This is characteristic of nondissociative capture that occurs at the low electron energies present in carbon dioxide at low values of E/P.

Diffusion of Electrons in Gases

As a stream of electrons moves through a gas at pressure p under the action of a uniform electric field E, the electrons will gain energy from the field but, in the steady state, this will be balanced by the energy lost in collisions with the molecules of the gas. In this steady state the swarm will possess a definite mean drift velocity w in the direction of the field and, as a result of the collisions with the gas molecules, the electron stream will diffuse with a characteristic diffusion coefficient K.

The diffusion of electrons in gases has been investigated, using a chamber similar to that first employed by Huxley.[27] Electrons enter a uniform field region through a small hole in a metal plate and diffuse as they drift a distance h along the direction of the field to coplanor collecting electrodes consisting of a central disk of radius b and an annular ring of outer radius c. The ratio R of the electron current to the central electrode to the current to both electrodes is:

$$R = \frac{1 - \frac{h}{\sqrt{h^2 + b^2}}\, e^{-w/2K\left(\sqrt{h^2+b^2}-h\right)}}{1 - \frac{h}{\sqrt{h^2 + c^2}}\, e^{-w/2K\left(\sqrt{h^2+c^2}-h\right)}} \quad .$$

From the measurements of R, the ratio w/K can be determined as a function

---

[27] L. G. H. Huxley and A. A. Zaazou, Proc. Roy. Soc. 196A, 402 (1949).

of E/p for the gas in question. Results of measurements in H_2, N_2, CH_4, and C_2H_4 are shown in Fig. 3.7. The results for hydrogen and nitrogen are in good agreement with those obtained by Crompton and Sutton[28] in a similar experiment. The results for C_2H_4 are appreciably lower than earlier measurements;[29] CH_4 had not been investigated previously. Measurements on argon have not yet given results independent of pressure and chamber geometry, and the investigation of argon and other gases of interest is being continued.

From the experimentally determined values of w/K, the mean energy of agitation of the electrons in the swarm can be determined if one assumes an energy distribution function. The electron energy is usually expressed in terms of the Townsend energy factor k, which is defined as the ratio of the mean energy of agitation of an electron to the mean energy of thermal agitation of a gas molecule. Then,

$$k = A \frac{NeE}{R_0 T} \frac{K}{w} \quad ,$$

---

[28]R. W. Crompton and D. J. Sutton, Proc. Roy. Soc. 215A, 467 (1952).
[29]J. Bannon and H. L. Brose, Phil. Mag. 6, 817 (1928).

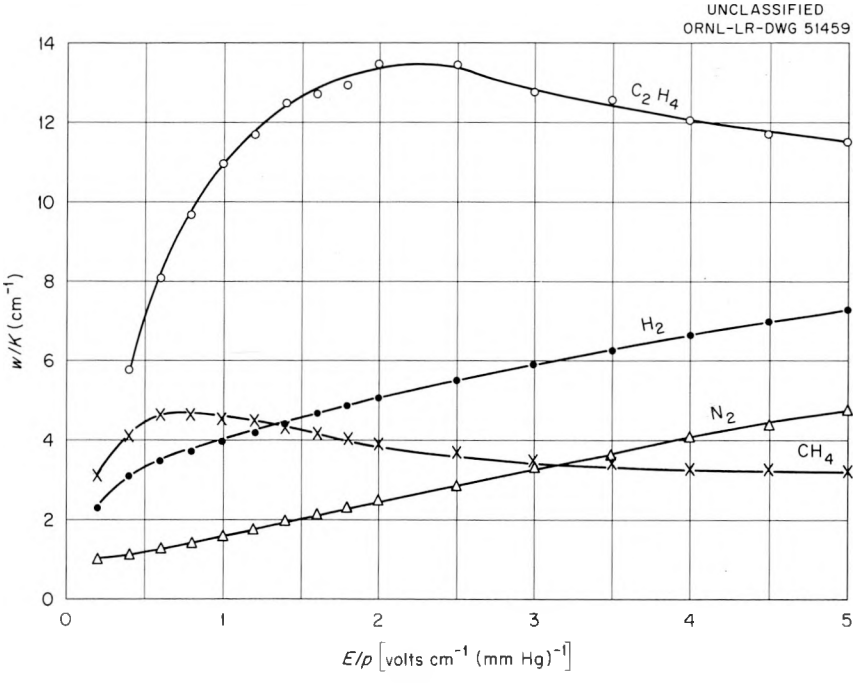

Fig. 3.7. Variation of the Ratio of Drift Velocity to Diffusion Coefficient for Electrons in Gases as a Function of E/p.

where

N = Avogadro's number,

e = the electronic charge,

R_0 = the gas constant,

T = the absolute temperature,

A = a constant having the value of unity for a Maxwellian distribution of electron velocities, and the value 0.875 for a distribution of the Druyvesteyn type.

Values of k as a function of E/p for the gases investigated are shown in Fig. 3.8; these values were computed for a temperature of 25°C and an electron velocity distribution of the Druyvesteyn type. By use of experimentally determined values of w/K and values of w obtained in an independent experiment,[30] for an assumed velocity distribution function, values of mean free path, average energy loss per collision, and collision cross sections as a function of E/p can also be inferred.

---

[30]T. E. Bortner, G. S. Hurst, and W. G. Stone, Rev. Sci. Instr. 28, 103 (1957).

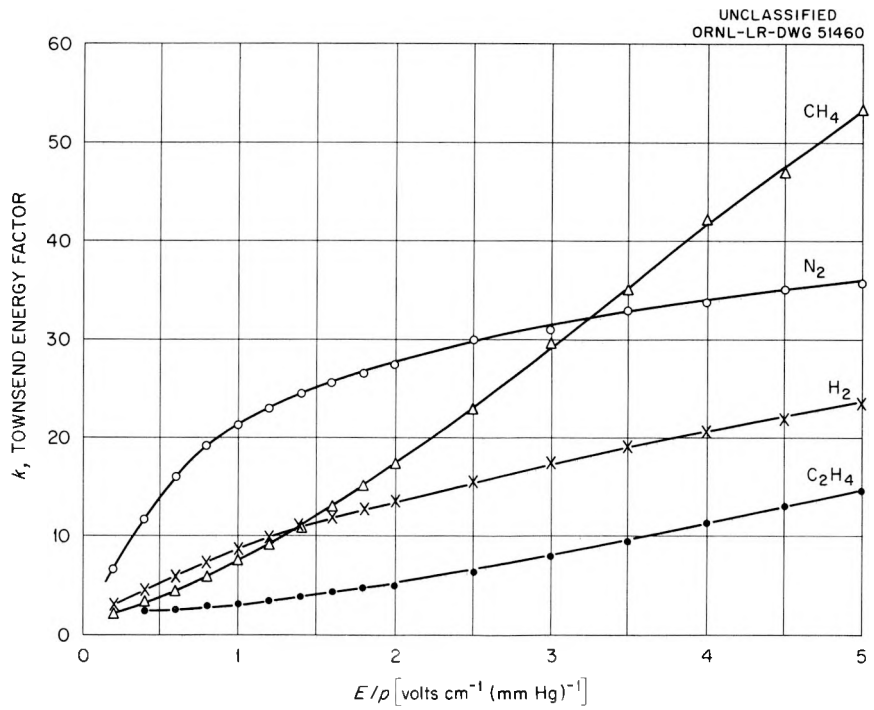

Fig. 3.8. Variation of Electron Agitation Energy with E/p at 25°C for an Assumed Electron Velocity Distribution of the Druyvesteyn Type.

Proportional Counter Studies of Single Electrons

Resolution in a proportional counter depends in part on the variation in the number of ion pairs produced by the ionizing particle, on the track orientation in the counter, and on the statistical variations in the size of the avalanches produced by individual electrons in the high-electric-field region near the collector electrode. A theory developed by Snyder[31] for this last contribution predicts a distribution in pulse heights for single electrons of the form $P_{N,\bar{N}} \approx (1/\bar{N})\, e^{-N/\bar{N}}$, where N and $\bar{N}$ are the gas amplification and the average gas amplification, respectively, for single electrons of low energy.

Pulse height distributions have been obtained in proportional counters of 2- and 4-cm diameters containing center wires of 0.0125-cm diameter and filled with a 50% argon–50% methane mixture to a pressure of 50 cm Hg. Photoelectrons from a gold cathode drifted through a uniform field region containing the same gas mixture as the counter and entered the counter through a slit. At the fields employed, the electrons had energies of about 1 ev as they entered the counter. The proportionality of the counter was determined by examining the pulse height distribution due to a Cr^{51} source.[32] The 5.01-kev x ray resulting from internal conversion in Cr^{51} will give a photoelectron from the argon of 2.05 kev, and the resulting K_α x ray from argon will escape from the counter part of the time. The resulting spectrum will consist of the full-energy 5.01-kev peak and the escape peak at 2.05 kev. The constancy of the ratio of these two-peak pulse heights as a function of counter voltage determines a region of proportional operation. The counter was operated at an average gas amplification of about 4×10^4. The linearity of the semilog plot down to the low pulse heights where noise is excessive is in agreement with theory. An earlier experiment by Curran et al.[33] gave a pulse height distribution which was fitted by a function of the type

$$P_{N,\bar{N}} = \frac{N^{1/2}}{\bar{N}}\, e^{-N/\bar{N}} \quad .$$

---

[31] H. S. Snyder, Phys. Rev. 72, 181 (1947).

[32] P. Rothwell and D. West, Proc. Phys. Soc. 63A, 541 (1950).

[33] S. C. Curran, J. Angus, and A. L. Cockcroft, Phil. Mag. 40, 929 (1949).

Calorimetric Measurement of Electron Stopping Power

Measurements of the stopping power of thin films for electrons have been extended to include elements of higher atomic number. The apparatus was redesigned because of the increased nuclear scattering found for heavier elements. In particular, a pilot run on a gold foil with the old calorimeter gave a stopping power which was 800% above theoretical expectations, whereas deviations of a few per cent at most were anticipated. Calculations showed that such errors would arise if singly scattered electrons could be absorbed in any part of the foil support ring. The calorimeter shown in Fig. 3.9 embodies several improvements over the previous model, the most important of which is that electrons which have been singly scattered from gold nuclei have a much smaller probability of being stopped by the foil ring. The new thinner ring subtends a solid angle of only 0.027 steradian, representing a reduction by a factor of 44 over that of the previous apparatus.

Reduction of the number of thermocouples and the mass of the foil ring results in a net gain in sensitivity and a reduction of the heat loss and time constant of the system. With a faster response, operation of the calorimeter at the constant temperature of the surroundings becomes possible if the heating by the beam is just balanced by thermoelectric cooling. Such operation has the additional advantage that the beam current may be integrated over long periods of time to achieve increased accuracy of this measurement.

Secondary electrons were directed back into the foil by plates adjacent to the foil and maintained at negative potentials of up to 2 kv with respect to the foil. Such potentials proved adequate during calibration of the calorimeter when the beam energy was reduced so that complete absorption of the beam in the foil was achieved. However, at higher beam energies higher suppressing voltages were required with the optimum voltage being half the beam energy. That is, any electron emerging from the foil with less than half the beam energy is a secondary electron by definition and should be reflected back into the foil. Unfortunately, higher voltages could not be used, and this limitation may have been responsible for the high stopping powers found for gold. Although there

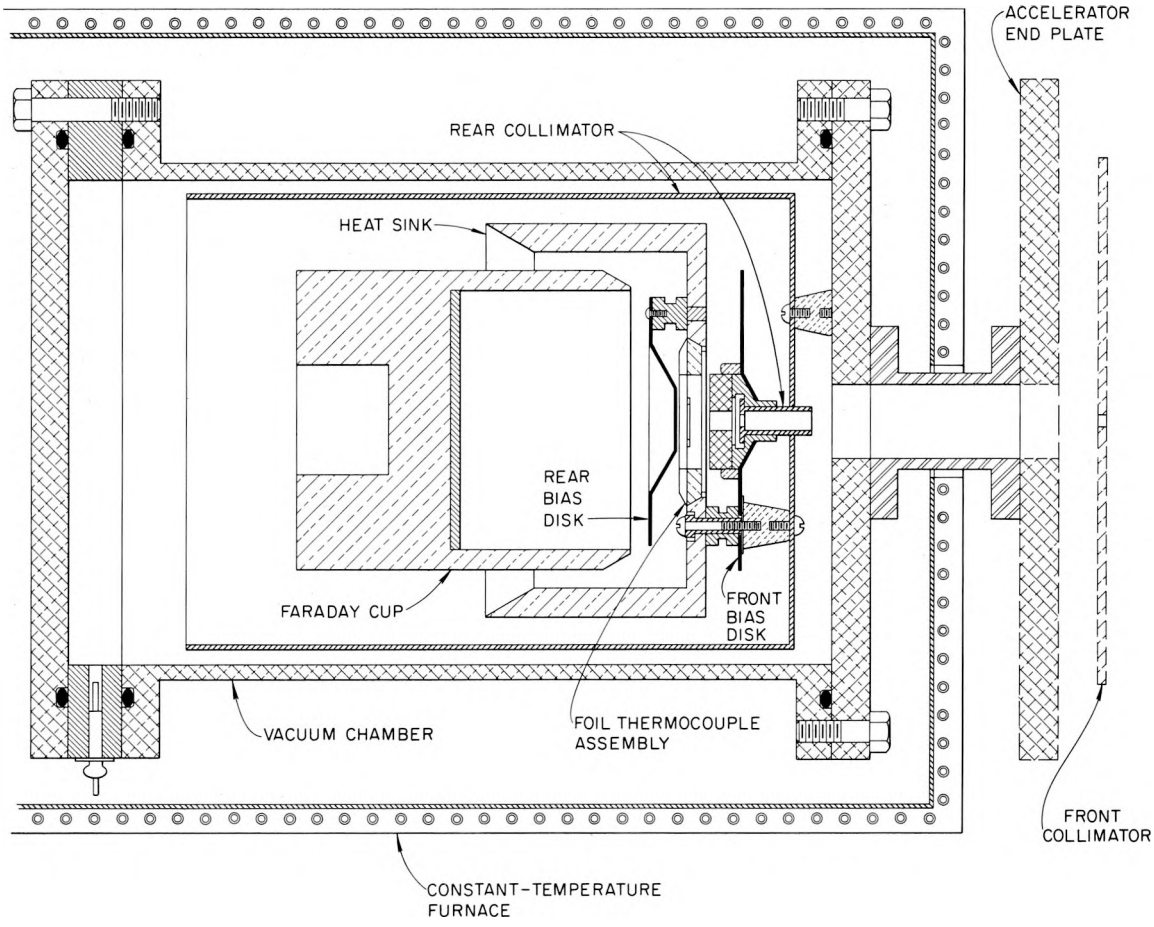

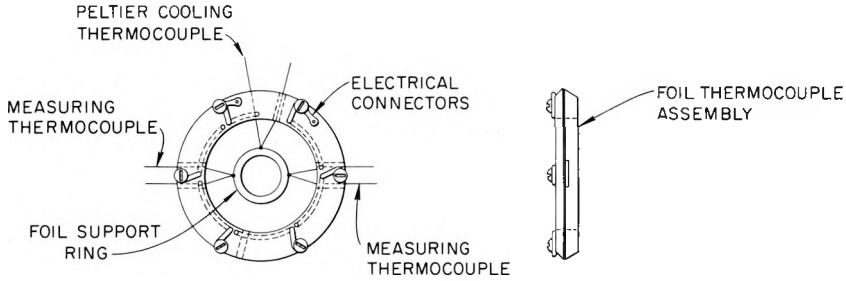

Fig. 3.9. Calorimeter for Measuring the Stopping Power.

was considerable variation from foil to foil, experimental stopping powers were usually about 20% higher than predicted by the Bethe formula above 50 kev and as much as 50% higher at 30 kev. As a result, the geometry of the suppressing plates was changed at the time that conduction cooling (see next section) replaced the thermoelectric cooling. The suppressing electrode is now a spherical grid centered about the foil, a situation much more amenable to theoretical analysis. That is, the probability that an electron will be reflected back into the foil is now a function of only its energy and the grid voltage, and does not depend on its angle of emission from the foil. Also, higher grid voltages may be used because of the introduction of better insulation and greater electrode spacings.

The Conduction Cooling Calorimeter

The calorimetric determination of energy absorption employed in the electron stopping power measurements has utilized a Peltier cooling thermocouple to balance out heating caused by the passage of the electron beam through the foil. Such measurements, however, failed to achieve the reproducibility or accuracy necessary for a really precise measurement of stopping power. The lack of reproducibility was probably due to a variation in the heat conductivity between the foil and the Peltier couple. The lack of accuracy was an inherent feature of the Peltier cooling method in making null calorimetric measurements. An index of the accuracy of any null method is the ratio of the power conducted into or out of the system per centigrade degree to the power level of operation. That is, any temperature monitoring instrument has a lower limit to its sensitivity, and, within this limit, power conducted into or out of the system is unobservable. For the Peltier method the net cooling power is $P = \pi Ti - i^2(\rho\ell/A)$ for a Peltier couple of resistivity ρ, length ℓ, cross section area A at a Kelvin temperature T. Here i is the cooling current and π the thermoelectric power of the couple. Here and henceforth it will be assumed for simplicity that the thermocouple wires are identical except for thermoelectric power. This situation exists for the constantan-Manganin couples which have usually been employed here. The equation states that the net cooling is the difference between the Peltier cooling and

the i^2R heating due to the flow of cooling current through the thermocouple wires. It may be noted that although the total heat generated is $i^2[\rho(2\ell)/A]$, only half is conducted toward the cooling junction. The graph of P vs i is a parabola with a maximum cooling of

$$P_{max} = \frac{(\pi T)^2}{4(\rho\ell/A)} \quad .$$

Now if a measuring thermocouple is connected to the foil-Peltier couple system, the ratio noted above may be written as follows:

$$R = \frac{4KA}{\ell[(\pi T)^2/4(\rho\ell/A)]} = \frac{16K\rho}{(\pi T)^2} \quad ,$$

where K is the heat conductivity.

The value of R for constantan-Manganin couples is about 1 per degree centigrade. Thus, if a good thermocouple galvanometer is used which produces a noticeable deflection for a temperature change of 10^{-3} °C, a theoretical accuracy of about 0.1% is obtainable. However, practical considerations raise this number to 0.5% or higher.

Clearly a substantial increase in accuracy can be achieved only through a fundamental change in the design of the calorimeter. Consider a foil which is connected by only a measuring thermocouple to the surroundings. Cooling is produced by conduction along the couple wires. That is, the wires lead from the junction through a cold reservoir and back to room temperature where connection with the galvanometer is made. If the system is operating at a power level P, with the cold reservoir at a temperature ΔT below room (and foil) temperature, then the ratio R defined above is $R = (P/\Delta T)/P = 1/\Delta T$. Thus, R takes on the values 0.036, 0.0127, and 0.0051 per degree centigrade for cold reservoirs filled with ice water, acetone–dry ice, and liquid nitrogen, respectively, and the accuracy of the system is improved by two orders of magnitude. A calorimeter embodying these principles has been constructed and is being tested.

Plasma-Light Experiment

The discrete energy losses suffered by fast electrons passing through thin metal foils[34] have been attributed to the plasma oscillation of free electrons in the metal. Ferrell,[35] in 1958, suggested that the decay of this excitation should be accompanied by the emission of radiation at the plasma frequency. For example, aluminum, with a 14.8-ev characteristic energy loss, should emit light at 837 A. Ferrell's theory, however, does not contain the effects of retardation and consequently is not complete. He predicts that the intensity of radiation at the plasma frequency in the forward direction is zero because of the competition of interband damping with the radiative decay.

A complete classical treatment of stimulated emission from a finite foil having a realistic dielectric variation with frequency has been described by Ritchie.[36] The angular distribution of radiation at the plasma frequency, according to Ritchie, varies as cos θ, when θ is measured from the foil normal. A preliminary experiment to detect this radiation has been described in a previous report.[37] The electrons from a series of radioactive phosphorus-Bakelite plaques were used to bombard a thin aluminum foil. It was reported at that time that no blackening was observed on the photographic plate.

The present report describes an experiment designed to investigate this phenomenon by using an accelerator as a source of high-energy electrons. A schematic diagram of the apparatus is shown in Fig. 3.10. The maximum energy available from the accelerator (120 kev) was utilized because the intensity of light emitted is directly proportional to v/c for a foil of the optimum thickness, where v is the electron velocity and c the velocity of light. Exposures with currents as high as 5 μa or 2.5×10^{13} electrons per second for 2 hr have been used, although the usual exposures have been at 0.7 μa for 20 min.

---

[34]A. W. Blackstock, R. H. Ritchie, and R. D. Birkhoff, Phys. Rev. 100, 1078 (1955).

[35]R. A. Ferrell, Phys. Rev. 111, 1214 (1958).

[36]R. H. Ritchie et al., H-P Ann. Prog. Rep. July 31, 1959, ORNL-2806, p 137.

[37]G. S. Hurst et al., H-P Ann. Prog. Rep. July 31, 1959, ORNL-2806, p 155.

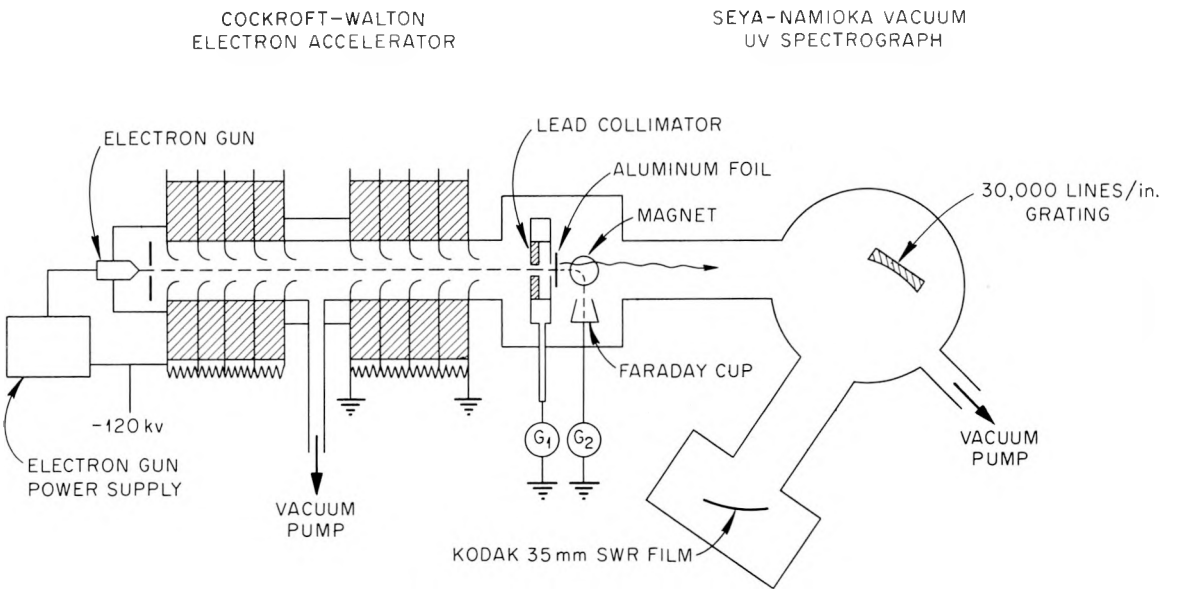

Fig. 3.10. Schematic Diagram of Plasma-Light Experiment.

The apparatus used to analyze the light emission is a Seya-Namioka vacuum ultraviolet spectrograph built by the Jarrell-Ash Company of Newtonville, Mass. The focal length of the instrument is 50 cm with an f/12 aperture at 1300 A. The unique feature of the spectrograph is that the entrance and exit slits are fixed while only the grating rotates[38,39] to cover the wavelength region from 0 to 10,000 A. The grating used in this experiment was a 30,000 lines-per-inch glass grating, coated with aluminum and optimized at 1100 A. The region from 0 to 4500 A is scanned with this grating.

In order to test the performance of the instrument, a gaseous discharge tube was constructed in which hydrogen, helium, neon, and other gases could be excited by a 14-kv sign transformer. Figure 3.11 shows densitometer tracings of the 584-A line of helium and the 1215-A Lyman-alpha line in hydrogen. The linear dispersion of the instrument was determined experimentally and is plotted as a function of wavelength in Fig. 3.12.

---

[38]M. Seya, Sci. of Light (Tokyo) 2, 8 (1952).

[39]T. Namioka, Sci. of Light (Tokyo) 3, 15 (1953).

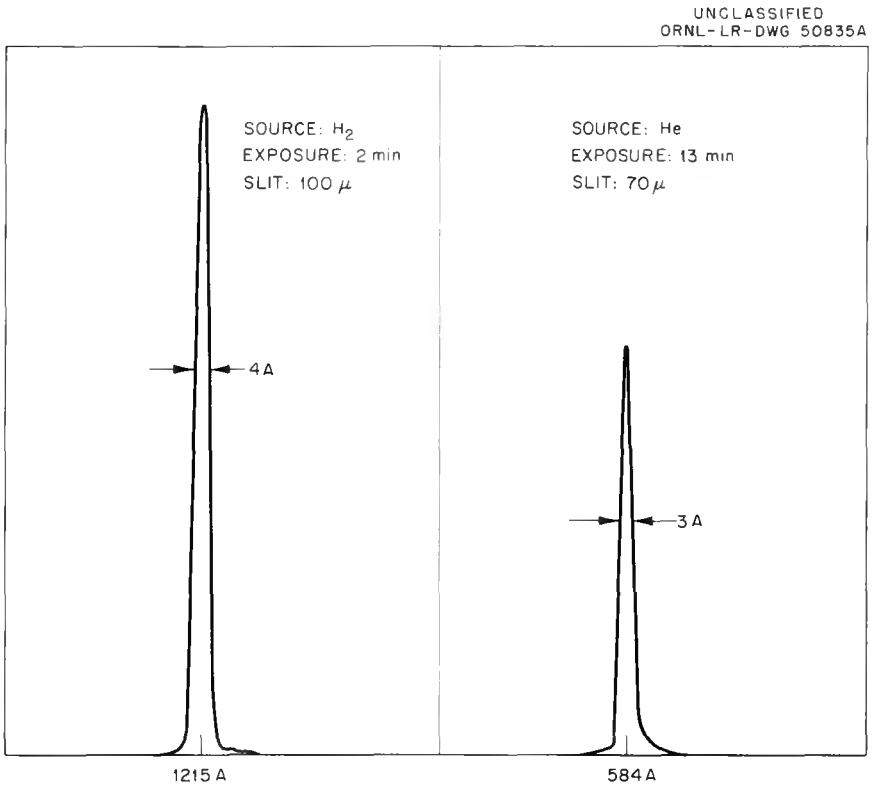

Fig. 3.11. Densitometer Tracings of Ultraviolet Lines Produced by Gaseous-Discharge Tube.

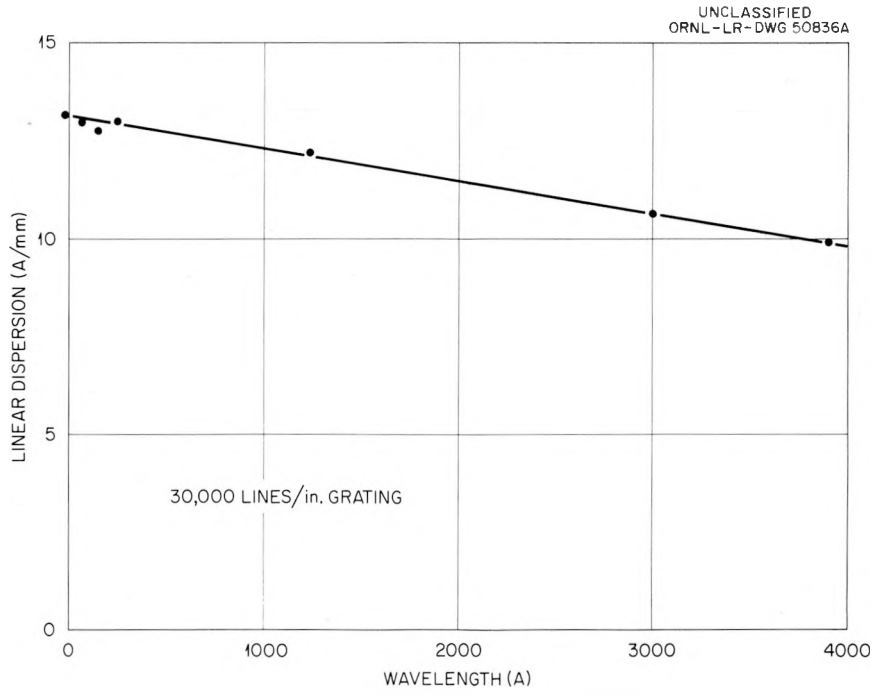

Fig. 3.12. Linear Dispersion vs Wavelength for Ultraviolet Spectrograph.

The aluminum foils used in the experiment were vacuum-evaporated onto Formvar and Zapon backings directly in the plasma-light apparatus, since it is known that a coating of aluminum oxide 40 to 50 A thick forms on the surface of aluminum in a few minutes at atmospheric pressures. Several runs were begun within 2 min after the foils, ranging from 270 A (10 $\mu g/cm^2$) to 540 A (20 $\mu g/cm^2$), were made. Thicknesses were calculated from

$$t = \frac{m}{4\pi r^2} ,$$

where m is the mass of aluminum evaporated and r is the distance from the source to the foil.

Kodak's SWR film,[40] a specially sensitized film for use in the far ultraviolet region, was used to detect the radiation emitted by the foils.

No blackening of the film has been observed at 837 A, where a sharp line has been predicted by Ferrell. Instead, a fairly broad continuum with a peak at approximately 2000 A has been observed. No blackening has been observed from 2200 A to the upper limit of the grating at 4500 A. The interpretation of this observation has not been completed. The influence of film sensitivity as a function of wavelength, the reflectivity of the aluminum-coated grating in this region, and several other factors have yet to be evaluated.

Plans are being made to investigate the radiation emitted by magnesium and sodium, which have characteristic energy losses at 10.6 ev (1170 A) and 6 ev (2100 A), respectively. The optical problems are simplified considerably at these wavelengths. The reflectance of aluminum, with which the grating is coated, is only 5% at 837 A, but increases to 30% at 1170 A and is 85% at 2100 A.[41]

Improved Calculations for the Spherical Condenser Spectrometer

The study of the generation, diffusion, and absorption of electrons in irradiated matter has been considerably hampered by the lack of a suitable low-energy electron spectrograph which would have a high transmission

---

[40] Kodak Photographic Plates for Scientific and Technical Use, 7th ed., p 6, Eastman Kodak Co., Rochester, New York, 1953.

[41] J. B. Sabine, Phys. Rev. 55, 1064 (1939).

for electrons originating in extended sources. The inverse square electric field between two concentric charged spheres provides a focusing of charged particles which leave a point source on the inner sphere as shown in Fig. 3.13. An analysis of the transmission, resolution, and line profile shape which may be obtained with a spectrometer utilizing this focusing has been carried out analytically and graphically.[42] The essential features of this study may be summarized as follows: the transmission is found to be $T = \chi/4$, and the energy resolution (width of the line profile at half height) $\delta = \chi^2/16$, where χ is the supplement to the central angle through which the particle rotates between the source and the slit. An approximate calculation of the operating characteristics for a source on

[42]R. H. Ritchie, J. S. Cheka, and R. D. Birkhoff, Nuclear Instr. & Methods 6, 157 (1960).

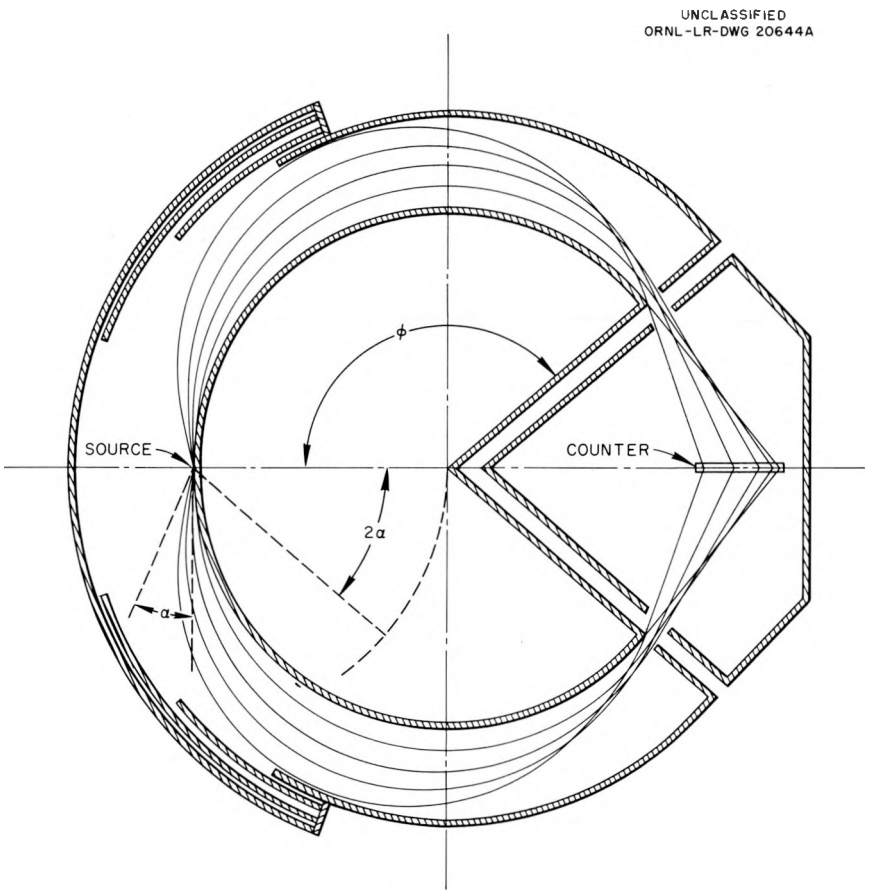

Fig. 3.13. Schematic Cross-Sectional View of the Spherical Condenser Spectrometer.

the inner sphere but not on the axis of symmetry was carried out previously[43] and indicated that such a spectrometer would perform almost as well for nonaxial sources (and hence extended, disk sources) as for point sources. Before construction was started, however, it was deemed advisable to improve the calculations to take into account more precisely the boundary effects imposed by the spheres and slits. The more realistic boundary conditions complicated the calculation to the extent that the problem was coded for the IBM 704 computer. It will suffice to quote the results of these calculations.

The transmission $\bar{t}$ for a point on the inner sphere but off the axis by an amount $\eta = h\chi$ (in units of the inner sphere radius) is given for various values of h as a function of the energy parameter $d = \delta/\chi^2$ in Fig. 3.14. These line profiles show, for example, that when $\chi = 1$, the transmission and resolution are 25 and 6.3% for an axial source, and 13 and 9% for a source located on the inner sphere but displaced from the axis a distance equal to 30% of the radius of the inner sphere.

[43]R. D. Birkhoff et al., H-P Ann. Prog. Rep. July 31, 1958, ORNL-2590, p 128.

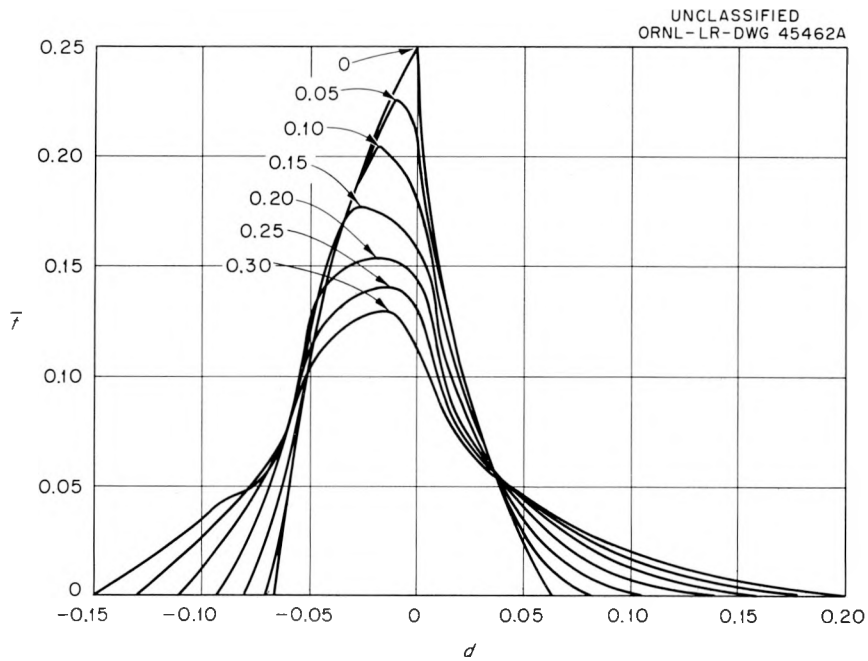

Fig. 3.14. Line Profiles for a Point Source on the Inner Sphere but Off the Axis of Symmetry. Numbers on curves are the source displacements h.

Appropriate combinations of the above profiles yield the composite profiles for disk sources, as shown in Fig. 3.15, where the numbers on the curves refer to the radii of the disks in units as above. For a source radius equal to the source displacement taken in the example above, and the highest transmission (occurring for $X = 1$), the transmission and energy resolution are 16 and 7.7% respectively. It would appear that the conclusions of the earlier calculation are substantiated and that a simple electrometer (rather than a counter) will suffice as a particle detector because of the large source and transmission. Construction of such a spectrometer will be started this year.

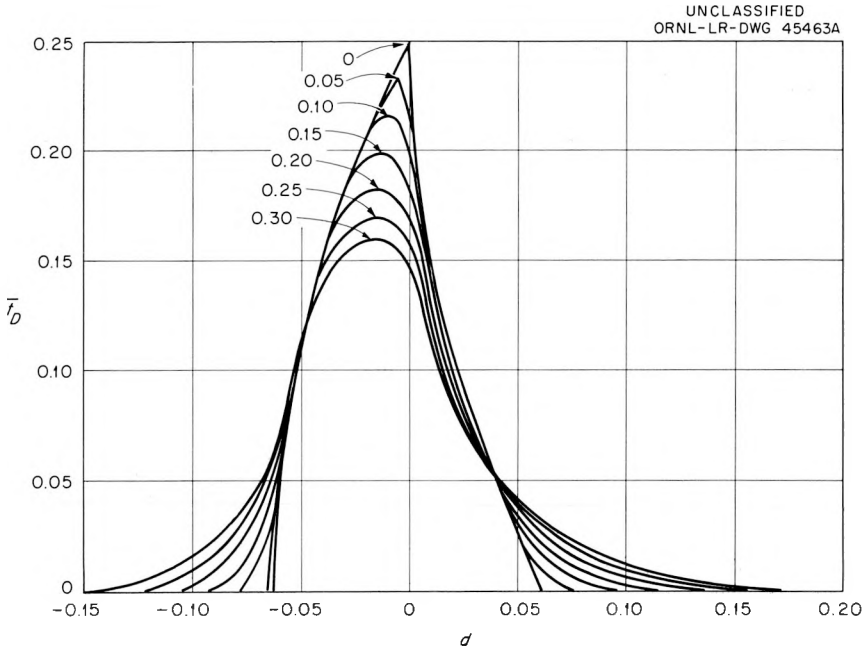

Fig. 3.15. Line Profiles for a Disk Source on the Inner Sphere. Numbers on curves are the source radii h.

Response of Anthracene as a Function of LET and Its Use in an LET Meter

Previous work at this Laboratory has shown that the response of anthracene to alpha particles, protons, and electrons is well represented by an equation given by Birks wherein the specific fluorescence is equal to the specific energy loss divided by a factor depending on the specific energy loss,

$$\frac{dS}{dx} = \frac{A(dE/dx)}{[1 + kB(dE/dx)]} \quad ,$$

where the constants A, k, and B are the same for all radiations. It is interesting to note that the factor in the denominator of the above, which essentially measures the decreased ability of anthracene to fluoresce for particles of high dE/dx, is very close numerically to the "administrative" RBE given in NBS Handbook 59.[44] The two are given in Fig. 3.16 where the close similarity may be noted. The substantial variation of this factor over the range of LET thought to be significant biologically, suggests that layers of anthracene, thin compared with particle ranges, may be employed in an LET meter. More particularly, such a device may be constructed from a sandwich of a thin layer of anthracene and a thin inorganic phosphor. A particle traversing these layers at any angle will cause a pulse height proportional to dS/dx in the anthracene and proportional to dE/dx in the

[44] Permissible Dose from External Sources of Ionizing Radiation, National Bureau of Standards Handbook 59 (Sept. 24, 1954).

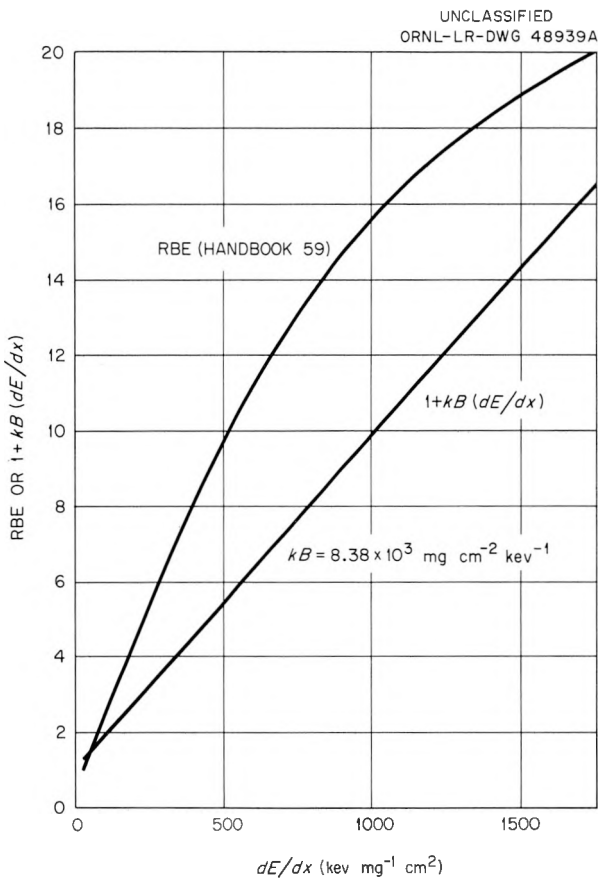

Fig. 3.16. The RBE from Handbook 59 and Birks' Factor [1 + kB (dE/dx)] as a Function of dE/dx.

other layer. The dE/dx of the particle may be computed then from the ratio of pulse heights (which is independent of the angle of traversal) and the above equation.

The feasibility of the above instrument rests primarily on whether uniform layers of phosphor may be produced which are thin compared with the ranges of moderately energetic recoil protons. In Fig. 3.17 the pulse-height distribution obtained from alpha particle bombardment of an anthracene crystal 1.04 mg/cm^2 in thickness is shown. The crystal is prepared by evaporation of anthracene from a heated stainless steel boat in high vacuum directly onto the face of a photomultiplier. The collimated alpha source may be rotated about the crystal plane so that bombardment angles of 60 and 70.5° may be employed. Incidence at such angles produces path lengths of two and three times the crystal thickness, respectively,

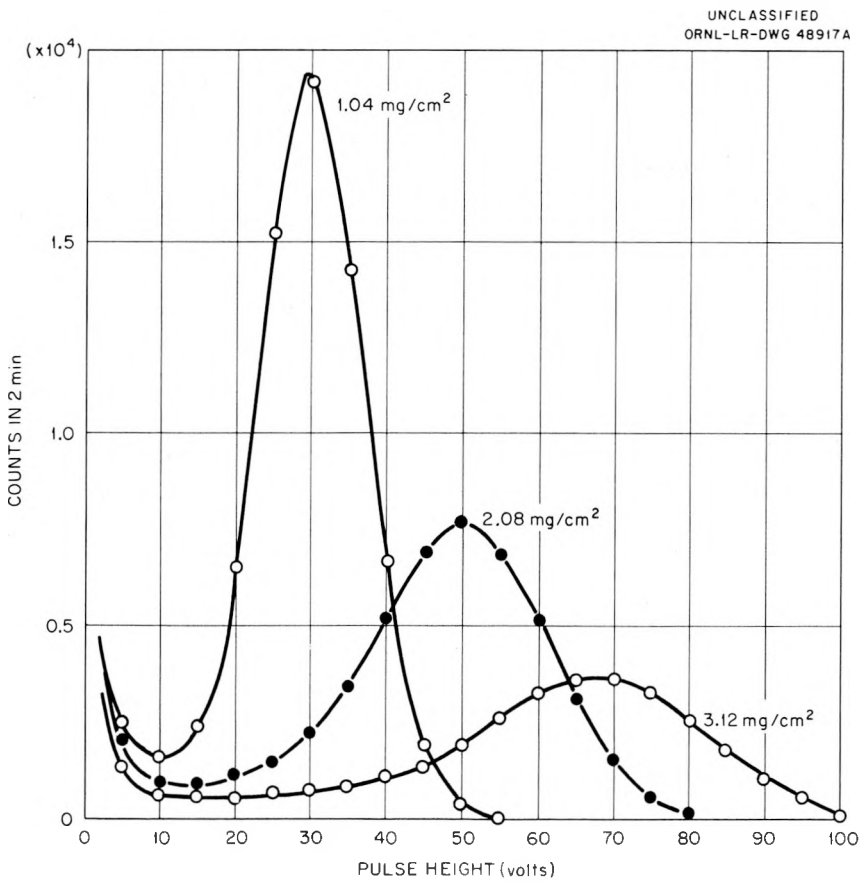

Fig. 3.17. Pulse-Height Distributions for an Anthracene Crystal 1.04 mg/cm^2 Thick Irradiated by Alpha Particles at 0, 60, and 70.5° to the Normal.

and the corresponding pulse-height distributions are given in Fig. 3.17. Similar distributions are given for thinner layers, 0.51 and 0.19 mg/cm^2, respectively, in Figs. 3.18 and 3.19.

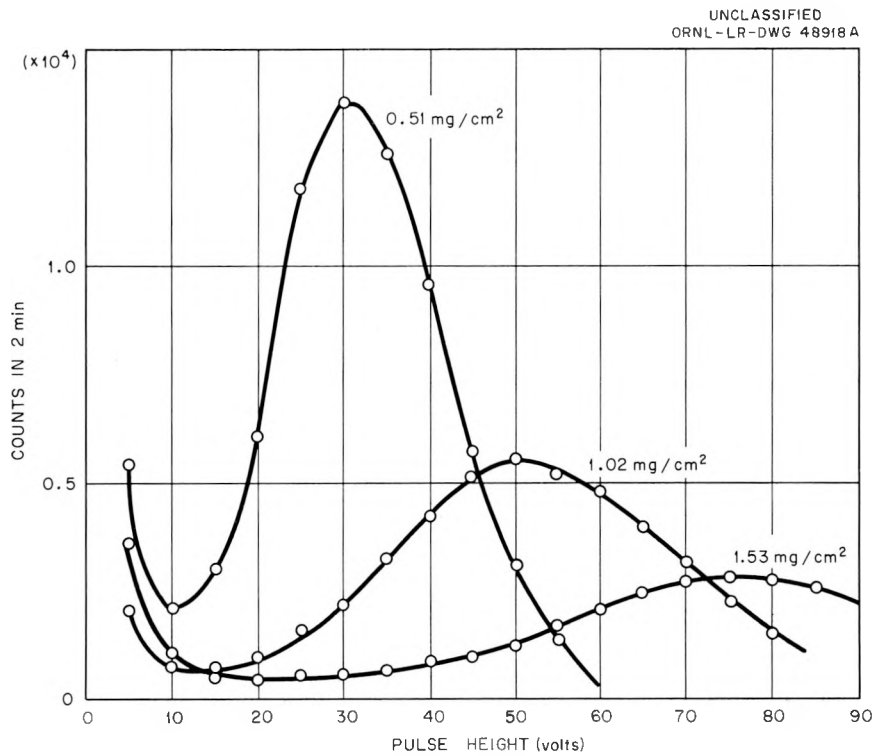

Fig. 3.18. Pulse-Height Distributions for an Anthracene Crystal 0.51 mg/cm^2 Thick Irradiated by Alpha Particles at 0, 60, and 70.5° to the Normal.

Attempts to produce similar fluorescing layers of ZnS(Ag) for the other half of the sandwich have not been entirely successful to date, but evaporation techniques are being improved continuously and it is felt that suitable phosphors will be available soon. The separation of the two pulses will be made on the basis of the great differences in decay times in the two phosphors [0.032 and 10 μsec for anthracene and ZnS(Ag), respectively]. A dual amplifier 256-channel analyzer with a special input to permit such discrimination has been ordered and will be received soon.

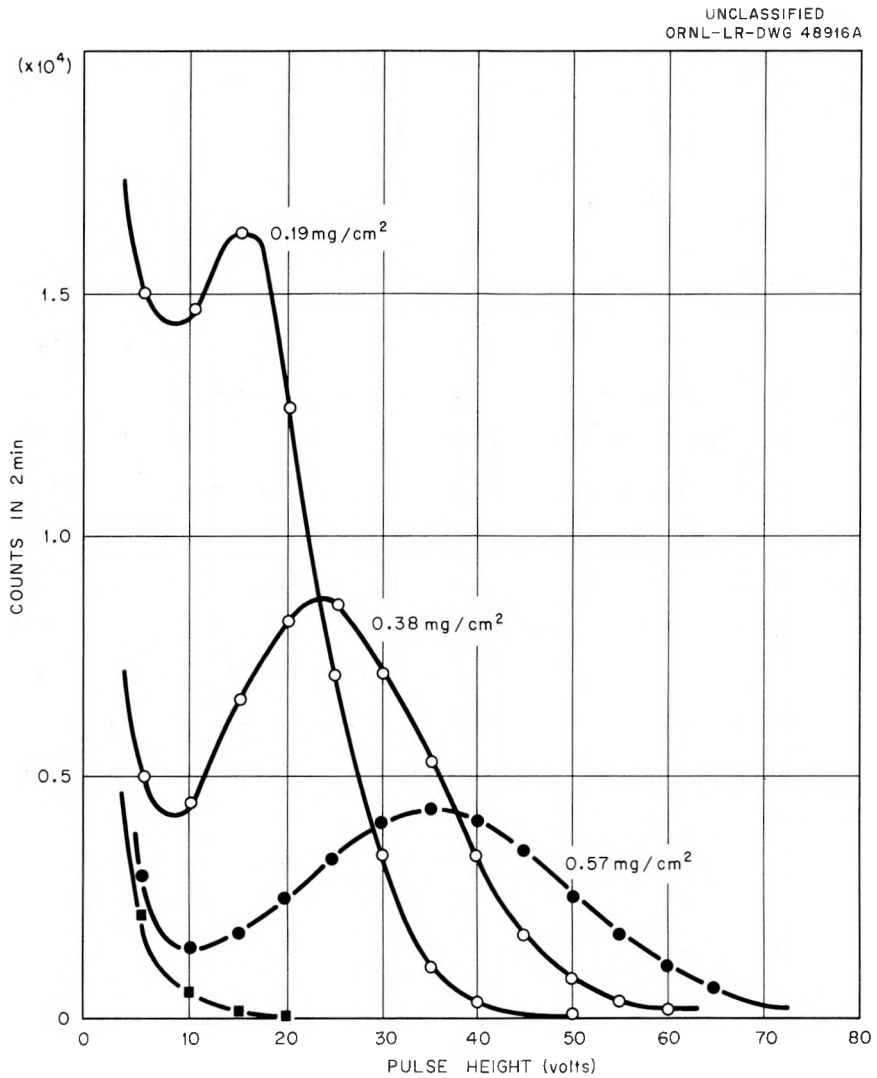

Fig. 3.19. Pulse-Height Distributions for an Anthracene Crystal 0.19 mg/cm^2 Thick Irradiated by Alpha Particles at 0, 60, and 70.5° to the Normal.

DOSIMETRY METHODS

F. J. Davis

A. E. Carter
R. W. Granlund[45]
J. A. Harter
P. W. Reinhardt
R. M. Simmons
E. B. Wagner

A G-M Tube Gamma-Ray Dosimeter with Low Neutron Sensitivity

A small halogen-type Geiger-Mueller counter can be arranged with suitable shields to provide an instrument whose response is (a) independent of energy for x or gamma radiation above approximately 150 kev, (b) insensitive to fast neutrons, and (c) insensitive to thermal neutrons.

The counter used is a Philips No. 18509 micro G-M counter.[46] The unshielded counter shows considerable energy dependence below 200 kev. As shown by Fig. 3.20, the counter can be made to furnish readings of exposure dose in r that are essentially independent of gamma-ray energies down to 150 kev by shielding the counter with lead and tin as shown in Fig. 3.21.

---

[45]AEC Health Physics Fellow.

[46]Manufactured by N. V. Philips Gloelampenfabrieken, Amsterdam, The Netherlands.

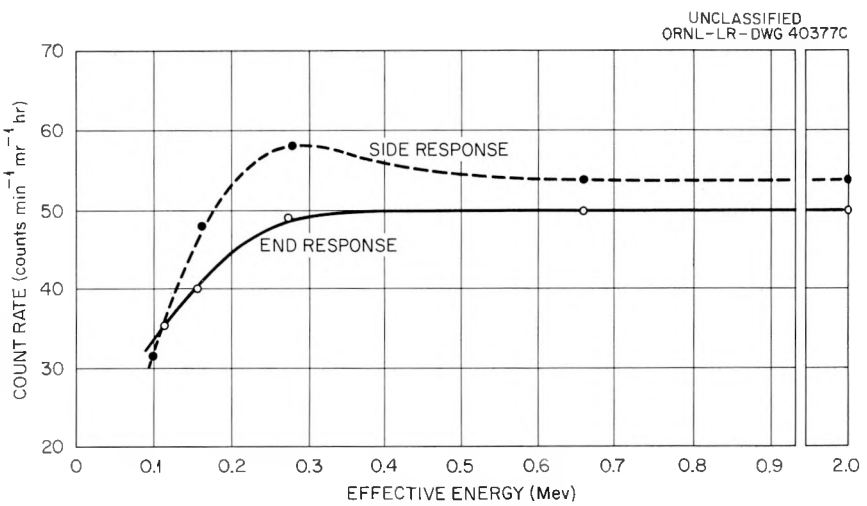

Fig. 3.20. Response of the Shielded Counter as a Function of Gamma-Ray Energy.

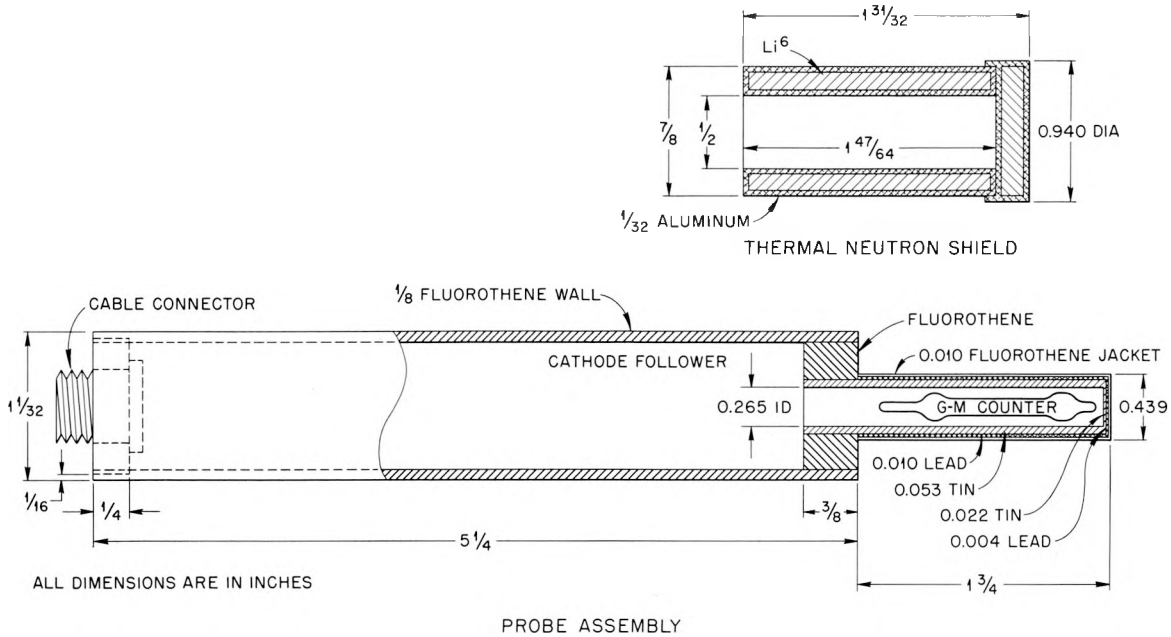

Fig. 3.21. Schematic Diagram of Probe Unit, Showing Lithium Shield for Thermal Neutrons.

The counter is capable of indicating gamma dose rates from 0.1 mr/hr to 300 r/hr. The response as a pulse device is essentially linear from 0.1 mr/hr to 5 r/hr. The response as a current device is approximately logarithmic from 2 to 150 r/hr.

By calculation it can be shown that the main contribution to the fast-neutron response is due to inelastic collisions in the gamma-energy correction shield and is a maximum at a neutron energy of about 5.0 Mev. An upper limit to the neutron response at 5 Mev is calculated to be 0.15%, and experiments indicate that it is less than 0.5%.

Experimentally it was found that the response of the counter to thermal neutrons is low, requiring about 5×10^9 neutrons/cm^2 to produce the same response as 1 r of gamma radiation. With the addition of a lithium shield, about 1.5×10^{12} neutrons/cm^2 would be required to produce the same response as 1 r of gamma radiation.

Silicon-Gold Surface Barrier Fission Counters

Fission foils of U^{235}, Np^{237}, and U^{238} have been prepared by plating 0.3 to 7.0 mg of material on 3.5-cm^2 metal disks. By counting the fission

fragments from these foils with a silicon diode, we produce a measure of the neutron flux above the threshold of these nuclides. Instead of Pu^{239}, ordinarily used in the threshold-detector units, U^{235} is used because of its lower alpha activity. When U^{235} is shielded by B^{10}, its curve of neutron cross section vs energy has approximately the same shape as that for Pu^{239}. The foils are placed 0.005 in. from the gold surface when in use but are removable from the diode counter to prevent alpha damage when not in use. The detectors are of a suitable size to be placed inside the B^{10} shields used in the standard threshold-detector units.

Threshold-Detector Measurements

To measure the effect of a concrete wall on the neutron dose from a critical assembly, the experimental arrangement shown in Fig. 3.22 was set up. Complete threshold-detector units were placed on each side of a 1-ft-thick concrete wall; a control unit was placed 5 ft from the edge of the wall and at the same distance from the critical assembly as the unit on the side of the wall facing the source. The measurements show increase

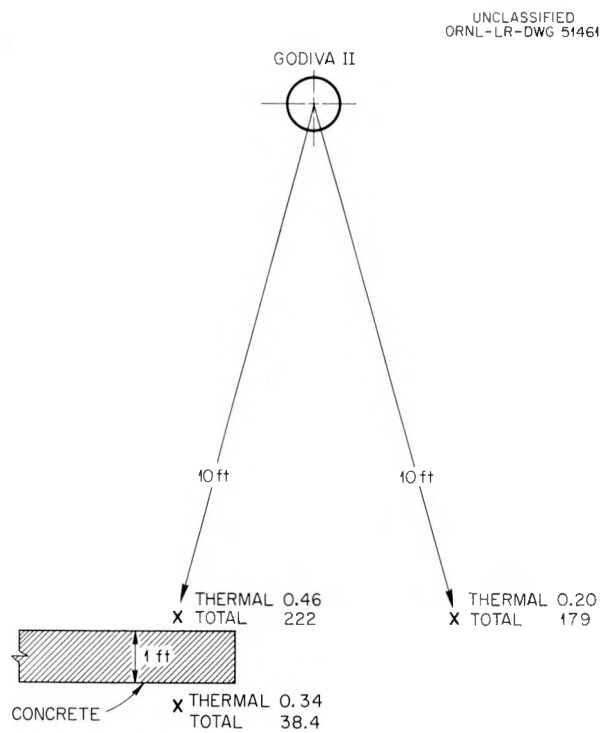

Fig. 3.22. Effect of Wall on Neutron Dose.

in the thermal-neutron dose on both sides of the wall with little attenuation through the wall. The dose due to fast neutrons shows an appreciable buildup on the front face of the wall and a large attenuation through the wall. The actual dose measurements are shown in the same figure.

A comparable experiment to measure the variation of the neutron dose around the waistline of a person was made, using a phantom with a dosimetry belt containing sulfur, gold, and cadmium-shielded gold at each of eight positions. Figure 3.23 shows the positions and the corresponding measurements. The thermal-neutron measurement obtained from the difference between the activity of the gold and that of the cadmium-shielded gold is N_T, and N_S is the fast-neutron measurement obtained from the sulfur activity and represents the number of neutrons above the sulfur threshold of 2.5 Mev. The attenuation of the thermal flux through the body is of the order of a factor of 2; the fast-neutron flux is attenuated by a factor of 10. Such a belt, if worn by a person exposed to a critical excursion, would indicate his orientation with respect to the source.

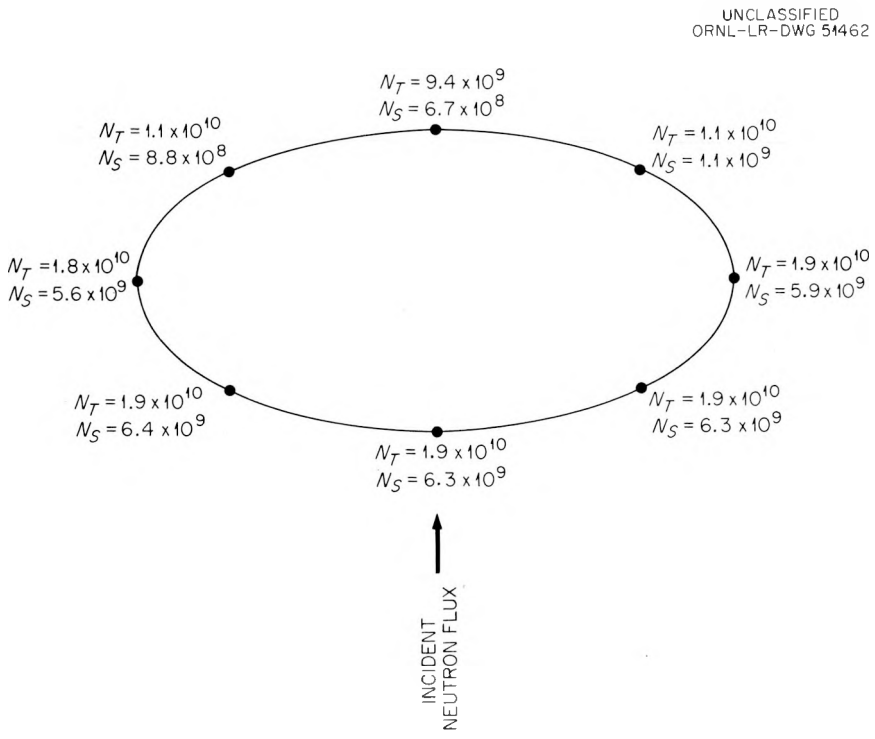

Fig. 3.23. Effect of Person on Neutron Dose.

Figure 3.24 shows the effect on the thermal-neutron flux by the B^{10} balls and cadmium shields used in the threshold-detector units. The relative gold activation shows there is very little thermal-flux depression except possibly near the B^{10} ball.

Extended Source Calibration Area (ESCA)

At the request of the Division of Biology and Medicine, USAEC, a source field is being prepared for use in calibration and intercomparison of instrumentation in aircraft used for radiation surveys by the AEC, the U.S. Geological Survey, Edgerton, Germeshausen, and Grier, Inc., and ORNL. The area chosen for the source field is located in the Frenchman Flat Area at the Nevada Test Site. The area is remarkably level and shows a general background of 15 μr/hr. A grid of 361 sources spaced at 100-ft intervals will extend over an area 1800 ft square. For ground calibration, the center source will be replaced by 100 sources at 10-ft intervals, each source 1/100 of the magnitude of the outer sources. The source configuration is shown in Fig. 3.25. Since the center of the small sources is at the center of four sources making a 10-ft square, the ground measurements can be an average of measurements made in a grid the plane of which is 3 ft above this 10-ft square. Two sets of sources, Co^{60} and Cs^{137}, will be available for measurements. These sources have been chosen for their long half life. Cobalt-60 has a gamma-ray spectrum similar to the spectrum of natural background, and Cs^{137} has a gamma-ray spectrum similar to I^{131} and $Te^{132} + I^{132}$ encountered in a reactor incident. The Radsafe Division of the Reynolds Electric Engineering Company will place, recover, and store the sources.

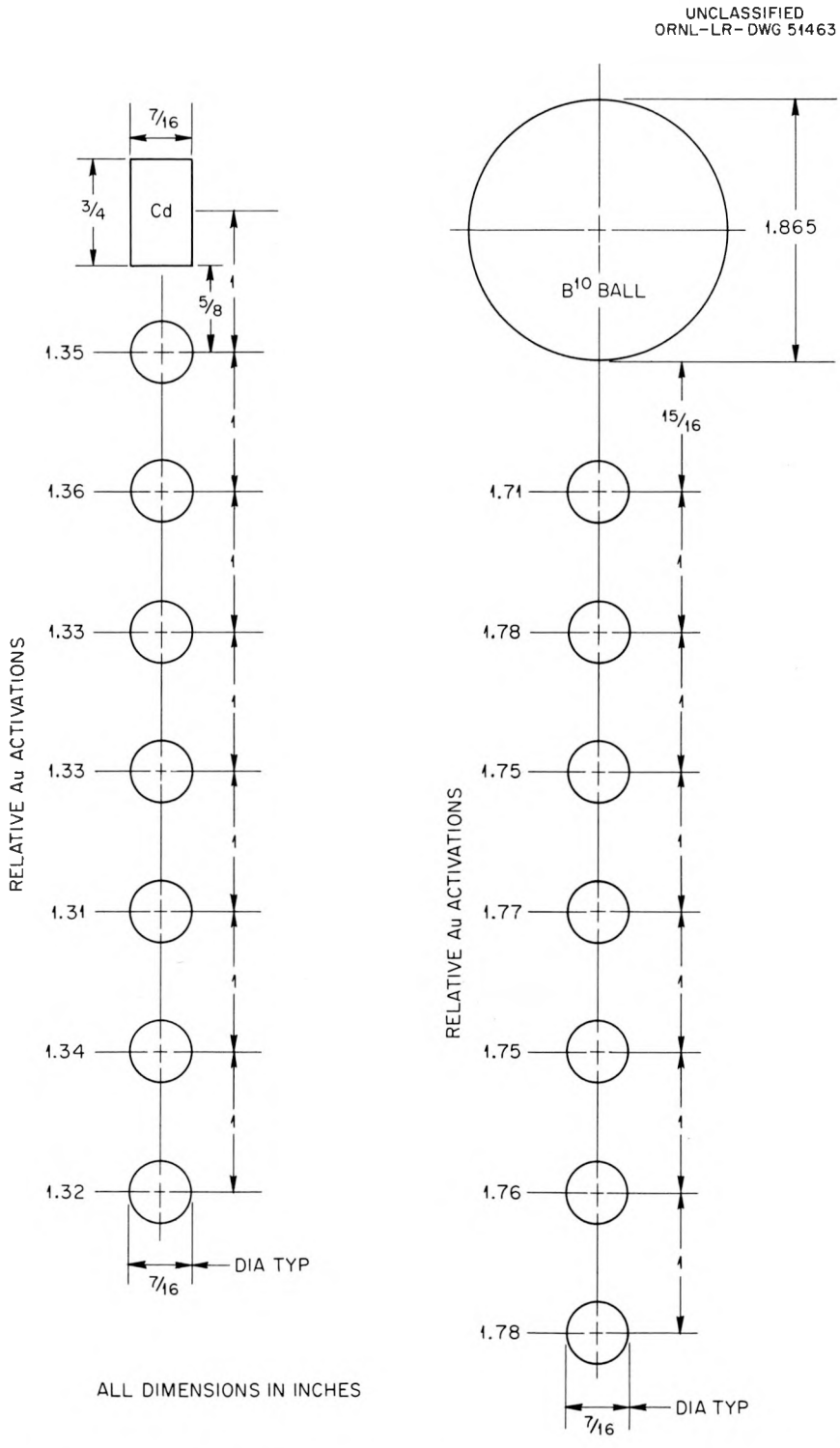

Fig. 3.24. Effect of Thermal Flux Depression Near B^{10} Balls and Cadmium.

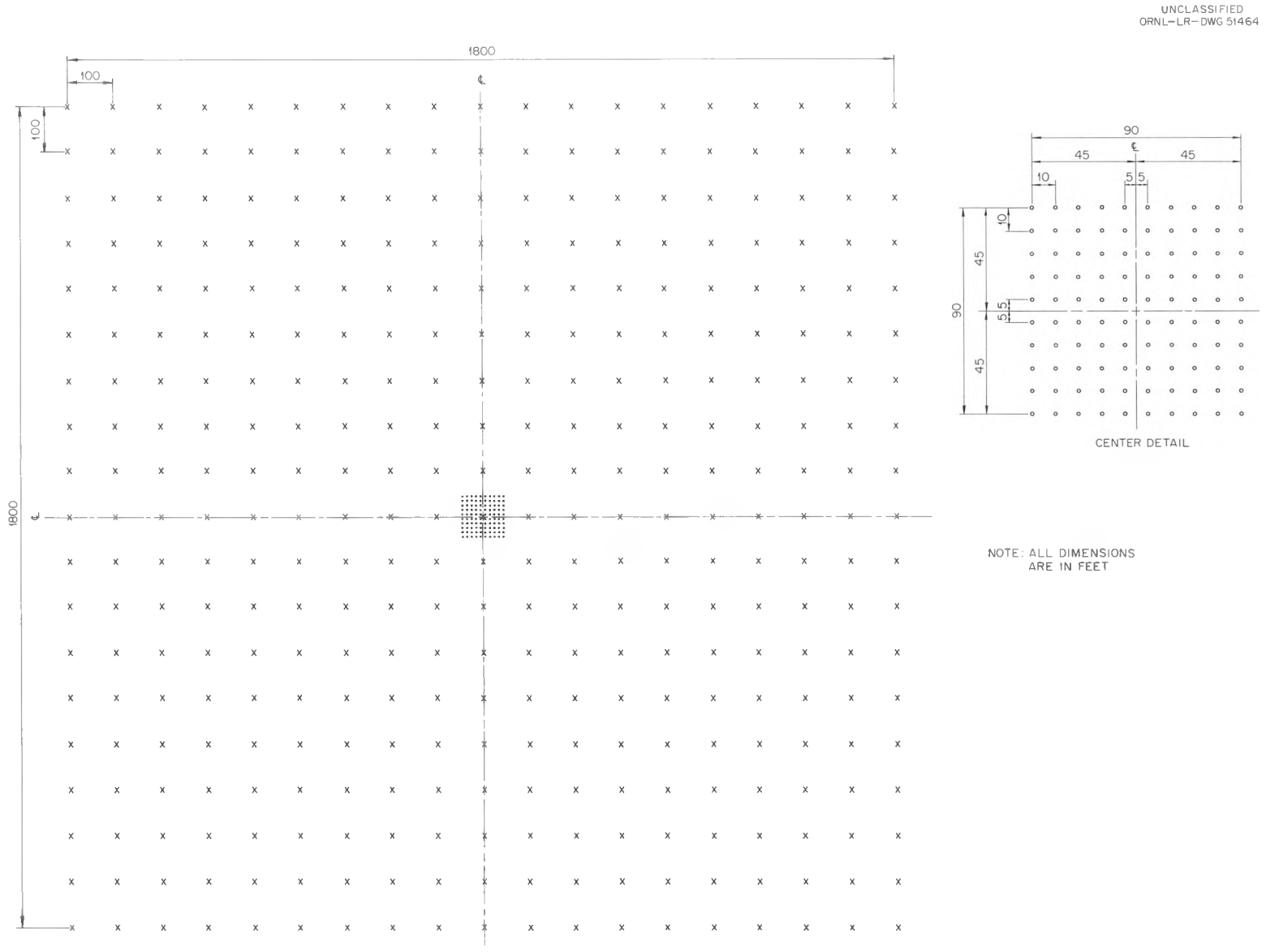

Fig. 3.25. Extended Source Calibration Area Grid.

DOSIMETRY APPLICATIONS

J. A. Auxier

J. C. Ashley[47]
C. H. Bernard[47]
J. S. Cheka
D. W. Forester[47]
A. L. Frank[47]
R. Goodman
W. E. Kiker[47]
T. Ishihara[48]
W. W. Ogg
F. W. Sanders
W. H. Shinpaugh, Jr.
T. D. Strickler[47]
J. H. Thorngate

Dosimetric Investigation of the Yugoslav Radiation Accident

On October 15, 1958, a nuclear radiation accident occurred at the Boris Kidrič Institute near Belgrade, Yugoslavia. Six persons received gross doses of neutrons and gamma rays. Five of these were given bone-marrow transplants at the Curie Hospital in Paris; one of the five died. The number of persons exposed and the type of treatments given increased the importance of determining the radiation exposures.

After the accident the reactor was not molested and remained in essentially the same condition as at the time of the accident until early in 1960, although the heavy water had been removed from the storage tank for use in another reactor.

The reactor consists of a heavy-water-moderated lattice of natural uranium rods of about 2.5-cm diameter encased in aluminum. The fuel rods are about 2 m in length and form a uniform vertical array suspended in a cylindrical aluminum tank 2 m in diameter as shown in Fig. 3.26.

To obtain the radiation exposures of the six individuals, the following general approach was taken: (1) Measurement of the gamma exposure doses at the points of interest, (2) measurement of the first-collision neutron doses at the points of interest, (3) measurement of the gross neutron spectrum, and (4) measurement of the blood sodium activation per unit fast-neutron dose. With the neutron-to-gamma dose ratios measured, and the individual neutron dose determined by the sodium activity, the total dose could be calculated. Fortunately, the sodium activation had been measured after the accident; the six persons were

---

[47]Summer employee.

[48]Alien guest from the Japan Atomic Energy Research Establishment, Tokai-Mura, Japan.

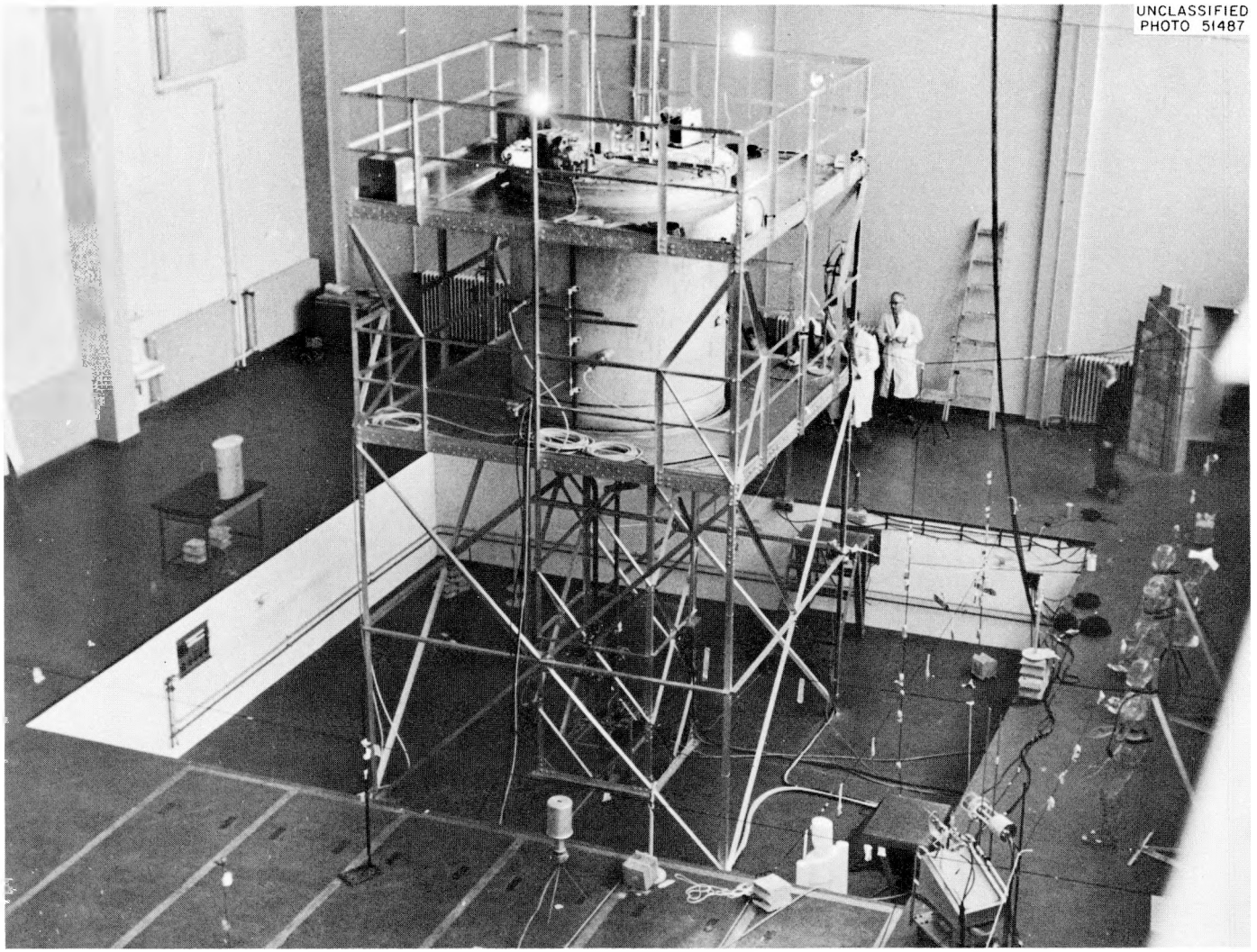

Fig. 3.26. General View of the Boris Kidrič Reactor.

flown to Paris and the measurements made there. The blood sodium activation was evaluated by using plastic-shell phantoms filled with NaCl solution.

Although the final results of the experiments cannot be given until the results of the cross-calibration checks have been completely analyzed, some of the important data can be discussed. Table 3.2 shows a comparison of the flux from the Boris Kidrič reactor and that from the assembly involved in the Y-12 excursion as measured by the various threshold detectors. Except for the thermal component, the spectrum is an insensitive function of position. Figure 3.1 shows the "adopted" spectrum used in the dose calculations; this calculated spectrum agrees well with the threshold-detector results except for the thermal component. Thermal-neutron fluxes were measured at the points of interest because of the sensitivity of the flux to geometry. The calculation of this spectrum is discussed in the Theoretical Physics of Dosimetry section (Chap. 3). The ratio of gamma dose to neutron dose is shown in Table 3.3 for several typical points.

Blood Na^{24} Evaluation Studies

Analyses of Na^{24} in the blood of persons exposed to nuclear accidents have been used[49] and recommended[50] as a tool in neutron dosimetry.

---

[49] Accident Radiation Excursion at the Y-12 Plant, Y-1234 (June 16, 1958).

[50] G. S. Hurst and R. H. Ritchie (eds.), Radiation Accidents: Dosimetry Aspects of Neutron and Gamma-Ray Exposures, ORNL-2748A (Nov. 2, 1959).

Table 3.2. Comparison of Neutron Spectra (Relative Flux Intensities for the Various Threshold Detectors) for Two Critical Assemblies

Threshold Detector	Boris Kidrič (ZPR)			Y-12 Excursion
	Station 1	Station 9	Station 10	
Pu	1.00	1.00	1.00	1.00
Np	0.36	0.35	0.35	0.89
U	0.20	0.18	0.19	0.54
S	0.094	0.088	0.090	0.25
Au	3.91	3.63	3.87	0.45

Table 3.3. Experimentally Determined Gamma-to-Neutron Dose Ratios for Various Positions near the Boris Kidrič Reactor

Position	Neutron Dose per Unit Monitor (rad neutron^{-1} cm^2)	D_γ/D_n
	$\times 10^{-6}$	
1	1.01	3.9
2	0.80	4.0
3	0.67	4.1
3a	0.59	4.3
4	0.57	4.2
8	0.48	4.0
9	0.76	4.5
10	0.64	4.7

However, further research was indicated in order to define better the range of application of the technique and the factors influencing the accuracy of results obtained by its use. The analysis of various parameters affecting the activation of Na^{23} to Na^{24} in the body can most conveniently be made by utilizing phantoms. However, before the use of a phantom could be justified it was necessary to show that a homogeneous phantom could be substituted for a live animal in these studies. Consequently, an experiment was conducted using the Los Alamos Godiva II Reactor to determine the stability of homogeneous phantoms in these studies. A burro and a phantom containing an aqueous NaCl solution were irradiated, sampled, and compared. To avoid the difficulty of constructing a phantom of the exact size and shape of a particular animal, in this case the burro, the following procedure was used. A burro with its legs folded and tied was placed in an aluminum tank as shown in Fig. 3.27. The tank was filled with an aqueous NaCl solution and the tank and burro were exposed to neutrons from the Godiva II reactor. Samples of the burro blood serum and the NaCl solution were taken, and the Na^{24} concentrations were determined by using a scintillation counter. For a

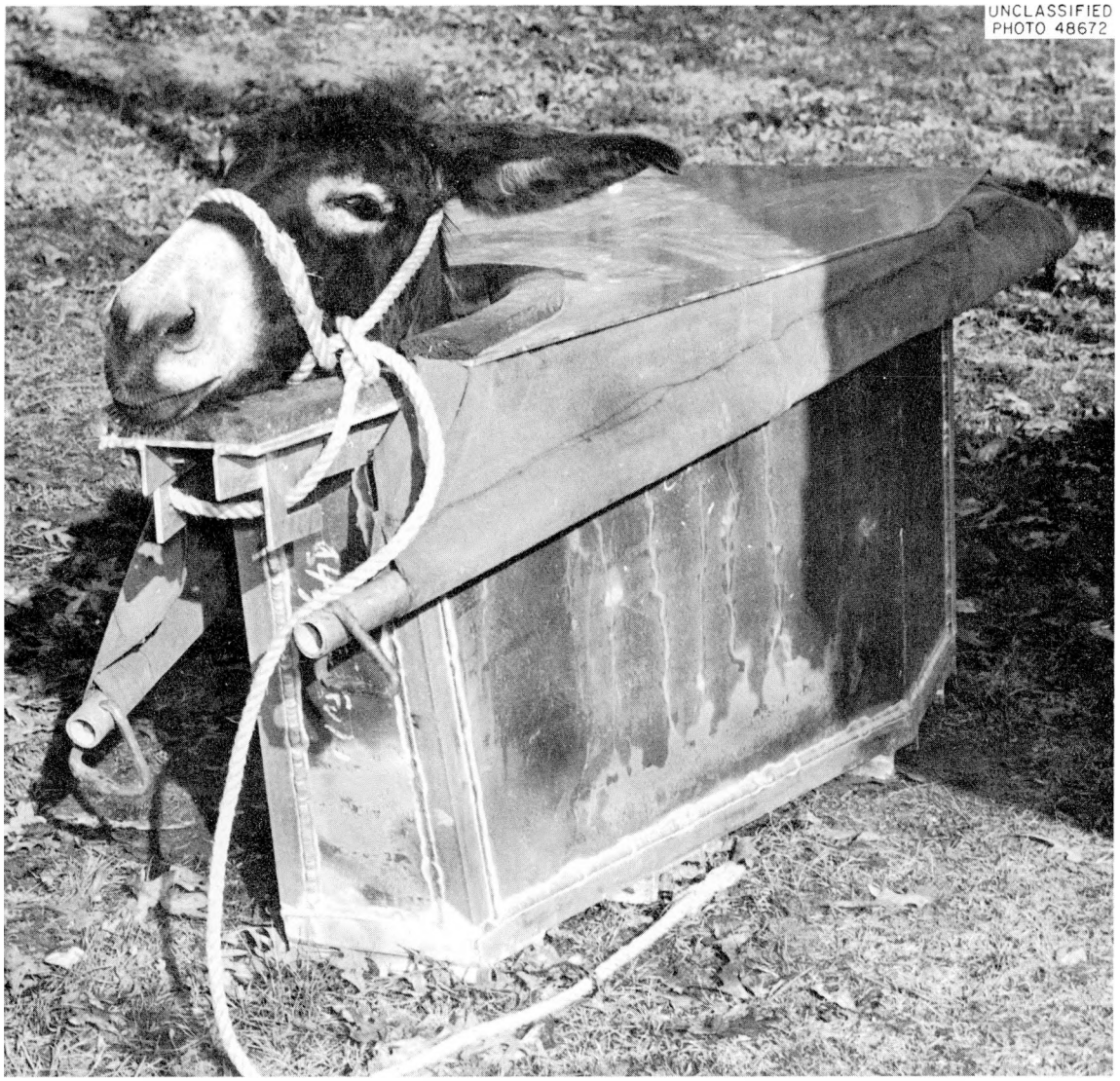

Fig. 3.27. Burro Submerged in Solution of NaCl Used in Phantom Studies.

second irradiation the tank was filled with NaCl solution and irradiated in the same position as in the first exposure. The irradiation exposure was determined by threshold detectors and by a secondary monitor of the flux. The tank can be considered to contain two regions. In the first irradiation, one region was occupied by the burro and the other region occupied by the NaCl solution around it. In the second irradiation, the regions were the same in size, shape, and location as in the first irradiation; however, they were both occupied by NaCl solution. Each region contained the same number of sodium atoms in each exposure. In

the outer region the distribution of sodium was homogeneous in both exposures; the sodium distribution in the inner region was heterogeneous in the first exposure and homogeneous in the second. The ratio of Na^{24} to Na^{23} was determined for each region in the first exposure and for the average (by stirring) of the two regions in the second exposure. The ratios of the concentrations from the first exposure were weighted by the volumes of the regions and averaged, and the resulting concentration ratio was compared with the concentration ratio determined for the second exposure. The difference between the two average ratios (approximately 3%) is less than the experimental error, and from this it was assumed that a phantom with a homogeneous distribution of sodium can be used to approximate an animal for this type of study.

Further studies were conducted using plastic-shell phantoms of human size which are commercially available.[51] These compartmented phantoms are constructed to represent the mean size of U.S. Air Force personnel, measure 5 ft 9 in. tall, and, when filled with tissue-equivalent material, weigh 162 lb. For these experiments the compartments were filled with an NaCl solution and the Na^{24}-to-Na^{23} ratio was determined as a function of fast-neutron dose for each of the compartments. A second phantom constructed of ten circular and elliptical cylindrical bottles was also used. Measurements of the effect of orientation on the sodium activation were made with these phantoms. All exposures were made with the centers of the phantoms 3 m from the center of the reactor and with the midline of the phantom at the same height above the floor as the reactor. The average sodium activation in these phantoms exposed under these conditions was 15% less when the side of the phantom was toward the reactor than when the phantom faced the reactor.

Various cylindrical phantoms were also exposed to neutrons from the Godiva reactor in order to determine approximately the effect of phantom size on sodium activation. These data are shown in Fig. 3.28.

A second experiment at the Godiva assembly involved the exposure of several burros from which blood samples were taken and analyzed for sodium activation. As the burro weights ranged from approximately 300 lb

---

[51]These phantoms were developed by W. Langham, LASL, in conjunction with Alderson Research Associates, Inc., Long Island, N.Y.

to almost 500 lb, a determination of the sodium activation as a function of burro weight was possible. Figure 3.29 is a plot of body weight vs Na^{24} concentration.

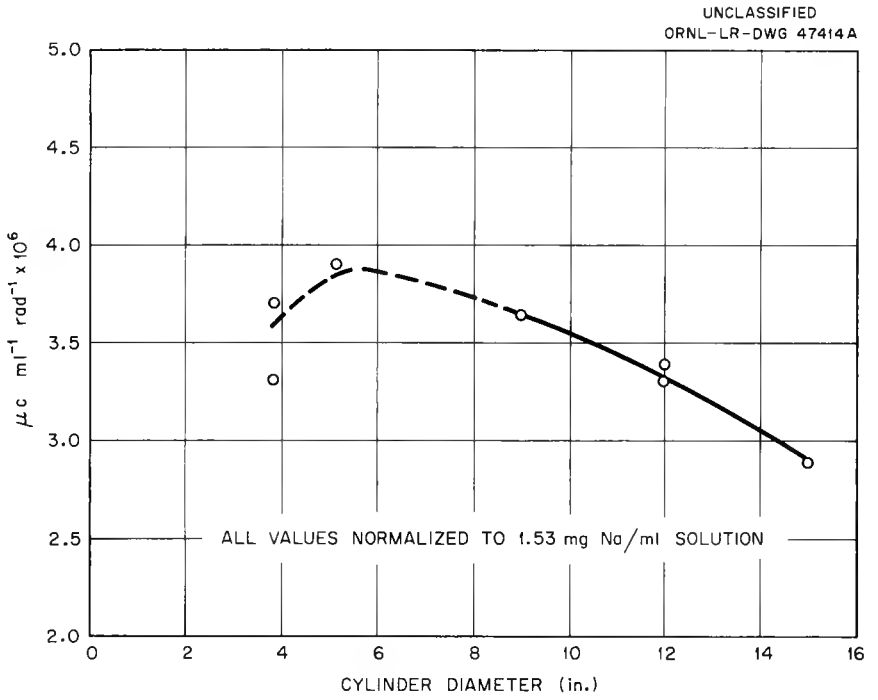

Fig. 3.28. Sodium-24 Concentration in Cylinders of Aqueous Solution of NaCl as a Function of Diameter.

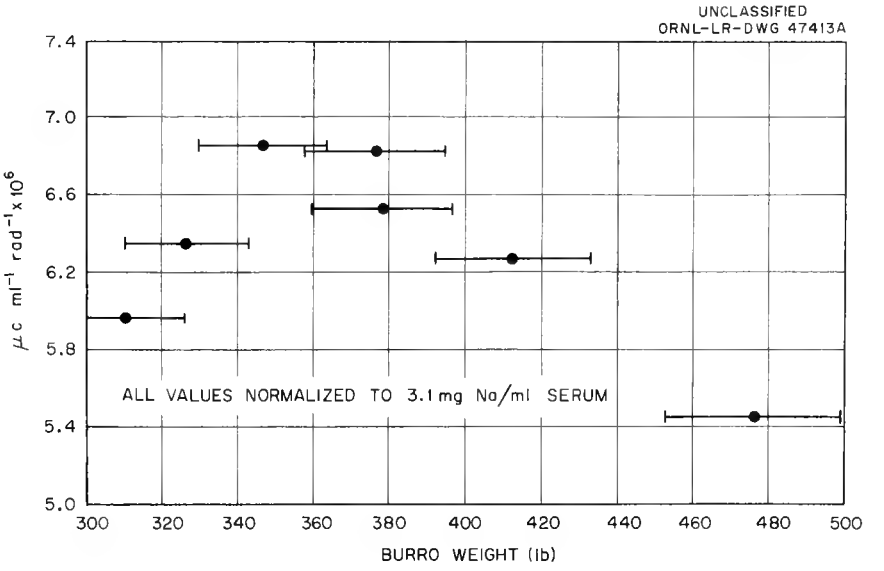

Fig. 3.29. Sodium-24 Concentration in Blood Serum from Burros Exposed to Radiation from Godiva II as a Function of Weight.

Experimental Evaluation of the Radiation Fallout Protection Afforded by Typical Oak Ridge Houses

The protection afforded against a simulated fallout radiation has been experimentally evaluated for nine typical houses in the Oak Ridge area.[52] This experiment, in support of the AEC community self-protection program, supplemented work done under more controlled but less typical conditions.[53-55] Houses were chosen to represent a variety of construction materials, topographical conditions, and sizes, and included three types of Oak Ridge cemesto houses, two wood frame houses, and one concrete block house with a basement fallout shelter. The protection factor (ratio of open-field exposure dose rate to exposure dose rate in the house) in all of these houses ranged from 2 to 5 on the main floor and from 5 to 30 in the basement, except in the basement fallout shelter where the protection factor was greater than 100.

All the basements in which measurements were made had at least part of one wall and some windows exposed above ground level, and most of the radiation exposure dose inside these basements entered through these walls and from sources on the roofs. Generally, the dose rate in the basements of wood frame houses would be greater by a factor of about 2 for basements with one exposed wall than for buried basements.

The data obtained in the Oak Ridge experiments can be compared with measurements made under more controlled conditions in Nevada.[53] The protection factors on the main floor are higher, in general, than those measured in Nevada for single-story structures. This can be attributed

---

[52] T. D. Strickler and J. A. Auxier, Experimental Evaluation of the Radiation Protection Afforded by Typical Oak Ridge Homes Against Distributed Sources, CEX-59.13 (Apr. 14, 1960).

[53] J. A. Auxier et al., Experimental Evaluation of the Radiation Protection Afforded by Residential Structures Against Distributed Sources, CEX-58.1 (Jan. 19, 1959).

[54] C. Eisenhauer, Analysis of Experiments on Light Residential Structures with Distributed Co^{60} Sources, NBS-6539 (Oct. 15, 1959).

[55] E. T. Clark, J. F. Batter, Jr., and A. L. Kaplan, Measurement of Attenuation in Existing Structures of Radiation from Simulated Fallout, TO-B 59-4 (Apr. 27, 1959).

to several factors. The houses are built, generally, with higher foundations, and the source locations were limited to within approximately 20 ft of the house, resulting in greater attenuation by foundation walls. In addition, the Oak Ridge homes were fully furnished. The basement protection factors are generally less than those measured in Nevada. This is attributed to the fact that the Oak Ridge houses are on sloping lots and the basements are partially or totally above ground on at least one side.

PHYSICS OF TISSUE DAMAGE

R. D. Birkhoff

J. G. Carter D. R. Nelson

Low-Temperature Thermoluminescence of Amino Acids and Proteins

One measure of the effect of ionizing radiation on proteins and their constituent amino acids is their ability to emit light after gamma irradiation. The catalytic capability of those proteins possessing enzymatic function presumably depends upon a small number of amino acid side chains at the surface of the enzyme which are maintained in the requisite configuration by the secondary and tertiary bonding in the molecule. It was first suggested by L. G. Augenstine[56,57] that radiation possibly destroys enzymatic activity by disrupting the essential configuration of the molecule. According to Augenstine, for inactivation to proceed a restricted, but specific, portion [a group of bonds known collectively as a "weak link," which includes disulfides (S-S) and a limited number of other intramolecular bonds and is presumably involved in maintaining the unique topography of the active site] of the enzyme configuration must be disrupted. For this disruption to occur it was postulated that the energy from ionizing radiation must move from the site of initial absorption and become preferentially localized in the weak link. It is presumed that an

---

[56]L. G. Augenstine, p 119–24 in Information Theory in Biology (ed. by H. Quastler), University of Illinois Press, Urbana, 1953.

[57]L. G. Augenstine, p 287 in Symposium on Information Theory in Biology (ed. by H. P. Yockey), Pergamon Press, London, 1958.

extensive sequence of events may be involved between absorption and localization.

In some materials it is possible to arrest this sequence. With appropriate experimental control, such as the irradiation at low temperature used in this study, some of the metastable products involved in the sequence can be investigated.

It is known that proteins yield amino acids upon hydrolysis; that the amino acids are at least in large part joined to each other in the vast protein molecule by peptide linkage; that many of the same amino acids have been isolated from widely different proteins; and that in many proteins, and even in certain enzymes and hormones, there is no evidence that the proteins are constituted of any elements of structure other than amino acids. In previous work[58] it was found that both proteins and amino acids which are irradiated at liquid-nitrogen temperature exhibit thermoluminescence. Preliminary calculations, however, indicated that the thermoluminescence from the enzyme trypsin was not simply a properly normalized composite of that arising from its constituent amino acids in the isolated crystalline form. Thus, one aim of this research was to investigate experimentally this possibility for three proteins in addition to trypsin.

In the previous work[58] the occurrence of ring structures in the chemical makeup of an amino acid increased the thermoluminescence by a factor of as much as 10^4 over "nonring" amino acids. Thus a second aim of this research was to evaluate the relative importance of crystalline structure and chemical makeup as factors determining the thermoluminescence from irradiated amino acid samples.

Glow Curves from Proteins and Corresponding Amino Acid Mixtures

The glow curves from trypsin, chymotrypsin, chymotrypsinogen, and insulin[59] are shown by the dashed lines in Fig. 3.30. Portions of the

---

[58]L. G. Augenstine et al., Radiation Effects at the Macromolecular Level (to be published).

[59]Samples of insulin were supplied by W. W. Davis, Director of the Physiochemical Research Division, Lilly Research Laboratories, Eli Lilly and Co.

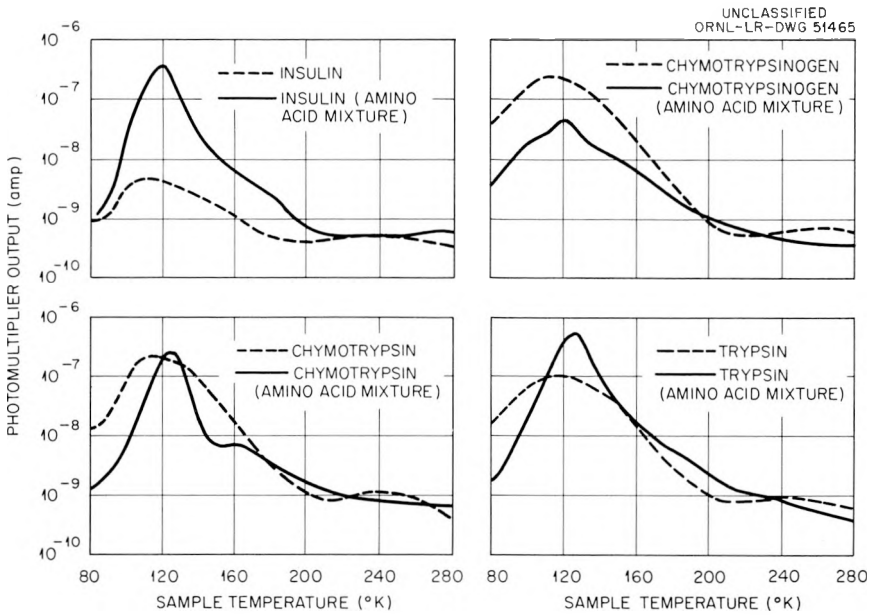

Fig. 3.30. Composite Glow Curves of Four Proteins and Their Corresponding Amino Acid Mixtures.

various constituent amino acids were carefully pulverized and blended according to their percentage (by weight[60]) composition.[61] The glow curves from these mixtures are shown by the solid lines in Fig. 3.30. If one neglects any possible effects of impurities on the glow curves these results indicate that the thermoluminescence from a protein is not the sum of the glow curves for its constituent amino acids. This means that although the gamma radiation interacts with electrons in the crystal essentially at random, the displaced electrons and associated holes do not become trapped and bound at random. This preferential localization is in accord with features of the weak-link hypothesis discussed previously.

Amino Acid Glow Curves

Glow curves for powdered L-amino acid preparations were found to have a number of peaks in the temperature range examined (77 to 273°K). The glow curves of the 23 amino acid preparations can be separated roughly

---

[60]R. J. Block and K. W. Weiss, p 294 in Amino Acid Handbook, Thomas, Springfield, Ill., 1956.

[61]Samples of insulin (amino acid mixtures), chymotrypsinogen (amino acid mixtures), and chymotrypsin were supplied by A. D. McLaren, College of Agriculture, University of California.

into two categories. The first group (see Fig. 3.31) contains L-tyrosine, L-tryptophan, L-histidine-HCl-H_2O, and L-phenylalanine. The first three have one predominant peak in the range 100 to 137°K, with maximum intensities of approximately 10, 3, and 0.3 μa, respectively, and activation energies ranging from 0.130 ev for L-histidine-HCl-H_2O to 0.517 ev for L-tyrosine. L-Phenylalanine has two peaks with maximum intensities of 0.6 μa at 125 and 137°K, with activation energies of 0.300 and 0.213, respectively. The remaining amino acids (see Figs. 3.32–3.34) constitute a second group whose maximum intensities are much less than the above listed values and whose activation energies vary from 0.020 ev for L-threonine to 0.267 ev for L-cysteine-HCl-H_2O. The majority of the amino acids in this group have peaks in the range 160 to 170°K and/or between 100 and 110°K. The maximum intensities of the peaks in this second group range from a low of 0.0002 μa for glycine and a few others to a high of 0.053 μa for L-hydroxyproline.

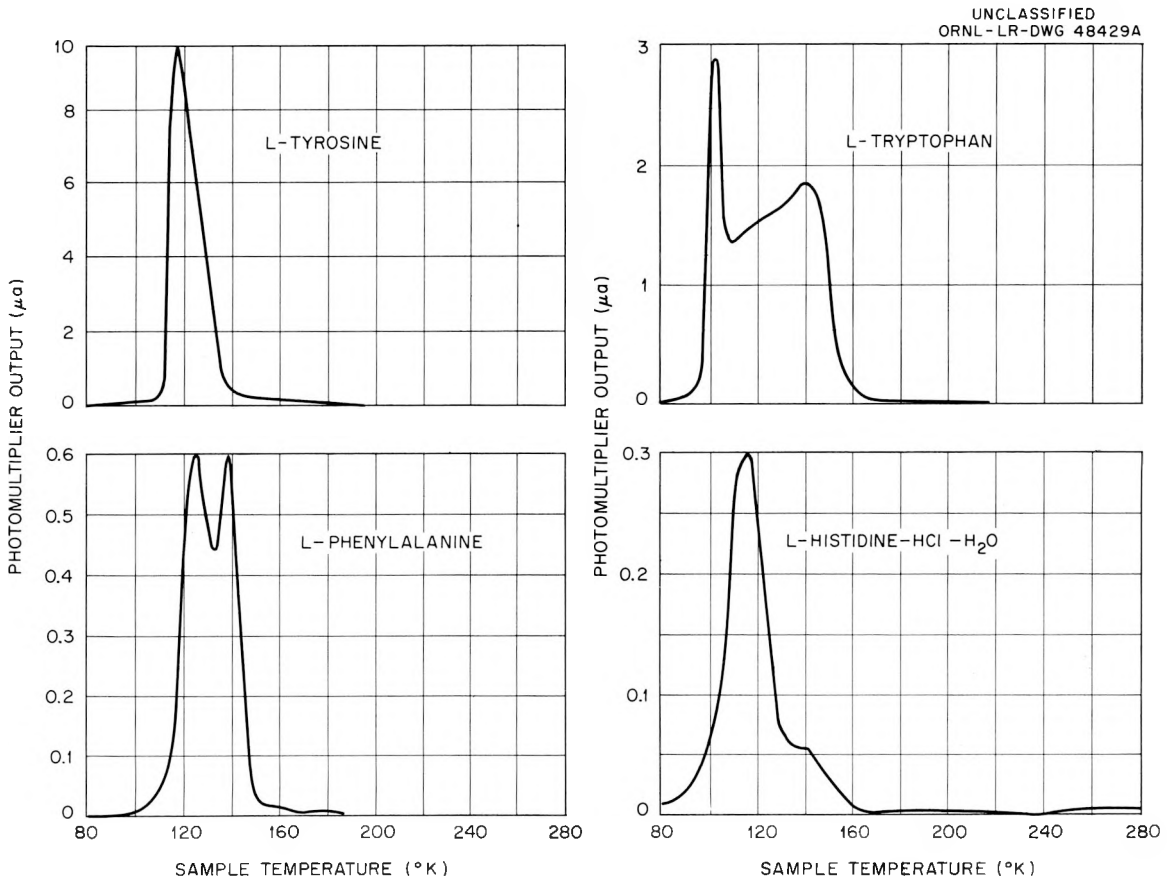

Fig. 3.31. Composite Glow Curves of Ring Structure Containing Amino Acids.

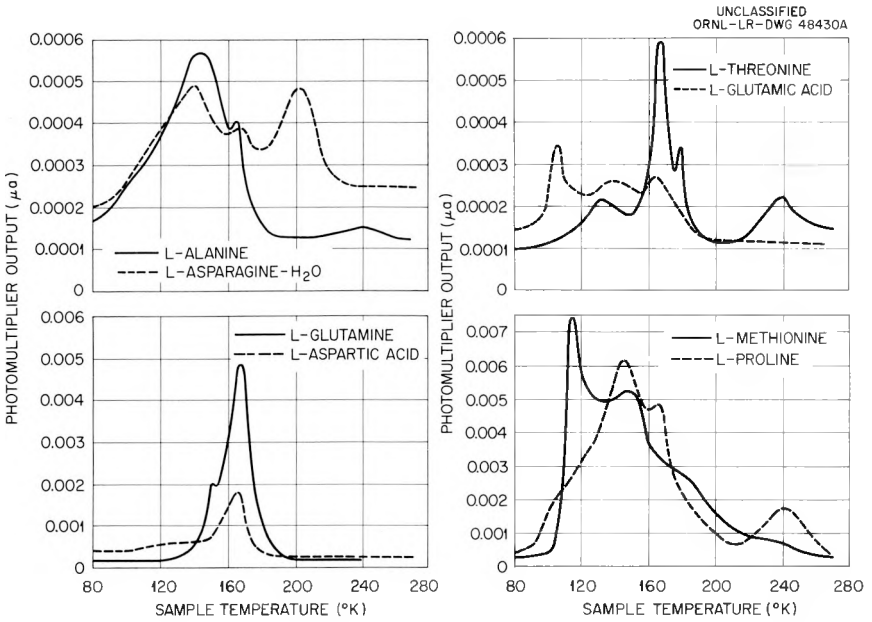

Fig. 3.32. Composite Glow Curves of the Amino Acids Belonging to the Orthorhombic and Monoclinic Crystalline Systems.

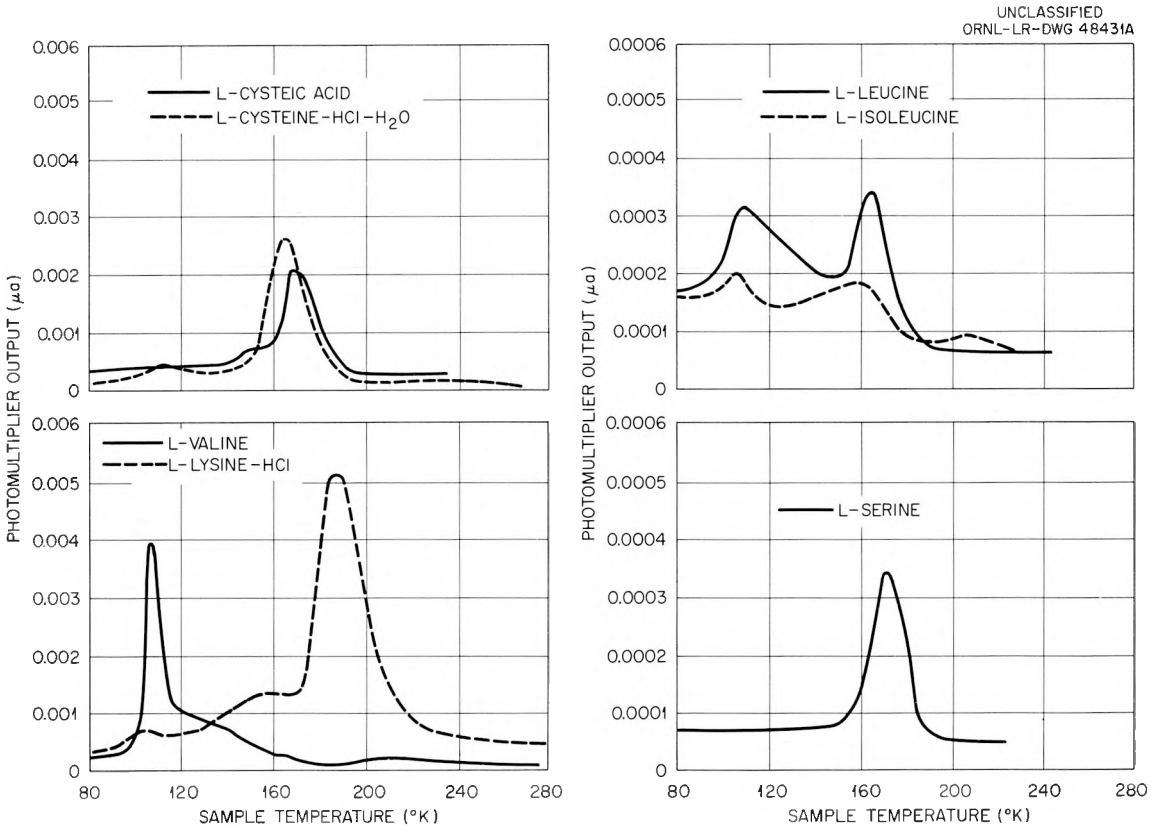

Fig. 3.33. Composite Glow Curves of Low-Intensity Amino Acids.

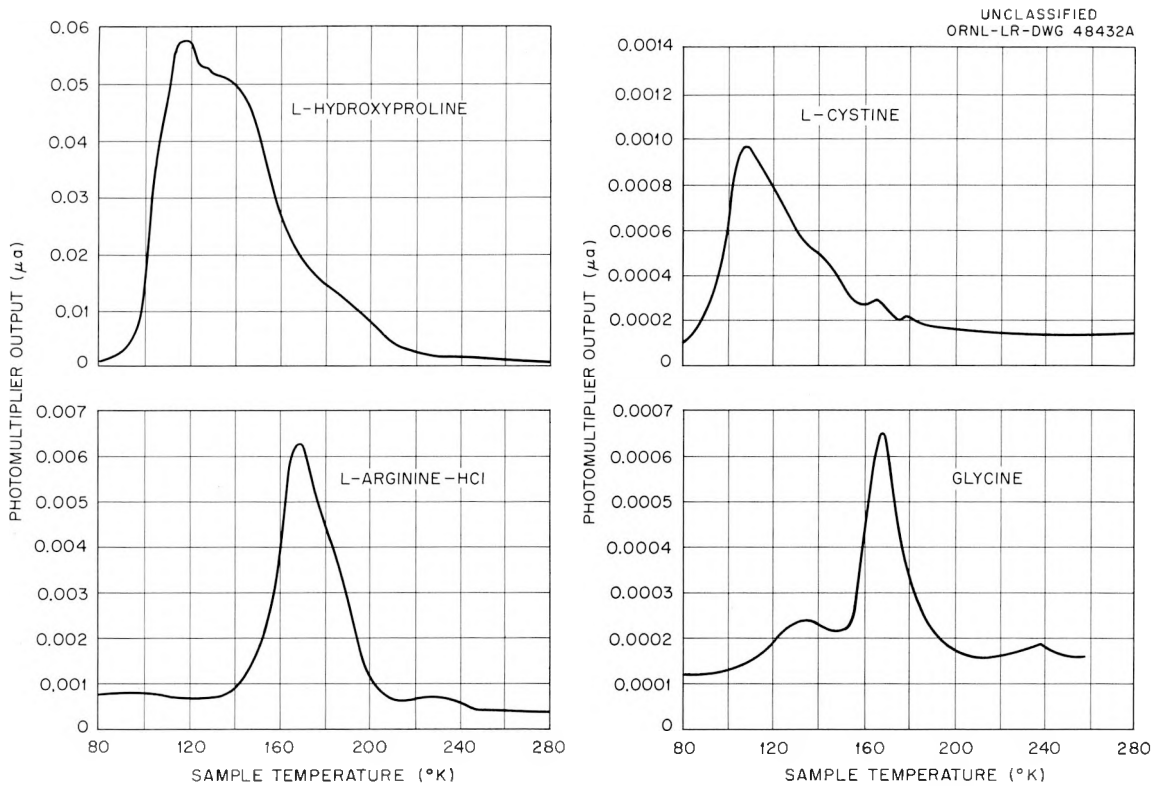

Fig. 3.34. Composite Glow Curves of Four Remaining Amino Acids.

The most intense peaks seem to be associated with ring structures. This possibly may be correlated with the fact that these compounds are those most readily destroyed when proteins are irradiated.[58] Correspondingly, the low-intensity peak at about 165°K may be associated with the aminoacetic acid backbone common to all amino acids. A very remote possibility which can seemingly be ruled out is the effect of ice. With the present experimental methods ice has a glow curve consisting of one major peak at 163°K with an intensity of 0.003 μa, and an activation energy of 0.314 ev. Thus, for the very small water contents expected in the protein and amino acid samples, the contribution to the glow curves from ice should be negligible. The present results with ice differ slightly from the results obtained by Grossweiner and Matheson[62] who found a peak at 156°K and an activation energy of 0.32 ev. However, they used purer water and a greatly different freezing technique.

---

[62]L. I. Grossweiner and M. S. Matheson, J. Chem. Phys. 22, 1514 (1954).

Effect of Crystalline Structure on the Glow Curves of Amino Acids

The importance of a ring structure, that is, chemical composition, in determining the nature of the glow curve is pointed out in the section above. If the glow curves were wholly or in part due to the crystalline structure of the materials, then it would seem that there should be a repetition of peaks in the glow curves of amino acids belonging to the same crystalline system.

Crystallographic data for ten amino acids are included in Table 3.4. From an examination of this table and the corresponding plots in Figs. 3.31, 3.32, and 3.34, it is apparent that the eight amino acids belonging to the orthorhombic system with a primitive unit cell containing four molecules and space group $P2_12_12_1$ do not have closely related glow curves. In fact, the most striking result is that the peak intensities vary by as much as a factor of 10^3 within this group. This seems to be conclusive evidence that chemical composition is much more important than crystalline structure in determining thermoluminescence.

Two peaks, however, are observed most frequently: one at approximately 165°K appears in all but L-hydroxyproline and L-histidine-HCl-H_2O,

Table 3.4. Crystallographic Data for Ten Amino Acids

Amino Acid	Crystalline System	Molecules per Unit Cell	Space Group
L-Alanine	Orthorhombic	4	$P2_12_12_1$
L-Asparagine-H_2O	Orthorhombic	4	$P2_12_12_1$
L-Aspartic acid	Monoclinic	4	$P2_1$
L-Cystine	Hexagonal	6	$P6_1$
L-Glutamic acid	Orthorhombic	4	$P2_12_12_1$
L-Glutamine	Orthorhombic	4	$P2_12_12_1$
L-Histidine-HCl-H_2O	Orthorhombic	4	$P2_12_12_1$
L-Hydroxyproline	Orthorhombic	4	$P2_12_12_1$
L-Proline	Orthorhombic	4	$P2_12_12_1$
L-Threonine	Orthorhombic	4	$P2_12_12_1$

the other at approximately 140°K is present in all of the eight but L-glutamine, L-proline, and L-threonine. However, this also does not appear to be a property of the orthorhombic crystalline system per se. As has already been stated in the previous section, the peak at approximately 165°K appears in most of the amino acids investigated, and may be associated with the aminoacetic acid backbone. For example, L-cystine and L-aspartic acid, which belong to the hexagonal and monoclinic systems and whose space groups are $P6_1$ and $P2_1$, respectively, also exhibit this 165°K peak (see Table 3.4).

Role of the Level of Purity

It is known that small amounts of impurities greatly affect the luminescence of many inorganic solids.[63] Ghormley and Levy[64] found that impurities had a large effect on the magnitude and spectral distribution of the emitted light, although the temperatures and relative heights of the glow curve peaks were not significantly affected. For example, glow curves obtained from air-grown and vacuum-grown single crystals of LiF were quite different above room temperature, but below room temperature were the same with respect to the temperature and relative heights of the peaks, although the vacuum-grown crystals gave a tenfold greater light emission throughout the temperature range. This difference in output was attributed to the quenching action of the impurities in the air-grown crystals. Their observations led them to conclude that impurities did not significantly affect the glow curves of the ionic crystals they studied, in the temperature range 77°K to room temperature.

The effect of impurities could be studied by adding controlled amounts of known impurities or by purification to decrease the concentration of foreign materials. Instead of either of these methods, studies of the thermoluminescent properties of samples having different purities and from more than one supplier have been compared.

The glow curves obtained from the purest grade of amino acids from the California Corporation for Biochemical Research and Mann Research

---

[63]J. K. Rieke, J. Phys. Chem. 61, 633 (1957).

[64]J. A. Ghormley and H. A. Levy, J. Phys. Chem. 56, 548 (1952).

Laboratories, Inc., did not exhibit any appreciable differences in the maximum intensities and values of T' (temperature at which maximum intensity occurs) for L-histidine-HCl-H_2O and L-phenylalanine – both from the high-intensity group. However, there was a significant difference in the low-intensity amino acids, L-aspartic acid and L-alanine. Glow curves for L-aspartic acid and L-alanine showing the difference between samples from the two suppliers are presented in Fig. 3.35. With L-aspartic acid the intensities differ by a factor of about 10, and with L-alanine the shapes of the curves are different.

Another comparison was made between the glow curves obtained from samples having the highest purity commercially available and those having

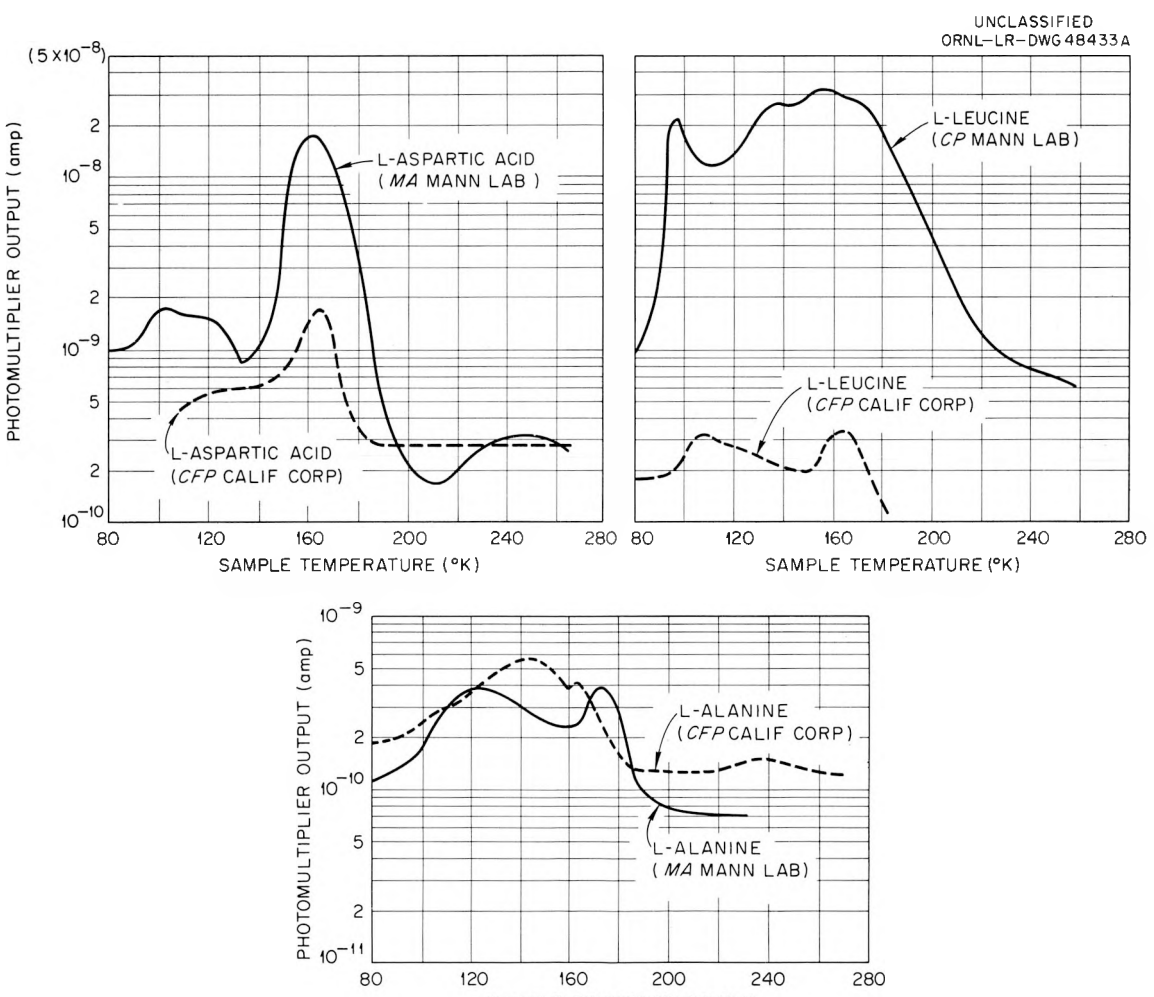

Fig. 3.35. Composite Glow Curves Showing Effect of Sample Purity.

a somewhat lower grade of purity of the following three amino acids: L-histidine-HCl-H_2O, L-tryptophan, and L-leucine. Of these, only L-leucine showed a striking difference. In Fig. 3.35 the glow curves for the two different grades of purity of L-leucine are presented. There is a hundredfold difference between the maximum intensities, and again the shape of the curve is changed. It is interesting to note that the properties of the glow curves from the high-intensity group (L-histidine-HCl-H_2O, L-phenylalanine, and L-tryptophan) seem less dependent on the purity of the samples than those from the low-intensity group (L-aspartic acid, L-alanine, and L-leucine).

4. INTERNAL DOSIMETRY

W. S. Snyder

ESTIMATION OF INTERNAL DOSE

Short-Term Exposure

W. S. Snyder

The estimation of dose to man from radioactive materials taken into the body is necessary for the protection of those occupationally exposed to such materials and also for other population groups that may be exposed. The Internal Dosimetry Section has worked closely with the ICRP and NCRP on these problems in the past and also has been called upon to participate in the current work of the Federal Radiation Council (FRC). One member of the section has been on assignment with Temporary Staff II of the FRC during part of this year while the second report is in preparation.

The dose in various organs must be estimated for short-term exposure and for continuous exposure to various radionuclides. The first report of the FRC has emphasized the importance of the maximum dose within a population, and the Internal Dosimetry Section is analyzing the data available on the distribution of trace elements in humans in order to obtain the variability of 48 isotopes with respect to age, sex, diet, and other factors. It has been found that f_2, the fraction of body burden in the critical tissue, seems to show a smaller variance among individuals than do the tissue concentrations. These preliminary indications are being analyzed to obtain confidence limits on the range of this parameter.

The dose from a short-term exposure, or from a single intake of radioactive material, has been estimated and compared with the dose from continuous exposure to the same material. It is found that if a continuous exposure level is set so that after 50 years of ingestion at this level the critical organ is exposed at a dose rate of R rems per quarter, then a single intake equal in amount to that ingested during a quarter of continuous exposure will deliver a total dose of R rems to the same organ during the 50 years immediately following the single ingestion. This simple rule provides a basis for interpreting the recommendations concerning single dose that have been given previously by the ICRP. The further study

of this problem is directed toward estimates for dose during shorter periods of time, which thus may be useful in assessing emergency situations.

Nonlinear Curve Fitting

B. R. Fish

W. S. Snyder C. F. Taylor

A method, called the fractionator, for fitting certain classes of nonlinear curves has been developed and is under study to define its convergence properties. One type of function that can be fitted by using this method is the linear combination of exponentials, $y = \sum_i a_i e^{-\alpha_i t}$, which is of wide use in the nuclear field. This form is of special interest to health physicists since many important processes may be represented by such a function, for example, radioactive decay of a mixture of isotopes or biological elimination of an internally deposited radionuclide. Bernard et al.[1] attempted to fit sums of exponentials to human excretion data and they found that the Deming method[2] and the Garwood method[3] were unstable and that Householder's modification[4] of Prony's method[5] did not yield tenable estimates of the parameters.

The fractionator, an iterative method, was derived by Fish[6] and may be described as follows: Let

$$Y_j = \text{the set of observed values} \quad , \tag{1}$$

and assume that, on the basis of an a priori model, a function,

$$y = \sum_i f_i(a_i, b_i, c_i, \ldots ; X) = \text{the true values} \quad , \tag{2}$$

may be chosen for which it is desired to derive an estimate of the parameters, a_i, b_i, c_i, etc. By choosing initial estimates for the parameters,

---

[1]S. R. Bernard et al., Fitting Linear Combinations of Exponentials to Human Uranium Excretion Data, ORNL-2364 (Dec. 26, 1957).

[2]W. E. Deming, Statistical Adjustment of Data, p 128–41, Wiley, New York, 1946.

[3]F. Garwood, Biometrika 32, 46–58 (1941).

[4]A. S. Householder, On Prony's Method of Fitting Exponential Decay Curves and Multiple-Hit Survival Curves, ORNL-455 (Sept. 19, 1949).

[5]E. T. Whittaker and G. Robinson, The Calculus of Observations, p 369–71, Blackie and Sons, London and Glasgow, 1944.

[6]B. R. Fish et al., H-P Ann. Prog. Rep. July 31, 1957, ORNL-2384, p 2.

and evaluating Eq. (2) for each X_j, a set of calculated values may be derived. Thus,

$$y_j = \sum_i f_i(a_{0i}, b_{0i}, c_{0i}, \ldots ; X_j) = \text{the initial calculated values} \quad . \quad (3)$$

Define

$$y_{ij} = f_i(a_i, b_i, c_i, \ldots ; X_j) = \text{the ith "subfunction" of } y_j \quad , \quad (4)$$

and

$$Y_{ij} = \text{the "subset of observed values" (subdata point) associated with } y_{ij} \quad , \quad (5)$$

such that

$$Y_j = \sum_i Y_{ij} \quad . \quad (6)$$

Then

$$\epsilon_j = Y_j - y_j = \text{error in } Y_j \text{ with respect to calculated values, } y_j, \text{ taken from a smooth curve which was chosen to approximate the true values} \quad . \quad (7)$$

Also,

$$\epsilon_j = \sum_i Y_{ij} - \sum_i y_{ij} = \sum_i (Y_{ij} - y_{ij}) \quad . \quad (8)$$

Define

$$\epsilon_{ij} = Y_{ij} - y_{ij} = \text{error in the subdata point due to error in the observed value at } X_j \quad . \quad (9)$$

If the total error ϵ_j is divided among the subdata sets in proportion to the calculated absolute value of the subfunction, then

$$\epsilon_{ij} = \epsilon_j \frac{|y_{ij}|}{\sum |y_{ij}|} \quad . \quad (10)$$

From Eqs. (9) and (10),

$$Y_{ij} = y_{ij} + \epsilon_j \frac{|y_{ij}|}{\sum |y_{ij}|} \quad , \quad (11)$$

and from Eqs. (7) and (11),

$$Y_{ij} = y_{ij} + \frac{|y_{ij}|}{\sum |y_{ij}|} (Y_j - y_j) \quad . \quad (12)$$

After the sets of "subdata" have been formed, as in Eq. (12), the subfunctions $y_{ij} = f_i(a_i, b_i, c_i, \ldots ; X_j)$ are each fitted to the respective subdata independently. The resulting estimates for the parameters are substituted for the initial estimates, and the process is repeated.

The fractionator method has been programmed for the Oracle, and test problems are being run to explore the convergence properties of the method. Table 4.1 summarizes the results of three runs using the exponential fractionator program with the same data in each case, but starting with different initial estimates. A "peel off" procedure[7] was used to obtain the "good" estimates; the other estimates were chosen in such a way as to place the maximum strain on the method; for example, the initial values of the exponents, α_1 and α_2, are so nearly the same for the very poor estimate that this is very close to the assumption of a single exponential. For this set of data, as it has in the case of others, the fractionator did converge and the results were the same, independent of starting estimate.

[7]W. Feurzeig and S. A. Tyler, ANL Quar. Rep., ANL-4401, p 14–29 (1950).

Table 4.1. Initial Estimates and Converged Values of the Parameters* of the Equation $y = ae^{-\alpha t} + be^{-\beta t}$

	Good Estimate	Poor Estimate	Very Poor Estimate	Same Final Result in Each Case
Parameter				
a	1.22	10.0	100.0	1.3246
α	0.2538	0.1	0.51	0.2267
b	1.65	0.1	0.02	1.5454
β	0.01429	0.01	0.50	0.01319
Number of iterations required to converge	375	333	357	
$\Sigma(Y - y)^2$	0.03559	58.37	9443.0	0.03104535

*Data used was taken from the study of acute inhalation of U_3O_8 by mice.

Interestingly enough, the good estimate required more iterations to converge than did either of the other estimates.

Two Oracle programs are available for exponential curve fitting. The EXFRAC I, used for convergence studies, punches the previous value of $\sum_j w_j(Y_j - y_j)^2$ and the computed values of the parameters onto paper tape at the end of each iteration. For the case of a two-component exponential, EXFRAC I requires 7 sec noncomputing time per iteration plus an additional 0.38 sec per iteration for each original data point. EXFRAC II punches out only the final results of a specified number of iterations (2.5 sec noncomputing time and 0.38 sec per data point for each iteration of a two-component exponential). A polynomial fractionator program is available for fitting polynomials up to the ninth degree. This function is of research interest only and was chosen to compare the fractionator results with a known least-squares procedure. The theoretical work and the numerical experiments will continue, and interim reports will be issued as significant results are obtained.

Experience with the fractionator method has shown no tendency for it to become unstable, and it has converged, or was converging, on every occasion of its use. The "circle-of-convergence" for the exponential fractionator seems to be almost limitless: it appears that any set of initial estimates will lead to convergence if all numbers are within the range of the floating-point subroutines ($10^{38} \geq X \geq 10^{-38}$). Convergence is very slow, frequently requiring as many as 150 or 200 iterations, and this is especially true when there are large errors in the observed data.

Additional effort should be directed toward producing a convergence theorem, and work should be done on one of the available schemes for accelerating convergence. After the slow-convergence problem has been solved, consideration can be given to measures of dispersion.

Spectrographic Analysis of Human Tissue

I. H. Tipton[8]

M. J. Cook M. A. Kastenbaum[9]
K. K. McDaniel

Most of the data on humans used by the authors of the ICRP Recommendations in Handbook 69 (ref 10) have been obtained from this study. A description of the method and a large part of the results of analyses of tissues of subjects from the U.S. have been published[11] and some comparisons made between these values and those for tissues from subjects of different geographical origin.[12] Spectrographic analysis of foreign tissues and statistical treatment of data have continued at the University of Tennessee. The ashing laboratory at ORNL has been moved into the Spectrochemistry Section of the Analytical Chemistry Division, and the routine spectrographic analyses are being transferred to this group.

The range of values for the concentration of an element in a tissue is wide, and the frequency distribution is not normal for most elements: the number of samples is different for each geographical and age group, and certain elements are not observed in all samples of a tissue. If an element is not detected in a particular sample, this does not necessarily mean that the concentration is zero but that it is less than the lower limit of sensitivity of the method. All these factors argue against the use of common statistical procedures in the treatment of the data. The median, high, low, 33.3 and 66.7 percentile, and mean values for the concentration of a number of elements in kidney, liver, and lung have been determined. These quantities for the concentrations of calcium, of strontium, and for the strontium-to-calcium ratio in kidney for the various geographical groups are given in Table 4.2. These elements occur in every sample. The grouping is the same as reported previously.[12] Table 4.3

---

[8]Consultant, University of Tennessee, Knoxville.

[9]Mathematics Panel.

[10]Natl. Bur. Standards (U.S.), Handbook No. 69 (June 5, 1959).

[11]I. H. Tipton, p 27 in Metal-Binding in Medicine, ed. by M. J. Seven, Lippincott, Philadelphia, Pa., 1960.

[12]M. J. Cook et al., H-P Ann. Prog. Rep. July 31, 1959, ORNL-2806, p 194–201.

Table 4.2. Strontium and Calcium in Kidney

Spectrographic analysis of human tissue

Geographical Groups	No. of Samples	Median Age		Ash (% of wet sample)	Dry Weight (% of wet sample)	Ash (% of dry sample)	Ca (% in ash)	Sr (ppm in ash)	$\frac{Sr}{Ca} \times 10^4$
U.S. adults	161	40	Median	1.1	24		0.80	5.1	5.8
			High	2.9	39		3.7	28	33
			Low	0.44	14		0.27	0.6	0.9
			33.3 percentile	1.0	23		0.67	4.0	4.4
			66.7 percentile	1.1	26		0.95	6.7	7.5
			Mean	1.1	24		0.81	6.2	6.3
Swiss	9	59	Median			4.7	1.8	6.0	3.8
			High			6.0	2.2	14	13
			Low			2.5	1.1	3.3	2.1
			Mean			4.4	1.7	7.6	4.9
African	44	34	Median			5.0	0.82	6.8	8.5
			High			14	3.2	38	19
			Low			1.3	0.34	2.0	3.7
			Mean			5.0	0.91	8.7	8.9
Asian Caucasian	43	39	Median			4.2	0.60	8.2	12
			High			5.5	1.8	27	70
			Low			1.3	0.36	2.1	1.7
			Mean			3.9	0.71	11	19
Asian oriental	57	40	Median			4.7	1.3	7.6	6.9
			High			11	7.0	240	39
			Low			2.0	0.26	2.4	3.0
			Mean			4.7	1.5	18	8.9

Table 4.3. Comparison of Foreign Groups with U.S. Adults: Calcium, Strontium, and Sr/Ca in Kidney

Spectrographic analysis of human tissue

Geographical Group		Calcium	Strontium	$\frac{Sr}{Ca}$
Swiss	% above highest U.S. value			
	% within upper 1/3 of U.S. values	100	44	11
	% within middle 1/3 of U.S. values		44	22
	% within lower 1/3 of U.S. values		11	67
	% lower than lowest U.S. value			
Africian	% above highest U.S. value		2	
	% within upper 1/3 of U.S. values	30	50	63
	% within middle 1/3 of U.S. values	49	34	28
	% within lower 1/3 of U.S. values	21	14	9
	% lower than lowest U.S. value			
Asian Caucasian	% above highest U.S. value			19
	% within upper 1/3 of U.S. values	19	63	67
	% within middle 1/3 of U.S. values	21	28	7
	% within lower 1/3 of U.S. values	60	9	7
	% lower than lowest U.S. value			
Asian oriental	% above highest U.S. value	5	7	4
	% within upper 1/3 of U.S. values	63	58	35
	% within middle 1/3 of U.S. values	23	32	51
	% within lower 1/3 of U.S. values	7	4	11
	% lower than lowest U.S. value	2		

shows a comparison of foreign with U.S. subjects by indicating the percentage of the total number of individuals in a foreign group with values which fall above, within, or below the values for U.S. adults (age > 20).

To determine whether the differences between the various groups are significant, the Two Sample Sign Test as described by White[13] has been applied to these quantities. Tables 4.4–4.6 indicate the significance of the variations of the concentrations of calcium and strontium and the strontium-to-calcium ratio in the kidney with geographical location. The numbers indicate the probability that two groups are from the same population. For example, p = 0.01 means that the probability that two groups are alike is only 1%; that is, the chances that they are different is 99%. The tables show which of two different populations is higher. If the probability that the populations are alike is greater than 30%, the value for p has been placed in both columns, high-low and low-high. A value of p greater than 0.05 indicates no difference between the groups at the 95% confidence level.

The same kind of comparison among age groups in the U.S. population is given in Tables 4.7–4.10. Unfortunately there were not enough foreign

[13] C. White, Biometrics 8, 33 (1952).

Table 4.4. Significance of Difference Among Geographical Groups: Calcium in Kidney

Spectrographic analysis of human tissue

Values for p, probability that two groups are from same population; p > 0.05 indicates that two groups are different at the 95% confidence level

Low \ High	All U.S.	All Swiss	All African	All Asian Caucasian	All Asian Oriental
All U.S.		< 0.001	> 0.50		< 0.001
All Swiss					
All African	> 0.50	< 0.001			< 0.001
All Asian Caucasian	< 0.001	< 0.001	0.001		< 0.001
All Asian Oriental		0.030			

Table 4.5. Significance of Difference Among Geographical Groups: Strontium in Kidney

Spectrographic analysis of human tissue

Values for p, probability that two groups are from same population; $p > 0.05$ indicates that two groups are different at the 95% confidence level

Low \ High	All U.S.	All Swiss	All African	All Asian Caucasian	All Asian Oriental
All U.S.		0.162	0.009	< 0.001	< 0.001
All Swiss			> 0.50	0.19	0.35
All African		> 0.50		0.15	0.30
All Asian Caucasian					> 0.50
All Asian Oriental				> 0.50	

Table 4.6. Significance of Difference Among Geographical Groups: Sr/Ca in Kidney

Spectrographic analysis of human tissue

Values for p, probability that two groups are from same population; $p > 0.05$ indicates that two groups are different at the 95% confidence level

Low \ High	All U.S.	All Swiss	All African	All Asian Caucasian	All Asian Oriental
All U.S.			< 0.001	< 0.001	0.077
All Swiss	0.020		0.001	0.004	0.001
All African				0.001	
All Asian Caucasian					
All Asian Oriental			0.086	0.001	

Table 4.7. Comparison of U.S. Age Groups with U.S. Adults: Calcium, Strontium, and Ca/Sr in Kidney

Spectrographic analysis of human tissue

Age Group		Calcium	Strontium	$\frac{Sr}{Ca}$
45 days to 12 years	% above highest U.S. value			14
	% within upper 1/3 of U.S. values	14	13	29
	% within middle 1/3 of U.S. values		13	
	% within lower 1/3 of U.S. values	86	75	57
	% lower than lowest U.S. value			
13 to 19 years	% above highest U.S. value			
	% within upper 1/3 of U.S. values		27	13
	% within middle 1/3 of U.S. values	38	9	75
	% within lower 1/3 of U.S. values	63	64	13
	% lower than lowest U.S. value			
20 to 29 years	% within upper 1/3 of U.S. values	10	26	55
	% within middle 1/3 of U.S. values	40	39	20
	% within lower 1/3 of U.S. values	50	35	25
30 to 39 years	% within upper 1/3 of U.S. values	30	24	27
	% within middle 1/3 of U.S. values	43	33	32
	% within lower 1/3 of U.S. values	27	43	41
40 to 49 years	% within upper 1/3 of U.S. values	32	27	32
	% within middle 1/3 of U.S. values	36	42	36
	% within lower 1/3 of U.S. values	32	30	32
50 to 59 years	% within upper 1/3 of U.S. values	39	19	22
	% within middle 1/3 of U.S. values	17	39	30
	% within lower 1/3 of U.S. values	44	42	48

Table 4.7 (continued)

Age Group		Calcium	Strontium	$\frac{Sr}{Ca}$
60 to > 60 years	% within upper 1/3 of U.S. values	61	58	22
	% within middle 1/3 of U.S. values	28	21	39
	% within lower 1/3 of U.S. values	11	21	39

Table 4.8. Significance of Difference Among Age Groups (U.S.): Calcium in Kidney

Spectrographic analysis of human tissue

Values for p, probability that two groups are from same population; $p > 0.05$ indicates that two groups are different at the 95% confidence level

Low \ High	45 Days to 12 Years	20 to 29 Years	40 to 49 Years	60 Years
45 Days to 12 Years		← * > 0.05	0.007	< 0.001
20 to 29 Years			0.076	0.076
40 to 49 Years				0.002
60 Years				

*The arrow points to the lower group, although the difference is not significant at the 95% level.

samples from the different age groups to make a factorial study of age and geographical location. The fact that calcium in the kidney was significantly higher in the Swiss may reflect the greater median age of this group.

Except for the somewhat lower values for U.S. adults, the differences in concentration of strontium in the kidney throughout the world are not significant. The significant variation in the strontium-to-calcium ratio for the kidney is due to the variation in calcium rather than in strontium.

Table 4.9. Significance of Difference Among Age Groups (U.S.): Strontium in Kidney

Spectrographic analysis of human tissue

Values for p, probability that two groups are from same population; $p > 0.05$ indicates that two groups are different at the 95% confidence level

Low \ High	45 Days to 12 Years	20 to 29 Years	40 to 49 Years	60 Years
45 Days to 12 Years		0.059	0.041	0.011
20 to 29 Years			> 0.50	0.037
40 to 49 Years		> 0.50		< 0.001

Table 4.10. Significance of Difference Among Age Groups (U.S.): Sr/Ca in Kidney

Spectrographic analysis of human tissue

Values for p, probability that two groups are from same population; $p > 0.05$ indicates that two groups are different at the 95% confidence level

Low \ High	45 Days to 12 Years	20 to 29 Years	40 to 49 Years	60 Years
45 Days to 12 Years		← > 0.05*	> 0.50	← > 0.05
20 to 29 Years				
40 to 49 Years	> 0.50	0.126		1.00
60 Years		0.097	1.00	

*The arrow points to the lower group, although the difference is not significant at the 95% level.

It appears, therefore, that the common use of the strontium-to-calcium ratio as an indication of the strontium level is not adequate, at least for soft tissue.

In establishing MPC's for the general population of any one country or for the world at large, more specific information about the variation of an element in the body with age and geography is needed. Statistical studies of some 25 elements in 12 tissues is in progress.

APPLIED RADIOBIOLOGY

B. R. Fish

Inhalation Studies

G. W. Royster, Jr.

U. S. Davis, Jr.
G. J. Dodson
M. B. Edwards
J. A. Payne[14]
H. E. Stokinger[15]
J. L. Thompson

A chronic inhalation study[16] in which small amounts of U_3O_8 dusts were administered to dogs has been completed. The animals were allowed to inhale uranium in the form of a dust. The compound and the dosage level were chosen to simulate conditions which could be experienced in local processing areas. Other inhalation projects begun during last year have been completed. All of these studies were directed primarily at obtaining information applicable to the estimation of an existing internal deposit in humans.

Adult female beagles were administered weekly single inhalations of U_3O_8 dust by means of a muzzle mask and a two-way valve.[16,17] The aerosol consists of discrete particles having a narrow range in size. None of the particles exceed 1.2 μ and over 99% of the aerosol is greater than 0.2 μ in diameter; the mass median size is 0.75 μ. The aerosol concentration was maintained at 0.5 mg/m^3 in a 1-m^3 plastic box, and the dogs

---

[14]Co-op student.

[15]Consultant, USPHS.

[16]B. R. Fish et al., H-P Ann. Prog. Rep. July 31, 1959, ORNL-2806.

[17]S. R. Bernard et al., H-P Ann. Prog. Rep. July 1957, ORNL-2380, p 4.

were allowed to breathe 0.05 m^3 of the aerosol every week. The total inhaled quantity of 25 μg per week corresponds to the amount of uranium an employee could inhale each week if he were exposed continually to the plant allowable air limit while at work in one of the local installations. Urine samples are collected from the dogs on the fifth and sixth days after each inhalation in order to simulate the industrial practice of collecting Monday morning urine samples.

Figure 4.1 illustrates the buildup of uranium in the lung tissue and in the pulmonary lymph nodes during the exposure period. The concentration of uranium in the lung is apparently equilibrating after about six to nine months of repeated weekly exposures. However, the uranium concentration in the pulmonary lymph nodes continues to increase and surpasses the concentration of uranium in the lung within seven to eight months after beginning the exposure. In one beagle, autopsied three years after a single inhalation of uranium oxide fume, the uranium concentration in the pulmonary lymph nodes was 70 times greater than in the general lung tissue, and 40% of the uranium in the region of the chest was stored in these lymph nodes. Other interesting facts to be seen in Fig. 4.1 are that the urinary uranium excretion rate is equilibrating and that over a considerable portion of the exposure period, the ratio of lung burden to

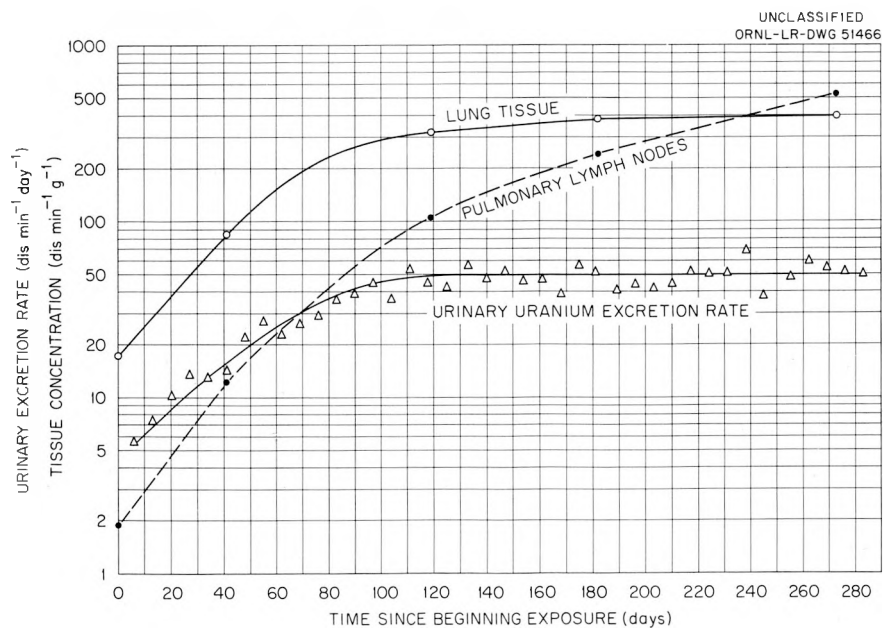

Fig. 4.1. Chronic Inhalation of U_3O_8.

urinary uranium excretion rate is constant and is approximately 520, that is, 400(average weight of lungs)/50. If this were to apply to the human case, 35,500 dis/min of eneriched uranium in the lung (gives a dose of 15 rems per year to the lung) would correspond to 68 dis/min (alpha) excreted in the urine per day.

All of the data from the inhalation study program has not been analyzed. Reports will be published as each phase is finished.

Aerosol Project

F. G. Karioris[18].

B. R. Fish M. B. Edwards

Exploding-Wire Aerosol Generator

An exploding-wire aerosol generator[19] for the production of U_3O_8 fume has been fabricated and is undergoing tests to evaluate its characteristics. In this device, a 4000-j capacitor is discharged through a uranium wire to generate an aerosol which may be used for animal inhalation studies in conjunction with exposure chambers available in this laboratory.[20,21] Previous work[22] has shown need for a generator whose output is reproducible in concentration and particle size.

Although there are many methods of generating solid aerosols,[23] these are not suitable for the production of small quantities of very toxic materials. An aerosol generator,[20] in which small uranium chips are burned, has low yield and produces an aerosol whose concentration varied by as

---

[18]Temporary employee.

[19]F. G. Karioris and B. R. Fish, Uranium Oxide Smoke from Exploding Wires, paper presented at the Fifth Annual Meeting of the Health Physics Society, Boston, Mass., July 1, 1960.

[20]S. R. Bernard et al., H-P Semiann. Prog. Rep. July 31, 1956, ORNL-2151, p 1–4.

[21]B. R. Fish et al., H-P Ann. Prog. Rep. July 31, 1959, ORNL-2806, p 189–90.

[22]B. R. Fish et al., H-P Ann. Prog. Rep. July 31, 1959, ORNL-2806, p 185.

[23]L. Silverman and C. E. Billings, J. of APCA 6(2), 1–8 (1956).

much as a factor of 10 in a series of trials.[22] The exploding-wire phenomenon[24,25] has many applications, but little attention has been given to the smoke produced by each wire explosion that takes place in air. In 1946, Abrams et al.[26] generated uranium and plutonium aerosols by discharging a high-energy capacitor through aluminum foil in which small specimens were wrapped. By this method, however, the aerosol was heavily contaminated with aluminum and the yields reported were variable, ranging from 0.9 to 54% for similar attempts.

Wires of pure uranium metal can be exploded electrically in air to produce a U_3O_8 aerosol in the apparatus shown in Fig. 4.2. A 20-μf capacitor bank may be charged to voltages up to 20 kv and discharged through

---

[24]W. G. Chace, A Bibliography of the Electrically Exploded Wire Phenomenon, AFCRC-TN-58-457 (1958).

[25]W. G. Chace and H. K. Moore (ed.), Exploding Wires, Plenum Press, New York, 1959.

[26]R. Abrams et al., Production and Analysis of Radioactive Aerosols, CH-3629 (1946).

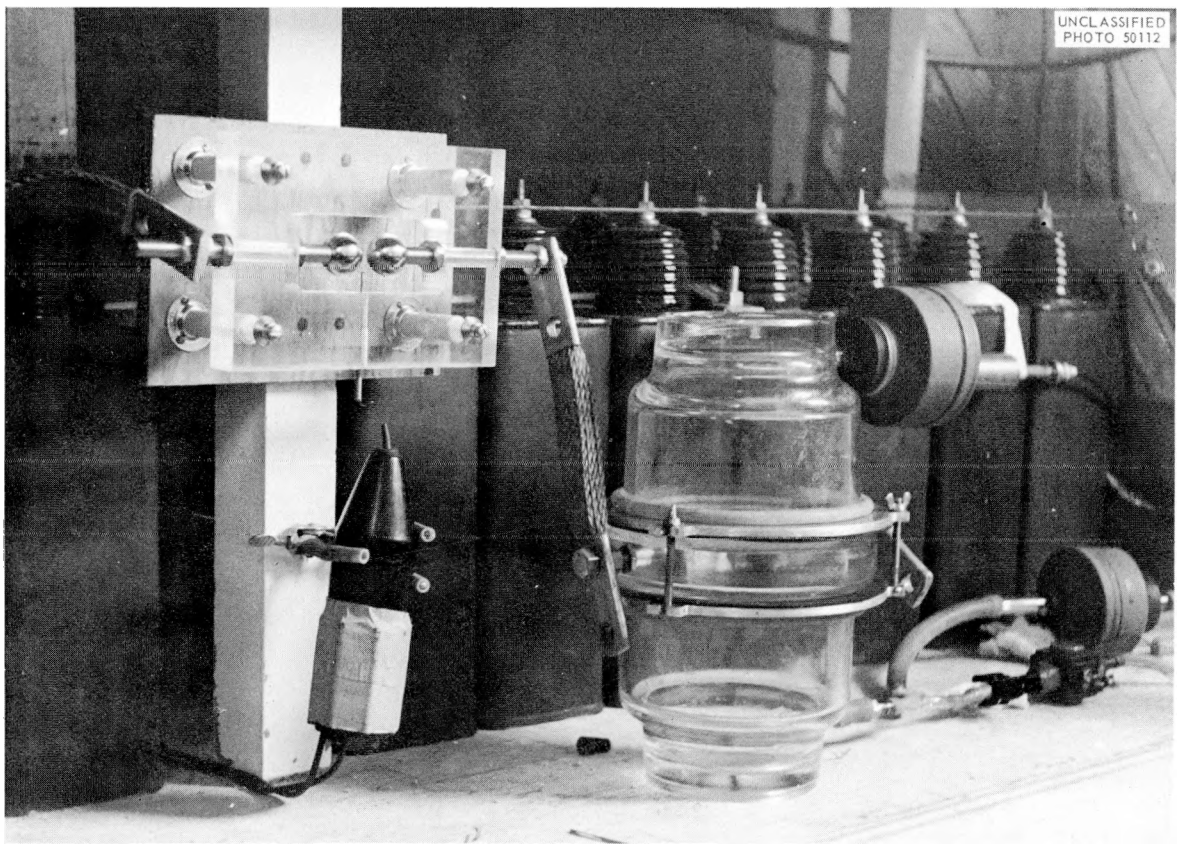

Fig. 4.2. Exploding-Wire Aerosol Generating Apparatus.

a measured mass of wire clamped between stainless steel electrodes in a glass explosion chamber. Discharge of the capacitor is initiated by using a high-frequency leak tester to ionize the air in a simple series sphere gap, and surge currents of 60,000 amp have been observed in a coaxial shunt of conventional design.[27]

Triggering the sphere gap results in a noisy explosion accompanied by a brilliant flash of white light, and the explosion chamber can be seen to fill instantly with white smoke which persists for about 2 min before showing noticeable evidence of instability. When observed in a beam of light, the concentrated U_3O_8 smoke appears to coagulate rapidly after 3 min, feathery strands 2 cm long can be seen floating about in the air inside the chamber after 5 min, and much of the solid material settles out in 10 min. Within the first minute following the explosion, aerosols produced in the explosion chamber can be sampled by a thermal precipitator for particle size determinations and then collected on a Millipore filter for yield and reproducibility studies.

Good reproducibility of concentration is a necessary characteristic for aerosol research. In addition, high yield is desirable when highly toxic or costly materials are used. The data in Table 4.11 show that for explosions with 6 kv or more the yield of the exploding-wire generator is

[27]W. G. Chace and E. H. Cullington, Instrumentation for Studies of the Exploding Wire Phenomenon, AFCRC-TR-57-235 (August 1957).

Table 4.11. Uranium Oxide Aerosol Yield from Exploding-Wire Generator

Voltage on Capacitor (kv)	Number of Trials	Yield (%)	Standard Error (%)
6	4	81.5	±6.9
8	5	85.1	±2.8
10	18	84.0	±3.2
12	10	85.9	±3.5
15	4	91.3	±4.3

about 85% and is reproducible to approximately ±4%. Since x-ray diffraction analysis has shown that the particles are composed of U_3O_8 with less than 5% contamination by β-UO_2, the percentage yield can be calculated from the weight of solid collected after the explosion of a known weight of uranium. This technique has been confirmed in several instances by using a chemical method.[28] Immediately after the explosion, the yield is uniformly distributed in the 4.7-liter chamber so that concentrations can be determined. The aerosol has been drawn through as much as 10 ft of 3/8-in.-ID tubing with no significant loss of particulate matter.

Analysis of data from 18 trials at 10 kv using uranium wires in the range 4.7 to 26.2 mg shows that yield is somewhat dependent on the mass of wire exploded. By the method of least squares, these data can be fitted to the line $Y = 90.2 - 0.6lm$, where Y is the per cent yield and m is the number of milligrams of wire used. For this case, the standard error of the estimate is −3.2%. Over the range of 6 to 15 kv, the yield may increase slowly with increasing voltage on the capacitor.

Current studies indicate that the uranium oxide aerosol produced is typical of fume. Electron photomicrographs show chains and agglomerates composed of spherical particles with a count median diameter of approximately 0.02 μ. There is some evidence that the particle size may depend on the voltage used to explode the wire, but further work is required to establish this relationship.

In addition to uranium, wires of Al, Cu, Fe, Mg, and Th have been exploded in the apparatus to produce their respective oxide aerosols. It is expected that the device will function as well with plutonium or neptunium when such work is undertaken.

Ingestion of Uranium Compounds

B. R. Fish

J. A. Payne[29] J. L. Thompson

Studies of the absorption into the body of orally ingested uranium were begun in order to check the basis which was used in establishing the

---

[28]G. W. Royster, Jr., Health Phys. 2, 291–94 (1960).
[29]Co-op student.

handbook[30,31] values for MPC of uranium in water. This work was of a preliminary nature and included only the determination of the fraction of the ingested dose which was retained by the body. The need to examine the ingestion criteria was seen as the result of a human exposure case in which, apparently, 50 times more uranium was absorbed into the bloodstream than was predicted by the parameter noted for uranium in the ICRP report on internal dose.[31] Within two days, more than 0.5% of the ingested uranium was recovered in the man's urine.

Ten mongrel dogs were given single oral doses of UO_2F_2 in water: seven of these received 0.7 mg of U per kg of body weight (simulating the human case cited above); and the other three dogs received 0.007 mg of U per kg. Six dogs were given single oral doses of uranyl nitrate in water: three each at dose levels of 0.7 and 0.007 mg of U per kg. One beagle was administered weekly doses of UO_2 in food (5.8 mg of U per kg weekly); another was given weekly doses of U_3O_8 in food (6.5 mg of U per kg weekly).

Radiochemical analysis has been completed for all of the ingestion exposure groups. Results of the study of UO_2F_2 ingestion at the dose level, 0.700 mg of U per kg, are described in detail elsewhere[32] and summarized in this report. The results of ingestion studies will be published upon completion of data interpretation.

In the case of UO_2F_2 ingestion, at the higher dose level (0.7 mg of U per kg), an average of 1.55% (standard deviation 0.21%) of the ingested uranium was absorbed into the bloodstream: the lowest value was 0.83% and the highest was 2.30%. The urinary uranium excretion rates of these seven dogs, expressed in per cent of the absorbed dose excreted per day, is shown in Fig. 4.3 and may be compared with the average urinary excretion rates of 11 mongrel dogs which were given single intravenous injections of uranyl nitrate.[33]

---

[30] Natl. Bur. Standards (U.S.), Handbook No. 69 (June 5, 1959).

[31] Addendum to ICRP Publication I (1958 Recommendations), Health Phys. 2, 317–20 (1960).

[32] B. R. Fish et al., Absorption of Uranium from the Gastrointestinal Tract of Dogs Following Ingestion of UO_2F_2, (in manuscript).

[33] J. R. Muir et al., H-P Ann. Prog. Rep. July 31, 1958, ORNL-2590.

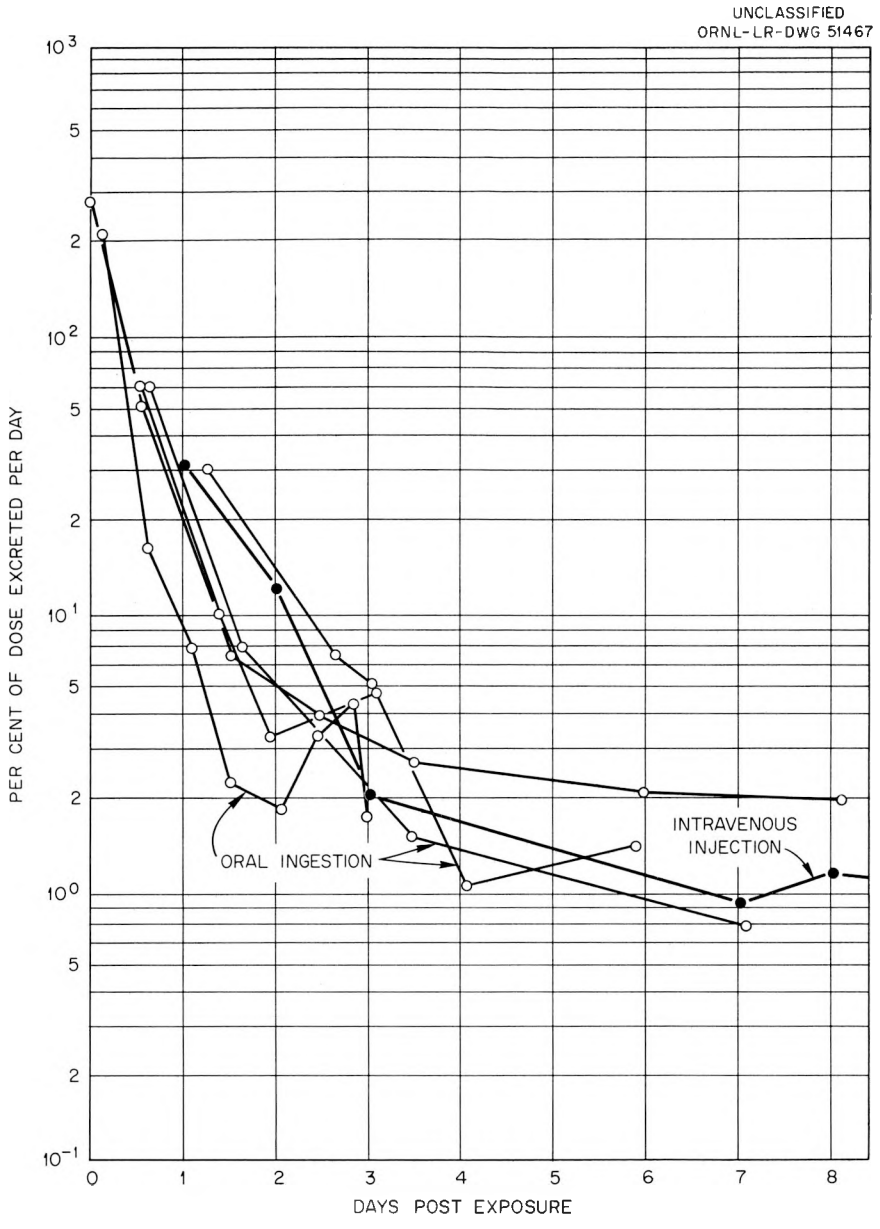

Fig. 4.3. Comparison of Urinary Excretion Rates for Single Oral Ingestion of UO_2F_2 and Single Intravenous Injection of Uranyl Nitrate from Mongrel Dogs.

The ICRP handbook[31] lists the fraction of an oral dose that is absorbed from the gastrointestinal (GI) tract into the bloodstream, f_1, to be 0.0001 for soluble compounds of uranium. Preliminary results of the ingestion study indicate that f_1 may be more nearly 0.01 for UO_2F_2. There does not appear to be any significant difference in the pattern of urinary excretion of absorbed uranium, whether it reaches the bloodstream via the

GI tract or whether it is injected directly into the bloodstream. Questions relating to the effect upon GI absorption attributable to gravimetric dose level, compound differences, and repeated exposure will be dealt with in the final report for this project. Other factors which should be investigated include the relationship of these animal data to man (a possible species difference), and the possibility that a prolonged transit time through the GI tract might significantly increase the total absorption.

Distribution and Excretion of Uranium

J. R. Muir

B. R. Fish
N. L. Gillum
E. S. Jones
J. L. Thompson

The study of the deposition of soluble uranium compounds in the animal body previously reported[34] has been extended to a new dose level and also extended in time. The new dose level was used at a concentration of 0.5 μg of U^{233} per ml. All techniques and other dose levels used were as previously described.

The percentage deposition in the kidneys indicates some differences between the two highest and the two lowest dose levels (see Fig. 4.4). The two highest dose levels represent the range of doses reported in a study with humans.[35] There appears to be a different retention pattern for the high doses as contrasted with the low doses, with an apparent difference in biological half lives for the kidney. The 0.1 μg of U per g of body weight dose is the most erratic of the group and approximates the lower dose levels reported by Bernard.[35]

---

[34]J. R. Muir et al., H-P Ann. Prog. Rep. July 31, 1959, ORNL-2806, p 191.

[35]S. R. Bernard, Health Phys. 1, 288–305 (1958).

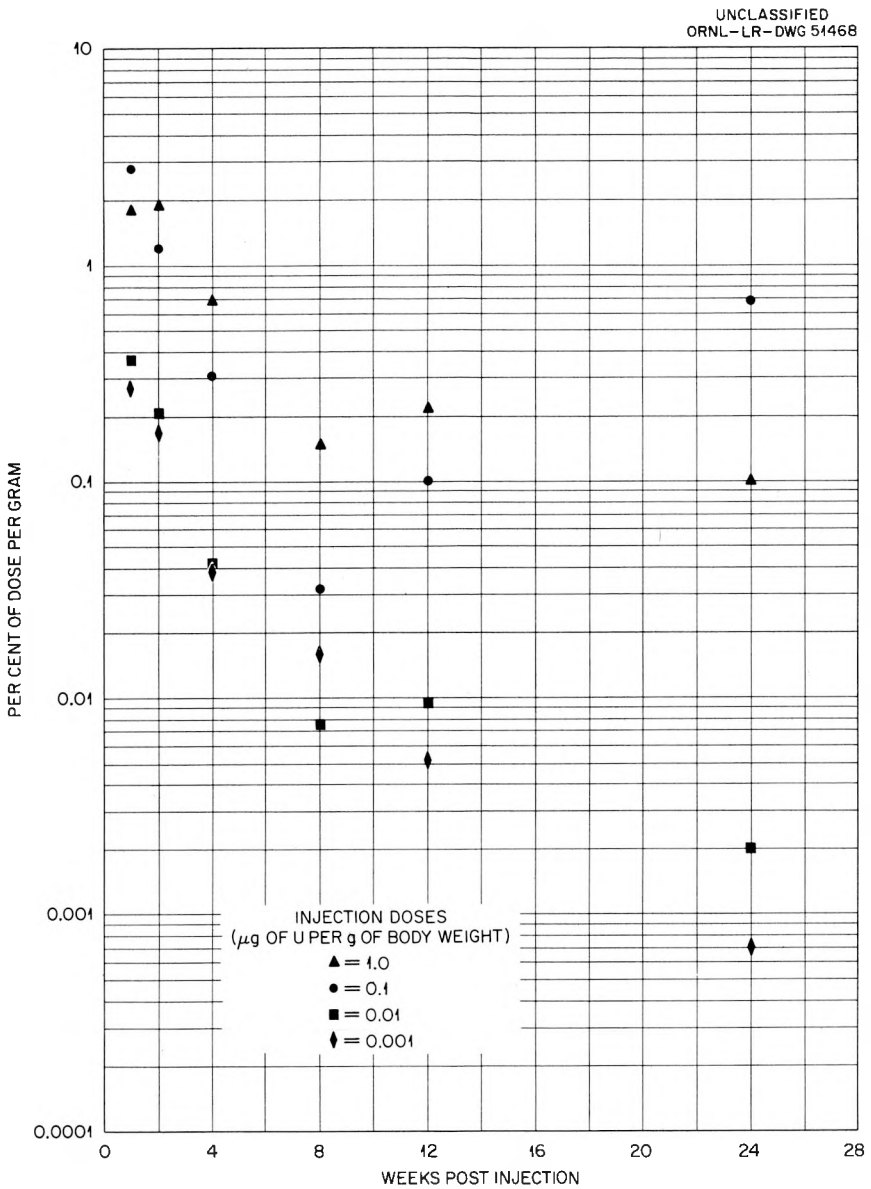

Fig. 4.4. Percentage Deposition of Uranium in Kidneys of Female White Rats Following Intravenous Injection.

Autoradiographic Studies on Nonuniform Distribution of Uranium in the Rat Kidney

E. S. Jones

L. J. Casarett[36]
G. J. Dodson
B. R. Fish
N. L. Gillum
M. A. Kastenbaum[37]
J. R. Muir
G. W. Royster, Jr.
J. L. Thompson
A. C. Upton[38]

The nonuniform distribution factor (ref 39), N, has been defined by Hindmarsh et al.[40] as the ratio of the number of tracks per unit field in a specific area to the average number of tracks per unit field for the entire organ. This is used by ICRP Committee II in formula calculations. The need of data on soft tissue led to the development of the present method (previously reported[41]). Direct observations of alpha tracks from uranium deposited in half kidneys of rats have been made by track counting in autoradiograms and compared with alpha activity in corresponding half kidneys. The highest concentration is usually in the cortex and the factor denoted as N, whereas in two cases of higher concentration in the medulla, N_m is used.

Counting has been completed on ten kidneys with the corresponding alpha activity on six of these compared with the counting. Detailed records on the location of the tracks in the histological units and some observations on the pathological conditions have been made. The majority of the latter work is still to be done on accompanying slides. Seventeen half kidneys are ready for counting, three are being exposed to photographic emulsion, and 14 are ready for sectioning. Data may be obtained on 16 other kidneys. Also, there are kidney tissues remaining from the Boston studies.[42]

---

[36]University of Rochester.

[37]Mathematics Panel.

[38]Biology Division.

[39]Report of Committee II on Permissible Dose for Internal Radiation, ICRP Publication 2, Pergamon, London, 1959.

[40]M. Hindmarsh et al., Brit. J. Radiol. 31(370), 518 (1958).

[41]E. S. Jones, H-P Ann. Prog. Rep. July 31, 1959, ORNL-2806, p 194.

[42]S. R. Bernard, Health Phys. 1(3), 288 (1958).

The uranyl nitrate concentrations injected, the type of rats used, the methods, and measuring of alpha activity in the ashed material are those described by J. R. Muir.[43] One additional level of 0.001 mg of U per kg of body weight was used. In this paper these levels are designated as high (Q-1), intermediate (Q-2), low (Q-3), and lowest (Q-4). The rats are in two groups: (1) serially sacrificed at 1, 2, 4, 8, and 12 weeks, designated as a, b, c, d, and e; and (2) serially sacrificed at 1, 2, 4, and 10 days, designated as A, B, C, and D. There has been only slight modification of the method as previously reported.[44] Sections have been cut at 8 μ and liquid emulsion (Eastman) has been used. In the counting, when dense agglomerates are present, an estimate of the number of tracks is formed by a count of one-fourth of the mass.

The amount of deposition of uranium in rat kidneys has been described by Muir.[43] Figure 4.5 shows photomicrographs of kidneys from rats with the two highest dose levels. Figure 4.5a and b shows cortex and contrasting medulla at the high dose level and Fig. 4.5c and d the same at the intermediate level. Figure 4.6 shows the alpha activity after different doses as evident at different times of sacrifice.

Of two control rats in the same environment, but without injection, one showed 26.5 dis min^{-1} g^{-1} and the other 3.02, averages of the two kidneys of each rat.

An extensive study of distribution of uranium tracks in the different histological units of the kidney is in process. In the rat Q-2, G-E, there was more activity in the medulla. Both kidneys show an N_m of 1.5. In the cortex more tracks were found in distal tubules than in proximal tubules. It should be noted that this animal was sacrificed 84 days after injection.

Table 4.12 gives the nonuniform distribution factor, N, for ten kidneys based on track counting and is compared with N based on alpha activity of six of the corresponding half kidneys ashed. Considering the cortex to be 70% of the entire kidney,[45] the formula for calculating N is as

---

[43]J. R. Muir, H-P Ann. Prog. Rep. July 31, 1959, ORNL-2806, p 191.

[44]E. S. Jones, H-P Ann. Prog. Rep. July 31, 1959, ORNL-2806, p 194.

[45]M. Arataki, Am. J. Anat. 36, 422 (1926).

UNCLASSIFIED
PHOTO 51442

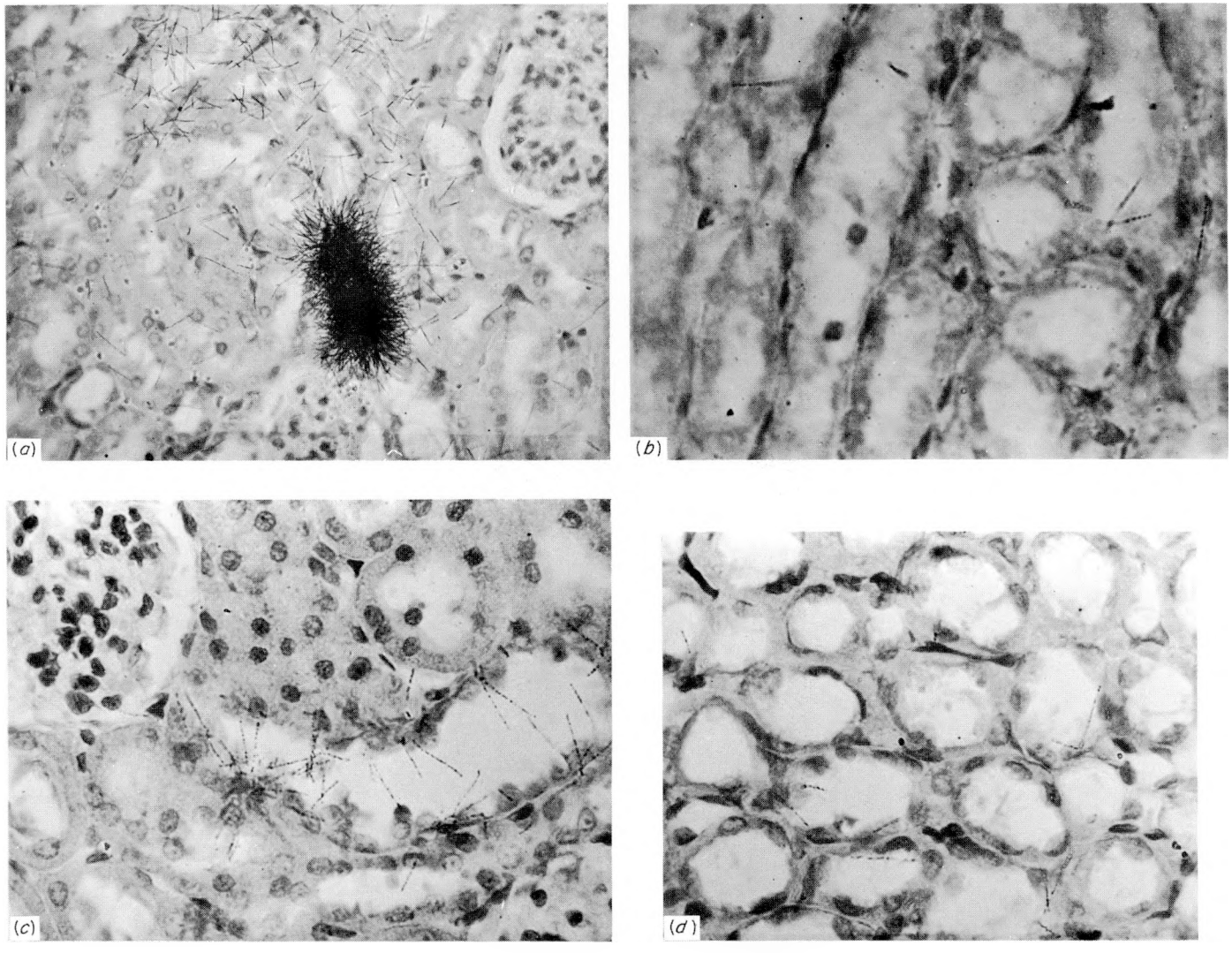

Fig. 4.5. Deposition of Uranium in Rat Kidney. (a) Cortex, high-level dose, 1-day post injection. Ca. 250X. (b) Medulla, high-level dose, 1-day post injection. Ca. 400X. (c) Cortex, intermediate dose, 28-day post injection. Ca 500X. (d) Medulla, intermediate dose, 28-day post injection. Ca. 400X. Reduced 21%.

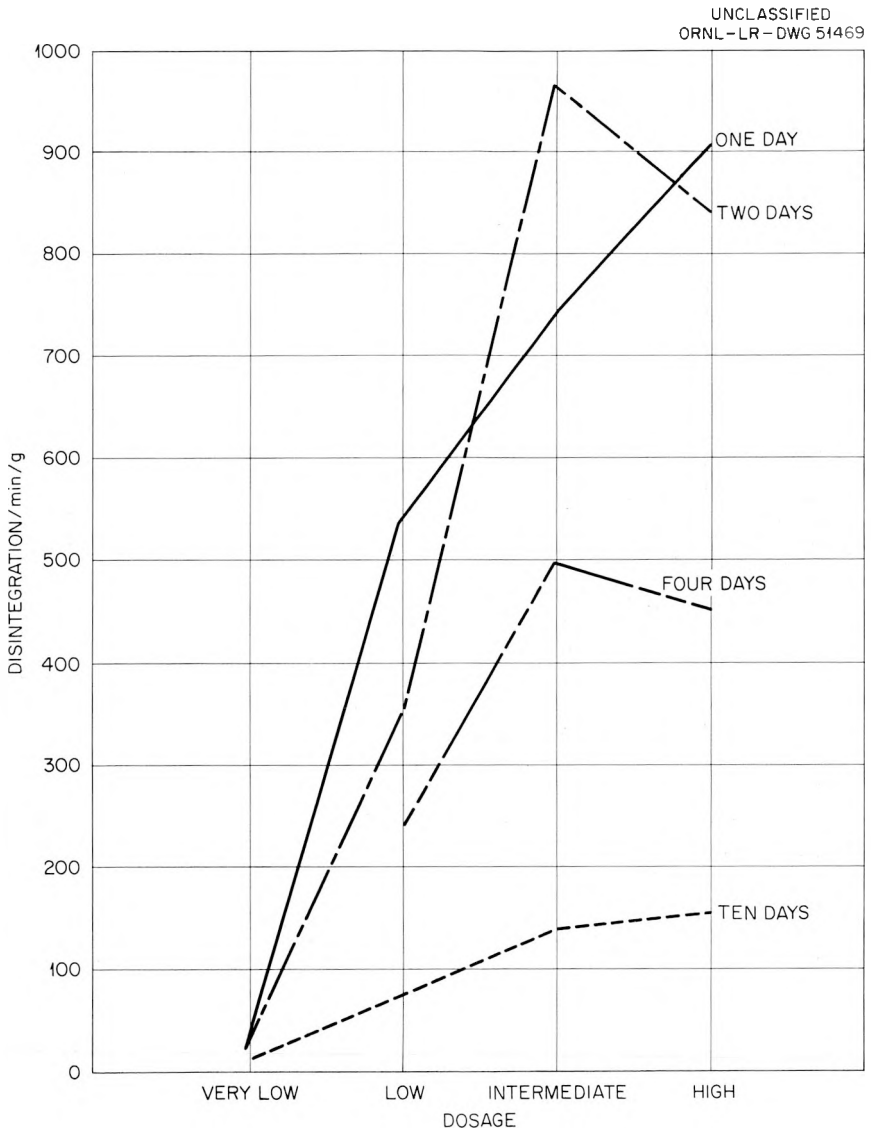

Fig. 4.6. Amount of Alpha Activity After Different Doses of Uranium.

follows:

Let

c = counts per field in D days in the cortex,

m = counts per field in D days in the medulla,

K = counts per field over entire half kidney.

In the kidneys counted then

$$K = 0.7c + 0.3m,$$

$$N = \frac{c}{K},$$

$N_m = \frac{m}{K}$ = nonuniform distribution factor when higher activity is in the medulla.

Table 4.12. Nonuniform Distribution Factor on Basis of Track Counting and Alpha Activity

No. of Animal	Dosage	Time of Isotope in Animal (days)	Location of Kidney in Body	Tracks Counted					Material Ashed						
				c, Counts per Field in Cortex	m, Counts per Field in Medulla	Entire Half Kidney		N[b]	Cortex		Medulla		Corresponding Entire Kidney		N'[e]
						Weight (g)	K,[a] Counts per Field		Weight (g)	C[c]	Weight (g)	M[c]	Weight (g)	K'[c,d]	
Q-1A	High	1	left	437.5	48.2	0.49	320.7	1.36	0.52	13,123.8	0.08	2014.9	0.60	9791.1	1.34
			right	526.1	56.5	0.63	385.2	1.36	0.48	6,740.0	0.05	1124.1	0.53	4565.2	1.48
Q-1B3	High	2	left	168.13	21.58	0.45	124.17	1.35	0.69	7,251.4	0.13	781.8	0.82	5310.5	1.36
Q-1Rcx	High	28	left	53	5.38	0.52	38.7	1.36	0.52	1,274.8	0.16	590.6	0.68	969.5	1.31
			right	39.86	5.1	0.72	29.4	1.36	0.28	1,503.6	0.16	1202.5	0.44	1413.3	1.06
Q-2Rc	Intermediate	28	right	115	5.0	0.44	82	1.4	0.64	4,731.4	0.06	1705.0	0.7	3823.5	1.24
Q-2,G-D	Intermediate	56	left	1.6	0.28	0.71	1.2	1.33							
			right	1.75	1.19	0.82	1.58	1.11							
Q-2,G-E	Intermediate	84	left	27.7	52.96	0.96	35.3	1.5 N_m							
			right	50.37	102.66	0.95	66	1.55 N_m							

[a] $K = 0.7c + 0.3m$.

[b] $N = c/K$.

[c] Disintegrations per minute per gram.

[d] $K' = 0.7C + 0.3M$.

[e] $N' = C/K'$.

In the kidneys ashed let

C = dis min^{-1} g^{-1} in cortex,

M = dis min^{-1} g^{-1} in medulla,

K' = dis min^{-1} g^{-1} over entire ashed half kidney,

$K' = 0.7c + 0.3M$,

$$N = \frac{C}{K'} .$$

The average of eight half kidneys gave N as 1.33 with a range of 1.1 to 1.4. The factor for the ninth and tenth kidneys which showed more activity in the medulla gave an N_m of 1.5. Figuring the factor from six ashed half kidneys, the average N was found to be 1.3 with a range of 1.06 to 1.48.

Based on eight kidneys, evidence points to the nonuniform distribution factor, N, for the rat kidney as approximately 1.3.

5. EDUCATION, TRAINING, AND CONSULTATION

E. E. Anderson

AEC FELLOWSHIP PROGRAM

E. E. Anderson M. F. Fair

Twenty-eight students completed the course in Applied Radiation Physics at Vanderbilt University in May 1960. Eighteen of these were AEC Fellows, five were from the Nuclear Engineering Department of the University, two were Air Force officers, two were students from Greece (one sponsored by the International Atomic Energy Agency and the other by the International Cooperation Administration), and one was a student from Burma (sponsored by the International Atomic Energy Agency). Twenty people reported to ORNL in June for their applied health physics training. Thirteen were AEC Fellows (including one from Puerto Rico), three were Air Force officers, one was from India, one was from The Philippines, and two were from Greece. Five of the Fellows were granted extensions to the Fellowship to complete the requirements for the MS degree. One of the Fellows has chosen to do his research at the Health Physics Division and four will return to Vanderbilt University. The AEC Fellows for the 1960-61 program were selected in March 1960, and a group of 19 will enroll at Vanderbilt University in September 1960.

OTHER ACTIVITIES

E. E. Anderson M. F. Fair K. Z. Morgan

Personnel from the Health Physics Division spent several weeks at the Puerto Rico Nuclear Center at Mayaguez and San Juan, providing instruction in general health physics and consulting on the Center's health physics curriculum.

A ten-week course in health physics was conducted by the Health Physics Division of ORNL and the Special Training Division of the Oak Ridge Institute of Nuclear Studies for personnel of the Atomic Energy Commission and from state departments of health. Twenty participants attended the course from January 11, 1960, to March 18, 1960.

A 12-hr lecture course was presented for 21 persons from the Chemical Technology Division from March 21, 1960, to April 18, 1960.

A 60-hr course in health physics was presented by the Division for the foreign ORSORT program. This was a combined lecture and laboratory course covering all aspects of health physics.

Members of the section gave lectures on various topics in health physics to NSF-AEC Institutes in Radiation Biology for High School Teachers, to university groups under the ORINS-ORNL lecture program, to military groups, and to professional societies.

One of the staff is a member of the AIBS Advisory Committee on Education and Training to the Division of Biology and Medicine, and is also a member of the AEC Fellowship Board, advisory to ORINS on the AEC Fellowship program in Health Physics.

During the year a total of eight trainees associated with nuclear energy programs in this country and abroad, trained in various phases of applied health physics. The name and home agency for each individual assigned for training follow: I. Miyanaga, Japan; T. Ishihara, Japan; S. Okuyama, Japan; M. Srivanik, Thailand; S. Subbaratram, India; S. Danali, Greece; B. Rock, AEC, Washington, D.C.; and Major C. H. Colgin, Fort McClellan, Alabama.

Lectures and discussion periods on particular phases of health physics were given for the following:

1. U.S. Public Health Service,
2. ORNL Orientation Program,
3. MIT Practice School,
4. ORINS Radioisotope Techniques Course,
5. ORINS UT-AEC Military Veterinary Radiological Health Course.

PUBLICATIONS

S. I. Auerbach, "Biological Contamination and Dispersal of Radioactive Wastes: Dispersal by Insects," Nuclear Safety 1, 64–65 (1960).

J. A. Auxier, "Evaluation of Residential Structures for Shielding Against Fallout Radiation," p 148–51 in Biological and Environmental Effects of Nuclear War, Hearings Before the Special Subcommittee on Radiation of the Joint Committee on Atomic Energy, Congress of the United States, U.S. Government Printing Office, Washington, 1959.

R. L. Blanchard, B. Kahn, and R. D. Birkhoff, "The Preparation of Thin, Uniform, Radioactive Sources by Surface Adsorption and Electrodeposition," Health Phys. 2, 246–55 (1960).

W. B. Cottrell, L. A. Mann, F. L. Parker, and G. D. Schmidt, Environmental Analysis of NS "Savannah" Operation at Camden, ORNL-2867 (Rev.) (May 5, 1960).

K. E. Cowser, Potential Hazard of Ruthenium in the ORNL Waste-Pit System, ORNL CF-60-3-93 (1960).

F. J. Davis, "Instrumentation in Aircraft for Radiation Measurements," p 24–27 in A Compendium of Information for Use in Controlling Radiation Emergencies, Including Lecture Notes for a Training Session at Idaho Falls, Feb. 12–14, 1958, TID-8206.

F. J. Davis, "Radiation Monitoring of Large Areas," Nuclear Safety 1, 52–53 (1959).

P. H. Doyle and J. Neufeld, "On the Behavior of Plasma at Ionic Resonance," Phys. Fluids 2, 390–92 (1959).

R. A. Finston, H. H. Hubbell, Jr., W. G. Stone, and R. D. Birkhoff, Measurements of Electron Flux in Irradiated Media by AC Methods, ORNL-2732 (Aug. 31, 1959).

J. C. Howell and P. B. Dunaway, Long-Term Ecological Study of the Oak Ridge Area: II. Observations on the Mammals with Special Reference to Melton Valley, ORNL CF-59-10-126 (Oct. 26, 1959).

G. S. Hurst, "Fast Neutron Dosimetry," chap. IV.G in Fast Neutron Physics, vol IV (ed. by J. B. Marion and J. L. Fowler), Interscience, New York, 1960.

G. S. Hurst, "Dosimetry of Direct Radiation from Nuclear Weapons," p 140–47 in Biological and Environmental Effects of Nuclear War, Hearings Before the Special Subcommittee on Radiation of the Joint Committee on Atomic Energy, Congress of the United States, U.S. Government Printing Office, Washington, 1959.

G. S. Hurst and R. H. Ritchie (eds.), Radiation Accidents: Dosimetric Aspects of Neutron and Gamma-Ray Exposures, ORNL-2748, Part A (Nov. 2, 1959).

G. S. Hurst and T. D. Strickler, "Alpha Particle Ionization of Binary Gas Mixtures," chap. V.4 in Penetration of Charged Particles in Matter (ed. by E. A. Uehling), National Academy of Sciences–National Research Council, Washington, D.C., 1960.

G. S. Hurst, R. H. Ritchie, and L. C. Emerson, "Accidental Radiation Excursion at the Oak Ridge Y-12 Plant. III. Determination of Radiation Doses," Health Phys. 2, 121–33 (1959).

D. G. Jacobs and T. Tamura, "Retentions and Movement of Radioisotopes in Soils," Nuclear Safety 1(3), 65–69 (1960).

F. Kalil, W. G. Stone, H. H. Hubbell, Jr., and R. D. Birkhoff, Stopping Power of Thin Aluminum Foils for 12 to 127 kev Electrons, ORNL-2731 (Sept. 3, 1959).

S. V. Kaye, "Gold-198 Wires Used to Study Movements of Small Mammals," Science 131, 824 (1960).

W. J. Lacy, F. M. Empson, and I. R. Higgins, "Physical and Chemical Properties of Nuclear Power Reactor Waste Solutions," Ind. Eng. Chem. 51, 83A–86A (1959).

P. K. Lee and S. I. Auerbach, Determination and Evaluation of the Radiation Field Above White Oak Lake Bed, ORNL-2755 (Feb. 12, 1960).

K. Z. Morgan, "Health Physicists Play Important Role in Radiation Hazard Control," Safety Standards 8(6), 12–14 (1959).

K. Z. Morgan, "Human Exposure to Radiation," Bull. Atomic Scientists 15, 384–89 (1959).

K. Z. Morgan, "Some Problems in the Control of Criticality," p 261, and "Immediate Evaluation of External Radiation Doses and Internal Contaminations in the Event of a Radiation Accident," p 339, in Health Physics in Nuclear Installations, Organization for European Economic Co-operation, European Nuclear Energy Agency, Paris, December 1959.

K. Z. Morgan, "Radiation: Protection and Health Physics," p 502 in Medical Physics, vol III, The Year Book Publishers, Chicago, 1960.

K. Z. Morgan, "Protection from Ionizing Radiation," and "Dosimetry of Internal Radioactive Isotopes," p 250–337 in Selected Materials on Radiation Protection Criteria and Standards: Their Basis and Use, Joint Committee on Atomic Energy, Congress of the United States, U.S. Government Printing Office, Washington, 1960.

K. Z. Morgan, Chairman, ICRP Committee II, "Report of Committee II on Permissible Dose for Internal Radiation," Health Phys. 3 (1960).

K. Z. Morgan, I. H. Tipton, and M. J. Cook, "A Summary of Data That Was Used in the Revision of the Internal Dose Recommendations of the International Commission on Radiological Protection," p 17 in Health Physics, Progress in Nuclear Energy, Series 12, vol 1 (ed. by W. G. Marley and K. Z. Morgan), Pergamon, London, 1959.

J. Neufeld, "Occurrence of Vavilov-Čerenkov Radiation in a High-Temperature Plasma," Phys. Rev. 116, 1–3 (1959).

J. Neufeld, "Propagation of Electromagnetic Waves in a Multistream Medium at Gyromagnetic Resonance," Phys. Rev. 116, 19–20 (1959).

J. Neufeld, "Radiation Produced by an Electron Beam Passing Through a Dielectric Medium," Phys. Rev. 116, 785–87 (1959).

L. B. O'Kelly, G. S. Hurst, and T. E. Bortner, Measurement of Electron Attachment in Oxygen-Methane and Oxygen-Carbon Dioxide Mixtures, ORNL-2887 (Jan. 11, 1960).

J. S. Olson, "Biological Contamination and Dispersal of Radioactive Wastes: Contamination of Vegetation," Nuclear Safety 1, 62–64 (1960).

G. L. Plummer, Biometric Analysis of a Growth Response of Two Plant Species in a Radioactive Waste Area, ORNL-2903 (Apr. 11, 1960).

R. H. Ritchie, "Calculations of Energy Loss Under the Bias in Fast Neutron Dosimetry," Health Phys. 2, 73–76 (1959).

R. H. Ritchie and G. S. Hurst, "Penetration of Weapons Radiation: Application to the Hiroshima-Nagasaki Studies," Health Phys. 1, 390–404 (1959).

R. H. Ritchie, J. S. Cheka, and R. D. Birkhoff, "The Spherical Condenser as a High Transmission Particle Spectrometer," Nuclear Instr. & Methods 6, 157–63 (1960).

C. J. Rohde, "Studies on the Biologies of Two Mite Species, Predator and Prey, Including Some Effects of Gamma Radiation on Selected Developmental Stages," Ecology 40, 572–79 (1959).

G. W. Royster, Jr., "Electrodeposition of Uranium from Urine," Health Phys. 2, 291–94 (1960).

F. W. Sanders, A Feasibility Report on a Method of Direct Total Body Measurement of Enriched Uranium in Man, ORNL CF-59-6-107 (Aug. 7, 1959).

F. W. Sanders, J. A. Auxier, and J. S. Cheka, "A Simple Method of Minimizing the Energy Dependence of Pocket Ionization Chambers," Health Phys. 2, 308–9 (1960).

F. W. Sanders, G. S. Hurst, and T. E. Bortner, A Study of Alpha Particle Ionization in Argon Mixtures, ORNL-2807 (Oct. 9, 1959).

W. S. Snyder, "Range of Uncertainty of MPC Values," p 338 in Selected Materials on Radiation Protection Criteria and Standards: Their Basis and Use, Joint Committee on Atomic Energy, Congress of the United States, U.S. Government Printing Office, Washington, 1960.

W. S. Snyder, "The Scientific Basis for the Permissible Levels of Internal Contamination," p 29 in Health Physics in Nuclear Installations, Organization for European Economic Co-operation, European Nuclear Energy Agency, Paris, December 1959.

A. Sorathesn, G. Bruscia, T. Tamura, and E. G. Struxness, Mineral and Sediment Affinity for Radionuclides, ORNL CF-60-6-93 (1960).

T. D. Strickler and J. A. Auxier, Experimental Evaluation of the Radiation Protection Afforded by Typical Oak Ridge Homes Against Distributed Sources, CEX-59.13 (Apr. 14, 1960).

E. G. Struxness, "Disposal in Salt Formations," Ind. Radioactive Waste Disposal 3, 2077–80 (1959) (published hearings before the Special Subcommittee on Radiation of the Joint Committee on Atomic Energy, Congress of the United States, Jan. 28–30, Feb. 2–3, 1959).

E. G. Struxness, "Fixation and Ultimate Disposal," Ind. Radioactive Waste Disposal 3, 1852–55 (1959) (published hearings before the Special Subcommittee on Radiation of the Joint Committee on Atomic Energy, Congress of the United States, Jan. 28–30, Feb. 2–3, 1959).

T. Tamura and D. G. Jacobs, "Structural Implications in Cesium Sorption," Health Phys. 2, 391–98 (1960).

E. B. Wagner and G. S. Hurst, "Gamma Response and Energy Losses in the Absolute Fast Neutron Dosimeter," Health Phys. 2, 57–61 (1959).

W. K. Willard, "Avian Uptake of Fission Products from an Area Contaminated by Low-Level Atomic Wastes," Science 132, 148–50 (1960).

P. L. Ziemer, R. M. Johnson, and R. D. Birkhoff, Measurement of Stopping Power of Copper by Calorimetric Methods, ORNL-2775 (Dec. 17, 1959).

PAPERS

S. I. Auerbach
The Ecology of White Oak Lake Bed – A Radioactive Waste Area, IX International Botanical Congress, August 19–29, 1959, Montreal, Quebec, Canada.

J. A. Auxier
Dosimetry in a Reconstruction of the Reactor Excursion in Yugoslavia, Health Physics Society, Fifth Annual Meeting, June 29–July 1, 1960, Boston, Massachusetts.

J. A. Auxier
Human Data Derived from Japanese Experiences, Scientific Seminar on the Effects of Radiation on Man, July 29, 1960, Berea, Kentucky.

J. A. Auxier, C. H. Bernard, and W. T. Thornton
Silver Metaphosphate Glass for Gamma-Ray Measurements in Coexistent Neutron and Gamma Radiation Fields, Symposium on Selected Topics in Radiation Dosimetry, International Atomic Energy Agency, June 7–11, 1960, Vienna, Austria.

J. A. Auxier, F. W. Sanders, and W. S. Snyder (presented by W. S. Snyder), Na^{24} Activation in the Dosimetry of Nuclear Accidents, presented at Symposium on Radioactivity in Man, Vanderbilt University, April 18–19, 1960, Nashville, Tennessee.

R. D. Birkhoff and W. Happer
Angular Response of a Partially Shielded Cylindrical Dosimeter, Health Physics Society, Fifth Annual Meeting, June 29–July 1, 1960, Boston, Massachusetts.

R. D. Birkhoff and R. M. Johnson
Response of Anthracene as a Function of LET and Its Use in a LET Meter, Health Physics Society, Fifth Annual Meeting, June 29–July 1, 1960, Boston, Massachusetts.

W. J. Boegly, Jr., R. L. Bradshaw, F. M. Empson, and F. L. Parker
Disposal of Radioactive Wastes in Natural Salt – Field Experiments, Fifteenth Annual Purdue Industrial Waste Conference, Purdue University, May 3–5, 1960, Lafayette, Indiana.

J. S. Cheka
An Instrument for Measuring Gamma Radiation in the Presence of Neutrons, Japan Atomic Energy Research Institute, April 19, 1960, Tokai-Mura, Japan.

J. S. Cheka
A Proportional Counter for Measuring Fast Neutron Tissue Dose, Japan Atomic Energy Research Institute, April 19, 1960, Tokai-Mura, Japan.

J. S. Cheka
Film-Illustrated Talk on Radiation Measurements, Atomic Bomb Casualty Commission, March 1960, Hiroshima and Nagasaki, Japan.

J. S. Cheka
Gamma-Ray Dosimetry with Metaphosphate Glass, Japan Atomic Energy Research Institute, April 19, 1960, Tokai-Mura, Japan.

J. S. Cheka
Monitoring Neutron Exposures by Film, Japan Atomic Energy Research Institute, April 19, 1960, Tokai-Mura, Japan.

J. S. Cheka
Threshold Detectors for Neutron Monitoring, Japan Atomic Energy Research Institute, April 19, 1960, Tokai-Mura, Japan.

K. E. Cowser and E. G. Struxness
Disposal of Radioactive Wastes, Twenty-Third Annual Short Course for Superintendents of Water and Sewerage Systems, Louisiana State University, March 16–18, 1960, Baton Rouge, Louisiana.

F. J. Davis
Neutron Dose Determinations with Threshold Detectors, Symposium on Selected Topics in Radiation Dosimetry, International Atomic Energy Agency, June 7–11, 1960, Vienna, Austria.

P. B. Dunaway, Field Studies on Mammals at Oak Ridge National Laboratory, 69th Meeting, Tennessee Academy of Science, December 11–12, 1959, Nashville, Tennessee.

H. B. Eldridge and R. H. Ritchie
A Monte-Carlo Code for Calculating Gamma-Ray Attenuation, Health Physics Society, Fifth Annual Meeting, June 29–July 1, 1960, Boston, Massachusetts.

B. R. Fish
Inhalation of Uranium Aerosols by Mouse, Rat, Dog and Man, International Symposium on Inhaled Particles and Vapours, British Occupational Hygiene Society, March 29–April 1, 1960, Oxford, England.

G. S. Hurst
Capture of Low Energy Electrons in Oxygen, Institut du Radium, June 14, 1960, Paris, France.

G. S. Hurst
Dosimetry Considerations in Criticality Accidents, Seventh Annual Naval Reserve Nuclear Science Seminar, September 13–26, 1959, Brookhaven National Laboratory, Upton, N. Y.

G. S. Hurst
Human Data Derived from Radiation Accidents, Scientific Seminar on the Effects of Radiation on Man, Berea College, June 29, 1960, Berea, Kentucky.

G. S. Hurst and J. A. Auxier
Application of Radiation Dosimetry Studies on the Evaluation of Environmental and Biological Consequences of Nuclear War, Joint Committee on Atomic Energy, Congress of the U.S., Public Hearings on the Biological and Environmental Effects of Nuclear War, June 22–26, 1959, Washington, D.C.

G. S. Hurst and T. E. Bortner
Electron Capture in O_2, 1959 Gaseous Electronics Conference, October 14–16, 1959, Washington, D.C.

G. S. Hurst and E. B. Wagner
Special Counting Techniques in Mixed Radiation Dosimetry, Symposium on Selected Topics in Radiation Dosimetry, International Atomic Energy Agency, June 7–11, 1960, Vienna, Austria.

F. R. Karioris and B. R. Fish
Uranium Oxide Smoke from Exploding Wires, Health Physics Society, Fifth Annual Meeting, June 29–July 1, 1960, Boston, Massachusetts.

S. V. Kaye, A Study of the Eastern Harvest Mouse, Reithrodontomys h. humulis, American Society of Mammalogists, Fortieth Annual Meeting, June 19–23, 1960, Tacoma, Washington.

K. Z. Morgan
Dosimetry of Internal Radioactive Isotopes, Symposium on Radioactivity in Man, Vanderbilt University, April 18–19, 1960, Nashville, Tennessee.

K. Z. Morgan
Dosimetry Requirements for Protection from Ionizing Radiation, Symposium on Selected Topics of Radiation Dosimetry, International Atomic Energy Agency, June 7–11, 1960, Vienna, Austria.

K. Z. Morgan
Maximum Permissible Exposure to Man of Ionizing Radiation, given at AEC Industrial Health Personnel Meeting, November 17–18, 1959, New York, New York, and Tennessee Academy of Science, December 12, 1959, Nashville, Tennessee.

J. Neufeld and W. S. Snyder
Estimates of Energy Dissipation by Heavy Charged Particles in Tissue, Symposium on Selected Topics in Radiation Dosimetry, International Atomic Energy Agency, June 7–11, 1960, Vienna, Austria.

J. S. Olson
Diversity of Dune Ecosystems, Symposium on Sand Dune Systems, A.A.A.S. Meeting, December 30, 1959, Chicago, Illinois.

J. S. Olson
Energy Storage and the Balance of Producers and Reducers, Symposium: Energy Flow in Ecosystems, Ecological Society of America and the American Society of Limnology and Oceanography, A.I.B.S. Meeting, August 1959, State College, Pennsylvania.

J. S. Olson
Exponential Equations Relating Productivity, Decay and Accumulation of Forest Litter, IX International Botanical Congress, August 19–29, 1959, Montreal, Quebec, Canada.

F. L. Parker
Dispersal of Radioactive Contaminants in Fresh Water, Fifth Annual Conference on Water for Texas, Texas A. & M. College, September 11, 1960, College Station, Texas; also presented at the Annual Meeting of Tennessee Section of American Industrial Hygiene Association, October 9, 1959, Kingsport, Tennessee.

F. L. Parker, W. J. Boegly, Jr., R. L. Bradshaw, F. M. Empson, L. Hemphill, E. G. Struxness, and T. Tamura
Disposal of Radioactive Wastes in Natural Salt, International Scientific Conference on the Disposal of Radioactive Wastes, November 16–21, 1959, Monaco.

F. L. Parker, G. D. Schmidt, W. B. Cottrell, and L. A. Mann
Dispersion of Radiocontaminants in an Estuary, Health Physics Society, Fifth Annual Meeting, June 29–July 1, 1960, Boston, Massachusetts.

R. H. Ritchie, H. B. Eldridge, and V. E. Anderson
Calculation of the Radiation Yield from Fission Assemblies and Comparison with Experiments, Symposium on Selected Topics in Radiation Dosimetry, International Atomic Energy Agency, June 7–11, 1960, Vienna, Austria.

W. S. Snyder
Estimation of Body Burden and of Internal Dose, Annual Meeting of AEC Industrial Health Personnel, NYOO, November 17–18, 1959, New York, New York.

W. S. Snyder
Estimation of Dose Distribution Within the Body from Exposures to a Criticality Accident, Symposium on Selected Topics in Radiation Dosimetry, International Atomic Energy Agency, June 7–11, 1960, Vienna, Austria.

W. S. Snyder
Estimation of Dose from a Single Intake of Radioactive Materials, Health Physics Society Meeting, June 29–July 1, 1960, Boston, Massachusetts.

W. S. Snyder
Present Trends in Estimation of Internal Dose, presented at 5th Annual Bio-Assay and Analytical Chemistry Meeting, October 1–2, 1959, Gatlinburg, Tennessee.

W. S. Snyder
Theoretical Studies in Dosimetry, Biomedical Directors' Meeting, ORNL, October 6, 1959, Oak Ridge, Tennessee.

W. S. Snyder
Uncertainties in MPC Values for Thorium Isotopes, presented at Thorium Seminar, University of Rochester Atomic Energy Project, January 19–20, 1960, Rochester, New York.

T. D. Strickler and J. A. Auxier
The Oak Ridge House Shielding Program, Kentucky Association of Physics Teachers, October 24, 1959, Bowling Green, Kentucky.

E. G. Struxness
Ground Disposal of Radioactive Wastes, American Institute of Mining and Metallurgical Engineers Meeting, September 25, 1960, Gatlinburg, Tennessee.

E. G. Struxness, K. E. Cowser, W. de Laguna, D. G. Jacobs, R. J. Morton, and T. Tamura
Waste Disposal Research and Development in the USA, International Scientific Conference on the Disposal of Radioactive Wastes, November 16–21, 1959, Monaco.

T. Tamura and D. G. Jacobs
Structural Implications of Sorption by Alumino-Silicate Clays, Ion Exchange Conference, September 7–11, 1959, Gatlinburg, Tennessee.

E. B. Wagner and G. S. Hurst
A G-M Tube Gamma-Ray Dosimeter with Low Neutron Sensitivity, Health Physics Society, Fifth Annual Meeting, June 29–July 1, 1960, Boston, Massachusetts.

E. E. Anderson

Radiation Hazards and Current Practices in Radiation Protection, Duke University Marine Laboratory, August 6–7, 1959, Beaufort, North Carolina; Puerto Rico Nuclear Center, September 21–28, 1959, Mayaguez, Puerto Rico; US Naval Medical Research Laboratory, October 22–23, 1959, New London, Connecticut; RESA, January 11–13, 1960, Newport News, Virginia; University of North Carolina, January 25, 1960, Raleigh, North Carolina; Mississippi State University, April 19, 1960, State College, Mississippi; Texas Woman's University, April 21, 1960, Denton, Texas; University of Cincinnati, April 27, 1960, Cincinnati, Ohio; Cincinnati Altrusa Club, April 27, 1960, Cincinnati, Ohio.

Biological Problems of Interest to the Health Physicist, Puerto Rico Nuclear Center, September 21–28, 1959, Mayaguez, Puerto Rico.

Maximum Permissible Exposure Values (ICRP and NCRP), Puerto Rico Nuclear Center, September 21–28, 1959, Mayaguez, Puerto Rico.

Health Physics as a Profession, Symposium on Health Physics, Argonne National Laboratory, October 13, 1959, Lemont, Illinois; Symposium on Health Physics, Hotel Texas, October 16, 1959, Fort Worth, Texas.

Health Physics, Drexel Institute of Technology, March 29, 1960, Philadelphia, Pennsylvania; NSF Institute for High School Teachers, University of Chattanooga, June 22, 1960, Chattanooga, Tennessee; Tulane University Summer Institute in Radiation Biology, July 15, 1960, New Orleans, Louisiana.

The Profession of Health Physics, Texas Woman's University, April 21, 1960, Denton, Texas.

Radiation Protection Criteria and Standards: Their Basis and Use, Congressional Hearings, June 3, 1960, Washington, D.C.

Current Developments in Maximum Permissible Dose Recommendations, Robert A. Taft Sanitary Engineering Center, June 17, 1960, Cincinnati, Ohio.

The Concept of the Maximum Permissible Dose, Purdue University, July 11, 1960, Lafayette, Indiana.

Principles of Radiation Protection (Health Physics), University of North Dakota Summer Science Institute, July 19–20, 1960, Grand Forks, North Dakota; South Dakota State College Summer Science Institute, July 21–22, 1960, Brookings, South Dakota.

Maximum Permissible Exposure Values, University of North Dakota Summer Science Institute, July 19–20, 1960, Grand Forks, North Dakota; South Dakota State College Summer Science Institute, July 21–22, 1960, Brookings, South Dakota.

S. I. Auerbach

Characterization of Radiation Field on White Oak Lake Bed, Health Physics Division Seminar, ORNL, July 8, 1959, Oak Ridge, Tennessee.

Ecological Studies in Relation to Radioactive Wastes, Highlands Biological Station, July 30, 1959, Highlands, North Carolina; NSF Biology Institute, Knox College, July 1, 1959, Galesburg, Illinois; NSF Biology Institute, July 23, 1959, Purdue University, Lafayette, Indiana.

Radiation Wastes and Human Ecology, Traveling Teacher Course, ORINS, August 20, 1959, Oak Ridge, Tennessee.

Fate of Sr^{90} and Cs^{137} in White Oak Lake Bed Ecosystem, Bio-Medical Directors Meeting, ORNL, October 6, 1959, Oak Ridge, Tennessee.

Ecological Research in the Oak Ridge Area, Chemical Technology Division Seminar, ORNL, October 27, 1959, Oak Ridge, Tennessee.

Ecological Research at Oak Ridge National Laboratory, Biology Division Seminar, ORNL, November 5, 1959, Oak Ridge, Tennessee; Botany Department, University of Tennessee, November 19, 1959, Knoxville, Tennessee.

Ecology and the Radioactive Waste Problem; Biological Cycling of Sr^{90} and Cs^{137} in Radioactive Waste Areas, 3 lectures, Biology Departments, University of Puerto Rico, March 14–20, 1960, San Juan and Mayaguez, Puerto Rico.

Radiation Ecology. A.I.B.S. Lectures, Tusculum College, April 4–5, 1960, Greeneville, Tennessee.

The Role of Ecology in the Atomic Age, A.I.B.S. Lecture to Phi Sigma Society, Marquette University, April 10, 1960, Milwaukee, Wisconsin.

Fundamentals of Ecology and Radiation Ecology, Health Physics Fellowship Students, Vanderbilt University, May 9, 1960, Nashville, Tennessee.

K. E. Cowser

Process Waste Water Treatment, Health Physics Course for ORSORT Foreign Students, January 6, 1960, Oak Ridge, Tennessee; ORNL Ten-Week Course in Health Physics, March 15, 1960, Oak Ridge, Tennessee.

Waste Pits and Burial Grounds, Health Physics Course for ORSORT Foreign Students, January 11, 1960, Oak Ridge, Tennessee; ORNL Ten-Week Course in Health Physics, March 16, 1960, Oak Ridge, Tennessee.

Handling, Treatment, and Disposal of Chemical Processing Wastes at ORNL, Oak Ridge Chapter of American Society of Civil Engineers, January 13, 1960, Oak Ridge, Tennessee; U.S. Public Health Service Course on Environmental Health Aspects of Nuclear Reactor Operations, May 24, 1960, Oak Ridge, Tennessee; Health Physics Fellowship Program, Vanderbilt University, May 17, 1960, Nashville, Tennessee.

D. A. Crossley, Jr.

Accumulation of Radioactive Fission Products by Insects, Zoology and Entomology Department, University of Tennessee, February 16, 1960, Knoxville, Tennessee.

F. M. Empson

Radiation Problems Related to Public Health, College of Education, University of Tennessee, November 29, 1959, and May 23, 1960, Knoxville, Tennessee.

Tank Disposal and Calcination of Reactor Fuel Reprocessing Wastes, Health Physics Course for ORSORT Foreign Students, December 30, 1959, Oak Ridge, Tennessee.

Possible Disposition of Radioactive Wastes into Depleted Salt Mines, Salt Producers Association, May 11, 1960, Chicago, Illinois.

M. F. Fair

Health Physics, ORINS Traveling Teachers, August 5, 1959, Oak Ridge, Tennessee; ORINS Medical School, August 6 and December 10, 1959, March 24, 1960, Oak Ridge, Tennessee; ORINS, August 11, September 4, October 22, 1959, and May 12, 1960, Oak Ridge, Tennessee; US Public Health Service, October 19, 1959, Cincinnati, Ohio; NSF, December 15, 1959, Cookeville, Tennessee.

L. Hemphill

Origin and Nature of Fuel Process Waste, Health Physics Course for ORSORT Foreign Students, December 28, 1959, Oak Ridge, Tennessee; U.S. Public Health Service Course on Environmental Health Aspects of Nuclear Reactor Operations, May 24, 1960, Oak Ridge, Tennessee.

Waste Disposal, National Science Foundation Radiological Sciences Conference, North Texas State College, April 13–15, 1960, Denton, Texas.

D. G. Jacobs

Geochemical Studies on Radioactive Waste Disposal at ORNL, AEC Meeting on Disposal of Radioactive Wastes into the Ground, University of California, August 26, 1959, Berkeley, California.

Geochemical Studies in Radioactive Waste Disposal, Agronomy Department Seminar, University of Illinois, October 22, 1959, Urbana, Illinois.

Ground Dispersal of Radioactive Wastes, AEC Health Physics Fellowship Program, Vanderbilt University, May 16, 1960, Nashville, Tennessee.

K. Z. Morgan

Health Physics Applied Dosimetry Problems, presented at Research Council Meeting, ORNL, September 11, 1959, Oak Ridge, Tennessee.

Welcome Address, given at Bio-Assay and Analytical Chemistry Meeting, October 1–2, 1959, Gatlinburg, Tennessee.

Some Internal Dose Problems, presented at Bio-Medical Meeting, Oak Ridge, October 4–6, 1959; presented at Health Physics Division Information Meeting, ORNL, October 29–30, 1959, Oak Ridge, Tennessee.

Health Physics, given at Naval Reserve Seminar, ORINS, December 4, 1959, Oak Ridge, Tennessee.

Statement on the History and Philosophy of Laboratory Operations with Respect to the Clinch River, given at the Meeting on Clinch River Research Program, ORNL, December 18, 1959, Oak Ridge, Tennessee.

Internal Dose, lecture to Foreign Students, Reactor School, ORNL, December 21, 23, 1959, Oak Ridge, Tennessee.

Health Physics Problems Associated with Recent Accident at ORNL, Health Physics Seminar, ORNL, January 20, 1960, Oak Ridge, Tennessee.

Activities of the Health Physics Division of Oak Ridge National Laboratory, AEC Bio-Med Meeting, February 11–12, 1960, Chalk River, Canada.

Internal Dose, lecture to Health Physics Trainees, ORNL, February 23, 1960, Oak Ridge, Tennessee; lecture to students at Vanderbilt University, February 29, March 7–8, 1960, Nashville, Tennessee.

Allowable Biological Exposures to Radiation, Oak Ridge Section of the American Nuclear Society, April 5, 1960, Oak Ridge, Tennessee.

R. J. Morton

ORNL Waste Disposal Facilities and Field Studies (tour and lecture), ORSORT Course for College Professors, ORNL, August 13, 1959, Oak Ridge, Tennessee.

Ionizing Radiation in the Environment (panel discussion), Sixth Annual Seminar on Radiological Health, University of North Carolina and North Carolina State Board of Health, January 26, 1960, Chapel Hill, North Carolina.

Radioactive Waste Disposal (lecture) and Public Health Readiness to Meet Ionizing Radiation Responsibilities (panel discussion), Sixth Annual Seminar on Radiological Health, University of North Carolina and North Carolina State Board of Health, January 27, 1960, Chapel Hill, North Carolina.

Waste Management Facilities at ORNL (field tour and lecture), U.S. Public Health Service Course on "Reactor Environmental Health Problems," ORNL, May 24, 1960, Oak Ridge, Tennessee.

J. S. Olson

Rates of Succession and Soil Formation on Sand Dunes, Health Physics Division Seminar, ORNL, July 7, 1960, Oak Ridge, Tennessee.

Movement of Isotopes in Forests, Biomedical Directors Meeting, ORNL, October 6, 1959, Oak Ridge, Tennessee.

F. L. Parker

Disposal into Salt, Health Physics Course for ORSORT Foreign Students, January 4, 1960, Oak Ridge, Tennessee.

Surface Waterways Dispersion, ORNL Ten-Week Course in Health Physics, March 7, 1960, Oak Ridge, Tennessee.

Field Tests of Disposal of Radioactive Wastes in Natural Salt Formations, presented before the Committee on Waste Disposal of the Division of Earth Sciences of the National Academy of Sciences, National Research Council, March 26, 1960, Washington, D.C.

Fundamentals of Waste Disposal, AEC Health Physics Fellowship Program, Vanderbilt University, May 10, 1960, Nashville, Tennessee.

Disposal in Geological Formations, AEC Health Physics Fellowship Program, Vanderbilt University, May 10, 1960, Nashville, Tennessee.

R. H. Ritchie
Dosimetry of Vinča Accident, ORSORT Lecture, July 22, 1960, Oak Ridge, Tennessee.

W. S. Snyder
An Estimate of Gonad Dose Due to Internally Deposited Radionuclides and Theoretical Neutron Response of Threshold Detectors, Health Physics Division Information Meeting, ORNL, October 29–30, 1959, Oak Ridge, Tennessee.

E. G. Struxness
Summary of Waste Research at ORNL and Elsewhere in the USA, Health Physics Course for ORSORT Foreign Students, January 15, 1960, Oak Ridge, Tennessee.

T. Tamura
Ion Exchange Reactions of Clays, Tuskegee Institute, October 20, 1959, Tuskegee, Alabama.

Disposal Using Clay Minerals, Health Physics Course for ORSORT Foreign Students, January 13, 1960, Oak Ridge, Tennessee.

Statement on the Chemical Reactions Involved in the Disposal of Radioactive Wastes in Salt Formations, presented before the Committee on Waste Disposal of the Division of Earth Sciences of the National Academy of Sciences, National Research Council, March 26, 1960, Washington, D.C.

ORNL-2994
UC-41 — Health and Safety
TID-4500 (15th ed.)

INTERNAL DISTRIBUTION

1. C. E. Center
2. Biology Library
3. Health Physics Library
4-6. Central Research Library
7. Reactor Experimental Engineering Library
8-44. Laboratory Records Department
45. Laboratory Records, ORNL R.C.
46. L. B. Emlet (K-25)
47. J. P. Murray (Y-12)
48. A. M. Weinberg
49. J. A. Swartout
50. E. D. Shipley
51. K. Z. Morgan
52. M. L. Nelson
53. C. P. Keim
54. S. C. Lind
55. A. S. Householder
56. C. S. Harrill
57. C. E. Winters
58. A. H. Snell
59. E. H. Taylor
60. W. H. Jordan
61. T. A. Lincoln
62. A. Hollaender
63. F. L. Culler
64. H. E. Seagren
65. D. Phillips
66. M. T. Kelley
67. E. E. Anderson
68. R. S. Livingston
69. R. A. Charpie
70. K. E. Cowser
71. C. D. Susano
72. L. B. Farabee
73. F. J. Davis
74. R. J. Morton
75. C. E. Haynes
76. Hugh F. Henry (K-25)
77. E. G. Struxness
78. W. E. Cohn
79. H. H. Hubbell
80. D. E. Arthur
81. J. Neufeld
82. M. L. Randolph
83-84. P. M. Reyling
85. G. C. Williams
86. R. S. Cockreham
87. M. J. Skinner
88. J. C. Hart
89. T. H. J. Burnett
90. W. de Laguna
91. M. J. Cook
92. G. S. Hurst
93. S. R. Bernard
94. J. A. Lane
95. W. S. Snyder
96. L. Hemphill
97. L. B. Holland
98. J. L. Gabbard
99. D. G. Jacobs
100. R. L. Bradshaw
101. A. C. Upton
102. E. T. Arakawa
103. D. M. Davis
104. P. E. Brown
105. E. D. Gupton
106. J. C. Ledbetter
107. R. L. Clark
108. G. C. Cain
109. L. C. Johnson
110. W. Ogg
111. O. D. Teague
112. E. L. Sharp
113. E. J. Kuna
114. H. H. Abee
115. C. R. Guinn
116. A. D. Warden
117. E. B. Wagner
118. D. A. Crossley, Jr.
119. J. R. Muir
120. J. A. Auxier
121. M. F. Fair
122. S. I. Auerbach
123. G. W. Royster, Jr.
124. T. F. Lomenick
125. J. D. McLendon
126. F. W. Sanders

127. F. C. Maienschein
128. W. J. Boegly, Jr.
129. W. B. Nix
130. J. G. Carter
131. B. Fish
132. D. R. Nelson
133. S. V. Kaye
134. C. E. Breckinridge
135. H. B. Eldridge
136. R. M. Johnson
137. L. B. O'Kelly
138. P. W. Reinhardt
139. J. H. Thorngate
140. E. S. Jones
141. F. M. Empson
142. R. D. Birkhoff
143. R. H. Ritchie
144. J. A. Harter
145. W. G. Stone
146. J. S. Cheka
147. P. N. Hensley
148. R. W. Peelle
149. P. B. Dunaway
150. T. Tamura
151. V. H. Climent
152. R. M. Richardson
153. J. S. Olson
154. D. Bagwell (consultant)
155. T. E. Bortner (consultant)
156. P. H. Doyle (consultant)
157. U. Fano (consultant)
158. T. D. Strickler (consultant)
159. J. C. Frye (consultant)
160. W. H. Langham (consultant)
161. G. M. Fair (consultant)
162. R. E. Zirkle (consultant)
163. L. S. Taylor (consultant)
164. R. L. Platzman (consultant)
165. N. Wald (consultant)
166. ORNL – Y-12 Technical Library, Document Reference Section

EXTERNAL DISTRIBUTION

167. C. P. Straub, Public Health Service, Robert A. Taft Sanitary Engineering Center
168. R. M. Collier, University of Florida, Gainesville, Florida
169. Physics and Engineering Group, Balcones Research Center, RFD 4, Box 189, Austin, Texas
170. G. E. Thoma, St. Louis University Hospital, 135 South Grand Boulevard, St. Louis, Missouri
171. Vanderbilt University (Physics Library)
172. Massachusetts Institute of Technology (Department of Electrical Engineering)
173. University of California (Gerhard Klein)
174. H. Le Grande, U.S. Geological Survey, Box 433, Albuquerque, New Mexico
175. Lola Lyons, Librarian, Olin Industries, Inc., East Alton, Illinois
176. Jack Story, Health Physicist, North Carolina State College, Raleigh, North Carolina
177. J. H. Ebersole, USSS Nautilus, c/o Fleet Post Office, New York, New York
178. David S. Smith, Health and Safety Division, U.S. Atomic Energy Commission, Chicago Operations Office, P.O. Box 59, Lemont, Illinois
179. Division of Research and Development, AEC, ORO
180. S. C. Sigoloff, Edgerton, Germeshausen and Grier, Inc., P.O. Box 98, GoLeta, California
181. Robert Wood, Department of Physics, Memorial Center, 444 E. 68th St., New York 21, New York
182. John Wolfe, Division of Biology and Medicine, U.S. Atomic Energy Commission, Washington, D.C.

183. Orlando Park, Department of Biology, Northwestern University, Evanston, Illinois
184. Eugene Odum, Department of Zoology, University of Georgia, Athens, Georgia
185. W. T. Ham, Medical College of Virginia, Richmond, Virginia
186. F. H. W. Noll, Department of Physics, Berea College, Berea, Kentucky
187. Herbert E. Stokinger, Bureau of State Service, Department of Health Education and Welfare, Penn 14 Broadway, Cincinnati 2, Ohio
188. J. B. Lackey, University of Florida, Gainesville, Florida
189. J. J. Davis, Biology Operation, Hanford Atomic Power Operations, Seattle, Washington
190. Royal Shanks, Department of Botany, University of Tennessee Knoxville, Tennessee
191. Robert B. Platt, Department of Biology, Emory University, Atlanta, Georgia
192. C. H. Bernard, Physics Department, Texas A&M College Station, Texas
193. H. M. Borella, Edgerton, Germeshausen and Grier, Inc., P.O. Box 98, Goleta, California
194. J. S. Mendell, Rensselaer Polytechnic Institute, Troy, New York
195. H. P. Yockey, Aerojet-General Nucleonics, San Ramon, California
196. C. E. Dady, Watertown Arsenal, Ordnance Material Research Office, Watertown, Massachusetts
197. John I. Hopkins, Davidson College, Department of Physics, P.O. Box 327, Davidson, North Carolina
198. W. J. Lacy, Office of Civil Defense Mobilization, Battle Creek, Michigan
199. G. A. Andrews, Oak Ridge Institute of Nuclear Studies, Oak Ridge, Tennessee
200. E. P. Resner, States Marine Lines, c/o New York Shipbuilding Corp., Camden, New Jersey
201-203. J. A. Lieberman, Division of Reactor Development, AEC, Washington, D.C.
204-206. The Carey Salt Company, Hutchinson, Kansas (1 copy to H. J. Carey, Jr.)
207. C. Orr, Georgia Institute of Technology, Atlanta, Georgia
208. W. E. Lotz, Division of Biology and Medicine, AEC, Washington, D.C.
209. E. F. Gloyna, Department of Civil Engineering, University of Texas, Austin 12, Texas
210. J. S. Cragwall, Jr., U.S. Geological Survey, Surface Water Branch, 823 Edney Building, Chattanooga, Tennessee
211. H. H. Waesche, AEC Liaison Officer, Geochemical and Petrology Branch, U.S. Geological Survey, Naval Gun Factory, Building 213, Washington 25, D.C.
212. S. Leary Jones, Tennessee Department of Public Health, Cordell Hull Building, Nashville, Tennessee
213. H. C. Thomas, Chemistry Department, University of North Carolina, Chapel Hill, North Carolina

214. Glenn Gentry, Fish Management Division, Game and Fish Commission, Cordell Hull Building, Nashville, Tennessee
215. A. A. Schoen, Biology Division, U.S. Atomic Energy Commission, Oak Ridge, Tennessee
216. F. E. Gartrell, Health and Safety Division, Tennessee Valley Authority, Edney Building, Chattanooga, Tennessee
217. Vincent Schultz, Environmental Sciences Branch, Division of Biology and Medicine, U.S. Atomic Energy Commission, Washington 25, D.C.
218. A. G. Friend, U.S. Public Health Service, Robert A. Taft Sanitary Engineering Center, 4676 Columbia Parkway, Cincinnati 26, Ohio
219. D. W. Pierce, Manager, Chemical Effluents Technology, Chemical Research and Development, General Electric Company, Hanford Atomic Products Operation, Richland, Washington
220. O. W. Kochtitzky, Tennessee Valley Authority, 717 Edney Building, Chattanooga, Tennessee
221. Leslie Silverman, Industrial Engineering, Department of Industrial Hygiene School of Public Health, Harvard University, 55 Shattuck Street, Boston 15, Massachusetts
222. J. Wade Watkins, U.S. Bureau of Mines, Bartlesville, Oklahoma
223. Kansas State Board of Health, Topeka, Kansas (Dwight F. Metzler)
224. Kansas State Geological Survey, Lawrence, Kansas (Frank C. Foley)
225. W. R. Thurston, Executive Secretary, Division of Earth Sciences, National Academy of Sciences — National Research Council, Washington, D.C.
226. C. S. Shoup, Biology Division, U.S. Atomic Energy Commission, Oak Ridge, Tennessee
227-857. Given distribution as shown in TID-4500 (15th ed.) under Health and Safety category (100 copies — OTS)